IDENTIFICATION OF PEPTIDYLARGININE DEIMINASE-2 (PADI2) AS A POTENTIAL ONCOGENE AND THERAPEUTIC TARGET

A Dissertation

Presented to the Faculty of the Graduate School

of Cornell University

In Partial Fulfillment of the Requirements for the Degree of

Doctor of Philosophy

by

John L. McElwee

January 2014

IDENTIFICATION OF PEPTIDYLARGININE DEIMINASE-2 (PADI2) AS A POTENTIAL ONCOGENE AND THERAPEUTIC TARGET

John L. McElwee, Ph. D.

Cornell University 2014

Breast cancer is the most frequently diagnosed cancer in women, with over 1 million new cases in the world each year. Recently, in addition to genetic mutations, numerous studies have found that epigenetics plays a direct role in the etiology of breast cancer. The PADIs are a family of epigenetic enzymes that catalyze citrullination, with previous work in our lab showing that PADIs can convert both protein and histone arginine to citrulline, leading to the disruption of protein-protein interactions, as well as direct transcriptional downregulation. Previous research has suggested a potential oncogenic role for PADI2 in breast cancer, though no formal analysis existed. The studies herein investigate the potential role of PADI2 as a novel oncogene and therapeutic target in the treatment of breast cancer *in vitro* and *in vivo*.

First, using an *in vitro* model of breast cancer progression (MCF10AT), we show that PADI2 is upregulated upon the malignant transformation of cells, especially in MCF10DCIS cells, which recapitulate the highly invasive comedo-like ductal carcinoma *in situ* (DCIS) tumors seen in humans. Secondly, using RNA-seq, we show that *PADI2* is highly correlated with *HER2/ERBB2* overexpression across 57 breast cancer cell lines. We concluded this study by validating the use of our first-generation PADI inhibitor, Cl-amidine, as a therapeutic agent for the treatment of breast cancer both *in vitro* and *in vivo*.

Following this, we further investigated the functional relationship between PADI2 and HER2 expression. Interestingly, PADI2 appears to function both upstream

and downstream of HER2, potentially indicating a role in an oncogenic positive-feedback loop with HER2. Previous evidence from our lab established that PADI2 functions as an ER co-activator via the citrullination of histone H3 arginine 26 (H3R26) at ER-target gene promoters. We show here that PADI2 can bind to the HER2 promoter and downstream ERE; thus, suggesting that the epigenetic regulation of HER2 gene expression by PADI2 occurs via similar mechanisms to ER-target genes. Moreover, we were able to validate our highly potent next-generation PADI inhibitor, BB-Cl-amidine, in the treatment of breast cancer cells *in vitro*.

Lastly, using a mouse model of PADI2 overexpression (MMTV-FLAG-PADI2), we found that 20% of mice developed skin lesions after five months. These tumors express high levels of transgenic human PADI2 and display markers of increased inflammation and invasiveness-EMT. Furthermore, a subset of these tumors showed via histopathological analysis to have undergone malignant progression to highly invasive squamous cell carcinomas.

Collectively, these studies provide functional and mechanistic evidence establishing PADI2 as a potential novel oncogene and target for cancer therapy.

BIOGRAPHICAL SKETCH

John McElwee was born on May 25, 1976, in Nyack NY. He grew up a short distance away in Florida, NY. After attending St. Joseph's Grammar School, and John S. Burke Catholic HS, John ultimately ended up pursuing his baccalaureate degree at Binghamton University. At Binghamton University, John majored in Biological Sciences and minored in Biological Anthropology, receiving his Bachelor of Science degree in 1999. After graduating, he went on to work at Cornell University in the laboratory of Drs. Gustavo Aguirre and Greg Acland at the Baker Institute of Animal Health. It was here that John's interest in science grew, as he was involved in the burgeoning field of canine genomics, studying the genetics of canine eye diseases. John also worked briefly in the laboratory of Dr. Antje Baeumner, working on the development of biological sensors for the detection of select bio-warfare agents, such as *Bacillus anthracis*. John's last position at Cornell was in the laboratory of Dr. Alex Travis, where he worked in the field of reproductive biology, using the mouse as a model. Armed with a diverse background in molecular biology and genetics, John ventured outside of academia, working for Regeneron Pharmaceuticals. It was here that John developed his love for mouse genetics, working within the molecular group at VelociGene, which was directly responsible for generating mouse models of disease for the validation of novel therapeutic targets. While working on the KOMP project at VelociGene, John decided that independent research was his ultimate goal. In 2007, John enrolled at Cornell University as a graduate student in Comparative Biomedical Sciences, and after rotating, joined the lab of Dr. Scott Coonrod in the summer of 2008.

I would like to dedicate this work to my parents, especially my mother, who has given me unwavering support and guidance throughout my life.

ACKNOWLEDGEMENTS

The best science is always the work of many, and I owe a great deal of gratitude to the many people who have helped along the way. First, I would like to thank my mentor, Dr. Scott Coonrod, who provided me with enough freedom to take this dissertation project into new and exciting areas of cancer research. His passion for science, and unwavering support over the years, has helped me to reach my full potential as an independent scientist. I also owe a special thanks to my special committee: Drs. John Schimenti, Paul Soloway, and David Lin, for their support and enthusiasm, in addition to many insightful discussions during my doctoral training.

Although this work has taken several years of hard work, my many coworkers in the Coonrod lab have made this time enjoyable. My fellow graduate students, Boram Kim, Dr. Sunish Mohanan, and Sachi Horibata, have always been there for me whenever I needed science and/or personal support. Specifically, I want to thank Sunish for his expertise in pathology, which has been an invaluable resource during the course of my many *in vivo* studies. In addition, he has provided great conversation in areas ranging from politics, to potential careers post-dissertation. Next, I want to thank Sachi, who in addition to being a master at *in vitro* cancer assays, always brings a smile to the lab with her happy demeanor (and delicious baked goods). I must not forget the many postdocs in the lab, who have provided invaluable support and a wealth of knowledge to help my research move along properly. Thanks to Dr. Xuesen Zhang, who has taught me the basics of ChIP and helped with the many hours of subsequent troubleshooting. Special thanks to Dr. Brian Cherrington, who was instrumental in getting my project off the ground, and for always being there for support, both inside and outside the lab (many stories for both). In addition, thanks to Dr. Eric Morency, who was also a great sounding board for anything and everything

related to science, or life in general. I must also thank the research support staff of the Coonrod lab, especially our lab manager Lynne Anguish and our technician Kelly Sams, both have been invaluable in all areas of the lab, especially in the maintenance of our always expanding mouse colony. I have also enjoyed working with the many visiting veterinary leadership students during the summers, especially Dr. Heike Breuer, who provided a great deal of support and much needed fun during the summer following my A-exam, in addition to introducing me to the German language. This summer, I had the pleasure of working with the first Croatian leadership student, Iva Cvitaš, who provided a great deal of support for the transgenic project, as well as some much needed distraction from thesis writing. I must not forget the valuable contributions of my two great undergrads, Josephine Chen and Dalton McLean. Josephine became my cloning machine, and was invaluable in plowing through the many constructs (most of which unfortunately ended up in the negative data pile) used during my graduate research. Dalton has also provided me with much needed research support, and under my tutelage, has become a master at qPCR – always striving for the perfect run with no QC flags.

Lastly, I would like to thank all my family and friends for their support during this long journey down the doctoral research road. In addition, a big thanks to my fellow graduate students here at Cornell, who have made my time as a doctoral student much more enjoyable and rewarding. I will always be grateful to these future friends and colleagues for all their help and support during my time at Cornell University

TABLE OF CONTENTS

LIST OF FIGURES

LIST OF TABLES

LIST OF ABBREVIATIONS

AD	Alzheimer's disease
AI	Aromatase inhibitor
AIB1	Amplified in breast cancer
AKT	Murine thyme viral (v-AKT) oncogene homolog-1
ALEXA-seq	Alternative expression analysis by sequencing
AMD	Age-related macular degeneration
AP-1	Activator protein-1
BB-Cl-amidine	Biphenyl-benzimidazole-Cl-amidine
BRCA1/2	Breast cancer gene 1 and 2
CAM	Cl-amidine
CBP	CREB binding protein
CDK	Cyclin-dependent Kinase
cDNA	Complementary DNA
ChIP	Chromatin immunoprecipitation
CK	Cytokeratin
Cl-amidine	N-α-benzoyl-N5-(2-chloro-1-iminoethyl)-L-orn amide
CLS	Crown-like structure
CMV	Cytomegalovirus promoter
COPD	Chronic obstructive pulmonary disease
COX2	Cyclooxygenase-2
CSC	Cancer stem cell
DAPI	4',6-diamidino-2-phenylindole
DCIS	Ductal carcinoma in situ
DMBA	Di-methyl-benzanthracene

DNA	Deoxyribonucleic acid
E2	17ß-estradiol
ECM	Extracellular matrix
EGF	Epidermal growth factor
EGFR	Epidermal growth factor receptor (HER1)
EMT	Epithelial-to-mesenchymal transition
ER	Estrogen receptor alpha
ERBB2	Erythroblastic leukemia viral oncogene homolog-2
ERE	Estrogen response element
ERK	Extracellular regulated kinase
ERKO	Estrogen receptor knockout
ET	Extracellular trap
FACS	Fluorescence activated cell sorting
FOXA1	Forkhead box A1
GAPDH	Glyceraldehyde 3-Phosphate Dehydrogenase
GSK3ß	Glycogen synthase kinase 3 beta
H&E	Hematoxylin and eosin
H3Cit2,8,17	Histone H3 citrulline 2,8,17
H3Cit26	Histone H3 citrulline 26
H3R2,8,17	Histone H3 arginine 2,8,17
H3R26	Histone H3 arginine 26
H3K27	Histone H3 lysine 27
H3K27ac	Histone H3 acetyl lysine 27
H4Cit3	Histone H4 citrulline 3
H4R3	Histone H4 arginine 3
HDAC	Histone deacetylase

HER2	Human epidermal growth factor receptor-2
HER3	Human epidermal growth factor receptor-3
HER4	Human epidermal growth factor receptor-4
IF	Immunofluorescence
IGF	Insulin-like growth factor
IGF1R	Insulin-like growth factor type 1 receptor
IHC	Immunohistochemistry
IL6	Interleukin 6
IL8	Interleukin 8
KD	Knock-down (genetic)
KO	Knock-out (genetic)
LAP	Lapatinib
MAPK	Mitogen activated protein kinase
MBP	Myelin basic protein
MEK	MAPK/ERK Kinase
MET	Macrophage extracellular trap
MMTV	Mouse mammary tumor virus
MMTV-LTR	Mouse mammary tumor virus long terminal repeat
mRNA	Messenger RNA
MS	Multiple sclerosis
MYC	Myelocytomatosis viral oncogene
NCoR	Nuclear receptor co-repressor
NET	Neutrophil extracellular trap
Neu	Neuro/glioblastoma derived oncogene homolog (avian)
NFkB	Nuclear factor kappa B
NRG	Neuregulin/heregulin

p300	E1A binding protein p300
PADI1	Peptidylarginine deiminase-1
PADI2	Peptidylarginine deiminase-2
PADI3	Peptidylarginine deiminase-3
PADI4	Peptidylarginine deiminase-4
PADI6	Peptidylarginine deiminase-6
PARP	Poly (ADP-ribose) Polymerase
PAS	Periodic acid-Schiff
PCNA	Proliferating cell nuclear antigen
PCR	Polymerase chain reaction
PEA3	Polyomavirus enhancer activator-3 (ETV4)
PGK	Phosphoglycerate kinase promoter
PI3K	Phosphatidylinositol 3-kinase
PR	Progesterone receptor
pRb	Retinoblastoma protein (RB1)
PyMT	Polyoma middle T antigen
qRT-PCR	Quantitative real-time PCR
RA	Rheumatoid arthritis
RAS	Rat sarcoma viral oncogene
RNA	Ribonucleic acid
RNA-seq	RNA sequencing
RTK	Receptor tyrosine kinase
SCC	Squamous cell carcinoma
SERD	Selective estrogen receptor down-regulator
SERM	Selective estrogen receptor modulator
shRNA	Short hairpin RNA

siRNA	Small interfering RNA
SMAD	SMA- and –MAD related
SP-1	Specificity protein 1
S-phase	Synthesis phase of the cell cycle
SRC	Steroid receptor co-activator
SV40	Simian virus 40
TCGA	The cancer genome atlas
TF	Transcription factor
TFF1	Trefoil factor-1
Tg	Transgenic
TGFß	Transforming growth factor beta
TGFα	Transforming growth factor alpha
TNBC	Triple negative breast cancer
TPA	12-O-tetradecanoylphorbol-13-acetate
UV	Ultraviolet
VEGF	Vascular endothelial growth factor

CHAPTER ONE

INTRODUCTION

1.1 Breast cancer

1.1.1 Origin of breast cancer molecular subtypes

In the United States, around 25% of all deaths are due to cancer [1], which translates to ~600,000 deaths per year. Among women, breast cancer is the most commonly diagnosed cancer (~29%), and is second only to lung and bronchial cancers for cancer-related deaths (~14%) [1]. While there has been a decrease in overall breast cancer incidence, largely due to enhanced screening and awareness, breast cancer is still the leading cause of death among women ages 20-59 [1]. There are many risk factors associated with the development of breast cancer, including, but not limited to: genetic predisposition (e.g. *BRCA1* and *BRCA2* [2, 3]), high mammary tissue density, early menarche, late menopause, age at first pregnancy, parity, breast-feeding, and many additional environmental risk factors [4]. Interestingly, some of these risk factors have recently been linked to the intrinsic breast cancer subtypes, with the majority of traditional breast cancer risk factors associated with luminal A tumors, the most common subtype [5]. In addition, weight gain (i.e. increased mammary tissue density) is more strongly associated with luminal B tumors, age at menopause was significantly associated with the human epidermal growth factor receptor-2 (HER2)-type, and hormonal treatment (estrogen + progestin) is strongly associated with basal-like tumors [4]. Interestingly, increased parity was found to be associated with a reduced risk of luminal A tumors; however, there was an increased risk of more malignant basal-like tumors [5, 6]. While early detection and targeted therapies have greatly reduced the incidence of mortality, the prognosis for women with locally advanced and metastatic breast cancer remains poor. Until recently, the predominant method of determining breast cancer prognosis has been via histological type, tumor grade, and lymph node involvement. Breast cancer is a highly heterogeneous disease, and while these histological parameters might be clinically useful, they offer little insight into the

molecular mechanisms behind this pathological diversity. Over the past decade, with improved sequencing and other genomics-based technologies, several groups have worked toward the molecular classification of breast cancer subtypes [7, 8]. Perou et al. first used microarray-based analysis of invasive breast tumors to define a list of ~500 "intrinsic genes", whose expression varied in the tumors from different patients [7]. Following up that study, Sorlie et al. further refined this gene expression pattern, indicating the existence of four molecular "intrinsic" subtypes of breast cancer (Luminal A, Luminal B, HER2-enriched, and Basal-like), establishing a molecular foundation for the distinct tumor subtypes. These four core "intrinsic" subtypes, in addition to the more recently identified Claudin-low and Normal breast-like groups, have repeatedly been observed across different studies [9], including recent data from the full genome and exome sequencing of primary breast tumors [10]. These studies have also translated to the clinic, as multiple prognostic gene signature tests are currently in use to predict the likelihood of relapse, including the 70-gene prognostic gene signature (MammaPrint), the Oncotype DX, and the Genomic Grade Index [11-15]. Remarkably, the different gene expression profiles correlate well with patient survival, with luminal A tumors having the most favorable prognosis, followed by luminal B tumors, while patients with HER2-positive and basal-like subtypes have the shortest survival time (**Table 1.1**). The ability to identify a patient's tumor subtype greatly increases the chance of successful treatment using targeted therapies for those breast cancers. Unfortunately, the use of gene-expression profiling is not as widespread in clinical settings as it should be; however, in an effort to correlate clinical parameters with gene-expression driven subtypes, five immunohistochemical (IHC) makers have been used as surrogates to define the different subtypes: estrogen receptor alpha (ESR1 or ER), progesterone receptor (PR), human epidermal growth factor receptor-2 (HER2 or ERBB2), cytokeratin 5/6 (CK5/6) and epidermal growth factor receptor

Table 1.1: Prevalence of breast cancer subtypes and current targeted therapies (% statistics from Susan G. Komen)

Subtype	ER/HER2 Status	Prevalence	Notes	Targeted Therapies
Luminal A	**ER+** and **HER2-**	42-59%	Most common and best prognosis	Tamoxifen (SERMs), SERDs, AIs
Luminal B	**ER+** and **HER2+**	6-19%	Slightly worse prognosis	Tamoxifen (SERMs), SERDs, AIs, and anti-HER2 mAb inhibition (e.g. Herceptin)
HER2-enriched	**ER-** and **HER2+**	14-20%	Often poor prognosis	Anti-HER2 (Herceptin, Lapatinib)
Basal-like/Triple-negative	**ER-** and **HER2-**	7-12%	Often aggressive, worst prognosis	EGFR inhibitors (Cetuximab), PARP or MEK inhibitors

(EGFR) [16]. These IHC marker defined phenotypes have been shown to be associated with clinical characteristics similar to those seen in gene expression defined subtypes. In addition, these IHC markers are able to identify distinct biological characteristics associated with the differences between short and long-term outcomes [17-19]. Recently, the PAM50 breast cancer subtype test has shown concordance with these standard clinical molecular markers, more specifically, with ER and HER2. In the absence of gene expression profiling, these two clinical markers have shown high agreement between protein biomarker scoring via IHC and gene expression [20]. This current attempt to compare and incorporate new genomic assays with old and new molecular markers, especially with regard to patient treatment and/or selection for clinical trials, remains highly challenging; however, consensus recommendations have recently been made regarding the incorporation of these parameters in the management of breast cancer therapy [21].

1.1.2 Luminal-like breast cancer subtype

The luminal-like breast cancer subtype(s) have an expression pattern reminiscent of normal epithelial cells of the mammary gland and account for nearly 70% of all breast cancers [22]. In particular, these cancers are estrogen receptor (ER) and progesterone receptor (PR)-positive, and often have higher expression of genes associated with ER signaling. The luminal-like subtype (**Table 1.1**) can be further divided into luminal A, which is usually low-grade and has the best prognosis, and luminal B, which is commonly of higher histological grade, more proliferative, and has a significantly worse prognosis [8]. Furthermore, in addition to being ER- and PR- positive, the luminal B tumors have been shown in several studies to be HER2-positive [17-19, 23, 24]. The most common target of therapy for luminal breast cancers is the estrogen receptor, which belongs to the steroid hormone receptor family (reviewed in Xu et al. [25]), which also

includes retinoic acid, vitamin D, and the thyroid hormone receptor. While there are two ER genes, ERα and ERβ, each with its own tissue distribution [26], ERα has been shown to act as an oncogene in the mammary gland, while ERβ may act as a tumor suppressor and regulator of ERα activity [27]. For the purposes of this work, I will only refer to ERα, herein called ER. ER signaling is required for the development of many tissues; however, there has been much work establishing a role for ER in the mammary gland development [28]. Interestingly, mammary glands from genetically modified mice harboring a deletion of ER (ERKO) do not undergo ductal morphogenesis or alveolar development. This disrupted signaling results in reduced estrogen-responsive gene products in the mammary gland, in addition to reduced mammotropic hormones, both of which contribute to the ERKO mammary phenotype [29-31]. ER functions as a ligand-activated transcription factor, and exists as a monomer when not ligand-bound. As a monomer, ER associates with co-repressor heat shock proteins (HSPs) such as Nuclear Receptor Co-Repressor (NCoR), Histone Deacetylase (HDAC) and Metastasis Associated Antigen-1 (MTA-1) [32]. The endogenous ligand for ER is 17β-estradiol (E2), a cholesterol derivative under the control of the hypothalamic-pituitary-gonadal endocrine axis [33]. Upon ligand binding, ER undergoes a conformation change, which allows the release of co-repressors and the recruitment of co-activators like Steroid Receptor Co-activator-1 (SRC1), Amplified in Breast Cancer (AIB1), or p300 and CBP-Associated Factor (PCAF) [32]. The activation of ER leads to receptor dimerization, enabling importation into the nucleus where it is able to bind specific DNA sequences or estrogen response elements (ERE) in the promoters of target genes leading to the increase in gene expression of ER-target genes (**Figure 1.1**). ER rarely binds to chromatin directly, and the loading of ER onto the promoter regions requires the presence of pioneer factors, such as the Forkhead Box Protein A1, (FOXA1). ER target genes subsequently regulate many cellular processes including

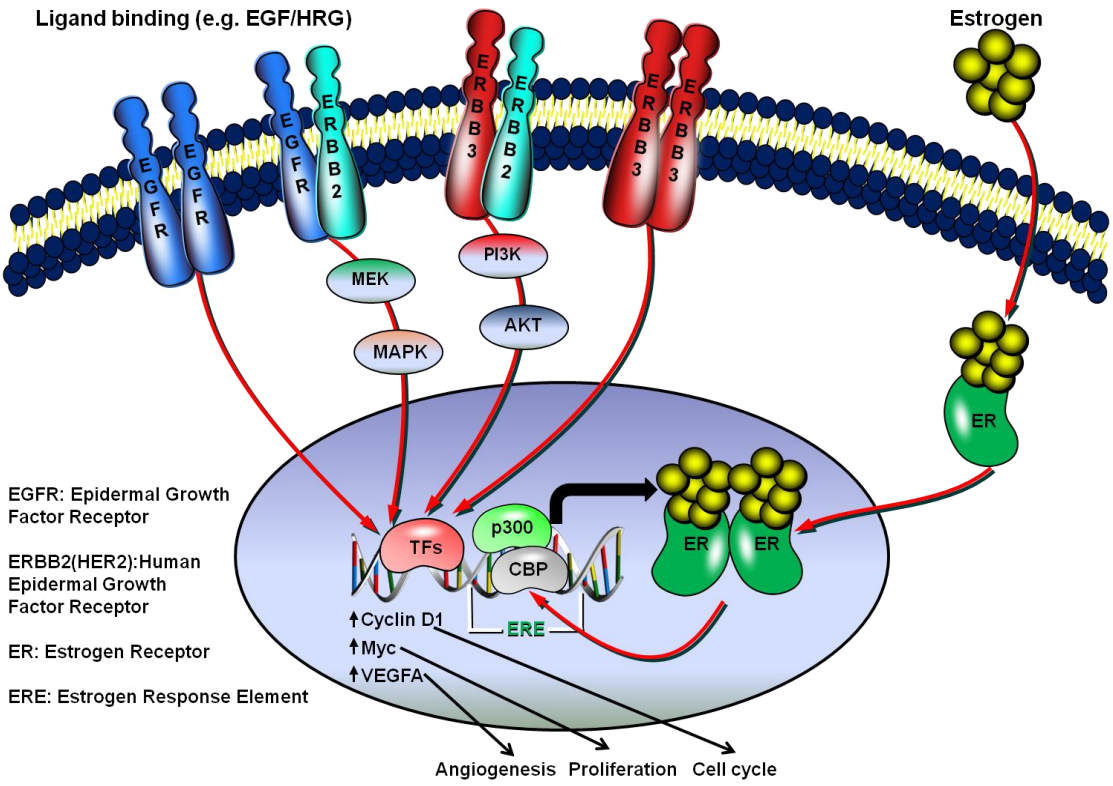

<u>Figure 1.1:</u> The ERBB2/HER2 and estrogen receptor signaling pathways in breast cancer signaling. The ERBB or HER family consists of four closely related type 1 transmembrane tyrosine kinase receptors: EGFR, also known as ERBB1, ERBB2 (also known as HER2), ERBB3, and ERBB4. The role of ERBB4 in cancer is not clear, therefore not represented here. HER2 is an orphan receptor; however, it is the preferred heterodimer partner. Ligand binding leads to the dimerization of ERBB proteins and trans- or auto-phosphorylation at tyrosine residues, which can then serve as docking sites for adaptor molecules. Two key signaling pathways are the MAPK pathway, which stimulates proliferation, and the PI3K-AKT pathway, which promotes tumor cell survival. The estrogen receptor, upon binding of estrogen, dimerizes and is transported to the nucleus, where it can bind directly to the ERE and drive transcription of target genes, or bind to transcription factors at the promoter (e.g. AP1, SP1, NFκB).

proliferation, cell cycle, invasion and metastasis (angiogenesis) [34-38]. These activated ER complexes have also been shown to act as co-activators of other transcription factors via protein-protein interactions, including Fos/Jun and AP-1 (activator protein-1) or SP-1(specificity protein-1), and Nuclear factor-κB (NFκB), thus affecting the transcription of genes that do not harbor EREs by indirect DNA binding [39-42]. This non-classical transcriptional regulation accounts for almost 1/3rd of the genes regulated by ER [32]. The estrogen receptor also possesses the capacity for rapid (seconds to minutes after E2 stimulus) signaling via extranuclear mechanisms that are independent of its transcriptional activity [43]. For example, the rapid activation of components downstream of Growth Factor Receptors or Receptor Tyrosine Kinases (RTK), such as Insulin-like Growth Factor-1 Receptor (IGF1R), EGFR, and HER2, is thought to occur by ligand-dependent activation of membrane-bound ER [44, 45]. Membrane-bound ER can regulate the expression of various components of growth factor signaling cascades via activation of MAPK and PI3K [43]. On the other hand, growth factor signaling via the same pathways (IGF1R, EGFR, and HER2) can activate ER and promote transcription of ER target genes in a ligand-independent manner [46-51]. This signaling is thought to occur via activation of downstream genes that ultimately leads to the phosphorylation and activation of ER [48]. This cross-talk between ER and growth factor signaling has implications for resistance to hormone therapy, as this signaling increases ER co-activator expression, ultimately resulting in tamoxifen-induced ER transcription activity [52].

There are currently three classes of drugs used to target estrogen signaling: (1) selective estrogen receptor modulators (SERMs), (2) selective estrogen receptor downregulators (SERDs), and (3) aromatase inhibitors (AIs). Tamoxifen and raloxifene are two of the most commonly prescribed SERMs, and tamoxifen has proven effective in treating most luminal subtype breast cancers. In addition, studies

have shown that SERMs, such as tamoxifen and raloxifene, may also be beneficial in long-term preventative treatment of patients with increased breast cancer risk factors [53]. SERMs function antagonistically by binding to ER and preventing estrogen binding, while also holding ER in an inactive conformation, thereby preventing the recruitment of co-activators and inhibiting ER-mediated transcription [54]. Moreover, tamoxifen bound ER actually mimics ER-bound to co-repressor complexes [55]. There is some thought that SERMs might have tissue-specific pharmacology, due to the cell-type specific profile of ER co-regulators [56]. The second class of ER antagonists used to treat luminal-like cancers, SERDs, acts by binding ER and preventing receptor dimerization, thereby inhibiting DNA binding. In addition, SERDs, such as fulvestrant (ICI 182,780; Faslodex), also act by inducing down-regulation of ER via receptor degradation [57]. More recently, aromatase inhibitors (AIs), such as letrozole, inhibit the enzyme aromatase, which catalyzes the conversion of testosterone to estradiol. Letrozole has been shown to be more effective in treating luminal-like cancers than Tamoxifen, and has been approved for the treatment of ER-positive breast cancers in post-menopausal women [58-60].

Tamoxifen is currently the most widely used therapy for luminal-like breast cancers, and has been recommended for ER-positive breast cancers in high-risk pre- and post-menopausal women, in addition to treatment for metastatic luminal-like cancers [61]. Interestingly, while tamoxifen is normally an antagonist to ER in the mammary gland, it has been found to be agonistic in other tissues (e.g. endometrium of the uterus), and its use is associated with a 2-fold increase in the rates of uterine cancer [61, 62]. Furthermore, many women do not respond to tamoxifen treatment due to *de novo* resistance, and many more eventually relapse due to acquired resistance. One of the most commonly documented mechanisms of resistance is overexpression of growth factor receptors, particularly EGFR and HER2 [50, 51, 63]. In addition, the

expression of co-activator proteins, such as SRC1, AIB1, and Polyomavirus Enhancer Activator-3 (PEA3), have been shown to correlate with endocrine resistance in breast cancer [64]. Particularly, the AIB1 gene has been shown to be critical in the development of tamoxifen resistance via ER/HER2 cross-talk [50, 65], and the role of AIB1 in breast cancer has been reviewed extensively elsewhere [66]. MCF7 breast cancer cells (ER+ luminal A) overexpressing HER2 (MCF-7/HER2-18 [67]) that were treated with tamoxifen showed cross-phosphorylation and activation of ER and EGFR/HER2 receptors. This was coincident with the phosphorylation and activation of the signaling molecules AKT and MAPK, as well as AIB1. Shou et al. have shown that tamoxifen treated MCF7/HER2-18 cells recruit co-activator complexes (ER, AIB1, CBP, p300) to the canonical ER-regulated gene, pS2, or Trefoil Factor-1 (*TFF1*). Conversely, tamoxifen treatment recruited co-repressor complexes to the control MCF7 cells that were not overexpressing HER2. Interestingly, Shou et al. were able to reverse the activating effects of tamoxifen by treating the cells first with Gefitinib, an EGFR inhibitor. This result has been repeated, albeit more effectively, using lapatinib, a dual EGFR/HER2 inhibitor [68]. Hurtado et al. have elucidated the mechanism behind this tamoxifen resistance, showing AIB1 outcompetes PAX2 for binding to a novel ERE in intron 4 of *HER2/ERBB2*, directly resulting in increased *HER2* expression via chromatin looping back onto the *HER2* promoter [65]. This cooperative action of different growth factor receptors, especially EGFR/HER2, and other intracellular signaling pathways (e.g. AIB1) in the luminal-like breast cancer subtype, especially endocrine resistance cells, suggests that targeting multiple pathways along with the ER might be a more effective treatment. Currently, there are multiple trials testing the efficacy of both HER2 and EGFR inhibitors along with tamoxifen, though this demonstrates the need for further research towards the discovery of novel genes involved in ER and EGFR/HER2 signaling and cross-talk.

1.1.3 HER2/ERBB2-amplified breast cancer subtype

The *HER2* gene, also known as Erythroblastic Leukemia Viral Oncogene Homolog-2 (*ERBB2*), is a member of the EGFR/HER family of tyrosine kinases. This family consists of four members, commonly referred to as EGFR (HER1, or ERBB1), HER2 (ERBB2, HER2/neu), HER3 (ERBB3), and HER4 (ERBB4). *HER4* is the only gene that has not been clearly linked to cancer pathogenesis, though recent work has implicated a role for HER4 as a tumor suppressor [69]. The EGFR/HER family proteins are type I transmembrane growth factor receptors that function to activate intracellular signaling pathways in response to extracellular signals. These membrane-spanning receptors consist of an extracellular ligand-binding domain, a transmembrane domain, and an intracellular tyrosine kinase domain (**Figure 1.1**). Unlike other members of the EGFR/HER family, HER2 is an orphan receptor, in that it lacks the capacity to bind a ligand. However, HER2 is the preferred dimerization partner, as it has the strongest catalytic kinase activity, and HER2-containing dimers have the strongest signaling functions [70, 71]. This increased kinase activity has been attributed to the fact that HER2 constitutively maintains an active conformation, normally achieved upon ligand binding in other family members [72, 73]. In addition, heterodimers containing HER2 are characterized by slow rates of ligand dissociation and slow receptor endocytosis [70, 74]. Conversely, HER3 lacks a functional kinase domain and is catalytically inactive [75]. Interestingly, although individually both HER2 and HER3 are incomplete signaling molecules, HER2/HER3 dimers form the most active signaling heterodimer of the family, and are essential for many biological and developmental processes, in addition to being implicated in many breast cancers [76]. EGFR/HER2 dimers are also important in mammary tumorigenesis, conferring both proliferative and invasive functions via prolonged activation of downstream mitogen-activated protein kinase (MAPK) signaling [77]. While EGFR/HER2 dimers signal through the MAPK pathway, the

HER2/HER3 dimers primarily signal downstream via the phosphatidylinositol 3-kinase (PI3K)-AKT pathway. HER2 lacks binding sites for the p85 subunit of PI3K; however, HER3 contains seven p85-docking sites [78]. HER2 tumors have been shown to require both alleles of *AKT1* for increased proliferation and migration [79], and mutant PIK3CA accelerates HER2-driven transgenic mammary tumors, while also inducing resistance to combination anti-HER2 therapies [80]. The PI3K-AKT pathway has been shown to regulate cell growth and proliferation, survival, and translation via the proliferation gene cyclin D1, nuclear receptor co-activators SRC1 and AIB1, and transcription factors such as NFκB, PEA3, and COX2. There are a large number of genes downstream of HER2 signaling, including, but not limited to, *JAB1* [81, 82], *PEA3* [83, 84], *FOXAI* [85], *FOXMI* [86, 87], and *GRB7* [88]. HER2 has also been found to signal often in positive feedback loops, including genes such as *ADAM12* [89], *ERα36* [90], *BEX2* [91], *MED1* [92], and the inflammatory gene, *IL6* [93]. These signaling loops enhance the oncogenic signaling of HER2 and drive tumorigenesis, and in the case of MED1, tamoxifen resistance.

HER2 protein overexpression or gene amplification (17q12 amplicon) accounts for approximately 25-30% of all breast carcinomas [94]. Tumors that are of the HER2 subtype are associated with poor prognostic factors, including highly proliferative and large tumors, higher grade, and nodal involvement [17, 18]. In addition to very aggressive clinical characteristics, these HER2-positive tumors have also been shown to have a high rate of recurrence [8]. While the majority of HER2-positive tumors are hormone receptor negative, some are ER-positive and usually cluster with the luminal B subtype. While amplification of the HER2 region is the most common cause of HER2 overexpression, there are many tumors still described by the HER2-positive subtype with no apparent gene amplification [95]. This is most likely due to the large number of downstream targets of HER2 that can be upregulated upon increased HER2

protein expression, even in the absence of amplification; thus, driving signaling that is the signature of HER2-amplified breast cancers. Current therapeutic options for HER2-positive breast cancers include standard cytotoxic chemotherapy, combined with trastuzumab (Herceptin), a monoclonal antibody that binds to the extracellular domain of HER2. Trastuzumab has led to the improvement of patient outcome, including overall survival, especially in the adjuvant treatment of metastatic breast cancer [96]. However, despite these great achievements, greater than 60% of HER2-positive tumors do not respond to trastuzumab monotherapy, with initial responders developing resistance within 1 year [94, 97]. The currently defined methods of trastuzumab resistance include: (1) the inability of trastuzumab to bind the constitutively active truncated form of HER2 receptor that is found in up to 60% of HER2-positive tumors, as well as the masking of the HER2 epitope by Mucin-4 (MUC4) [98] or CD44/hyaluronan complexes [99]; (2) alternative signaling through the insulin-like growth factor-1 receptor (IGFR1) [100]; (3) upregulation of downstream signaling pathways, like SRC [101, 102] and/or AKT [103]; (4) increase in the number of EGFR/HER3 heterodimers [104], and other receptors including c-Met and β-integrins [105]; and (5) failure to trigger immune-mediate responses [106]. Despite these problems, since the introduction of HER2-targeted therapy via trastuzumab, the prognostic stratification of breast cancer subtypes has shifted towards luminal B tumors having a decreased risk of recurrence when compared with luminal A tumors [107]. This study has also shown that the luminal B tumors, which are ER+/HER2+, have a better response to trastuzumab than HER2-positive subtype (HER2+/ER-) tumors. This is most likely due to the different pathways involved in the signaling, as luminal B tumors are more likely to signal through the PI3K/AKT pathway, while HER2+/ER- tumors through EGFR/RAS/MAPK pathway, though more research is needed in this area to elucidate these differences. As previously mentioned, HER2 overexpression plays a key role in

the development of tamoxifen resistance, so those patients receiving treatment for both HER2 and ER might be predicted to have a greater response to therapy. For those HER2+/ER- tumors, lapatinib has been used with success more recently. O'Brien et al. have shown that while PI3K/AKT signaling in HER2+/ER- cell lines can confer resistance to trastuzumab, the cell lines were highly sensitive to lapatinib treatment [108]. Overall, trastuzumab has been shown to reduce the risk of recurrence in patients by 52%, and the risk of death by 33%, when compared to chemotherapy alone[109]. While trastuzumab is still the most widely used therapy for treating HER-positive breast cancers, there remains an incomplete understanding of the mechanisms behind the resistance to this drug. This has highlighted the pressing need to discover and validate novel targets of HER2-positive breast tumors, so that additional treatments may be used in combination with, or in the place of, trastuzumab as adjuvant therapy to cancers of the HER2-subtype.

1.1.4 Basal-like breast cancer subtype

Basal-like tumors, which account for 15-25% of all breast cancers, are a group of ER-negative tumors named after their morphological and genetic relationship to normal basal/myoepithelial cells of the mammary gland. Tumors with the basal-like phenotype were initially described using IHC for cytokeratins (CK), as these tumors showed increased expression of CK5, 14, and 17, normally found in the basal cells of the mammary gland [110]. While the majority of basal-like tumors are triple negative, in that they lack expression of ER, PR, and HER2, the two are not synonymous. In addition to being hormone receptor-negative, basal-like tumors are further described by the positive expression of EGFR and CK5/6 [17]. Despite a well-defined subtype that has been validated through microarray experiments [7, 8], and more recently through sequencing [10], the basal-like tumors tend to be rather heterogeneous. In addition, these

breast cancers have distinctive clinical presentations, varied histological features, and different responses and outcomes to chemotherapy [8, 17, 111, 112]. Basal-like breast cancers are more likely to affect younger women (<50 years of age), and are more prevalent in African-American women [113, 114]. Tumors of this subtype are usually high grade, more likely to metastasize, and have a higher risk of recurrence and death within five years of diagnosis [115]. This aggressive clinical manifestation is evidenced by the pattern of metastases, as the primary tumor often spreads to the brain and lungs, making treatment much more difficult and worsening the prognosis [116]. Unfortunately, due to the lack of druggable targets (e.g. ER and HER2), patients with basal-like tumors are often just treated with surgery and standard chemotherapy regimens. This absence of targeted therapies has increased the need for the identification of genes involved in the propagation of tumors of this subtype. Many different molecular pathways are implicated in aggressive basal-like cancers, with the hallmark of these tumors being an increase in genetic instability. These cancers frequently have DNA gains and losses, suggesting defective DNA repair pathways [117]. There are currently a number of subtype specific markers being investigated, including EGFR, caveolin-1 and -2, p-cadherin, osteonectin, and αβ-crystallin[118-122]. More recently, the sequencing of basal-like tumors has revealed a similarity of these cancers with high-grade serous ovarian tumors, including mutations in the tumor protein-53 (*TP53* or *p53*), retinoblastoma protein-1 (*RB1* or *pRb*), and both *BRCA1* and *BRCA2* (breast cancer 1 and 2, early onset) [10]. The loss of *BRCA1* is highly associated with the risk of developing basal-like breast cancers, though these mutations are relatively rare in the general population (less than 1%). However, a woman carrying a *BRCA1* inactivating mutation is estimated to have a ~65% increased risk of developing breast cancer by age 70, and ~30-40% risk for developing ovarian cancer [123]. The *BRCA1* gene acts as a tumor suppressor, and the loss of *BRCA1* leads to increased chromosome instability;

ultimately, leading to the accumulation of additional deleterious mutations, often including *p53* and *pRb*. These three genes are involved in the cell cycle and DNA damage response pathways; therefore, mutations in all three is mostly likely responsible for the high proliferation rates of basal-like tumors. For this reason, patients with this subset of basal-like tumors are often a good candidate for the newly developed poly(adenosine diphosphate [ADP]-ribose) polymerase (PARP) inhibitors. PARP is a mediator of single strand DNA (ssDNA) break repair, and the inhibition of PARP results in the accumulation of ssDNA, which upon replication, is converted to double-strand breaks that are normally repaired by BRCA1. These double-strand breaks accumulate in the rapidly dividing cells and ultimately lead to cell death. While the outlook of PARP inhibitors sound promising, the two most advanced compounds in clinical trials, iniparib and olaparib, unfortunately did not make it past phase III and phase II respectively [124]. Other drugs that are currently in pre-clinical and clinical testing for basal-like tumors include sunitinib malate, a multiple receptor tyrosine kinase (RTK) inhibitor (including targeting of PDGF and VEGF)[125], and dasatinib, a c-Src inhibitor [126, 127]. The relative paucity of agents currently being tested for basal-like breast cancers only highlights the need for continued research towards the identification of novel therapeutic targets for these highly aggressive tumors.

1.1.5 MCF10AT model of basal breast cancer progression

The study of human breast cancer etiology is hampered by the lack of reproducible models that mimic the morphological events believed to be indicative of proliferative disease. The MCF10AT xenograft model of human breast cancer was developed in an attempt to meet this need (**Figure 1.2**) [128-132]. The human cell line MCF10A originated from the spontaneous immortalization of non-malignant breast epithelium. Transfection with mutated T24 H-Ras allowed MCF10A to acquire the ability for

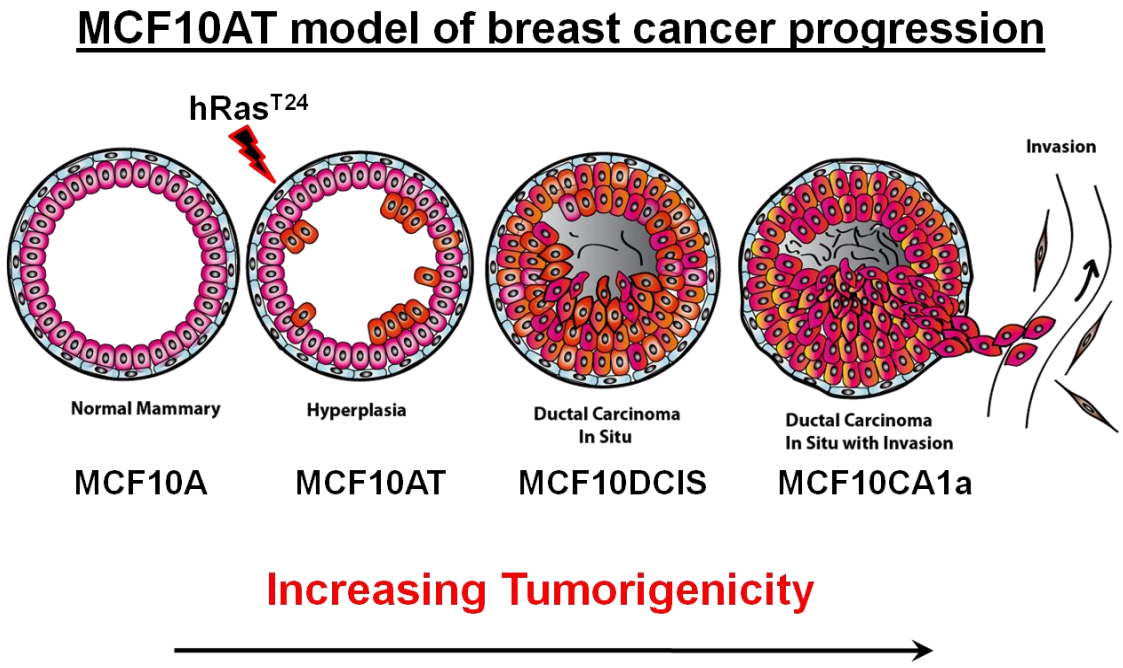

Figure 1.2: The MCF10AT model of basal breast cancer progression. Normal immortalized MCF10A cells were transformed with mutated T24 H-Ras (hRas), thereby acquiring the ability for xenograft growth in nude (nu/nu) mice. Pre-malignant lesions from xenografted MCF10AT cells were serially passaged in nude mice, leading to the isolation of further lesions that demonstrate a complex mix of morphological types and grades that recapitulate the morphological characteristics of the progression of human proliferative breast disease, including comedo-DCIS (MCF10DCIS) and invasive cancer (MCF10CA1a).

xenograft growth in immunodeficient (nude) mice. Serial passage of the H-Ras oncogene in transfected cells (MCF10AT) produces lesions in nude mice that demonstrate a complex of morphological types and grades that recapitulate the morphological characteristics of human proliferative breast disease, as well as, in a minority of mice, ductal carcinoma in situ or DCIS (MCF10DCIS.com), and invasive cancer (MCF10CA1a). Cell lines from this model encompass the entire range of human breast cancer progression, from benign normal tissue, to malignant/metastatic tumors. The majority of breast cancer originates as ductal hyperplasia, which eventually progresses to DCIS. The MCF10DCIS.com cell line, herein referred to as MCF10DCIS, has captured this stage of breast cancer progression, which is currently being diagnosed with high frequency. Furthermore, it represents the high-grade comedo-type DCIS, which is associated with a relatively high risk for subsequent development of invasive cancer [133]. Comedo DCIS lesions are populated by larger and more pleomorphic neoplastic cells, with clinical histology featuring the presence of intraluminal necrosis. Comedo DCIS lesions often demonstrate microinvasion [134], higher proliferation [135], and are more frequently HER2-positive compared to non-comedo lesions [136]. Therefore, the MCF10DCIS cell line might be the most appropriate target for chemoprevention regimens. The MCF10AT model, by the criteria of hormone receptor negativity and lack of amplification of the *HER2* locus, as well as by clustering of the parental MCF10A cell line with the basal-like subtype by transcriptional profiling, most closely models the development of basal-like human breast cancers with very poor prognosis [137]. This isogenic model of breast cancer is unique, in that it offers the opportunity to discover novel genes responsible for the progression of breast cancer. Furthermore, it allows for the investigation of these genes at specific stages during cancer development, in addition to testing and validating inhibitors to those genes, both *in vitro* and *in vivo*.

1.2 Peptidylarginine deiminase (PADI) enzyme family

1.2.1 Background of the PADI family of enzymes

The peptidylarginine deiminases (PADIs) are a family of calcium dependent post-translational modification enzymes that convert positively charged arginine residues to neutral citrulline residues on target proteins [138] . This activity is termed citrullination (**Figure 1.3a**) or deimination, and has been shown to have wide-ranging effects on target protein structure, function, and protein-protein interactions (**Figure 1.3b**) [139-142]. Furthermore, in addition to converting histone arginine residues to citrulline, PADI enzymes can also convert histone methylarginine to citrulline via "demethylimination" [143], leading to chromatin decondensation (**Figure 1.4**), which when occurring at gene promoters, can lead to an increase in gene expression [144-146]. The PADI family consists of five well-conserved members (~55% amino acid identity in humans), each differing in its pattern of substrate specificity and tissue distribution. Although there is some overlap, each PADI isozyme appears to target a unique set of cellular proteins. In particular, both PADI2 and PADI4 show expression in the mammary gland [147] and are regulated by estrogen *in vivo* [148]. The PADIs are all arranged within a highly organized gene cluster on human chromosome 1p36.13 and on the orthologous region of mouse chromosome 4E1. Interestingly, the 1p36 region is often mutated and deleted in multiple cancers and likely contains novel tumor suppressor genes [139-142], suggesting that PADI genes and citrullination may play a role in tumorigenesis. Recently, the citrullination of proteins has been linked to a variety of human diseases [149] (**Table 1.2**), including rheumatoid arthritis (RA) [142, 150], Alzheimer's disease (AD) [140, 151, 152], multiple sclerosis (MS) [141, 153-156], ulcerative colitis [157], psoriasis [158], chronic obstructive pulmonary disease (COPD) [159], lupus [160], glaucoma [161, 162], age-related macular degeneration (AMD) [163], and cancer (reviewed in Mohanan et al. [164]).

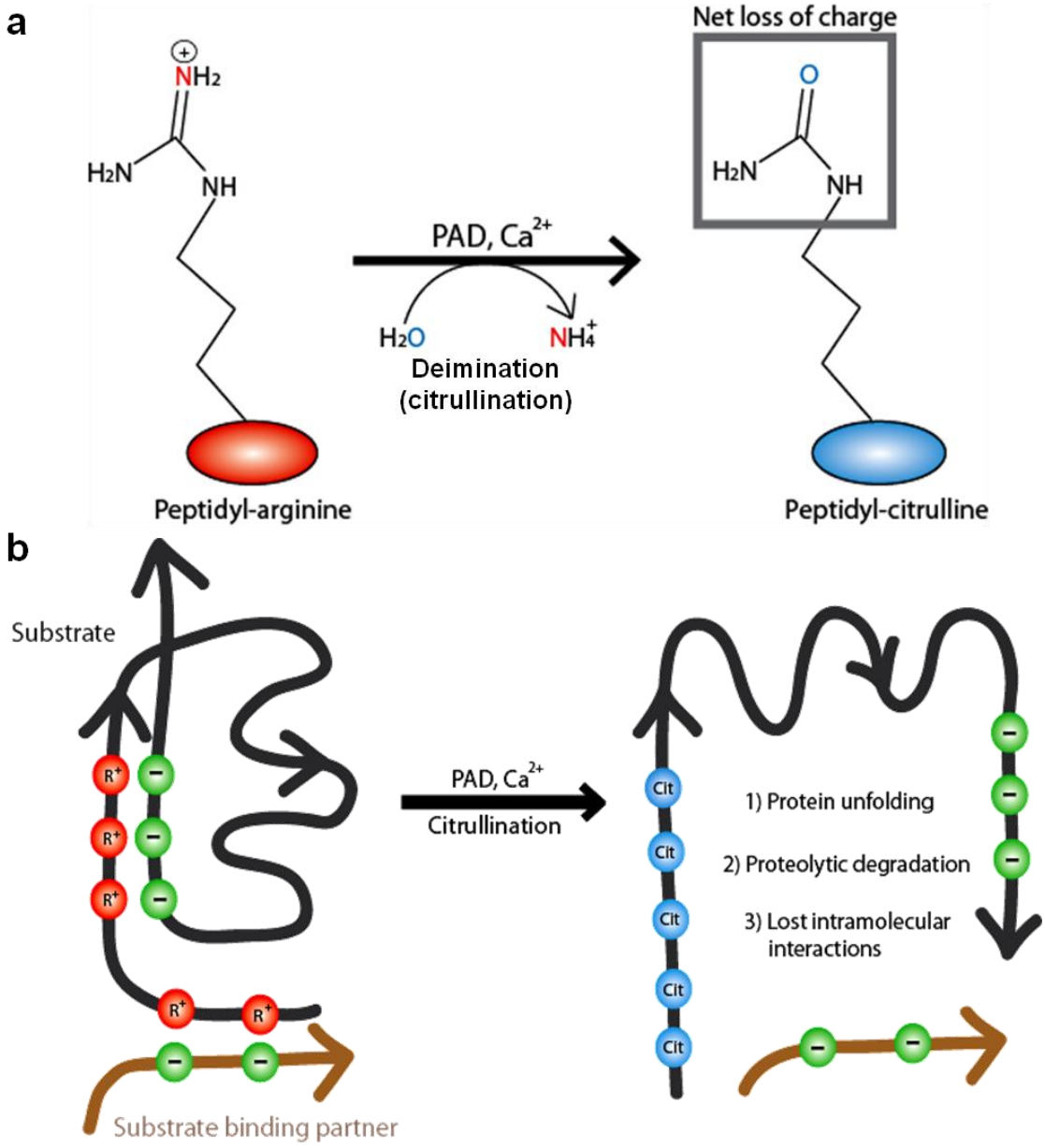

<u>Figure 1.3:</u> The enzymatic activity of peptidylarginine deiminase (PADI) isozymes. (a) The different PADI isozymes catalyze the conversion of positively charged protein arginine residues to neutral citrulline in a process called deimination, or citrullination. (b) The change in charge of proteins can lead to conformational changes or loss of protein-protein interactions. (Figure obtained from Horibata et al., *Jour. Repro. & Dev.*, 2012 [148])

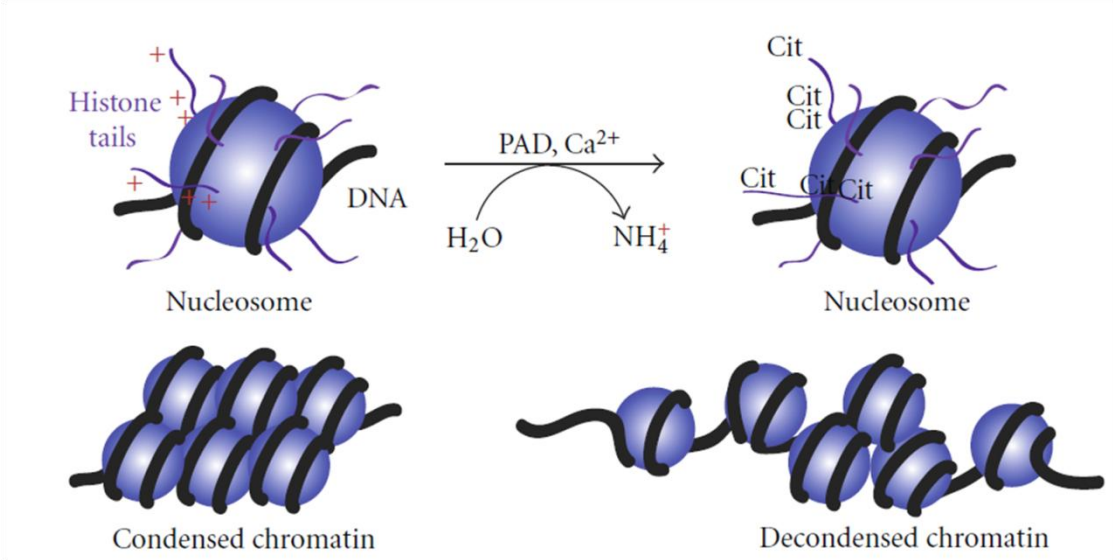

Figure 1.4: PADI-mediated histone tail citrullination leads to chromatin decondensation. PADI recruitment to target promoters by the relevant transcription factor is followed by deimination of N-terminal histone tails at specific residues, leading to a more open or "relaxed" chromatin architecture. This can have pronounced effects on gene expression of the target gene. (Figure obtained from Mohanan et al., *Bio. Res. Int.*, 2012 [164])

Table 1.2: PADI isozymes and various tissue specific roles and associated diseases

PADI Isozyme	Tissue Distribution	Subcellular Localization	Target Substrate	Physiological Role	Regulation of Expression	Associated Diseases
PADI1	Epidermis, Uterus	Cytoplasm	Keratin, Filaggrin	Skin differentiation, Terminal differentiation of keratinocytes	Retinoic acid, Estrogen	Skin disorders, Psoriasis, Oral SCC
PADI2	Sk. Muscle, Brain, Hematopoietic cells, Uterus, Mammary epithelium	Cytoplasm, Nucleus	MBP, Vimentin, Histones, IKKγ, CXCL8, ERα, HER2(ERBB2)	Potential role in brain development, Potential role in proliferation of reproductive tissues NET formation	Estrogen, EGF, HER2	RA, MS, AMD, Alzheimer's Disease, COPD, Cancer
PADI3	Hair follicles	Cytoplasm	Trichohyalin	Skin differentiation, Hair follicle formation, Terminal differentiation of keratinocytes	Retinoic acid	Skin disorders, Pancreatic Cancer
PADI4	Hematopoietic cells, Uterus, Mammary epithelium	Cytoplasm, Nucleus	Histones, ELK1, p53, GSK3β, Nucleophosmin	Cellular differentiation, Transcriptional co-repressor of p53, co-activator of ELK1, NET formation	Retinoic acid, Estrogen	RA, MS, Ulcerative Colitis, Cancer
PADI6	Oocyte, Ovary, Testis	Cytoplasm, Nucleus	α-Tubulin (cytoplasmic lattices)	Embryonic development, Cytoplasmic lattice formation, Fertility	Unknown	Unknown

1.2.2 Peptidylarginine deiminase-1 (PADI1)

PADI1 and PADI3 have been primarily characterized in the epidermis (basal to granular layer); with PADI3 being found to deiminate trichohyalin in hair follicles [165, 166] and PADI1 deiminating keratin (K1 and K10) and filaggrin during epidermal differentiation [167, 168]. It is thought that the deimination of keratin and filaggrin in the epidermis induces changes in the spatial organization of keratin intermediate filaments during keratinocyte maturation [158]. This modification is important for maintaining the barrier function of superficial keratinized epidermal cell layers [169-172]. The overexpression of PADI1 (potentially along with PADI2 and PADI3), which leads to abnormal levels of citrullinated keratin K1, has been reported in areas of the epidermis of psoriatic patients [173]. In addition, the loss of *PADI1* has been implicated in the development of Oral squamous cell carcinoma (OSCC), which is associated with substantial mortality and morbidity, with *PADI1* being identified as a biomarker for the early detection of invasive OSCC. Gene expression analysis found expression of *PADI1* to be downregulated in both dysplasia and OSCC, when compared with controls [174]. The deimination of protein arginine residues in the keratinocytes of oral mucosa by PADI1 forms an epidermal barrier; therefore, the down-regulation of PADI1 may allow the growth, expansion, and movement of tumor cells.

1.2.3 Peptidylarginine deiminase-2 (PADI2)

PADI2, the ancestral isozyme of the PADI family, is widely distributed and is highly expressed in both muscle [175, 176] and brain [152, 172], and is often associated with the deimination of myelin basic protein (MBP) and vimentin [177, 178]. The citrullination of MBP by PADI2 plays a key role in the pathogenesis of neurodegenerative disease, including MS [153, 177], while the citrullination of vimentin has been implicated in the development of AD[151, 152]. In addition, PADI2-mediated citrullination of the

intermediate filament vimentin in macrophages results in cytoskeletal disintegration and eventually apoptosis [179]. PADI2 is implicated in various inflammatory diseases, such as RA and COPD[159], and recent work has shown that PADI2 was linked to cytokine signaling during the immune-inflammatory response. For example, PADI2 can citrullinate IKKγ in macrophages, leading to the suppression of NFκB activity [180]. Additionally, PADI2 mediated citrullination of CXCL8 is also associated with modulation of the inflammatory response [181]. In macrophages, both *in vitro* and *in vivo*, PADI2 has been shown to catalyze histone H4 arginine 3 (H4R3) hypercitrullination, and the formation of extracellular traps (ETs). Specifically, these macrophage ETs (METs) were also seen in "crown-like structures" (CLSs), which are infiltrating macrophages found in the adipose tissue of mammary glands from obese patients. CLSs are associated with increased levels of inflammatory mediators, and Mohanan et al. have shown that increased PADI2 driven METs in CLSs plays a key role in promoting inflammatory signaling [182]. PADI2 is also abundantly expressed in the epithelium of the mammary gland, uterine endometrium, and in the pituitary gland [183, 184]. Previous investigators have found that PADI2 expression and citrullination in reproductive tissues is strongly linked to the estrous cycle, with both expression and enzymatic activity reaching their peak during the secretory phase of the cycle [148, 183-185]. While PADI2 has historically been defined as a cytoplasmic protein, recent evidence from our lab shows that PADI2 can localize to the nucleus, as well as directly bind chromatin to influence target gene expression [146, 186, 187]. In the canine mammary gland, estrous cycle regulated PADI2 expression in epithelial tissue correlates with citrulline levels, potentially indicating a role in gene expression. Recent evidence from our lab supports this prediction, as Zhang et al. have shown that PADI2 catalyzed citrullination of histone H3 arginine 26 (H3R26) facilitates ER target gene activation [146].

1.2.4 Peptidylarginine deiminase-3 (PADI3)

PADI3 has been implicated in pancreatic cancer, with gene expression analysis of the highly metastatic human pancreatic cancer cell line (L3.6pl) showing *PADI3* to be the most significant gene upregulated [188]. Furthermore, analysis of *PADI3* led to the identification of a PAD Intergenic Enhancer (PIE), an evolutionary conserved non-coding segment located 86-kb from the *PADI3* promoter. The PIE is a strong enhancer of the *PADI3* promoter in Ca2+ differentiated epidermal keratinocytes, and requires bound Activator Protein-1 (AP-1) factors, namely c-Jun and c-Fos [189]. The AP-1 complex has a central role in multiple processes involved in tumorigenesis, including proliferation, migration, invasion and metastasis. The long-range control of *PADI3* expression via AP-1 implicates a potential role of deimination during tumorigenesis. As previously mentioned, PADI3 (potentially along with PADI1 and PADI2) driven citrullination has been reported to be found in the epidermis of psoriatic patients [173].

1.2.5 Peptidylarginine deiminase-4 (PADI4)

PADI4 was originally found to be expressed during retinoic acid-induced HL-60 granulocyte differentiation and was originally thought to be the only PADI that localizes to the cell nucleus, likely via its distinct nuclear localization signal [190]. Hagiwara et al., (2002) found that activation of HL-60 granulocytes induced extensive protein citrullination that was mainly limited to the histones H2A, H3, H4, and nucleophosmin. Regarding the role of PADI4 in gene regulation, a number of reports have validated our original finding that PADI4 regulates gene activity and can act as a transcriptional co-repressor. For example, Cuthbert et al., [191] found that PADI4 targets the endogenous VEGF-A promoter and represses hormone-mediated gene induction, while Balint et al., demonstrated that PADI4 attenuated retinoid-regulated gene expression [192]. We have shown that in ER-positive MCF7 breast cancer cells, estrogen

stimulation enhances PADI4 binding and histone H4 citrullination at the canonical ER target gene *TFF1*, leading to transcriptional repression [193]. More recently, Yanming Wang, a former postdoctoral fellow in the Coonrod lab, has published a series of studies elucidating the role of PADI4 in the regulation of p53 target gene expression [145, 194-197]. More specifically, PADI4 serves as a p53 co-repressor to regulate histone arginine methylation at the p53-target gene *p21*/*WAF1*/*CIP1* promoter [195]. Furthermore, they show that histone arginine citrullination can coordinate with other histone modifications, HDAC2 in their case, to repress transcription [194]. This work utilized the specific PADI inhibitor, Cl-amidine, to dissect the mechanisms of PADI4 regulated gene expression. In addition, the combination of Cl-amidine with an HDAC inhibitor, suberoylanilide hydroxamic acid (SAHA), showed additive effects in inducing p21, GADD45, and PUMA expression, while inhibiting cancer cell growth in a p53-dependent manner. This important crosstalk between histone deacetylation and citrullination suggests that a combination of PADI4 and HDAC2 inhibitors serve as potential strategy for cancer treatment. Interestingly, a recent study found that citrullinated H4R3 (H4Cit3) levels are inversely correlated with p53 protein expression and with tumor size in non-small-cell lung carcinoma (NSCLC) tissues[197], potentially indicating a tumor suppressor function for PADI4. Reinforcing the role for PADI4 as a tumor suppressor, recent results from our lab showed that the dysregulation of PADI4-mediated citrullination of nuclear GSK3β activates TGF-β signaling, thereby inducing epithelial-to-mesenchymal (EMT) transition in breast cancer cells. Conversely, our lab has recently shown using a genome-wide analysis of chromatin-bound PADI4 that PADI4 can function as a co-activator for a range of oncogenic transcription factors [198]. Zhang et al. reported that the treatment of MCF7 cells with EGF leads to PADI4-mediated citrullination of the ELK1 oncogene at the c-Fos promoter. This PADI4-mediated citrullination facilitates the phosphorylation of

ELK1 by ERK1/2, which in turn, promotes the acetylation of histone H4 lysine 5 (H4K5), leading to increased transcription of the immediate early *c-Fos* oncogene. In addition, recent evidence has shown that PADI4 is overexpressed in numerous malignant, but not benign tumor types [139, 199, 200]. We have also shown that PADI4 promotes hypercitrullination of histones (including H4R3, and H3R2, 8, 17, and 26) and global decondensation, which when occurring in neutrophils, leads to neutrophil ETs (NETs). Primarily, TNFα treated blood neutrophils resulted in the release of extracellular chromatin that was extensively citrullinated at H4R3. This extracellular chromatin has been shown to entrap and kill invading pathogens [201-203]. Lastly, in addition to PADI4 functioning as a tumor suppressor and potential oncogene, the first PADI inhibitor, Cl-amidine (discussed in more detail later), was developed to treat disorders resulting from aberrant PADI4 expression. Interestingly, the treatment of several PADI4-expressing cancer cell lines with Cl-amidine elicited strong cytotoxic effects, while have no observable effect on non-cancerous lines, suggesting that PADIs may represent targets for new cancer therapies [204].

1.2.6 Peptidylarginine deiminase-6 (PADI6)

PADI6 is a maternal effect gene that is primarily expressed in oocytes and preimplantation embryos. We have shown using genetically modified mice (*PADI6*$^{-/-}$) that PADI6 is essential for embryonic development beyond the 2-cell stage [205]. Additionally, PADI6 localizes to poorly characterized cytoskeletal structures, termed cytoplasmic lattices, within oocytes and early embryos, and is required for lattice formation. Recent work from our lab has established that cytoplasmic lattices play a critical role in regulating microtubule-based activities during oocytes maturation and early development, as *PADI6*$^{-/-}$ mice had defects in microtubule mediated organelle repositioning [206, 207]. Interestingly, while this is the only isoform not specifically

implicated in having a potential role in cancer, a recent genome-wide association study (GWAS) in Icelanders shows a significant correlation between cutaneous basal cell carcinoma risk and mutations within the *PADI4/PADI6* locus on chromosome 1p36 [208]. The role for PADI6 in reproductive and developmental biology has been extensively reviewed elsewhere [148, 209, 210] and will not be discussed further.

1.2.7 PADI2 and potential links to cancer

Given that there are several studies showing a link between PADI4 and cancer, and the high degree of similarity in both tissue expression and enzymatic activity (i.e. citrullination of mammary epithelium), we hypothesized that PADI2 might also play a role in cancer, specifically breast cancer. Interestingly, the first paper to report the cloning of full-length human *PADI2* cDNA was by Ishigami et al., who found PADI2 to be highly expressed *in vitro* in a skin cancer cell line, HSC-1, which is derived from a human cutaneous squamous carcinoma [211]. Using a zebrafish model of Ewing's sarcoma (EWS-FLI1 fusion oncoprotein), Leacock et al. reported that *PADI2* is one of six overlapping genes conserved between human and zebrafish EWS-FLI driven small-round-blue-cell tumor (SRBCT) tumors [212]. Studies using mouse models of breast cancer have also shown a potential correlation between increased PADI2 levels and mammary tumors. Herschkowitz et al. identified *PADI2* as one of 106 genes most commonly identified to be overexpressed between human and mouse mammary carcinomas [213]. In addition, the MMTV-neu mouse model of HER2-positive breast cancer was shown to have elevated levels of *PADI2* in both hyperplastic (~2-fold) and primary tumors (~4-fold) of the mammary gland, when compared to matched-normal mammary epithelium [214]. In humans, *PADI2* is one of the most upregulated genes in luminal subtype breast cancer cell lines compared to basal cell lines [215, 216]. Additionally, gene expression profiling of 213 primary breast tumors with known

HER2/ERBB2 status identified *PADI2* as one of 29 overexpressed genes in HER2-positive tumors; thus, helping to define a *HER2/ERBB2+* gene expression signature [217]. Analyzing recent data from The Tumor Genome Atlas (TCGA) using the UCSC Cancer Genomics Browser, we see a correlation between *PADI2* expression and tumors of the HER2-subtype; however, we also see that *PADI2* is correlated with basal subtype tumors [218]. Moreover, using the Memorial Sloan Kettering Cancer Center (MSKCC) cBio Cancer Genomics Portal, both basal and HER2 subtype tumors show decreased survival when *PADI2* levels are increased [219, 220]. These results are interesting, especially with regard to our recent data indicating a relationship between *PADI2* and *HER2* across the luminal subtype [215, 216, 221]. However, these disparate results could potentially be attributed to differences in the tested samples, as well as experimental procedures, but there is no questioning that *PADI2* expression correlates with mammary tumorigenesis. Recent genomics/proteomics based studies have shown PADI2 to be the fifth most correlated gene with breast cancer progression [222], a known interacting protein with the c-Myc oncogene [223], in addition to being one of the genes known to differentiate ER–positive and –negative tumors [224].

These predictions and correlations between PADI2 and cancer have been supported by additional recent data from our laboratory. Comparative studies suggest that PADI2 nuclear expression in mammary carcinomas from human, canine, and feline, might be associated with tumor progression [225]. Surprisingly, using canine mammary tumor cells (CMT25), Cherrington et al. have shown that EGF stimulation increases the transcription of *PADI2*, and subsequently the citrullination of histone H3 arginine 2, 8, and 17. Furthermore, biochemical evidence *in vitro* shows definitively that PADI2 localizes to the nucleus of mammary epithelial cells, and that it associates with chromatin. Using truncation mutants, the motif responsible for nuclear localization was found to occur somewhere within the first 437 amino acids (aa) of the

PADI2 protein. Interestingly, the truncation of PADI2 from 665aa to 437aa, and then to 278aa, resulted in increasing proportions of PADI2 being targeted to the cell nucleus. Given that PADI2 does not contain a canonical nuclear localization signal (NLS), it is currently unclear how PADI2 gains entry to the nucleus. We hypothesize that PADI2 must contain a distinct nuclear directing motif or translocate to the nucleus via a protein-protein interaction with an additional NLS-containing protein. Both of these methods have been previously reported to occur in other proteins, such as ERKs, MEKs, and SMADs, which translocate to the nucleus via an NLS-independent mechanism [226, 227]. In addition, protein-protein interactions, such as the one between tissue transglutaminase (tTG) and vascular endothelial growth factor receptor-2 (VEGFR-2), facilitate nuclear importation upon stimulation [228]. Having provided evidence that PADI2 can localize to the nucleus, associate with chromatin, and regulate gene expression, we wanted to expand our understanding of PADI2 target gene modulation in breast cancer. As previously mentioned, PADI2 is known to correlate with estrogen stimulation *in vitro* and *in vivo*, so we wanted to examine globally the role of PADI2 in breast cancer cells upon estrogen stimulation. Using estrogen receptor-positive MCF7 breast cancer cells, Zhang et al. have shown that PADI2 interacts with ER following estrogen treatment, thereby catalyzing the site-specific citrullination of H3R26 (H3Cit26) at the promoters of nearly 200 ER target genes [146]. The H3Cit26 modification promotes the formation of a more relaxed/decondensed chromatin architecture around the target promoters; thus, facilitating ER target gene activation. This work was followed by an examination of the role for PADI2 during breast cancer progression, using the previously mentioned MCF10AT model (see **Chapter 2**). PADI2 levels were highest in the transformed, HER2-positive, cell lines of the MCF10AT model, especially in the comedo-DCIS cells (MCF10DCIS). HER2-positive tumors account for about 25–30% of invasive

ductal carcinomas of the breast and have a significantly poorer outcome, increased risk of recurrent disease, and shorter overall survival [94]. In ductal carcinoma *in situ* (DCIS) tumors, the incidence of HER2 overexpression/amplification is ≥ 60% [136, 229, 230], whereas benign and atypical breast lesions generally do not show any evidence of HER2 overexpression [231]. Given the high incidence of HER2 alterations in high-grade DCIS associated with comedo necrosis, HER2 overexpression, and potentially PADI2 overexpression, may confer a growth advantage to DCIS under ischemic conditions. We also examined the transcriptomic relationship between *PADI2* and *HER2* across a large number of breast cancer cell lines using RNA-seq, and reported that *PADI2* and *HER2* were highly correlated across the luminal subtype. Furthermore, we showed that *PADI2* was one of the top genes correlating with *HER2* expression in breast cancer cells [221]. This work suggests a functional relationship between these genes, which we now believe to occur via the same epigenetic mechanism as that seen in ER target genes. We ended this study by reporting the first successful use of our first-generation PADI inhibitor, Cl-amidine, to treat cancer cells both *in vitro* and *in vivo*. Specifically, Cl-amidine was able to significantly reduce the proliferation of breast cancer cells in 2D- and 3D- culture, as well as reduce the size of xenografted MCF10DCIS tumors, most likely via S-phase induced apoptosis and cell cycle arrest [221].

1.2.8 Peptidylarginine deiminase-inhibitors

Due to increasing evidence that the PADI family is involved in multiple diseases, including cancer, PADI inhibitors have generated substantial research interest in recent years. Most work in this field has focused on creating inhibitors for PADI4, which is dysregulated in rheumatoid arthritis [232, 233]. To date, Cl-amidine is the most potent PADI inhibitor and uses a chloroacetamidine warhead in place of the arginine substrate guanidinium group (**Figure 1.5**). This molecule irreversibly inhibits PADI

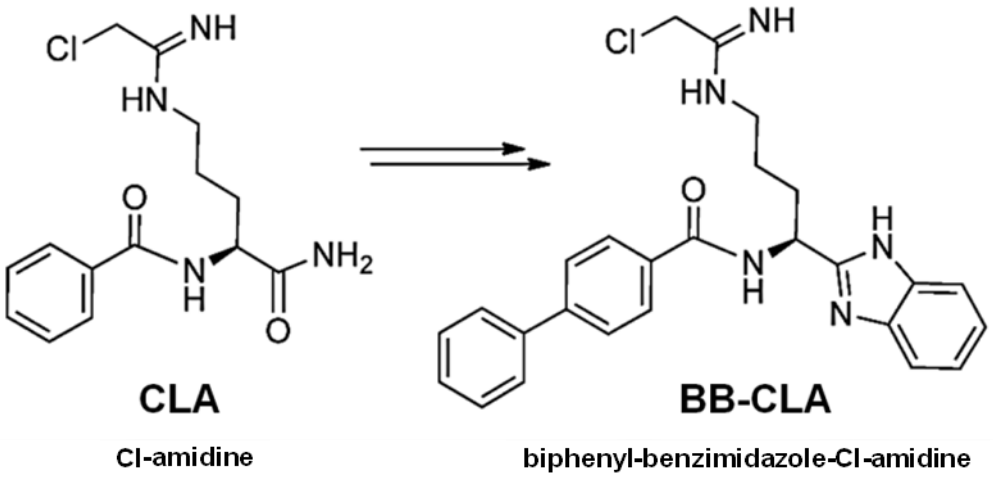

<u>Figure 1.5:</u> Chemical structure of both of the currently used small molecule pan-PADI inhibitors, first-generation Cl-amidine, and next-generation BB-Cl-amidine. The next-generation PADI inhibitor, BB-CLA, is more potent than its predecessor, Cl-amidine. This effect is likely due to the increased cellular permeability of the compound, which has increased hydrophobicity over Cl-amidine.

enzyme activity, is bioavailable, and preferentially targets the active form of these enzymes [232, 233]. In addition to our recent report on the treatment of MCF10DCIS cells *in vitro* and *in vivo*, previous research has shown Cl-amidine to be effective in decreasing the growth of several cancer cell lines (e.g. HL-60, HT-29, U2OS, and MCF7 cells). We also have unpublished data (see **Chapter 3**) showing that Cl-amidine (and BB-Cl-amidine) is effective at treating additional breast cancer cell lines, including BT-474, SKBR3, and MDA-MB-231cells. When administered in combination with other cancer drugs, such as doxorubicin or the HDAC inhibitor suberoylanilide hydroxamic acid (SAHA), Cl-amidine has a synergistic cytotoxic effect on cancer growth [195, 234-236]. Cl-amidine is highly specific for all PADI enzymes, with dose-dependent cytotoxicity and little-to-no effect in non-cancerous cell lines (i.e. HL-60 granulocytes and NIH3T3 cells) [236]. While we found that Cl-amidine suppressed tumor growth *in vivo*, the drug was well tolerated in our mice at a dose of 50 mg/kg/day during the study. Similarly, previous work found that doses of Cl-amidine up to 75 mg/kg/day in a mouse model of colitis [157], and up to100 mg/kg/day in a mouse model of RA [237], were well-tolerated without side effects. Our work using PADI inhibitors to target cancer *in vivo* was also validated by Wang et al., using a Cl-amidine derivative with increased cell permeability, YW3-56, which significantly suppressed cancer cell growth and reduced tumor size in mouse xenograft models of sarcoma [238]. This suggests that the development of new, more selective compounds, such as the second-generation PADI inhibitor, *o*-Cl-amidine, will help increase the effectiveness in future experiments [239]. We have currently been employing the next-generation PADI inhibitor, biphenyl-benzimidazole Cl-amidine (BB-Cl-amidine, **Figure 1.5**), which is ~3 fold more potent than Cl-amidine towards PADI2 in *in vitro* enzymatic assays, as well as over 100 fold more potent in decreasing cell growth *in vitro* in breast cancer cells (see **Chapter 3**). The increased potency of BB-Cl-amidine

over Cl-amidine is most likely due to its increased stability, in addition to increased cellular permeability, likely due to the higher hydrophobicity of the compound. While Cl-amidine (and more recently BB-Cl-amidine) has been important in numerous studies to help elucidate the role of PADIs in gene expression, the potential to develop this inhibitor into a novel epigenetic treatment of cancer, and specifically breast cancer, provides the impetus for our work.

1.3 Statement of purpose

Breast cancer is the most frequently diagnosed cancer in women, with over 1 million new cases in the world each year [240]. Recently, in addition to genetic mutations, numerous studies have found that epigenetics plays a direct role in the etiology of breast cancer. To this end, the goal of my research was to outline the role of peptidylarginine deiminase-2 (PADI2) in the progression of breast cancer. The PADIs are a family of epigenetic enzymes that catalyze citrullination, with previous work in our lab showing that PADI4 can convert both protein and histone arginine to citrulline, leading to the disruption of protein-protein interactions, as well as direct transcriptional downregulation. While PADI4 is downregulated in multiple cancers, perhaps indicating a tumor suppressor role, previous studies suggested a potential oncogenic role for PADI2 in breast cancer. However, despite this evidence, a formal experimental analysis of this relationship had yet to exist. The studies herein outline the role of PADI2 as an oncogene, especially in the progression of breast cancer, both *in vitro* and *in vivo*, as well as the validation of PADI inhibitors as a novel therapeutic agent.

In **Chapter 2**, we established a new line of evidence demonstrating that PADI2 plays a role in the oncogenic progression of breast cancer using the basal-like MCF10AT model. Furthermore, we showed using RNA-seq, that *PADI2* is highly

correlated with *HER2/ERBB2* overexpression across 57 breast cancer cell lines. We concluded this study with the first preclinical evidence showing that the PADI inhibitor, Cl-amidine, could be utilized as a therapeutic agent for the treatment of tumors *in vivo*. Following this, we wanted to investigate the functional relationship between PADI2 and HER2 expression. Interestingly, PADI2 appears to function in a positive-feedback loop with HER2, as PADI2 expression is both up- and downstream of HER2 signaling (**Chapter 3**). While we have previously established a role for PADI2 as an ER co-activator via citrullination of H3R26 at target gene promoters, it appears that PADI2 regulation of HER2 expression may occur in the same fashion at both the HER2 promoter and downstream ERE. Moreover, we established that the next-generation PADI inhibitor, BB-Cl-amidine, is nearly 100X more potent than first-generation Cl-amidine in reducing the growth of cancer cells. Lastly, we wanted to examine the potential role of ectopically expressed human *PADI2* in the development of carcinomas in mice (**Chapter 4**). Surprisingly, while the MMTV-FLAG-PADI2 mice did not develop any mammary tumors, we discovered that 20% of the mice developed skin lesions after five months. These tumors expressed high levels of transgenic human PADI2 and displayed markers of increased invasiveness (i.e. EMT). Furthermore, a subset of these tumors showed via histopathological analysis to have undergone malignant progression to highly invasive squamous cell carcinomas.

Collectively, these studies provide functional and mechanistic evidence establishing PADI2 as a potential novel oncogene and target for cancer therapy.

1.4 References

1. Siegel, R., Naishadham, D. & Jemal, A. Cancer statistics, 2013. *CA Cancer J Clin* **63**, 11-30 (2013).

2. Easton, D.F. et al. Breast cancer risks for BRCA1/2 carriers. *Science* **306**, 2187-91; author reply 2187-91 (2004).

3. Thompson, D. & Easton, D. The genetic epidemiology of breast cancer genes. *J Mammary Gland Biol Neoplasia* **9**, 221-36 (2004).

4. McPherson, K., Steel, C.M. & Dixon, J.M. ABC of breast diseases. Breast cancer-epidemiology, risk factors, and genetics. *BMJ* **321**, 624-8 (2000).

5. Tamimi, R.M. et al. Traditional breast cancer risk factors in relation to molecular subtypes of breast cancer. *Breast Cancer Res Treat* **131**, 159-67 (2012).

6. Millikan, R.C. et al. Epidemiology of basal-like breast cancer. *Breast Cancer Res Treat* **109**, 123-39 (2008).

7. Perou, C.M. et al. Molecular portraits of human breast tumours. *Nature* **406**, 747-52 (2000).

8. Sorlie, T. et al. Gene expression patterns of breast carcinomas distinguish tumor subclasses with clinical implications. *Proc Natl Acad Sci U S A* **98**, 10869-74 (2001).

9. Prat, A. & Perou, C.M. Deconstructing the molecular portraits of breast cancer. *Mol Oncol* **5**, 5-23.

10. TCGA. Comprehensive molecular portraits of human breast tumours. *Nature* **490**, 61-70 (2012).

11. Ma, X.J. et al. A two-gene expression ratio predicts clinical outcome in breast cancer patients treated with tamoxifen. *Cancer Cell* **5**, 607-16 (2004).

12. Paik, S. et al. A multigene assay to predict recurrence of tamoxifen-treated, node-negative breast cancer. *N Engl J Med* **351**, 2817-26 (2004).

13. Sotiriou, C. et al. Gene expression profiling in breast cancer: understanding the molecular basis of histologic grade to improve prognosis. *J Natl Cancer Inst* **98**, 262-72 (2006).

14. van 't Veer, L.J. et al. Gene expression profiling predicts clinical outcome of breast cancer. *Nature* **415**, 530-6 (2002).

15. Wang, Y. et al. Gene-expression profiles to predict distant metastasis of lymph-node-negative primary breast cancer. *Lancet* **365**, 671-9 (2005).

16. Blows, F.M. et al. Subtyping of breast cancer by immunohistochemistry to investigate a relationship between subtype and short and long term survival: a collaborative analysis of data for 10,159 cases from 12 studies. *PLoS Med* **7**, e1000279.

17. Carey, L.A. et al. Race, breast cancer subtypes, and survival in the Carolina Breast Cancer Study. *JAMA* **295**, 2492-502 (2006).

18. Tamimi, R.M. et al. Comparison of molecular phenotypes of ductal carcinoma in situ and invasive breast cancer. *Breast Cancer Res* **10**, R67 (2008).

19. Yang, X.R. et al. Hormonal markers in breast cancer: coexpression, relationship with pathologic characteristics, and risk factor associations in a population-based study. *Cancer Res* **67**, 10608-17 (2007).

20. Bastien, R.R. et al. PAM50 breast cancer subtyping by RT-qPCR and concordance with standard clinical molecular markers. *BMC Med Genomics* **5**, 44.

21. Kaufmann, M. & Pusztai, L. Use of standard markers and incorporation of molecular markers into breast cancer therapy: Consensus recommendations from an International Expert Panel. *Cancer* **117**, 1575-82.

22. Bhargava, R. et al. Prevalence, morphologic features and proliferation indices of breast carcinoma molecular classes using immunohistochemical surrogate markers. *Int J Clin Exp Pathol* **2**, 444-55 (2009).

23. Cheang, M.C.U., van de Rijn, M. & Nielsen, T.O. Gene expression profiling of breast cancer. *Annual review of pathology* **3**, 67-97 (2008).

24. Sihto, H. et al. Molecular subtypes of breast cancers detected in mammography screening and outside of screening. *Clin Cancer Res* **14**, 4103-10 (2008).

25. Xu, J., Wu, R.C. & O'Malley, B.W. Normal and cancer-related functions of the p160 steroid receptor co-activator (SRC) family. *Nat Rev Cancer* **9**, 615-30 (2009).

26. Couse, J.F. & Korach, K.S. Estrogen receptor null mice: what have we learned and where will they lead us? *Endocr Rev* **20**, 358-417 (1999).

27. Hartman, J., Strom, A. & Gustafsson, J.A. Estrogen receptor beta in breast cancer--diagnostic and therapeutic implications. *Steroids* **74**, 635-41 (2009).

28. Brisken, C. & O'Malley, B. Hormone action in the mammary gland. *Cold Spring Harb Perspect Biol* **2**, a003178 (2010).

29. Bocchinfuso, W.P. et al. Induction of mammary gland development in estrogen receptor-alpha knockout mice. *Endocrinology* **141**, 2982-94 (2000).

30. Bocchinfuso, W.P. & Korach, K.S. Mammary gland development and tumorigenesis in estrogen receptor knockout mice. *J Mammary Gland Biol Neoplasia* **2**, 323-34 (1997).

31. Lubahn, D.B. et al. Alteration of reproductive function but not prenatal sexual development after insertional disruption of the mouse estrogen receptor gene. *Proc Natl Acad Sci U S A* **90**, 11162-6 (1993).

32. Bedard, P.L., Freedman, O.C., Howell, A. & Clemons, M. Overcoming endocrine resistance in breast cancer: are signal transduction inhibitors the answer? *Breast Cancer Res Treat* **108**, 307-17 (2008).

33. Achermann, J.C. & Jameson, J.L. Fertility and infertility: genetic contributions from the hypothalamic-pituitary-gonadal axis. *Mol Endocrinol* **13**, 812-8 (1999).

34. Sabbah, M., Courilleau, D., Mester, J. & Redeuilh, G. Estrogen induction of the cyclin D1 promoter: involvement of a cAMP response-like element. *Proc Natl Acad Sci U S A* **96**, 11217-22 (1999).

35. Applanat, M.P., Buteau-Lozano, H., Herve, M.A. & Corpet, A. Vascular endothelial growth factor is a target gene for estrogen receptor and contributes to breast cancer progression. *Adv Exp Med Biol* **617**, 437-44 (2008).

36. Wang, C. et al. Estrogen induces c-myc gene expression via an upstream enhancer activated by the estrogen receptor and the AP-1 transcription factor. *Mol Endocrinol* **25**, 1527-38 (2011).

37. Castro-Rivera, E., Samudio, I. & Safe, S. Estrogen regulation of cyclin D1 gene expression in ZR-75 breast cancer cells involves multiple enhancer elements. *J Biol Chem* **276**, 30853-61 (2001).

38. Lamb, J., Ladha, M.H., McMahon, C., Sutherland, R.L. & Ewen, M.E. Regulation of the functional interaction between cyclin D1 and the estrogen receptor. *Mol Cell Biol* **20**, 8667-75 (2000).

39. Krishnan, V., Wang, X. & Safe, S. Estrogen receptor-Sp1 complexes mediate estrogen-induced cathepsin D gene expression in MCF-7 human breast cancer cells. *J Biol Chem* **269**, 15912-7 (1994).

40. Saville, B. et al. Ligand-, cell-, and estrogen receptor subtype (alpha/beta)-dependent activation at GC-rich (Sp1) promoter elements. *J Biol Chem* **275**, 5379-87 (2000).

41. Quaedackers, M.E., van den Brink, C.E., van der Saag, P.T. & Tertoolen, L.G. Direct interaction between estrogen receptor alpha and NF-kappaB in the nucleus of living cells. *Mol Cell Endocrinol* **273**, 42-50 (2007).

42. Kushner, P.J. et al. Estrogen receptor pathways to AP-1. *J Steroid Biochem Mol Biol* **74**, 311-7 (2000).

43. Heldring, N. et al. Estrogen receptors: how do they signal and what are their targets. *Physiol Rev* **87**, 905-31 (2007).

44. Kahlert, S. et al. Estrogen receptor alpha rapidly activates the IGF-1 receptor pathway. *J Biol Chem* **275**, 18447-53 (2000).

45. Levin, E.R. Plasma membrane estrogen receptors. *Trends Endocrinol Metab* **20**, 477-82 (2009).

46. Ignar-Trowbridge, D.M. et al. Peptide growth factors elicit estrogen receptor-dependent transcriptional activation of an estrogen-responsive element. *Mol Endocrinol* **7**, 992-8 (1993).

47. Ignar-Trowbridge, D.M., Pimentel, M., Parker, M.G., McLachlan, J.A. & Korach, K.S. Peptide growth factor cross-talk with the estrogen receptor requires the A/B domain and occurs independently of protein kinase C or estradiol. *Endocrinology* **137**, 1735-44 (1996).

48. Bunone, G., Briand, P.A., Miksicek, R.J. & Picard, D. Activation of the unliganded estrogen receptor by EGF involves the MAP kinase pathway and direct phosphorylation. *EMBO J* **15**, 2174-83 (1996).

49. Lee, A.V., Weng, C.N., Jackson, J.G. & Yee, D. Activation of estrogen receptor-mediated gene transcription by IGF-I in human breast cancer cells. *J Endocrinol* **152**, 39-47 (1997).

50. Shou, J. et al. Mechanisms of tamoxifen resistance: increased estrogen receptor-HER2/neu cross-talk in ER/HER2-positive breast cancer. *J Natl Cancer Inst* **96**, 926-35 (2004).

51. Knowlden, J.M. et al. Elevated levels of epidermal growth factor receptor/c-erbB2 heterodimers mediate an autocrine growth regulatory pathway in tamoxifen-resistant MCF-7 cells. *Endocrinology* **144**, 1032-44 (2003).

52. Osborne, C.K., Shou, J., Massarweh, S. & Schiff, R. Crosstalk between estrogen receptor and growth factor receptor pathways as a cause for endocrine therapy resistance in breast cancer. *Clin Cancer Res* **11**, 865s-70s (2005).

53. Vogel, V.G. et al. Update of the National Surgical Adjuvant Breast and Bowel Project Study of Tamoxifen and Raloxifene (STAR) P-2 Trial: Preventing breast cancer. *Cancer Prev Res (Phila)* **3**, 696-706 (2010).

54. Paige, L.A. et al. Estrogen receptor (ER) modulators each induce distinct conformational changes in ER alpha and ER beta. *Proc Natl Acad Sci U S A* **96**, 3999-4004 (1999).

55. Shiau, A.K. et al. The structural basis of estrogen receptor/coactivator recognition and the antagonism of this interaction by tamoxifen. *Cell* **95**, 927-37 (1998).

56. Heldring, N. et al. Structural insights into corepressor recognition by antagonist-bound estrogen receptors. *J Biol Chem* **282**, 10449-55 (2007).

57. Wakeling, A.E. & Bowler, J. Development of novel oestrogen-receptor antagonists. *Biochem Soc Trans* **19**, 899-901 (1991).

58. Regan, M.M. et al. Assessment of letrozole and tamoxifen alone and in sequence for postmenopausal women with steroid hormone receptor-positive breast cancer: the BIG 1-98 randomised clinical trial at 8.1 years median follow-up. *Lancet Oncol* **12**, 1101-8 (2011).

59. Chirgwin, J. et al. The advantage of letrozole over tamoxifen in the BIG 1-98 trial is consistent in younger postmenopausal women and in those with chemotherapy-induced menopause. *Breast Cancer Res Treat* **131**, 295-306 (2011).

60. Regan, M.M., Price, K.N., Giobbie-Hurder, A., Thurlimann, B. & Gelber, R.D. Interpreting Breast International Group (BIG) 1-98: a randomized, double-blind, phase III trial comparing letrozole and tamoxifen as adjuvant endocrine therapy for postmenopausal women with hormone receptor-positive, early breast cancer. *Breast Cancer Res* **13**, 209 (2011).

61. Visvanathan, K. et al. American society of clinical oncology clinical practice guideline update on the use of pharmacologic interventions including tamoxifen, raloxifene, and aromatase inhibition for breast cancer risk reduction. *J Clin Oncol* **27**, 3235-58 (2009).

62. Fisher, B. et al. Endometrial cancer in tamoxifen-treated breast cancer patients: findings from the National Surgical Adjuvant Breast and Bowel Project (NSABP) B-14. *J Natl Cancer Inst* **86**, 527-37 (1994).

63. Arpino, G., Wiechmann, L., Osborne, C.K. & Schiff, R. Crosstalk between the estrogen receptor and the HER tyrosine kinase receptor family: molecular mechanism and clinical implications for endocrine therapy resistance. *Endocr Rev* **29**, 217-33 (2008).

64. Fleming, F.J. et al. Expression of SRC-1, AIB1, and PEA3 in HER2 mediated endocrine resistant breast cancer; a predictive role for SRC-1. *J Clin Pathol* **57**, 1069-74 (2004).

65. Hurtado, A. et al. Regulation of ERBB2 by oestrogen receptor-PAX2 determines response to tamoxifen. *Nature* **456**, 663-6 (2008).

66. Lahusen, T., Henke, R.T., Kagan, B.L., Wellstein, A. & Riegel, A.T. The role and regulation of the nuclear receptor co-activator AIB1 in breast cancer. *Breast Cancer Res Treat* **116**, 225-37 (2009).

67. Benz, C.C. et al. Estrogen-dependent, tamoxifen-resistant tumorigenic growth of MCF-7 cells transfected with HER2/neu. *Breast Cancer Res Treat* **24**, 85-95 (1992).

68. Chu, I., Blackwell, K., Chen, S. & Slingerland, J. The dual ErbB1/ErbB2 inhibitor, lapatinib (GW572016), cooperates with tamoxifen to inhibit both cell proliferation- and estrogen-dependent gene expression in antiestrogen-resistant breast cancer. *Cancer Res* **65**, 18-25 (2005).

69. Uberall, I., Kolar, Z., Trojanec, R., Berkovcova, J. & Hajduch, M. The status and role of ErbB receptors in human cancer. *Exp Mol Pathol* **84**, 79-89 (2008).

70. Tzahar, E. et al. A hierarchical network of interreceptor interactions determines signal transduction by Neu differentiation factor/neuregulin and epidermal growth factor. *Mol Cell Biol* **16**, 5276-87 (1996).

71. Graus-Porta, D., Beerli, R.R., Daly, J.M. & Hynes, N.E. ErbB-2, the preferred heterodimerization partner of all ErbB receptors, is a mediator of lateral signaling. *EMBO J* **16**, 1647-55 (1997).

72. Cho, H.S. et al. Structure of the extracellular region of HER2 alone and in complex with the Herceptin Fab. *Nature* **421**, 756-60 (2003).

73. Garrett, T.P. et al. The crystal structure of a truncated ErbB2 ectodomain reveals an active conformation, poised to interact with other ErbB receptors. *Mol Cell* **11**, 495-505 (2003).

74. Lenferink, A.E. et al. Differential endocytic routing of homo- and hetero-dimeric ErbB tyrosine kinases confers signaling superiority to receptor heterodimers. *EMBO J* **17**, 3385-97 (1998).

75. Sierke, S.L., Cheng, K., Kim, H.H. & Koland, J.G. Biochemical characterization of the protein tyrosine kinase homology domain of the ErbB3 (HER3) receptor protein. *Biochem J* **322 (Pt 3)**, 757-63 (1997).

76. Baselga, J. & Swain, S.M. Novel anticancer targets: revisiting ERBB2 and discovering ERBB3. *Nat Rev Cancer* **9**, 463-75 (2009).

77. Karunagaran, D. et al. ErbB-2 is a common auxiliary subunit of NDF and EGF receptors: implications for breast cancer. *EMBO J* **15**, 254-64 (1996).

78. Schulze, W.X., Deng, L. & Mann, M. Phosphotyrosine interactome of the ErbB-receptor kinase family. *Mol Syst Biol* **1**, 2005 0008 (2005).

79. Ju, X. et al. Akt1 governs breast cancer progression *in vivo*. *Proc Natl Acad Sci U S A* **104**, 7438-43 (2007).

80. Hanker, A.B. et al. Mutant PIK3CA accelerates HER2-driven transgenic mammary tumors and induces resistance to combinations of anti-HER2 therapies. *Proc Natl Acad Sci U S A* (2013).

81. Hsu, M.C. et al. Jab1 is overexpressed in human breast cancer and is a downstream target for HER-2/neu. *Mod Pathol* **21**, 609-16 (2008).

82. Hsu, M.C., Chang, H.C. & Hung, W.C. HER-2/neu transcriptionally activates Jab1 expression via the AKT/beta-catenin pathway in breast cancer cells. *Endocr Relat Cancer* **14**, 655-67 (2007).

83. O'Hagan, R.C. & Hassell, J.A. The PEA3 Ets transcription factor is a downstream target of the HER2/Neu receptor tyrosine kinase. *Oncogene* **16**, 301-10 (1998).

84. Benz, C.C. et al. HER2/Neu and the Ets transcription activator PEA3 are coordinately upregulated in human breast cancer. *Oncogene* **15**, 1513-25 (1997).

85. Naderi, A., Meyer, M. & Dowhan, D.H. Cross-regulation between FOXA1 and ErbB2 signaling in estrogen receptor-negative breast cancer. *Neoplasia* **14**, 283-96 (2012).

86. Francis, R.E. et al. FoxM1 is a downstream target and marker of HER2 overexpression in breast cancer. *Int J Oncol* **35**, 57-68 (2009).

87. Koo, C.Y., Muir, K.W. & Lam, E.W. FOXM1: From cancer initiation to progression and treatment. *Biochim Biophys Acta* **1819**, 28-37 (2011).

88. Nencioni, A. et al. Grb7 upregulation is a molecular adaptation to HER2 signaling inhibition due to removal of Akt-mediated gene repression. *PLoS One* **5**, e9024 (2010).

89. Rao, V.H. et al. A positive feedback loop between HER2 and ADAM12 in human head and neck cancer cells increases migration and invasion. *Oncogene* **31**, 2888-98 (2011).

90. Kang, L., Guo, Y., Zhang, X., Meng, J. & Wang, Z.Y. A positive cross-regulation of HER2 and ER-alpha36 controls ALDH1 positive breast cancer cells. *J Steroid Biochem Mol Biol* **127**, 262-8 (2011).

91. Naderi, A., Liu, J. & Francis, G.D. A feedback loop between BEX2 and ErbB2 mediated by c-Jun signaling in breast cancer. *Int J Cancer* **130**, 71-82 (2011).

92. Cui, J. et al. Cross-talk between HER2 and MED1 regulates tamoxifen resistance of human breast cancer cells. *Cancer Res* **72**, 5625-34 (2012).

93. Hartman, Z.C. et al. HER2 overexpression elicits a proinflammatory IL-6 autocrine signaling loop that is critical for tumorigenesis. *Cancer Res* **71**, 4380-91 (2011).

94. Slamon, D.J. et al. Studies of the HER-2/neu proto-oncogene in human breast and ovarian cancer. *Science* **244**, 707-12 (1989).

95. Pusztai, L., Mazouni, C., Anderson, K., Wu, Y. & Symmans, W.F. Molecular classification of breast cancer: limitations and potential. *Oncologist* **11**, 868-77 (2006).

96. Murphy, C.G. & Fornier, M. HER2-positive breast cancer: beyond trastuzumab. *Oncology (Williston Park)* **24**, 410-5 (2010).

97. Esteva, F.J. et al. Phase II study of weekly docetaxel and trastuzumab for patients with HER-2-overexpressing metastatic breast cancer. *J Clin Oncol* **20**, 1800-8 (2002).

98. Scaltriti, M. et al. Expression of p95HER2, a truncated form of the HER2 receptor, and response to anti-HER2 therapies in breast cancer. *J Natl Cancer Inst* **99**, 628-38 (2007).

99. Carraway, K.L. et al. Muc4/sialomucin complex in the mammary gland and breast cancer. *J Mammary Gland Biol Neoplasia* **6**, 323-37 (2001).

100. Lu, Y., Zi, X., Zhao, Y., Mascarenhas, D. & Pollak, M. Insulin-like growth factor-I receptor signaling and resistance to trastuzumab (Herceptin). *J Natl Cancer Inst* **93**, 1852-7 (2001).

101. Zhang, S. & Yu, D. Targeting Src family kinases in anti-cancer therapies: turning promise into triumph. *Trends Pharmacol Sci* **33**, 122-8 (2011).

102. Zhang, S. et al. Combating trastuzumab resistance by targeting SRC, a common node downstream of multiple resistance pathways. *Nat Med* **17**, 461-9 (2011).

103. Chandarlapaty, S. et al. AKT inhibition relieves feedback suppression of receptor tyrosine kinase expression and activity. *Cancer Cell* **19**, 58-71 (2011).

104. Narayan, M. et al. Trastuzumab-induced HER reprogramming in "resistant" breast carcinoma cells. *Cancer Res* **69**, 2191-4 (2009).

105. Yang, X.H. et al. Disruption of laminin-integrin-CD151-focal adhesion kinase axis sensitizes breast cancer cells to ErbB2 antagonists. *Cancer Res* **70**, 2256-63 (2010).

106. Scaltriti, M. et al. Lapatinib, a HER2 tyrosine kinase inhibitor, induces stabilization and accumulation of HER2 and potentiates trastuzumab-dependent cell cytotoxicity. *Oncogene* **28**, 803-14 (2009).

107. Dawood, S., Broglio, K., Buzdar, A.U., Hortobagyi, G.N. & Giordano, S.H. Prognosis of women with metastatic breast cancer by HER2 status and trastuzumab treatment: an institutional-based review. *J Clin Oncol* **28**, 92-8 (2009).

108. O'Brien, N.A. et al. Activated phosphoinositide 3-kinase/AKT signaling confers resistance to trastuzumab but not lapatinib. *Mol Cancer Ther* **9**, 1489-502 (2010).

109. Romond, E.H. et al. Trastuzumab plus adjuvant chemotherapy for operable HER2-positive breast cancer. *N Engl J Med* **353**, 1673-84 (2005).

110. Rakha, E.A., Reis-Filho, J.S. & Ellis, I.O. Basal-like breast cancer: a critical review. *J Clin Oncol* **26**, 2568-81 (2008).

111. Carey, L.A. et al. The triple negative paradox: primary tumor chemosensitivity of breast cancer subtypes. *Clin Cancer Res* **13**, 2329-34 (2007).

112. Livasy, C.A. et al. Phenotypic evaluation of the basal-like subtype of invasive breast carcinoma. *Mod Pathol* **19**, 264-71 (2006).

113. Dent, R. et al. Triple-negative breast cancer: clinical features and patterns of recurrence. *Clin Cancer Res* **13**, 4429-34 (2007).

114. Morris, G.J. et al. Differences in breast carcinoma characteristics in newly diagnosed African-American and Caucasian patients: a single-institution compilation compared with the National Cancer Institute's Surveillance, Epidemiology, and End Results database. *Cancer* **110**, 876-84 (2007).

115. Millar, E.K. et al. Prediction of local recurrence, distant metastases, and death after breast-conserving therapy in early-stage invasive breast cancer using a five-biomarker panel. *J Clin Oncol* **27**, 4701-8 (2009).

116. Fulford, L.G. et al. Basal-like grade III invasive ductal carcinoma of the breast: patterns of metastasis and long-term survival. *Breast Cancer Res* **9**, R4 (2007).

117. Bergamaschi, A. et al. Distinct patterns of DNA copy number alteration are associated with different clinicopathological features and gene-expression subtypes of breast cancer. *Genes Chromosomes Cancer* **45**, 1033-40 (2006).

118. Nielsen, T.O. et al. Immunohistochemical and clinical characterization of the basal-like subtype of invasive breast carcinoma. *Clin Cancer Res* **10**, 5367-74 (2004).

119. Turner, N.C. & Reis-Filho, J.S. Basal-like breast cancer and the BRCA1 phenotype. *Oncogene* **25**, 5846-53 (2006).

120. Pinilla, S.M., Honrado, E., Hardisson, D., Benitez, J. & Palacios, J. Caveolin-1 expression is associated with a basal-like phenotype in sporadic and hereditary breast cancer. *Breast Cancer Res Treat* **99**, 85-90 (2006).

121. Moyano, J.V. et al. AlphaB-crystallin is a novel oncoprotein that predicts poor clinical outcome in breast cancer. *J Clin Invest* **116**, 261-70 (2006).

122. Peralta Soler, A., Knudsen, K.A., Salazar, H., Han, A.C. & Keshgegian, A.A. P-cadherin expression in breast carcinoma indicates poor survival. *Cancer* **86**, 1263-72 (1999).

123. Antoniou, A. et al. Average risks of breast and ovarian cancer associated with BRCA1 or BRCA2 mutations detected in case Series unselected for family history: a combined analysis of 22 studies. *Am J Hum Genet* **72**, 1117-30 (2003).

124. Guha, M. PARP inhibitors stumble in breast cancer. *Nat Biotechnol* **29**, 373-4 (2011).

125. Burstein, H.J. et al. Phase II study of sunitinib malate, an oral multitargeted tyrosine kinase inhibitor, in patients with metastatic breast cancer previously treated with an anthracycline and a taxane. *J Clin Oncol* **26**, 1810-6 (2008).

126. Tryfonopoulos, D. et al. Src: a potential target for the treatment of triple-negative breast cancer. *Ann Oncol* **22**, 2234-40 (2011).

127. Finn, R.S. et al. Dasatinib as a single agent in triple-negative breast cancer: results of an open-label phase 2 study. *Clin Cancer Res* **17**, 6905-13 (2011).

128. Pauley, R.J. et al. The MCF10 family of spontaneously immortalized human breast epithelial cell lines: models of neoplastic progression. *Eur J Cancer Prev* **2 Suppl 3**, 67-76 (1993).

129. Aslakson, C.J. & Miller, F.R. Selective events in the metastatic process defined by analysis of the sequential dissemination of subpopulations of a mouse mammary tumor. *Cancer Res* **52**, 1399-405 (1992).

130. Miller, F.R. Models of progression spanning preneoplasia and metastasis: the human MCF10AneoT.TGn series and a panel of mouse mammary tumor subpopulations. *Cancer Treat Res* **83**, 243-63 (1996).

131. Miller, F.R., Santner, S.J., Tait, L. & Dawson, P.J. MCF10DCIS.com xenograft model of human comedo ductal carcinoma in situ. *J Natl Cancer Inst* **92**, 1185-6 (2000).

132. Santner, S.J. et al. Malignant MCF10CA1 cell lines derived from premalignant human breast epithelial MCF10AT cells. *Breast Cancer Res Treat* **65**, 101-10 (2001).

133. Fisher, E.R. et al. Pathologic variables predictive of breast events in patients with ductal carcinoma in situ. *Am J Clin Pathol* **128**, 86-91 (2007).

134. Jaffer, S. & Bleiweiss, I.J. Histologic classification of ductal carcinoma in situ. *Microsc Res Tech* **59**, 92-101 (2002).

135. Meyer, J.S. Cell kinetics of histologic variants of in situ breast carcinoma. *Breast Cancer Res Treat* **7**, 171-80 (1986).

136. van de Vijver, M.J. et al. Neu-protein overexpression in breast cancer. Association with comedo-type ductal carcinoma in situ and limited prognostic value in stage II breast cancer. *N Engl J Med* **319**, 1239-1245 (1988).

137. Kadota, M. et al. Delineating genetic alterations for tumor progression in the MCF10A series of breast cancer cell lines. *PloS one* **5**, e9201 (2010).

138. Watanabe, K. & Senshu, T. Isolation and characterization of cDNA clones encoding rat skeletal muscle peptidylarginine deiminase. *J Biol Chem* **264**, 15255-60 (1989).

139. Chang, X. & Han, J. Expression of peptidylarginine deiminase type 4 (PAD4) in various tumors. *Mol Carcinog* **45**, 183-196 (2006).

140. Ishigami, A. et al. Abnormal accumulation of citrullinated proteins catalyzed by peptidylarginine deiminase in hippocampal extracts from patients with Alzheimer's disease. *J Neurosci Res* **80**, 120-128 (2005).

141. Mastronardi, F.G., Mak, B., Ackerley, C.A., Roots, B.I. & Moscarello, M.A. Modifications of myelin basic protein in DM20 transgenic mice are similar to those in myelin basic protein from multiple sclerosis. *J Clin Invest* **97**, 349-358 (1996).

142. Suzuki, A. et al. Functional haplotypes of PADI4, encoding citrullinating enzyme peptidylarginine deiminase 4, are associated with rheumatoid arthritis. *Nat Genet* **34**, 395-402 (2003).

143. Wang, Y. et al. Human PAD4 regulates histone arginine methylation levels via demethylimination. *Science* **306**, 279-83 (2004).

144. Wang, Y. et al. Histone hypercitrullination mediates chromatin decondensation and neutrophil extracellular trap formation. *J Cell Biol* **184**, 205-13 (2009).

145. Tanikawa, C. et al. Regulation of protein Citrullination through p53/PADI4 network in DNA damage response. *Cancer Res* **69**, 8761-9 (2009).

146. Zhang, X. et al. Peptidylarginine deiminase 2-catalyzed histone H3 arginine 26 citrullination facilitates estrogen receptor alpha target gene activation. *Proc Natl Acad Sci U S A* **109**, 13331-6 (2012).

147. Balandraud, N. et al. A rigorous method for multigenic families' functional annotation: the peptidyl arginine deiminase (PADs) proteins family example. *BMC Genomics* **6**, 153 (2005).

148. Horibata, S., Coonrod, S.A. & Cherrington, B.D. Role for peptidylarginine deiminase enzymes in disease and female reproduction. *J Reprod Dev* **58**, 274-82 (2012).

149. Jones, J., Causey, C. & Knuckley, B. Protein arginine deiminase 4 (PAD4): Current understanding and future therapeutic potential. *Current opinion in* (2009).

150. Chang, X., Zhao, Y., Sun, S., Zhang, Y. & Zhu, Y. The expression of PADI4 in synovium of rheumatoid arthritis. *Rheumatol Int* **29**, 1411-6 (2009).

151. Asaga, H., Akiyama, K., Ohsawa, T. & Ishigami, A. Increased and type II-specific expression of peptidylarginine deiminase in activated microglia but not hyperplastic astrocytes following kainic acid-evoked neurodegeneration in the rat brain. *Neurosci Lett* **326**, 129-32 (2002).

152. Asaga, H. & Ishigami, A. Protein deimination in the rat brain after kainate administration: citrulline-containing proteins as a novel marker of neurodegeneration. *Neurosci Lett* **299**, 5-8 (2001).

153. Musse, A.A. et al. Peptidylarginine deiminase 2 (PAD2) overexpression in transgenic mice leads to myelin loss in the central nervous system. *Dis Model Mech* **1**, 229-40 (2008).

154. Mastronardi, F.G., Ackerley, C.A., Roots, B.I. & Moscarello, M.A. Loss of myelin basic protein cationicity in DM20 transgenic mice is dosage dependent. *J Neurosci Res* **44**, 301-7 (1996).

155. Mastronardi, F.G., Noor, A., Wood, D.D., Paton, T. & Moscarello, M.A. Peptidyl argininedeiminase 2 CpG island in multiple sclerosis white matter is hypomethylated. *J Neurosci Res* **85**, 2006-16 (2007).

156. Mastronardi, F.G. et al. Increased citrullination of histone H3 in multiple sclerosis brain and animal models of demyelination: a role for tumor necrosis factor-induced peptidylarginine deiminase 4 translocation. *J Neurosci* **26**, 11387-96 (2006).

157. Chumanevich, A.A. et al. Suppression of colitis in mice by Cl-amidine: a novel peptidylarginine deiminase inhibitor. *American journal of physiology. Gastrointestinal and liver physiology* **300**, G929-38 (2011).

158. Ishida-Yamamoto, A. et al. Decreased deiminated keratin K1 in psoriatic hyperproliferative epidermis. *J Invest Dermatol* **114**, 701-5 (2000).

159. Ruiz-Esquide, V. et al. Anti-citrullinated peptide antibodies in the serum of heavy smokers without rheumatoid arthritis. A differential effect of chronic obstructive pulmonary disease? *Clin Rheumatol* **31**, 1047-50.

160. Nissinen, R. et al. Peptidylarginine deiminase, the arginine to citrulline converting enzyme, is frequently recognized by sera of patients with rheumatoid arthritis, systemic lupus erythematosus and primary Sjogren syndrome. *Scand J Rheumatol* **32**, 337-42 (2003).

161. Bhattacharya, S.K. Retinal deimination in aging and disease. *IUBMB Life* **61**, 504-9 (2009).

162. Bhattacharya, S.K., Bhat, M.B. & Takahara, H. Modulation of peptidyl arginine deiminase 2 and implication for neurodegeneration. *Curr Eye Res* **31**, 1063-71 (2006).

163. Bonilha, V.L. et al. Retinal deimination and PAD2 levels in retinas from donors with age-related macular degeneration (AMD). *Exp Eye Res* **111**, 71-8.

164. Mohanan, S. et al. Potential role of peptidylarginine deiminase enzymes and protein citrullination in cancer pathogenesis. *Biochem Res Int* **2012**, 895343 (2012).

165. Kanno, T. et al. Human peptidylarginine deiminase type III: molecular cloning and nucleotide sequence of the cDNA, properties of the recombinant enzyme, and immunohistochemical localization in human skin. *J Invest Dermatol* **115**, 813-23 (2000).

166. Nishijyo, T., Kawada, A., Kanno, T., Shiraiwa, M. & Takahara, H. Isolation and molecular cloning of epidermal- and hair follicle-specific peptidylarginine deiminase (type III) from rat. *J Biochem* **121**, 868-75 (1997).

167. Akiyama, K. & Senshu, T. Dynamic aspects of protein deimination in developing mouse epidermis. *Exp Dermatol* **8**, 177-86 (1999).

168. Nakashima, K. et al. Molecular characterization of peptidylarginine deiminase in HL-60 cells induced by retinoic acid and 1alpha,25-dihydroxyvitamin D(3). *J Biol Chem* **274**, 27786-92 (1999).

169. Nachat, R. et al. Peptidylarginine deiminase isoforms are differentially expressed in the anagen hair follicles and other human skin appendages. *J Invest Dermatol* **125**, 34-41 (2005).

170. Nachat, R. et al. Peptidylarginine deiminase isoforms 1-3 are expressed in the epidermis and involved in the deimination of K1 and filaggrin. *The Journal of investigative dermatology* **124**, 384-93 (2005).

171. Rawlings, A.V. & Harding, C.R. Moisturization and skin barrier function. *Dermatol Ther* **17 Suppl 1**, 43-8 (2004).

172. Senshu, T., Akiyama, K., Ishigami, A. & Nomura, K. Studies on specificity of peptidylarginine deiminase reactions using an immunochemical probe that recognizes an enzymatically deiminated partial sequence of mouse keratin K1. *J Dermatol Sci* **21**, 113-26 (1999).

173. Chavanas, S. et al. Peptidylarginine deiminases and deimination in biology and pathology: relevance to skin homeostasis. *J Dermatol Sci* **44**, 63-72 (2006).

174. Chen, C. et al. Gene expression profiling identifies genes predictive of oral squamous cell carcinoma. *Cancer Epidemiol Biomarkers Prev* **17**, 2152-62 (2008).

175. Takahara, H., Oikawa, Y. & Sugawara, K. Purification and characterization of peptidylarginine deiminase from rabbit skeletal muscle. *J Biochem* **94**, 1945-53 (1983).

176. Takahara, H., Okamoto, H. & Sugawara, K. Affinity chromatography of peptidylarginine deiminase from rabbit skeletal muscle on a column of soybean trypsin inhibitor (Kunitz)-Sepharose. *J Biochem* **99**, 1417-24 (1986).

177. Lamensa, J.W. & Moscarello, M.A. Deimination of human myelin basic protein by a peptidylarginine deiminase from bovine brain. *J Neurochem* **61**, 987-96 (1993).

178. Moscarello, M.A., Pritzker, L., Mastronardi, F.G. & Wood, D.D. Peptidylarginine deiminase: a candidate factor in demyelinating disease. *J Neurochem* **81**, 335-43 (2002).

179. Vossenaar, E.R. et al. Expression and activity of citrullinating peptidylarginine deiminase enzymes in monocytes and macrophages. *Ann Rheum Dis* **63**, 373-81 (2004).

180. Lee, H.J. et al. Peptidylarginine deiminase 2 suppresses inhibitory {kappa}B kinase activity in lipopolysaccharide-stimulated RAW 264.7 macrophages. *J Biol Chem* **285**, 39655-62.

181. Proost, P. et al. Citrullination of CXCL8 by peptidylarginine deiminase alters receptor usage, prevents proteolysis, and dampens tissue inflammation. *J Exp Med* **205**, 2085-97 (2008).

182. Mohanan, S., Horibata, S., McElwee, J.L., Dannenberg, A.J. & Coonrod, S.A. Identification of macrophage extracellular trap-like structures in mammary gland adipose tissue: a preliminary study. *Front Immunol* **4**, 67 (2013).

183. Takahara, H. et al. Expression of peptidylarginine deiminase in the uterine epithelial cells of mouse is dependent on estrogen. *J Biol Chem* **267**, 520-525 (1992).

184. Senshu, T., Akiyama, K., Nagata, S., Watanabe, K. & Hikichi, K. Peptidylarginine deiminase in rat pituitary: sex difference, estrous cycle-related changes, and estrogen dependence. *Endocrinology* **124**, 2666-2670 (1989).

185. Takahara, H. et al. Peptidylarginine deiminase of the mouse. Distribution, properties, and immunocytochemical localization. *J Biol Chem* **264**, 13361-8 (1989).

186. Cherrington, B.D., Morency, E., Struble, A.M., Coonrod, S.a. & Wakshlag, J.J. Potential role for peptidylarginine deiminase 2 (PAD2) in citrullination of canine mammary epithelial cell histones. *PloS one* **5**, e11768 (2010).

187. Cherrington, B.D. et al. Potential Role for PAD2 in Gene Regulation in Breast Cancer Cells. *PLoS One* **7**, e41242 (2012).

188. Nakamura, T., Fidler, I.J. & Coombes, K.R. Gene expression profile of metastatic human pancreatic cancer cells depends on the organ microenvironment. *Cancer Res* **67**, 139-48 (2007).

189. Chavanas, S. et al. Long-range enhancer associated with chromatin looping allows AP-1 regulation of the peptidylarginine deiminase 3 gene in differentiated keratinocyte. *PLoS One* **3**, e3408 (2008).

190. Nakashima, K., Hagiwara, T. & Yamada, M. Nuclear localization of peptidylarginine deiminase V and histone deimination in granulocytes. *J Biol Chem* **277**, 49562-8 (2002).

191. Cuthbert, G.L. et al. Histone deimination antagonizes arginine methylation. *Cell* **118**, 545-53 (2004).

192. Balint, B.L. et al. Arginine methylation provides epigenetic transcription memory for retinoid-induced differentiation in myeloid cells. *Mol Cell Biol* **25**, 5648-63 (2005).

193. Wang, Y. et al. Human PAD4 regulates histone arginine methylation levels via demethylimination. *Science (New York, N.Y.)* **306**, 279-83 (2004).

194. Li, P. et al. Coordination of PAD4 and HDAC2 in the regulation of p53-target gene expression. *Oncogene*.

195. Yao, H. et al. Histone Arg modifications and p53 regulate the expression of OKL38, a mediator of apoptosis. *J Biol Chem* **283**, 20060-8 (2008).

196. Guo, Q. & Fast, W. Citrullination of inhibitor of growth 4 (ING4) by peptidylarginine deminase 4 (PAD4) disrupts the interaction between ING4 and p53. *J Biol Chem* **286**, 17069-78 (2011).

197. Tanikawa, C. et al. Regulation of histone modification and chromatin structure by the p53-PADI4 pathway. *Nat Commun* **3**, 676 (2012).

198. Zhang, X. et al. Genome-wide analysis reveals PADI4 cooperates with Elk-1 to activate c-Fos expression in breast cancer cells. *PLoS Genet* **7**, e1002112 (2011).

199. Chang, X. & Fang, K. PADI4 and tumourigenesis. *Cancer cell international* **10**, 7 (2010).

200. Chang, X. et al. Increased PADI4 expression in blood and tissues of patients with malignant tumors. *BMC Cancer* **9**, 40 (2009).

201. Saffarzadeh, M. et al. Neutrophil extracellular traps directly induce epithelial and endothelial cell death: a predominant role of histones. *PLoS One* **7**, e32366 (2012).

202. Liu, C.L. et al. Specific post-translational histone modifications of neutrophil extracellular traps as immunogens and potential targets of lupus autoantibodies. *Arthritis Res Ther* **14**, R25 (2012).

203. Amulic, B. & Hayes, G. Neutrophil extracellular traps. *Curr Biol* **21**, R297-8 (2011).

204. Slack, J.L., Causey, C.P. & Thompson, P.R. Protein arginine deiminase 4: a target for an epigenetic cancer therapy. *Cellular and molecular life sciences : CMLS* (2010).

205. Yurttas, P. et al. Role for PADI6 and the cytoplasmic lattices in ribosomal storage in oocytes and translational control in the early mouse embryo. *Development* **135**, 2627-36 (2008).

206. Kan, R. et al. Potential role for PADI-mediated histone citrullination in preimplantation development. *BMC Dev Biol* **12**, 19 (2012).

207. Kan, R. et al. Regulation of mouse oocyte microtubule and organelle dynamics by PADI6 and the cytoplasmic lattices. *Dev Biol* **350**, 311-22 (2011).

208. Stacey, S.N. et al. Common variants on 1p36 and 1q42 are associated with cutaneous basal cell carcinoma but not with melanoma or pigmentation traits. *Nat Genet* **40**, 1313-1318 (2008).

209. Yurttas, P., Morency, E. & Coonrod, S. Use of proteomics to identify highly abundant maternal factors that drive the egg to embryo transition. *Reproduction* (2010).

210. Li, L., Zheng, P. & Dean, J. Maternal control of early mouse development. *Development* **137**, 859-70.

211. Ishigami, A. et al. Human peptidylarginine deiminase type II: molecular cloning, gene organization, and expression in human skin. *Arch Biochem Biophys* **407**, 25-31 (2002).

212. Leacock, S.W. et al. A zebrafish transgenic model of Ewing's sarcoma reveals conserved mediators of EWS-FLI1 tumorigenesis. *Dis Model Mech* **5**, 95-106 (2011).

213. Herschkowitz, J.I. et al. Identification of conserved gene expression features between murine mammary carcinoma models and human breast tumors. *Genome biology* **8**, R76 (2007).

214. Montañez-Wiscovich, M.E. et al. LMO4 is an essential mediator of ErbB2/HER2/Neu-induced breast cancer cell cycle progression. *Oncogene* **28**, 3608-18 (2009).

215. Mackay, A. et al. A high-resolution integrated analysis of genetic and expression profiles of breast cancer cell lines. *Breast cancer research and treatment* **118**, 481-98 (2009).

216. Blick, T. et al. Epithelial mesenchymal transition traits in human breast cancer cell lines parallel the CD44(hi/)CD24 (lo/-) stem cell phenotype in human breast cancer. *Journal of mammary gland biology and neoplasia* **15**, 235-52 (2010).

217. Bertucci, F. et al. Identification and validation of an ERBB2 gene expression signature in breast cancers. *Oncogene* **23**, 2564-2575 (2004).

218. Goldman, M. et al. The UCSC Cancer Genomics Browser: update 2013. *Nucleic Acids Res* **41**, D949-54 (2013).

219. Cerami, E. et al. The cBio cancer genomics portal: an open platform for exploring multidimensional cancer genomics data. *Cancer Discov* **2**, 401-4 (2012).

220. Gao, J. et al. Integrative analysis of complex cancer genomics and clinical profiles using the cBioPortal. *Sci Signal* **6**, pl1 (2013).

221. McElwee, J.L. et al. Identification of PADI2 as a potential breast cancer biomarker and therapeutic target. *BMC Cancer* **12**, 500 (2012).

222. Netzer, M., Fang, X., Handler, M. & Baumgartner, C. A coupled three-step network-based approach to identify genes associated with breast cancer. *BIOTECHNO 2012: The Fourth International Conference on Bioinformatics, Biocomputational Systems and Biotechniques*, 1-5 (2012).

223. Agrawal, P., Yu, K., Salomon, A.R. & Sedivy, J.M. Proteomic profiling of Myc-associated proteins. *Cell Cycle* **9**, 4908-21 (2010).

224. Rezaul, K. et al. Differential protein expression profiles in estrogen receptor-positive and -negative breast cancer tissues using label-free quantitative proteomics. *Genes Cancer* **1**, 251-71 (2010).

225. Cherrington, B.D. et al. Comparative analysis of peptidylarginine deiminase-2 expression in canine, feline and human mammary tumours. *J Comp Pathol* **147**, 139-46 (2012).

226. Yoon, S. & Seger, R. The extracellular signal-regulated kinase: multiple substrates regulate diverse cellular functions. *Growth Factors* **24**, 21-44 (2006).

227. Massague, J., Seoane, J. & Wotton, D. Smad transcription factors. *Genes Dev* **19**, 2783-810 (2005).

228. Dardik, R. & Inbal, A. Complex formation between tissue transglutaminase II (tTG) and vascular endothelial growth factor receptor 2 (VEGFR-2): proposed mechanism for modulation of endothelial cell response to VEGF. *Exp Cell Res* **312**, 2973-82 (2006).

229. Lodato, R.F., Maguire, H.C., Jr., Greene, M.I., Weiner, D.B. & LiVolsi, V.A. Immunohistochemical evaluation of c-erbB-2 oncogene expression in ductal carcinoma in situ and atypical ductal hyperplasia of the breast. *Mod Pathol* **3**, 449-54 (1990).

230. Bartkova, J., Barnes, D.M., Millis, R.R. & Gullick, W.J. Immunohistochemical demonstration of c-erbB-2 protein in mammary ductal carcinoma in situ. *Hum Pathol* **21**, 1164-7 (1990).

231. Allred, D.C. et al. Overexpression of HER-2/neu and its relationship with other prognostic factors change during the progression of in situ to invasive breast cancer. *Hum Pathol* **23**, 974-9 (1992).

232. Luo, Y. et al. Inhibitors and inactivators of protein arginine deiminase 4: functional and structural characterization. *Biochemistry* **45**, 11727-36 (2006).

233. Jones, J.E., Causey, C.P., Knuckley, B., Slack-Noyes, J.L. & Thompson, P.R. Protein arginine deiminase 4 (PAD4): Current understanding and future therapeutic potential. *Curr Opin Drug Discov Devel* **12**, 616-27 (2009).

234. Li, P. et al. Coordination of PAD4 and HDAC2 in the regulation of p53-target gene expression. *Oncogene* **29**, 3153-62 (2010).

235. Li, P. et al. Regulation of p53 target gene expression by peptidylarginine deiminase 4. *Mol Cell Biol* **28**, 4745-58 (2008).

236. Slack, J.L., Causey, C.P. & Thompson, P.R. Protein arginine deiminase 4: a target for an epigenetic cancer therapy. *Cell Mol Life Sci* **68**, 709-20 (2011).

237. Willis, V.C. et al. N-alpha-benzoyl-N5-(2-chloro-1-iminoethyl)-L-ornithine amide, a protein arginine deiminase inhibitor, reduces the severity of murine collagen-induced arthritis. *J Immunol* **186**, 4396-404 (2011).

238. Wang, Y. et al. Anticancer peptidylarginine deiminase (PAD) inhibitors regulate the autophagy flux and the mammalian target of rapamycin complex 1 activity. *J Biol Chem* **287**, 25941-53 (2012).

239. Causey, C.P. et al. The development of N-alpha-(2-carboxyl)benzoyl-N(5)-(2-fluoro-1-iminoethyl)-l-ornithine amide (o-F-amidine) and N-alpha-(2-carboxyl)benzoyl-N(5)-(2-chloro-1-iminoethyl)-l-ornithine amide (o-Cl-amidine) as second generation protein arginine deiminase (PAD) inhibitors. *J Med Chem* **54**, 6919-35 (2011).

240. Coughlin, S.S. & Ekwueme, D.U. Breast cancer as a global health concern. *Cancer Epidemiol* **33**, 315-8 (2009).

CHAPTER TWO

IDENTIFICATION OF PADI2 AS A POTENTIAL BREAST CANCER BIOMARKER AND THERAPEUTIC TARGET

* Manuscript from: John L. McElwee; Sunish Mohanan; Obi L. Griffith; Heike C. Breuer; Lynne J. Anguish; Brian D. Cherrington; Ashley M. Palmer; Louise R. Howe; Venkataraman Subramanian; Corey P. Causey; Paul R. Thompson; Joe W. Gray and Scott A. Coonrod. Identification of PADI2 as a potential breast cancer biomarker and therapeutic target. *BMC Cancer*. (2012) Oct 30; 12:500.

2.1 Summary

Introduction:

We have recently reported that the expression of peptidylarginine deiminase 2 (PADI2) is regulated by EGF in mammary cancer cells and appears to play a role in the proliferation of normal mammary epithelium; however, the role of PADI2 in the pathogenesis of human breast cancer has yet to be investigated. Thus, the goals of this study were to examine whether PADI2 plays a role in mammary tumor progression, and whether the inhibition of PADI activity has anti-tumor effects.

Methods:

RNA-seq data from a collection of 57 breast cancer cell lines was queried for PADI2 levels, and correlations with known subtype and HER2/ERBB2 status were evaluated. To examine PADI2 expression levels during breast cancer progression, the cell lines from the MCF10AT model were used. The efficacy of the PADI inhibitor, Cl-amidine, was tested *in vitro* using MCF10DCIS cells grown in 2D-monolayers and 3D-spheroids, and *in vivo* using MCF10DCIS tumor xenografts. Treated MCF10DCIS cells were examined by flow-cytometry to determine the extent of apoptosis and by RT^2 Profiler PCR Cell Cycle Array to detect alterations in cell cycle associated genes.

Results:

We show by RNA-seq that *PADI2* mRNA expression is highly correlated with *HER2/ERBB2* ($p = 2.2x10^{-6}$) in luminal breast cancer cell lines. Using the MCF10AT model of breast cancer progression, we then demonstrate that PADI2 expression increases during the transition of normal mammary epithelium to fully malignant breast carcinomas, with a strong peak of PADI2 expression and activity being observed in the MCF10DCIS cell line, which models human comedo-DCIS lesions.

Next, we show that a PADI inhibitor, Cl-amidine, strongly suppresses the growth of MCF10DCIS monolayers and tumor spheroids in culture. We then carried out preclinical studies in nude (nu/nu) mice and found that Cl-amidine also suppressed the growth of xenografted MCF10DCIS tumors by more than 3-fold. Lastly, we performed cell cycle array analysis of Cl-amidine treated and control MCF10DCIS cells, and found that the PADI inhibitor strongly affects the expression of several cell cycle genes implicated in tumor progression, including *p21*, *GADD45α*, and *Ki67*.

Conclusion:

Together, these results suggest that PADI2 may function as an important new biomarker for HER2/ERBB2+ tumors and that Cl-amidine represents a new candidate for breast cancer therapy.

Key words: Peptidylarginine deiminase, PAD2/PADI2, HER2/ERBB2, Breast Cancer, Luminal, Cl-amidine, Citrullination

2.2 Introduction

PADIs are a family of posttranslational modification enzymes that convert positively charged arginine residues on substrate proteins to neutrally charged citrulline, and this activity is alternatively called citrullination or deimination. The PADI enzyme family is thought to have arisen by gene duplication and localizes within the genome to a highly organized cluster at 1p36.13 in humans. At the protein level, each of the five well-conserved PADI members shows a relatively distinct pattern of substrate specificity and tissue distribution [1, 2]. Increasingly, the dysregulation of PADI activity is associated with a range of diseases, including rheumatoid arthritis (RA), multiple sclerosis, ulcerative colitis, neural degeneration, COPD, and cancer [3-5]. While the presumptive function of PADI activity in most diseases is linked to inflammation, the role that PADIs play in cancer progression is not clear. We and others, however, have found that PADI4 appears to play a role in gene regulation in cancer cells via histone tail citrullination. For example, in MCF7 breast cancer cells estrogen stimulation enhances PADI4 binding and histone H4 citrullination at the canonical ER target gene, *TFF1,* leading to transcriptional repression [6]. On the other hand, stimulation of MCF7 cells with EGF facilitates activation of *c-fos* via PADI4-mediated citrullination of the ELK1 oncogene [7]. Additionally, others have shown that citrullination of the p53 tumor suppressor protein affects the expression of p53 target genes *p21*, *OKL38*, *CIP1* and *WAF1* [8-10]. Interestingly, treatment of several PADI4-expressing cancer cell lines with the PADI inhibitor, Cl-amidine, elicited strong cytotoxic effects while having no observable effect on non-cancerous lines [11], suggesting that PADIs may represent targets for new cancer therapies.

Our current study suggests that PADI2 may also play a role in cancer progression, and this prediction is supported by several previous studies. For example, a mouse transcriptomics study investigating gene expression in MMTV-neu tumors

found that *PADI2* expression was upregulated ~2-fold in hyperplastic, and ~4-fold in primary neu-tumors, when compared to matched normal mammary epithelium [12]. In humans, *PADI2* is one of the most upregulated genes in luminal breast cancer cell lines compared to basal lines [13, 14]. Additionally, gene expression profiling of 213 primary breast tumors with known HER2/ERBB2 status identified *PADI2* as one of 29 overexpressed genes in HER2/ERBB2+ tumors; thus, helping to define a HER2/ERBB2+ gene expression signature [15]. Given these previous studies, our goal was to formally test the hypothesis that PADI2 plays a role in mammary tumor progression. For the study, we first documented PADI2 expression and activity during mammary tumor progression, and then investigated the effects of PADI inhibition in cell cultures, tumor spheroids, and preclinical *in vivo* models of breast cancer.

2.3 Materials and Methods

Cell culture and treatment with Cl-amidine

The MCF10AT cell line series (MCF10A, MCF10AT1kC1.2, MCF10DCIS.com, and MCF10CA1aC1.1) was obtained from Dr. Fred Miller (Barbara Ann Karmanos Cancer Institute, Detroit, MI, USA). This biological system has been extensively reviewed [16, 17] and culture conditions described [18-20]. The MCF7, BT-474, SK-BR-3, and MDA-MB-231 cell lines were from obtained from ATCC (Manassas, VA, USA) and cultured according to manufacturer's directions. All cells were maintained in a humidified atmosphere of 5% CO_2 at 37^o C. For the experimental treatment of cell lines with Cl-amidine, cells were seeded in 6-well plates (2×10^4) and collected by trypsinization 5d post-treatment. Counts were performed using a Coulter counter (Beckman Coulter, Fullerton, CA, USA) and are represented as mean fold difference in cell number after treatment. Cl-amidine was synthesized as previously described [21].

MMTV mice and the generation of MCF10DCIS xenografts and multicellular tumor spheroids

Tissues from the MMTV-neu mouse were a generous gift from Dr. Robert S. Weiss, Cornell University, and the MMTV-*Wnt-1* hyperplastic mammary glands and tumors were a gift of Dr. Louise R. Howe, Weill Cornell Medical College. MCF10DCIS xenograft tumors were generated by injecting 1 x 10^6 cells in 0.1 mL Matrigel (1:1) (BD Biosciences, San Jose, CA, USA) subcutaneously near the nipple of gland #3 in 6-week old female nude (nu/nu) mice (Taconic, Germantown, NY, USA). When the tumors reached ~200 mm^3, intraperitoneal injections of Cl-amidine (50 mg/kg/day) or vehicle control (PBS) were initiated and carried out for 14 days. Tumor volume was calculated by the formula: (mm^3) = ($d^2 \times D$)/2, where "d" and "D" are the shortest and longest diameters of the tumor, respectively. Tumor volume was measured weekly by digital caliper, and the differences between tumor volumes were evaluated by the non-parametric Mann–Whitney–Wilcoxon (MWW) test. Results are reported as mean ± SD. After 14 days, tumors were removed and either snap-frozen, placed in RNAlater (Qiagen Inc., Valencia, CA, USA), or added to 10% buffered formalin. Seven mice per group were used for each treatment. All mouse experiments were reviewed and approved by the Institutional Animal Care and Use Committees (IACUC) at Cornell University. Multicellular tumor spheroids were generated using the liquid overlay technique as previously described [22-24]. The spheroids were allowed to form over 48h and maintained up to 6–10 days for morphological analysis, then collected, rinsed with phosphate buffered saline, and fixed in 10% buffered formalin.

Assay of PADI activity

Cell lines were assayed for PADI activity as previously described [25, 26]. Briefly, citrulline levels were determined using BAEE (α-N-benzoyl-L-arginine ethyl ester) as

a substrate. After incubating lysates for 1h at 50°C with BAEE substrate mixture, the reaction was stopped by the addition of perchloric acid. The perchloric acid-soluble fraction was subjected to a colorimetric reaction with citrulline used as a standard and absorbance measured at 464 nm.

Immunohistochemistry (IHC) and immunofluorescence (IF)

IHC and IF experiments were carried out using a standard protocol as previously described [27]. Primary antibodies are as follows: anti-PADI2 1:100 (ProteinTech, Chicago, IL, USA), anti-ERBB2 (A0485) 1:100 (Dako, Carpentaria, CA, USA), anti-Cytokeratin 1:100 (Dako), and anti-p63 1:100 (Abcam, Cambridge, MA, USA). Sections prepared for IHC were incubated in DAB chromagen solution (Vector Laboratories, Burlingame, CA, USA) according to the manufacturer's protocol, washed, and then counterstained with hematoxylin. The IF slides were incubated in streptavidin conjugated-488 (Invitrogen, Carlsbad, CA, USA), washed, and then mounted using Vectashield containing DAPI (Vector Laboratories). Negative controls for both IHC and IF experiments were either rabbit or mouse IgG antibody at the appropriate concentrations. Tumor sections were examined for general morphological differences after hematoxylin and eosin (H&E) staining. Basement membrane integrity was determined using periodic acid-Schiff (PAS) stained slides, and was scored by SM on a scale of 0-3: 0- continuous with no breaching, 1- a few small interruptions, 2- several interruptions with breaching by tumor cells, 3- extensive loss of basement membrane with invasion of tumor cells over the breached area; observations were performed under 10X magnification.

Immunoblotting

Immunoblotting was carried out as previously described [27]. Primary antibodies were incubated overnight at 4°C using the following concentrations: anti-PADI2 1:1000 (ProteinTech) and anti-ErbB2 1:5000 (Dako). To confirm equal protein loading, membranes were stripped and re-probed with anti-β-actin 1:5000 (Abcam).

Quantitative Real-Time PCR (qRT-PCR)

RNA was purified using the Qiagen RNAeasy kit, including on-column DNAse treatment to remove genomic DNA. The resulting RNA was reverse transcribed using the ABI High Capacity RNA to cDNA kit according to the manufacturer's protocol (Applied Biosystems, Foster City, CA, USA). TaqMan Gene Expression Assays (ABI) for human PADI2 (Hs00247108_m1) and GAPDH (4352934E) were used for qRT-PCR. Data were analyzed by the $2^{-\Delta\Delta C(t)}$ method [28]. Data are shown as means ± SD from three independent experiments, and were separated using Student's t-test. For the analysis of cell cycle gene expression, cDNA was synthesized (RT^2 First Strand Kit, Qiagen) and samples analyzed for expression of 84 genes involved in cell cycle regulation by RT^2 Profiler PCR Cell Cycle Array (PAHS-020A, Qiagen). For data analysis, the RT^2 Profiler PCR Array software package was used and statistical analyses performed (n = 3). This package uses $\Delta\Delta C_T$–based fold change calculations and the Student's t-test to calculate two-tail, equal variance p-values.

Flow-cytometry

Monolayers of MCF10DCIS and MCF10A cells were seeded into 25 cm^2 flasks (2 x 10^6 cells) and treated with either Cl-amidine (200 μM or 400 μM), or 10μg/mL tunicamycin (apoptosis positive control). BT-474, SK-BR-3, and MDA-MB-231 cell lines were treated as previously described for MCF10DCIS and MCF10A; however,

they were also treated with 100 μM Cl-amidine. Cells were harvested after 4d using Accutase (Innovative Cell Technologies, Inc, San Diego, CA, USA), fixed, then permeabilized, and blocked in FACS Buffer (0.1M Dulbecco's phosphate buffered saline, 0.02% sodium azide, 1.0% bovine serum albumin, and 0.1% Triton X-100) containing 10% normal goat serum and stained (except the isotype controls) with rabbit anti-cleaved Caspase-3 antibody (Cell Signaling Technology, Inc, Danvers, MA, USA). Isotype controls were treated with normal rabbit IgG (Vector Laboratories) at 4 μg/mL. All samples were stained with secondary goat anti-rabbit IgG conjugated to Alexa-488 (Invitrogen) and DAPI (Invitrogen) according to the manufacturer's instructions. Cells were analyzed on a FACS-Calibur (BD Biosciences) or a Gallios (Beckman Coulter) flow-cytometer and data analyzed for percent apoptotic cells (cleaved Caspase-3+) and cell cycle analysis with FlowJo software (TreeStar, Inc, Ashland, OR, USA). Data are shown as means ± SD from three independent experiments, and were separated using Student's t-test.

RNA-seq analysis of breast cancer cell lines

Whole transcriptome shotgun sequencing (RNA-seq) was completed on breast cancer cell lines and expression analysis was performed with the ALEXA-seq software package as previously described [29]. Briefly, this approach comprises (i) creation of a database of expression and alternative expression sequence 'features' (genes, transcripts, exons, junctions, boundaries, introns, and intergenic sequences) based on Ensembl gene models, (ii) mapping of short paired-end sequence reads to these features, (iii) identification of features that are expressed above background noise while taking into account locus-by-locus noise. RNA-seq data were available for 57 lines (17 basal, 5 basal-NM, 6 claudin-low, 29 luminal). An average of 70.6 million (76bp paired-end) reads passed quality control per sample. Of these, 53.8 million reads

mapped to the transcriptome on average, resulting in an average coverage of 48.2 across all known genes. Log2 transformed estimates of gene-level expression were extracted for analysis with corresponding expression status values indicating whether the genes were detected above background level.

Statistical analysis

All experiments were independently repeated at least three times unless otherwise indicated. Values were expressed as the mean ± the SD. Means were separated using Student's t-test or by Mann-Whitney-Wilcoxon (MWW) test, with a p-value less than 0.05 considered as significantly different. Subtype specific expression in the RNA-seq analysis was determined by Wilcoxon signed-rank test. Correlations were determined by Spearman rank correlation. Genes were considered significantly differentially expressed or correlated if they had a p-value less than 0.05.

2.4 Results

PADI2 is overexpressed in transformed cells of the MCF10AT model of breast cancer progression

In order to investigate PADI2 expression during tumor progression, we first utilized TaqMan quantitative real-time PCR (qRT-PCR) to measure *PADI2* mRNA levels in cells from the MCF10AT tumor progression series (**Figure 2.1a**). As shown previously, these cell lines closely model the progression from normal (MCF10A), to hyperplastic (MCF10AT), to ductal carcinoma *in situ* (DCIS) with necrosis (MCF10DCIS.com), and finally to invasive/metastatic (MCF10CA1) breast cancer [16, 17, 30]. Results (**Figure 2.1b**) show that *PADI2* mRNA expression is elevated in the transformed cell lines, with the highest levels found in the comedo-DCIS MCF10DCIS.com cell line (hereafter MCF10DCIS). Additionally, PADI2 protein

levels closely correlated with *PADI2* mRNA levels across these lines, with the highest levels of PADI2 protein observed in the MCF10DCIS line. Given the previous microarray studies correlating *PADI2* expression with *HER2/ERBB2*, we also probed this cell line series with a well-characterized HER2/ERBB2 antibody and found that HER2/ERBB2 levels were also elevated in the transformed cell lines compared to the more normal MCF10A line (**Figure 2.1c**). We also tested whether the increase in PADI2 expression correlated with PADI2 enzymatic activity, with results (**Figure 2.1d**) showing that citrulline levels are, in fact, highest in the MCF10DCIS cell line; therefore, indicating a strong correlation between increased PADI2 expression and enzymatic activity. While these cell lines have been classified previously as basal-like [31], both MCF10A and MCF10DCIS have been shown to possess bipotential progenitor properties [19, 32, 33]. Furthermore, the MCF10AT cells have been reported to show the same multipotent properties [34], but until recently, there has only been one other report showing that HER2/ERBB2 is upregulated in the transformed lines of this series [35]. These data suggest that PADI2 activity may play a role in mammary tumor progression and that PADI2-mediated citrullination may be particularly relevant to comedo-DCIS biology.

Levels of PADI2 correlate with the luminal breast cancer subtype and HER2/ERBB2 overexpression

To test whether PADI2 displays a restricted expression pattern with respect to breast cancer subtype, we next investigated *PADI2* mRNA and protein expression in cell lines representing four common breast cancer subtypes: MCF7 (luminal A), BT-474 (luminal B), SK-BR-3 (HER2/ERBB2+), and MDA-MB-231 (basal). At the protein level, PADI2 was observed in both BT-474 (ER+, PR+, HER2/ERBB2+) and SK-BR-3 (ER-, PR-, and HER2/ERBB2 overexpressing) cell lines. Interestingly, the

Figure 2.1: PADI2 expression is highest in MCF10DCIS.com cells in the MCF10AT model of breast cancer progression. (a) The MCF10AT model is a series of cell lines that recapitulates the transition from normal epithelium to malignant carcinoma. (b and c) *PADI2* mRNA and protein expression is increased in transformed cells of the MCF10AT model, with very high levels seen in MCF10DCIS cells. Total RNA was isolated and *PADI2* mRNA levels were determined by qRT-PCR (TaqMan) using MCF10A cells as a reference and *GAPDH* normalization. Data were analyzed using the $2^{-\Delta\Delta C(t)}$ method and are expressed as the mean ± SD from three independent experiments (* $p < 0.001$). PADI2 expression levels were evaluated by subjecting whole cell lysates to SDS-PAGE and immunoblot analysis using an anti-PADI2 antibody. HER2/ERBB2 expression levels, detected using an anti-HER2 antibody, are also upregulated in the transformed cell lines when compared to the MCF10A levels. The blot was stripped and equal protein loading was determined by probing with a β-actin antibody. (d) Citrulline levels in the cell lines were determined by citrullination enzymatic assays, with the highest level of activity measured in the MCF10DCIS cells. Briefly, cell lysates were incubated with PADI substrate BAEE, and the reaction stopped with perchloric acid. The perchloric acid-soluble fraction was subjected to a colorimetric reaction with citrulline used as a standard and absorbance measured at 464 nm.

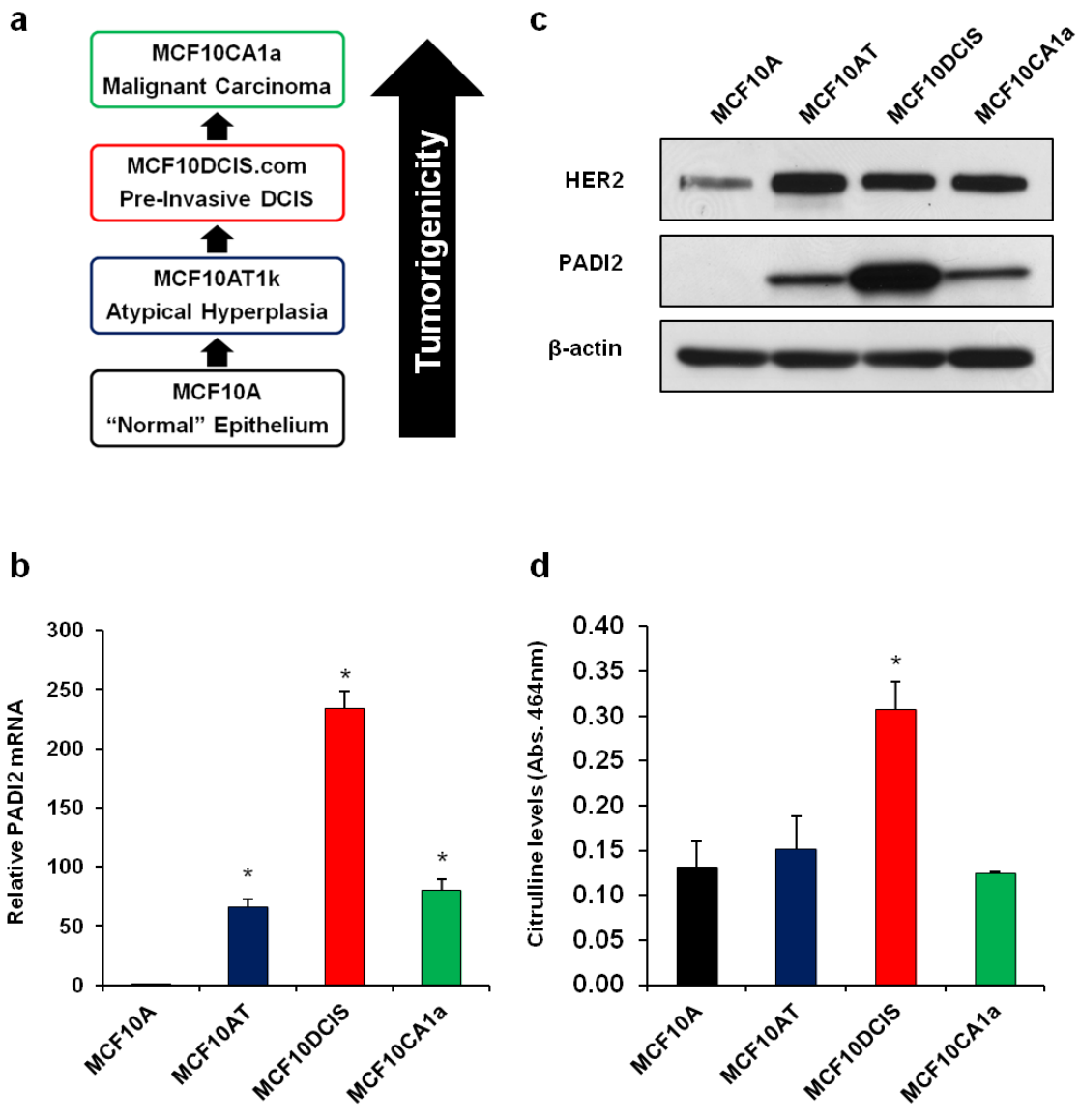
a
MCF10CA1a
Malignant Carcinoma
MCF10DCIS.com
Pre-Invasive DCIS
MCF10AT1k
Atypical Hyperplasia
MCF10A
"Normal" Epithelium
Tumorigenicity
c
MCF10A
MCF10AT
MCF10DCIS
MCF10CA1a
HER2
PADI2
β-actin
b
Relative PADI2 mRNA
300
250
200
150
100
50
0
MCF10A
MCF10AT
MCF10DCIS
MCF10CA1a
d
Citrulline levels (Abs. 464nm)
0.40
0.35
0.30
0.25
0.20
0.15
0.10
0.05
0.00
MCF10A
MCF10AT
MCF10DCIS
MCF10CA1a

comparison of PADI2 and HER2/ERBB2 protein levels across these four cell lines supports the hypothesis that these two proteins are coexpressed (**Figure 2.2a**). While the PADI2 protein expression is not observed in MCF7 cells in **Figure 2.2a**, a longer exposure of this film finds that PADI2 is weakly expressed in these cells (**Figure 2.3a**). Analysis of *PADI2* transcript levels in these lines finds that, as expected, *PADI2* mRNA is sharply elevated in the BT-474 line (**Figure 2.2b**), and is ~2 fold higher that that seen in the MCF10DCIS cells (**Figure 2.3b**) when compared to MCF10A cells. To test whether PADI2 expression is elevated in HER2/ERBB2 expressing cells *in vivo*, we next measured *PADI2* mRNA in normal murine mammary epithelium and in primary mammary tumors collected from MMTV-neu mice. Results indicate *PADI2* mRNA levels are ~15-fold higher in the HER2/ERBB2 overexpressing tumors compared to normal mammary tissue from littermate controls (**Figure 2.2c**). The ~15-fold increase in *PADI2* expression found in our study, compared to the ~4-fold increase found in the previous study [12], may simply reflect technical differences between the studies as we utilized TaqMan qRT-PCR compared to microarray analysis. We also investigated the level of *PADI2* mRNA in MMTV-*Wnt-1* mice, which is a basal mouse model of breast cancer [36-38]. The MMTV-*Wnt-1* model is unique in that it exhibits discrete steps in mammary tumorigenesis; the mammary glands are first hyperplastic, and then advance to invasive ductal carcinomas, finally culminating in fully malignant carcinomas that undergo metastasis [39]. Interestingly, we see that PADI2 levels are higher in the hyperplastic mammary glands (**Figure 2.2c**) when compared to normal mammary glands; however, the levels are less than those seen in the MMTV-neu tumors and are further reduced in the fully malignant MMTV-*Wnt-1* tumors.

To strengthen the hypothesis that PADI2 is primarily expressed in luminal breast cancer cell lines and is coexpressed with HER2/ERBB2, we next investigated

Figure 2.2: PADI2 expression is elevated in luminal B BT-474 cells, murine MMTV-neu tumors, and is correlated with the luminal subtype. (a) Four different breast cancer cell lines were selected to represent the common subtypes of breast cancer: MCF7 (luminal A), BT-474 (luminal B), SK-BR-3 (HER2/ERBB2+), and MDA-MD-231 (basal). Immunoblotting shows PADI2 protein expression is highest in both of the HER2/ERBB2 overexpressing cell lines, with the highest level seen in the luminal B BT-474 cells (ER+/PR+). (b) Relative *PADI2* mRNA levels in the cell lines compared to MCF10A. (c) Tumors from MMTV-neu mice (luminal subtype) show a ~15-fold increase in *PADI2* compared to normal mammary tissue. Both MMTV-*Wnt-1* hyperplastic mammary tissue and tumors (basal subtype) show elevated levels of *PADI2* compared to normal mammary tissue; however, *PADI2* expression levels in MMTV-*Wnt-1* tumors are ~10-fold less than those seen in the MMTV-neu tumors. *PADI2* mRNA levels were determined by qRT-PCR (TaqMan) using MCF10A cells as a reference and *GAPDH* normalization. Expression levels were analyzed using the $2^{-\Delta\Delta C(t)}$ method, and data are expressed as the mean ± SD from three independent experiments (* $p < 0.05$, ** $p < 1 \times 10^{-6}$). (d) RNA-seq analysis of 57 breast cancer cell lines shows that *PADI2* expression is significantly higher in luminal lines versus basal (* $p = 0.007$) and higher in basal versus basal-NM/claudin-low (** $p = 0.002$).

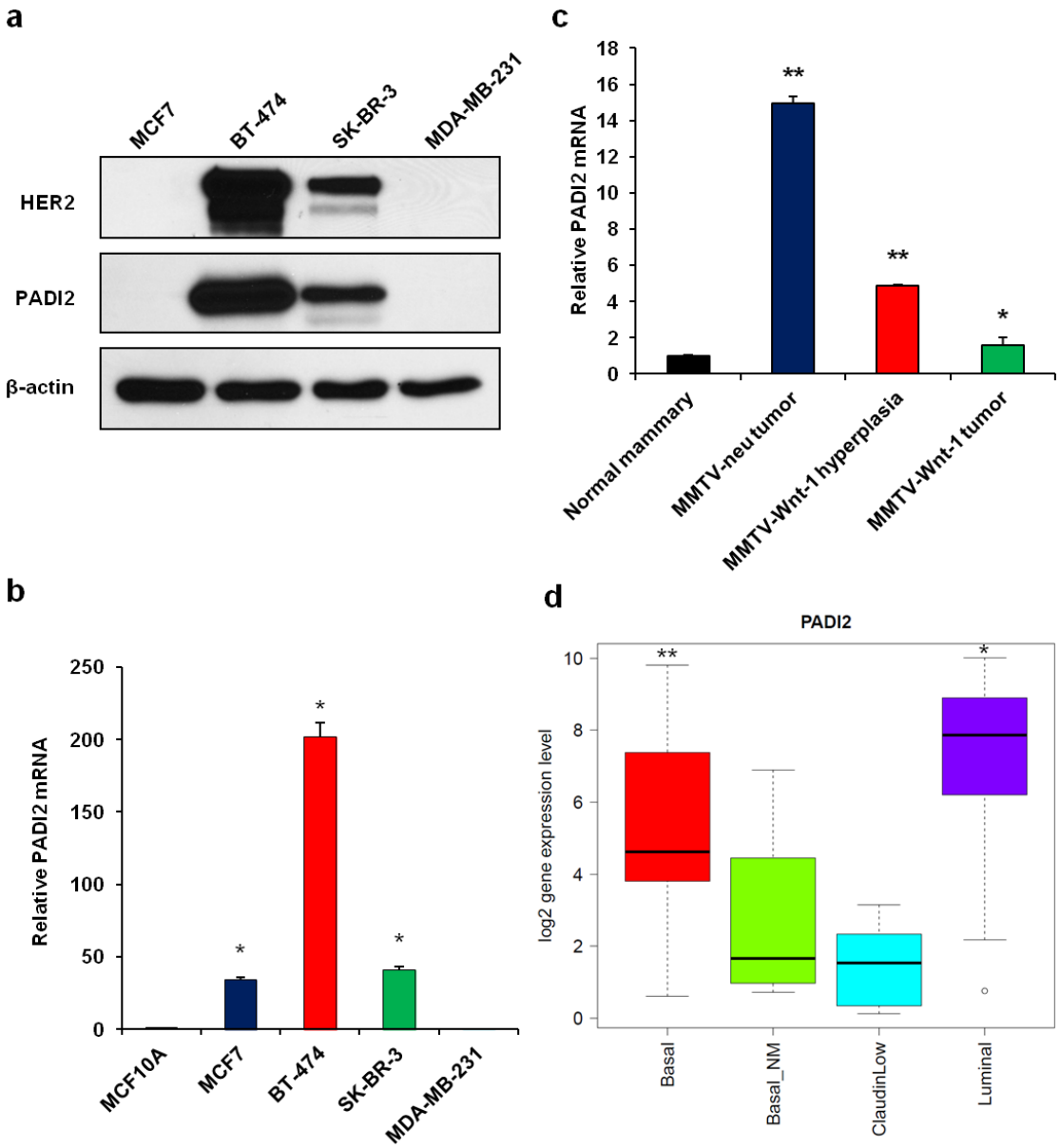
a
MCF7
BT-474
SK-BR-3
MDA-MB-231
HER2
PADI2
β-actin
c
Relative PADI2 mRNA
Normal mammary
MMTV-neu tumor
MMTV-Wnt-1 hyperplasia
MMTV-Wnt-1 tumor
b
Relative PADI2 mRNA
MCF10A
MCF7
BT-474
SK-BR-3
MDA-MB-231
d
PADI2
log2 gene expression level
Basal
Basal_NM
ClaudinLow
Luminal

<u>Figure 2.3:</u> Comparative expression levels of MCF10DCIS and HER2/ERBB2 expressing BT-474 and SK-BR-3 cell lines. (a) Overexposure of image in Figure 2a, showing that there are low levels of PADI protein found in the MCF7 cell line. (b) MCF10DCIS *PADI2* levels are about half that of BT-474 cells, with SK-BR-3 *PADI2* levels being about half of MCF10DCIS cells. These *PADI2* levels recapitulate the relationship seen at the protein level. Total RNA was isolated from MCF10A, MCF10DCIS, BT-474, and SK-BR-3 cell lines and *PADI2* mRNA levels were determined by qRT-PCR (TaqMan) using MCF10A cells as a reference and *GAPDH* normalization. Data were analyzed using the $2^{-\Delta\Delta C(t)}$ method and are expressed as the mean ± SD from three independent experiments (* $p < 0.005$).

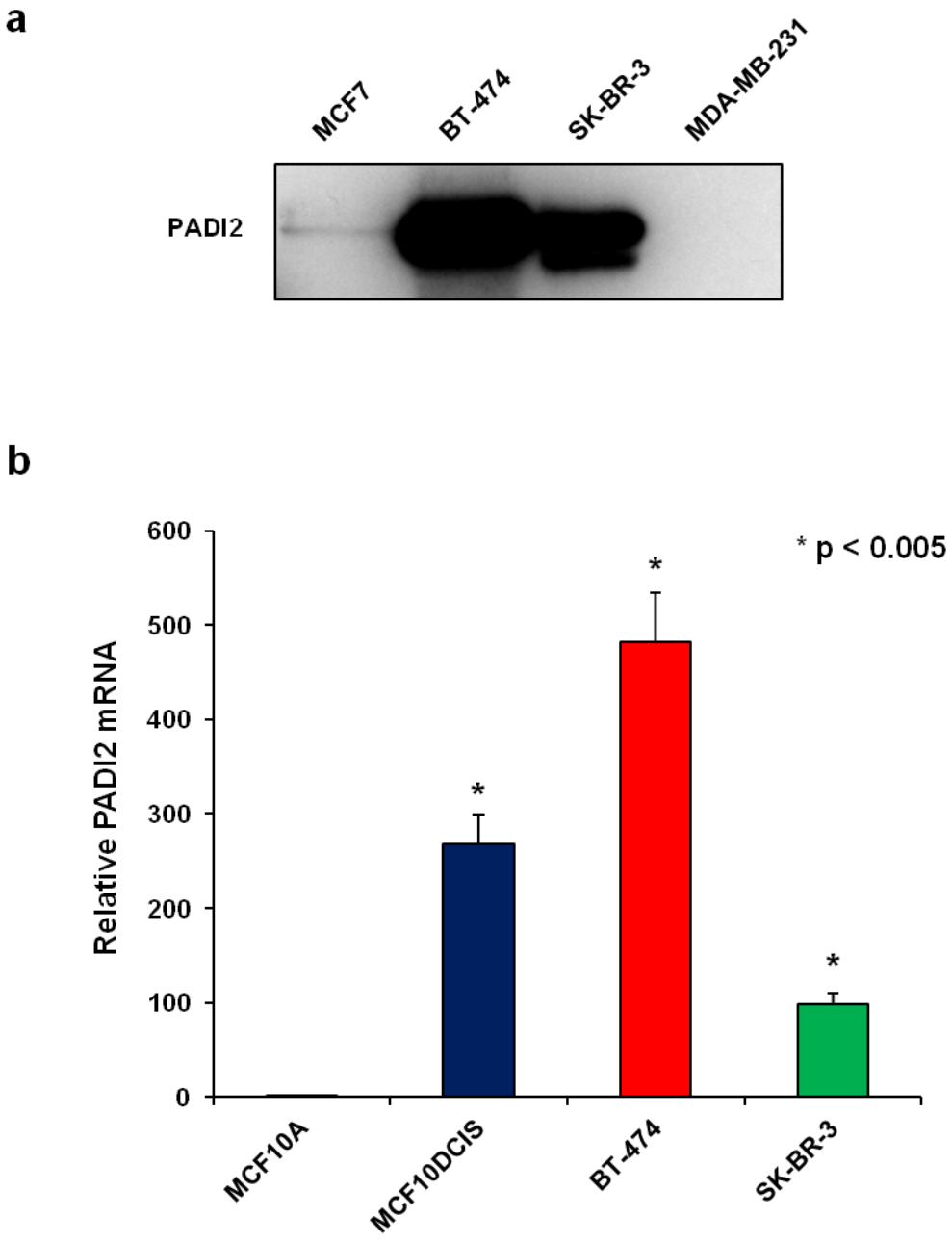
a
MCF7
BT-474
SK-BR-3
MDA-MB-231
PADI2
b
* p < 0.005
Relative PADI2 mRNA
600
500
400
300
200
100
0
MCF10A
MCF10DCIS
BT-474
SK-BR-3

PADI2 mRNA levels by querying RNA-seq datasets collected from 57 breast cancer cell lines. A summary of *PADI2* expression in these lines is shown in the **Figure 2.4**, with the most significant difference ($p = 3.59 \times 10^{-5}$) in *PADI2* expression across subtypes being found when luminal lines were compared with all non-luminal subtypes (**Figure 2.2d**). We then quantified the correlation between *PADI2* and *HER2/ERBB2* expression across the 57 cell lines. Results show that the correlation between *PADI2* and *HER2/ERBB2* overexpression is highly significant across the luminal, basal-NM (non-malignant), and claudin-low cell lines ($rho = 0.828$, $p = 2.2 \times 10^{-16}$) (**Figure 2.5**). Interestingly, a correlation between *PADI2* and *HER2/ERBB2* expression was not observed across the basal cell lines. In contrast, a significant anti-correlation was observed ($rho = -0.495$, $p = 0.045$), suggesting that the expression of these genes may be regulated by different mechanisms in these cell lines. Lastly, we queried the RNA-seq dataset to determine which genes were best correlated with *HER2/ERBB2* and *PADI2* expression in the luminal, basal-NM, and claudin-low lines to assess the relative strength of their coexpression. Only a single gene (*CCL17*) was as correlated with *PADI2* as *HER2/ERBB2* ($rho = 0.832$, $p = 2.2 \times 10^{-16}$), and *PADI2* represented the 13th most highly correlated gene with *HER2/ERBB2* (**Table 2.1**), thus suggesting co-regulation between HER2/ERBB2 and PADI2.

Inhibition of PADI activity reduces cellular proliferation in breast cancer cell lines

To investigate whether PADI2 expression is important for breast cancer cell proliferation, we next tested whether the pharmacological inhibition of PADI2 activity negatively affects the growth of tumor cells *in vitro.* We utilized the small molecule inhibitor Cl-amidine for this study because we have previously shown that this drug binds irreversibly to the active site of PADIs, thereby blocking activity *in vitro* and *in vivo* [40]. Cl-amidine functions as a "pan-PADI" inhibitor as it blocks the activity of all

Figure 2.4: ***PADI2*** **gene-level expression compared to distribution of all genes across 57 breast cancer cell lines.** Box-and-whisker plot of *PADI2* mRNA expression levels across 57 breast cancer cell lines were measured by RNA-seq. *PADI2* levels (black circles) are shown relative to all other genes in each cell line (interquartile range – colored boxes according to different subtype). *PADI2* is most highly expressed in the luminal lines (26/29 above background – black circles located in the upper quartile). PADI2 levels are significantly different in luminal cell lines when compared to all non-luminal cell lines ($p = 3.59 \times 10^{-5}$). (open circles = outliers)

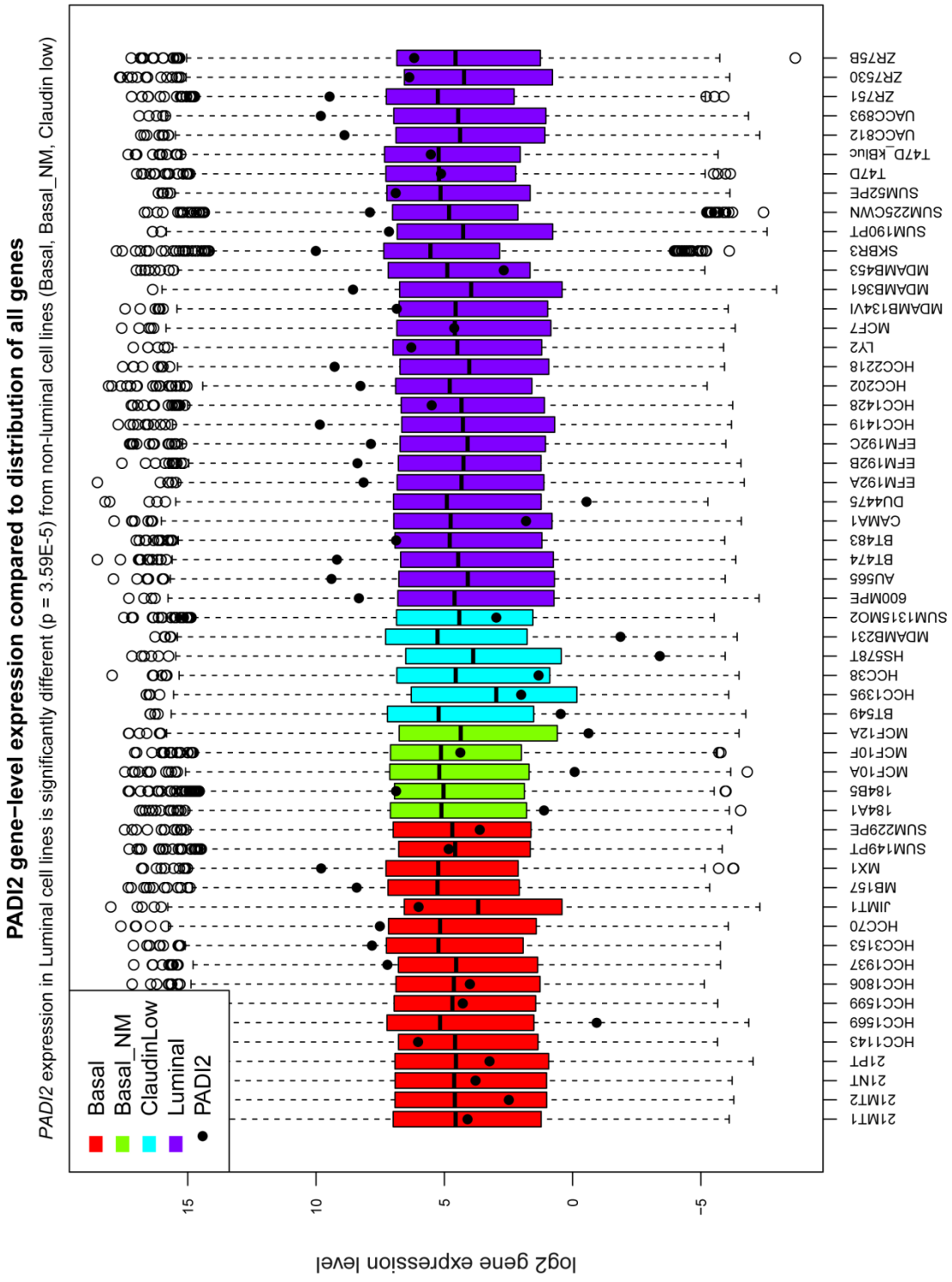
PADI2 gene−level expression compared to distribution of all genes
PADI2 expression in Luminal cell lines is significantly different (p = 3.59E-5) from non-luminal cell lines (Basal, Basal_NM, Claudin low)
Basal
Basal_NM
ClaudinLow
Luminal
PADI2
log2 gene expression level
15
10
5
0
−5
21MT1
21MT2
21NT
21PT
HCC1143
HCC1569
HCC1599
HCC1806
HCC1937
HCC3153
HCC70
JIMT1
MB157
MX1
SUM149PT
SUM229PE
184A1
184B5
MCF10A
MCF10F
MCF12A
BT549
HCC1395
HCC38
HS578T
MDAMB231
SUM1315MO2
600MPE
AU565
BT474
BT483
CAMA1
DU4475
EFM192A
EFM192B
EFM192C
HCC1419
HCC1428
HCC202
HCC2218
LY2
MCF7
MDAMB134VI
MDAMB361
MDAMB453
SKBR3
SUM190PT
SUM225CWN
SUM52PE
T47D
T47D_kBluc
UACC812
UACC893
ZR751
ZR7530
ZR75B

Figure 2.5: RNA-seq analysis of *PADI2* expression across 57 breast cancer cell lines shows subtype specific expression and high correlation with *HER2/ERBB2*. The Spearman correlation between *PADI2* and *HER2/ERBB2* overexpression was highly significant across the luminal, basal-NM, and claudin-low cell lines (rho = 0.828, $p = 2.2 \times 10^{-16}$). A significant anti-correlation between *PADI2* and *HER2/ERBB2* was observed across the basal cell lines (rho = -0.495, p = 0.045).

Basal cell lines PADI2-ERBB2 correlation
(rho = -0.0495, p = 0.0454)
Basal-NM, Claudin-low, and Luminal cell lines PADI2-ERBB2 correlation
(rho = 0.828, p = 2.2E-16)
Basal
rho = −0.556
p = 0.0276
Basal-NM
rho = 0.4
p = 0.517
Claudin-low
rho = 0.371
p = 0.497
Luminal
rho = 0.66
p = 0.000144
Log2 Gene Expression Level
0
5
10
15
ERBB2
PADI2
21MT1
21MT2
21NT
21PT
HCC1143
HCC1569
HCC1599
HCC1806
HCC1937
HCC3153
HCC70
JIMT1
MB157
MX1
SUM149PT
SUM229PE
184A1
184B5
MCF10A
MCF10F
MCF12A
BT549
HCC1395
HCC38
HS578T
MDAMB231
SUM1315MO2
600MPE
AU565
BT474
BT483
CAMA1
DU4475
EFM192A
EFM192B
EFM192C
HCC1419
HCC1428
HCC202
HCC2218
LY2
MCF7
MDAMB134VI
MDAMB361
MDAMB453
SKBR3
SUM190PT
SUM225CWN
SUM52PE
T47D
T47D_KBluc
UACC812
UACC893
ZR751
ZR7530
ZR75B

Table 2.1: Top genes that correlate with *HER2/ERBB2* expression. Genes identified by RNA-seq to be upregulated in HER2/ERBB2+ breast cancers were tested for correlation (Spearman's rho) and the top 13 genes are ranked from top to bottom, with *PADI2* exhibiting the 13th strongest correlation with *HER2/ERBB2* overexpression.

Table 2.1: Top genes correlating with *HER2/ERBB2* expression

Symbol	*Description*	*rho*
PGAP3	Post-GPI attachment to proteins 3 (PERLD1)	0.941
CREB3L3	CAMP responsive element binding protein 3-like 3	0.927
C2orf54	Chromosome 2 open reading frame 54	0.860
EFCAB4A	EF-hand calcium binding domain 4A	0.857
ARHGAP8	Rho GTPase activating protein 8	0.852
GRB7	Growth factor receptor-bound protein 7	0.851
TMEM210	Transmembrane protein 210	0.849
CLDN4	Claudin 4	0.847
MB	Myoglobin	0.846
ELF3	E74-like factor 3 (ets domain transcription factor, epithelial-specific)	0.842
TRIM3	Tripartite motif containing 3	0.839
PRSS8	Protease, serine, 8	0.829
PADI2	Peptidyl arginine deiminase, type II	0.828

active PADI family members (i.e. PADIs 1-4) with varying degrees of specificity [41]. Cultures from the MCF10AT cell line series were treated with 10, 50, or 200 μM of Cl-amidine, and the effects of the inhibitor on cell proliferation were quantified. Results showed a dose-dependent decrease in the growth of all cell lines. Additionally, given that 200 μM Cl-amidine decreased the growth of MCF10DCIS cells by 75% (**Figure 2.6a**), this cell line appeared to be particularly affected by the inhibitor. Given the high level of PADI2 expression in the MCF10DCIS line, this finding suggests that PADI2 is likely playing an important role in the growth of MCF10DCIS cells. Importantly, while Cl-amidine also suppressed the growth of MCF10DCIS cells at lower concentrations, these doses did not inhibit the growth of the non-tumorigenic "normal" MCF10A line. These data suggest that Cl-amidine is not generally cytotoxic. In addition, citrulline levels in the Cl-amidine treated MCF10DCIS cells were significantly reduced, suggesting that the inhibitory effect of Cl-amidine was specifically due to the blockade of PADI activity (**Figure 2.6b**). In order to test the potential anti-tumor efficacy of Cl-amidine in a physiological model, we investigated the effects of this inhibitor on the growth of MCF10DCIS tumor spheroids. Spheroids grown from this cell line have been shown by others to form acinar-like structures that closely recapitulate the comedo-DCIS lesions that form in MCF10DCIS xenografts [18, 20, 42]. Results from our studies found that Cl-amidine treatment significantly reduces tumor spheroid diameter (**Figure 2.6c**). Representative images of the effects of Cl-amidine on the growth of MCF10DCIS monolayers and spheroids are shown in **Figure 2.6d**.

Cl-amidine alters the expression of cell cycle associated genes and induces apoptosis

The observed effects of Cl-amidine on cell proliferation suggested that this drug might affect tumor growth by altering the expression of genes involved in cell cycle

Figure 2.6: PADI inhibitor Cl-amidine inhibits proliferation in breast cancer cell lines grown in monolayer and spheroid cultures. (a) Relative mean fold difference in proliferation for the MCF10AT progression model cell lines at increasing concentrations of Cl-amidine after 5d treatment ($n = 3$, * $p < 0.05$, ** $p < 0.005$, *** $p < 0.0005$). (b) Citrulline levels for MCF10DCIS cells treated with 200 μM Cl-amidine were measured and compared to PBS control MCF10DCIS cells. Data represent ($n = 3$, * $p < 0.005$) (c) Multicellular spheroids were treated with 200 μM Cl-amidine and the diameter was measured and recorded in microns ($n = 3$, * $p < 0.05$). (d) Phase contrast images (10X) of MCF10DCIS cells grown in monolayer (2D) or multicellular spheroids (3D) treated with either vehicle (PBS) or 200 μM of Cl-amidine (scale bar = 100 μm). (e and f) MCF10A and MCF10DCIS cells were treated with different concentrations of Cl-amidine (0 μM, 200 μM, and 400 μM) and (f) 10μg/mL Tunicamycin, and analyzed by flow-cytometry. Data represent percent apoptotic cells (cleaved Caspase-3 positive) or percentage of cells in various phases of the cell cycle (DAPI), and are expressed as the mean ± SD from three independent experiments (* $p < 0.005$, ** $p < 0.005$).

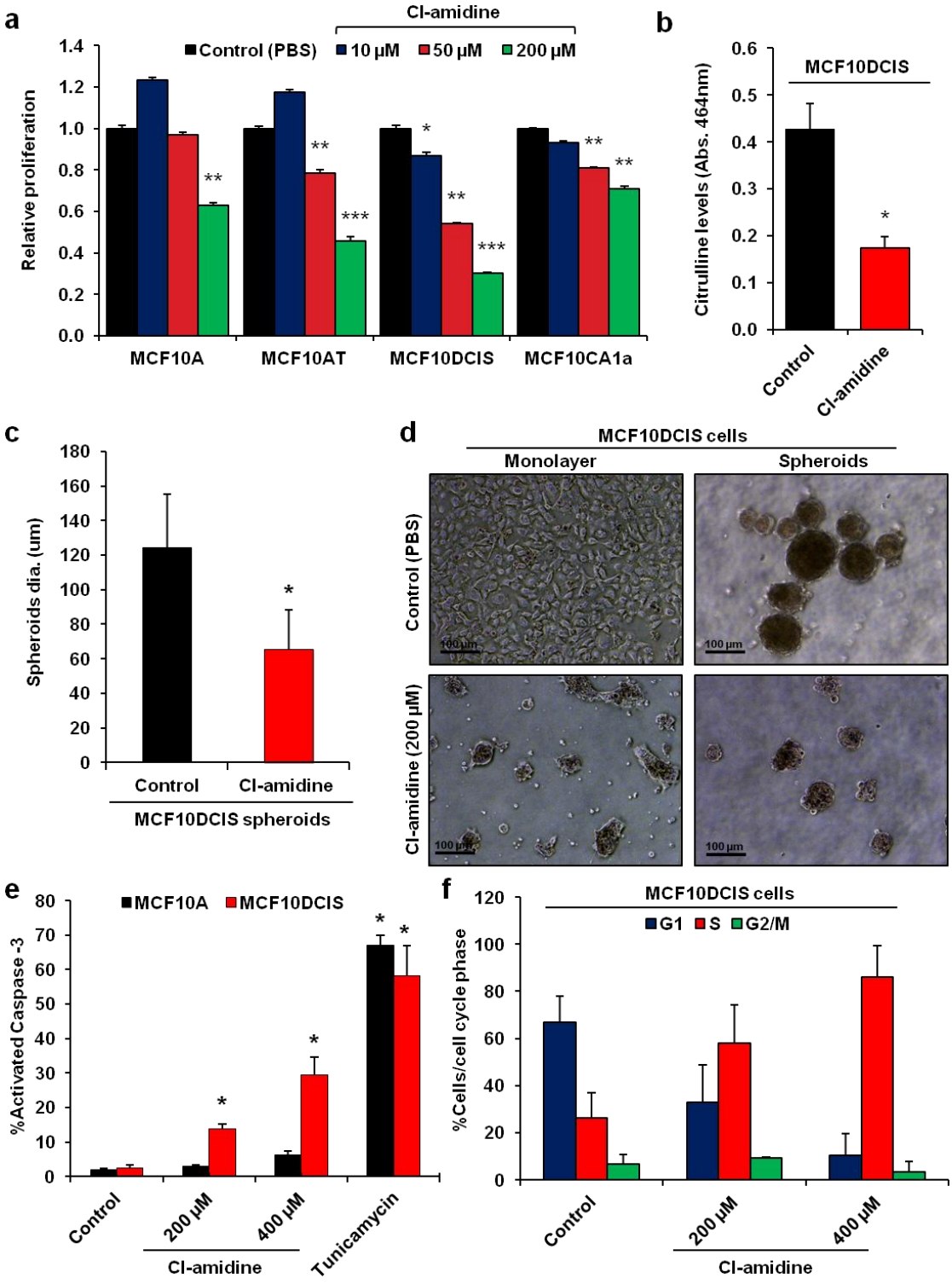
a
Cl-amidine
Control (PBS)
10 µM
50 µM
200 µM
Relative proliferation
MCF10A
MCF10AT
MCF10DCIS
MCF10CA1a
b
MCF10DCIS
Citrulline levels (Abs. 464nm)
Control
Cl-amidine
c
Spheroids dia. (um)
Control
Cl-amidine
MCF10DCIS spheroids
d
MCF10DCIS cells
Monolayer
Spheroids
Control (PBS)
Cl-amidine (200 µM)
100 µm
e
MCF10A
MCF10DCIS
%Activated Caspase -3
Control
200 µM
400 µM
Tunicamycin
Cl-amidine
f
MCF10DCIS cells
G1
S
G2/M
%Cells/cell cycle phase
Control
200 µM
400 µM
Cl-amidine

progression. To test this hypothesis, mRNA from the Cl-amidine treated and control MCF10DCIS cells was examined for the expression of cell cycle associated genes using the RT^2 Profiler PCR Cell Cycle Array via qRT-PCR. Using a threshold value of 2-fold expression change and a statistical significance of $p < 0.05$, we found that Cl-amidine affected the expression of a subset of genes (for the full unsorted list see McElwee et al., supplemental data [43]), with the top 10-upregulated and -downregulated genes presented in **Table 2.2**. Importantly, previous studies have shown that increased expression of *GADD45α*, the second most highly upregulated gene in our study, leads to cell cycle arrest and apoptosis in a range of cell types, including breast cancer cells [44]. This observation suggested that, in addition to affecting cell cycle gene expression (e.g. *p21*), Cl-amidine might also alter MCF10DCIS cell growth by inducing apoptosis. To test this hypothesis, we next treated MCF10A and MCF10DCIS cells with increasing concentrations of Cl-amidine for 4 days. Cells were fixed and labeled with anti-activated Caspase-3 antibody or DAPI, and then analyzed by flow-cytometry. Results show that Cl-amidine treatment significantly increased the percent of apoptotic MCF10DCIS cells in a dose-dependent manner (**Figure 2.6e**). In contrast, the MCF10A cells were largely unaffected. Furthermore, we also show that treatment of MCF10DCIS cells with Cl-amidine appears to induce cell cycle arrest in S-phase (**Figure 2.6f**). Lastly, we wanted to see whether the increase in apoptosis occurs earlier after treatment, so we tested the cells again following 2 days of treatment, but were unable to see any effect (**Figure 2.8a**). However, this was not surprising, as the effects of Cl-amidine are most pronounced after 3 days of treatment (data not shown). Taken together, it appears that Cl-amidine treatment after 4 days leads to S-phase coupled apoptosis, which is an intrinsic mechanism that prevents DNA replication of a damaged genome in a mammalian cell [45]. We also tested the effects of Cl-amidine on HER2/ERBB2 overexpressing cell lines

<u>Table 2.2:</u> Top 10 genes that are up- and down-regulated in MCF10DCIS cells after treatment with 200 μM Cl-amidine for 5 days. MCF10DCIS cells were treated with 200 μM Cl-amidine after seeding (5×10^4), and total RNA was collected 5d post-seeding. The mRNA for each group was tested on the RT^2 Profiler PCR Cell Cycle Array (SABiosciences Corporation, catalog number PAHS-020A). The PCR array was designed to study the profile of 84 human cell cycle related genes. Using a threshold value of 2-fold expression change and a statistical significance of $p < 0.05$, we found that Cl-amidine affected the expression of a subset of genes, with the top 10 up- and down-regulated genes displayed here.

Table 2.2: Top 10 cell cycle genes up- and down-regulated in MCF10DCIS cells after Cl-amidine treatment

Symbol	*Description*	*Fold Change*	*p-value*
Genes upregulated			
CDKN1A	Cyclin-dependent kinase inhibitor 1A (p21, Cip1)	17.68	1.06E-03
GADD45A	Growth arrrest and DNA-damage-inducible, alpha	13.53	3.57E-03
ATM	Ataxia telangiectasia mutated	9.61	6.91E-04
DIRAS3	DIRAS family, GTP-binding RAS-like 3	8.87	2.41E-04
HERC5	Hect domain and RLD 5	8.20	2.31E-03
RAD17	RAD17 homolog (S. pombe)	7.50	2.20E-05
CUL2	Cullin 2	6.57	7.37E-04
CCNE1	Cyclin E1	6.18	5.51E-04
ATR	Ataxia telangiectasia and Rad3 related	5.83	1.77E-04
CCNT2	Cyclin T2	5.68	1.15E-04
Genes downregulated			
MCM5	Minichromosome maintenance complex component 5	-8.45	3.23E-02
CDK1	Cyclin-dependent kinase 1	-8.14	2.88E-03
CDC20	Cell division cycle 20 homolog (S. cerevisiae)	-7.90	2.00E-06
GTSE1	G-2 and S-phase expressed 1	-6.62	4.84E-03
MCM2	Minichromosome maintenance complex component 2	-6.40	7.55E-04
MKI67	Antigen identified by monoclonal antibody Ki-67	-5.11	7.60E-05
CCNF	Cyclin F	-5.07	1.10E-02
BIRC5	Baculoviral IAP repeat containing 5 (Survivin)	-4.49	1.10E-02
BCL2	B-cell CLL/lymphoma 2	-4.14	1.70E-05
CCND2	Cyclin D2	-3.74	3.95E-02

BT-474 and SK-BR-3. Again, we see a reduction in cell growth (**Figure 2.7a**) and an increase in apoptosis (**Figure 2.7b**) that is coupled to S-phase cell cycle arrest (**Figure 2.7c**) for both BT-474 and SK-BR-3. These results show that Cl-amidine is effective in inhibiting the growth of luminal-HER2/ERBB2+ cell lines, BT-474 and SK-BR-3, and agree with previously reported data on Cl-amidine inhibition of growth in MCF7 cells [8, 9, 11, 46]. We wanted to test whether there would be any effect on a basal cell line, and chose MDA-MB-231 for comparison. Surprisingly, we see an effect on both cell growth and apoptosis (**Figure 2.8b and c**), albeit a smaller effect on apoptosis than we see in BT-474 and SK-BR-3. While this is interesting, and perhaps suggests the expression of a different PADI family member in this basal cell line, we have focused on PADI2 expressing cancers for this study, which are predominantly luminal and HER2/ERBB2 expressing. Taken together, these results suggest that Cl-amidine blocks the growth of MCF10DCIS cells by inducing cell cycle arrest and apoptosis. This prediction is supported by our previous finding that Cl-amidine can also drive apoptosis in lymphocytic cell lines *in vitro* [3]. Importantly, the lack of an apoptotic effect on MCF10A cells suggests that Cl-amidine may primarily target tumor cells for killing. Consistent with this possibility is the fact that Cl-amidine did not affect the growth of non-tumorigenic NIH3T3 cells and HL60 granulocytes [11].

PADI2 is highly expressed in the luminal epithelium of xenograft tumors derived from MCF10DCIS cells

Given that PADI2 expression is elevated in the MCF10DCIS cell line, we investigated PADI2 expression and localization in primary tumors derived from MCF10DCIS-injected mouse xenografts. Previous studies have shown that when MCF10DCIS cells are injected into the mammary fat-pad of immunodeficient nude (nu/nu) mice, tumors develop within 2-3 weeks. These tumors faithfully recapitulate the human comedo-

Figure 2.7: HER2/ERBB2 expressing cell lines BT-474 and SK-BR-3 show decreased proliferation after treatment with Cl-amidine. (a) BT-474 and SK-BR-3 cell lines were treated with increasing concentrations of Cl-amidine (0 μM, 100 μM, 200 μM, and 400 μM) over 4d and analyzed by flow-cytometry. Cell counts show a dose-dependent decrease in the growth of both BT-474 and SK-BR-3 (* $p < 0.05$, ** $p < 0.001$). (b) Apoptosis levels (cleaved Caspase-3 positive) significantly increase over the control in both BT-474 and SK-BR-3 cells after 200 μM and 400 μM of Cl-amidine. Tunicamycin (10μg/mL) is shown as a control for apoptosis (* $p < 0.05$, ** $p < 0.01$, *** $p < 0.001$). (c) Cell cycle analysis of Cl-amidine treated cells (DAPI) indicates S-phase arrest occurs in both BT-474 and SK-BR-3 cell lines. Data are expressed as the mean ± SD from three independent experiments.

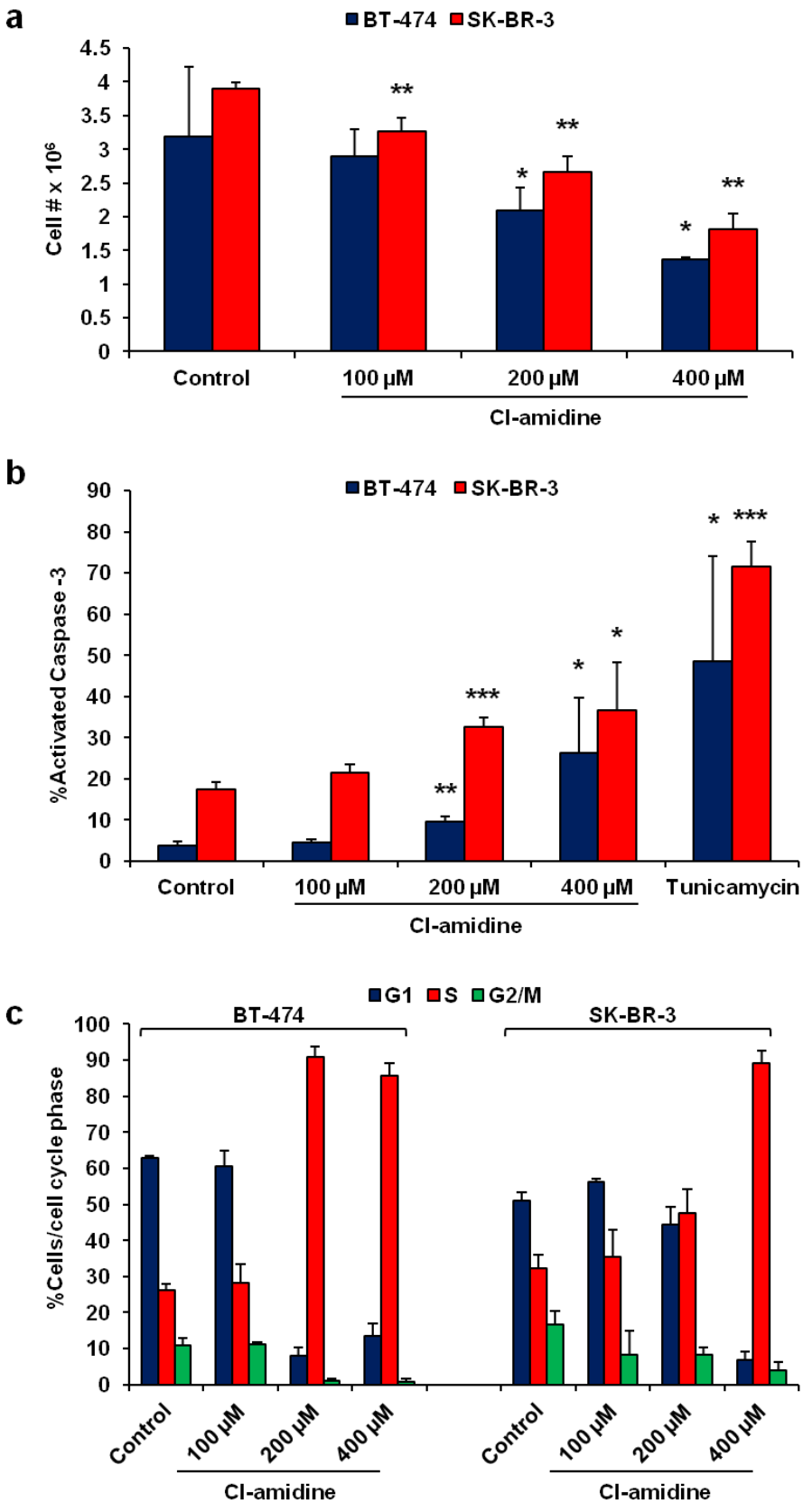
a
BT-474
SK-BR-3
Cell # x 10⁶
4.5
4
3.5
3
2.5
2
1.5
1
0.5
0
**
**
*
**
*
**
Control
100 µM
200 µM
400 µM
Cl-amidine
b
BT-474
SK-BR-3
%Activated Caspase -3
90
80
70
60
50
40
30
20
10
0
**
***
*
*
*
***
Control
100 µM
200 µM
400 µM
Tunicamycin
Cl-amidine
c
G1
S
G2/M
BT-474
SK-BR-3
%Cells/cell cycle phase
100
90
80
70
60
50
40
30
20
10
0
Control
100 µM
200 µM
400 µM
Control
100 µM
200 µM
400 µM
Cl-amidine
Cl-amidine

<u>Figure 2.8:</u> Flow-cytometry analysis of apoptosis in MCF10A and MCF10DCIS cell lines, and both proliferation/cell-growth and apoptosis in MDA-MB-231 cells. (a) MCF10A and MCF10DCIS cells were treated with different concentrations of Cl-amidine (0 μM, 200 μM, and 400 μM) and 10μg/mL Tunicamycin, and analyzed by flow-cytometry. Data represent percent apoptotic cells (cleaved Caspase-3 positive) after 2d and are expressed as the mean ± SD from three independent experiments (* $p < 0.05$, ** $p < 0.001$). (b) MDA-MB-231 cells were treated with increasing concentrations of Cl-amidine (0 μM, 100 μM, 200 μM, and 400 μM) over 4d and analyzed by flow-cytometry. Cell counts (DAPI) show a dose-dependent decrease in the growth (* $p < 0.001$). (c) Apoptosis levels (cleaved Caspase-3 positive) significantly increase over the control only after treatment with 400 μM of Cl-amidine. Tunicamycin (10μg/mL) is shown as a control for apoptosis (* $p < 0.01$). Data are expressed as the mean ± SD from three independent experiments.

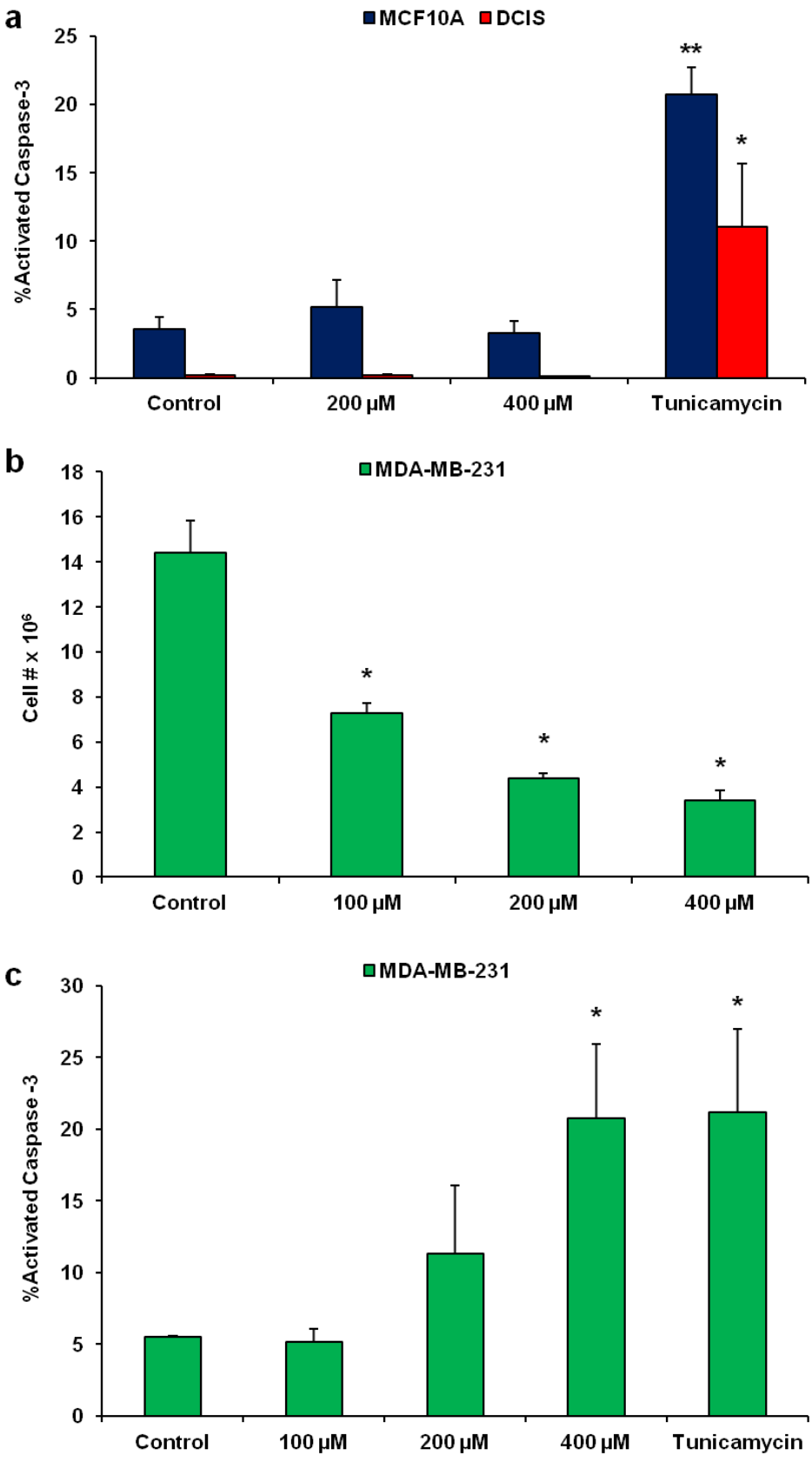
a
MCF10A
DCIS
%Activated Caspase-3
25
20
15
10
5
0
**
*
Control
200 µM
400 µM
Tunicamycin
b
MDA-MB-231
Cell # x 10⁶
18
16
14
12
10
8
6
4
2
0
*
*
*
Control
100 µM
200 µM
400 µM
c
MDA-MB-231
%Activated Caspase -3
30
25
20
15
10
5
0
*
*
Control
100 µM
200 µM
400 µM
Tunicamycin

DCIS condition, with the basement membrane limiting duct-like structure being comprised of an outer myoepithelial layer, an inner layer of luminal epithelial cells, and a central necrotic lumen [18, 19, 47, 48]. We chose to use subcutaneous injections instead of orthotopic or intraductal [49] methods, as previous work by Hu et al showed that the progression and phenotype of the MCF10DCIS tumors grown subcutaneously in the mammary fat pad were highly similar to human high-grade comedo-DCIS tumors [19]. In our study, we found that PADI2 protein expression was restricted to the luminal epithelium of the duct-like structures in the MCF10DCIS xenografts, and was not observed in the stromal tissue or the necrotic core (**Figure 2.9a, panel I and II**). At the subcellular level, PADI2 appears to be expressed in both the cytoplasmic and nuclear compartments of luminal epithelial cells (**Figure 2.9a, panel II**). This observation supports our recent findings that PADI2 can be targeted to the nucleus of both human normal mammary tissue and breast cancer cells [50] and regulate gene activity via citrullination [50, 51].

Next, we examined whether the observed correlation between PADI2 and HER2/ERBB2 expression also occurred *in vivo.* We found that both HER2/ERBB2 and PADI2 were expressed within the luminal epithelium of MCF10DCIS tumors (**Figure 2.9a, panel III and IV**). Interestingly, a previous report by Behbod et. al. found low levels of HER2/ERBB2 in MCF10DCIS tumors that were grown intraductally. We predict that the disparity between this data and our data may be due to differences in the microenvironment. We then quantified *PADI2* mRNA in the MCF10DCIS xenografts by qRT-PCR, and found that *PADI2* levels were significantly higher in the tumors when compared to monolayer cultures (**Figure 2.9b**). We also carried out immunofluorescence (IF) analysis of these tumors to examine PADI2 intratumoral localization. We found that PADI2 protein expression appears entirely limited to cytokeratin-positive luminal epithelial cells (**Figure 2.9c, panel I and III,**

Figure 2.9: PADI2 is expressed in MCF10DCIS xenograft tumors and localizes to the luminal epithelium. (a) MCF10DCIS cells (1 x 10^6) were injected subcutaneously into female nude (nu/nu) mice (Charles River) and comedo-DCIS tumors formed after 2 weeks. Tumor sections were probed with an (I, II) anti-PADI2 antibody (1:100) or (III, IV) anti-ERBB2 (1:100), and counterstained with hematoxylin. The black arrows indicate the luminal epithelium of the duct-like structures in DCIS tumors (I, III – 20X, scale bar = 200 µm; II, IV – 100X, scale bar = 50 µm). While the HER2/ERBB2 staining is predominantly cytoplasmic (IV), there are some nuclei staining positively for PADI2 (II). (b) Tumors were collected; two sections from each mouse were sampled and total RNA was isolated. *PADI2* mRNA levels were determined by qRT-PCR (TaqMan) using MCF10A cells as a reference and *GAPDH* normalization. *PADI2* levels were higher in the tumor samples than normally found in the MCF10DCIS cells. Data were analyzed using the $2^{-\Delta\Delta C(t)}$ method, and are expressed as the mean ± SD from three independent experiments (* $p < 0.005$). (c) Immunofluorescence staining (40X) shows that PADI2 is expressed in the luminal but not myoepithelium cells in MCF10DCIS tumors. Tumors were probed with anti-PADI2 (II, III, V, VI – green fluorescent signal), anti-cytokeratin (I, III – luminal marker – red fluorescent signal), and anti-p63 (IV, VI – myoepithelial marker – red fluorescent signal). Nuclei were stained with DAPI (blue fluorescent signal). The dashed arrows delineate the luminal epithelium layer, while the dashed straight line delineates the myoepithelium layer, which is adjacent to the basement membrane. In the merged images, the co-localization of cytokeratin and PADI2 can be seen in the luminal epithelium (III), while in contrast, PADI2 is absent from the p63 stained myoepithelium (VI).

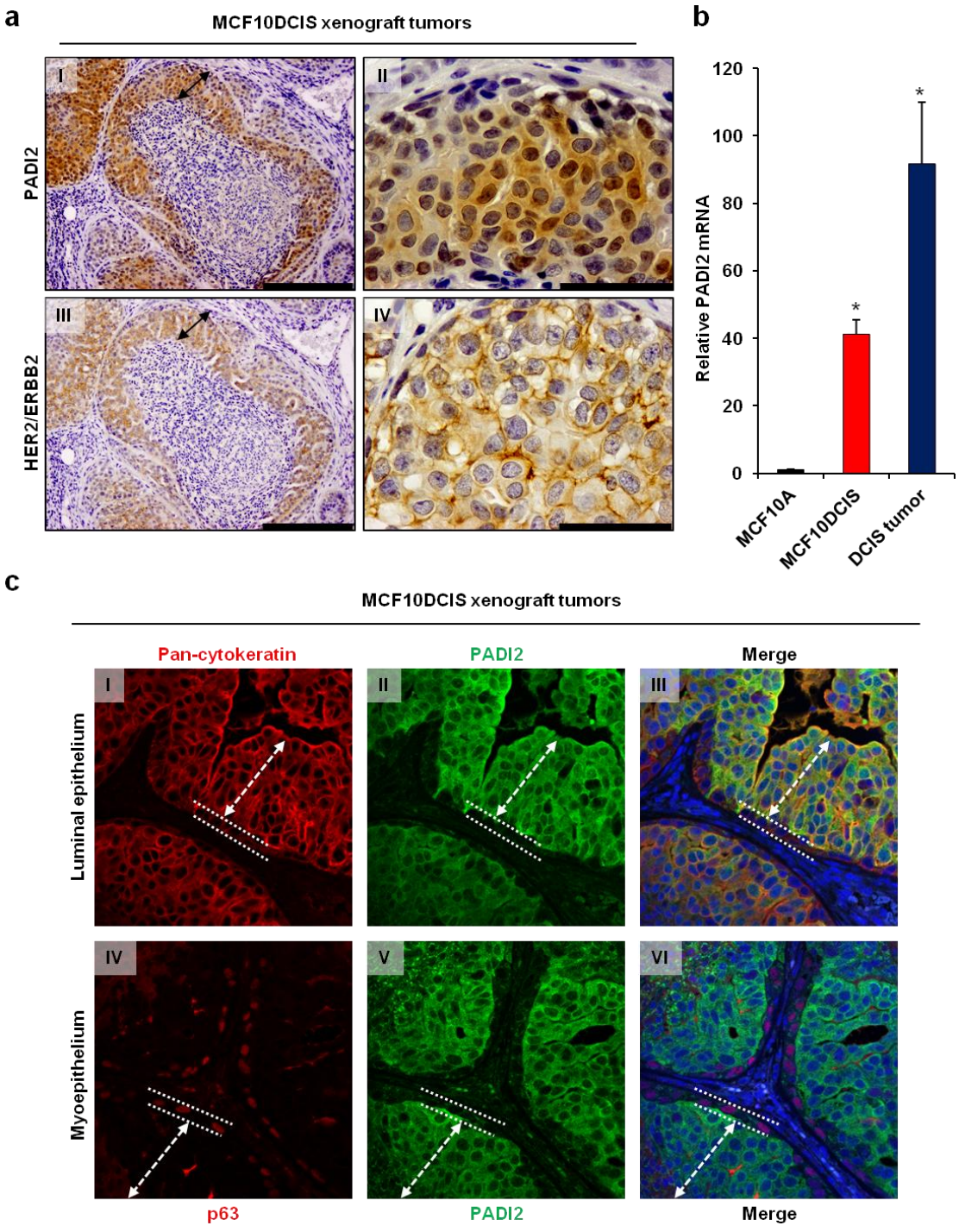
a
MCF10DCIS xenograft tumors
PADI2
HER2/ERBB2
I
II
III
IV
b
Relative PADI2 mRNA
120
100
80
60
40
20
0
*
*
MCF10A
MCF10DCIS
DCIS tumor
c
MCF10DCIS xenograft tumors
Pan-cytokeratin
PADI2
Merge
Luminal epithelium
Myoepithelium
I
II
III
IV
V
VI
p63
PADI2
Merge

<u>Figure 2.10:</u> Immunofluorescence staining of MCF10DCIS xenografts for PADI2, luminal epithelium (pan-cytokeratin), and myoepithelium (p63). (A) MCF10DCIS cells (1×10^6) were injected subcutaneously into female nude (nu/nu) mice (Charles River) and comedo-DCIS tumors formed after 2 weeks. Tumors were probed with anti-PADI2 (green fluorescent signal), anti-cytokeratin (luminal marker – red fluorescent signal), and anti-p63 (myoepithelial marker – red fluorescent signal). Nuclei were stained with DAPI (blue fluorescent signal). Immunofluorescence staining (63X) shows that PADI2 is expressed in the luminal but not myoepithelium cells in MCF10DCIS tumors. In addition, there is some evidence for PADI2 expression in the nucleus.

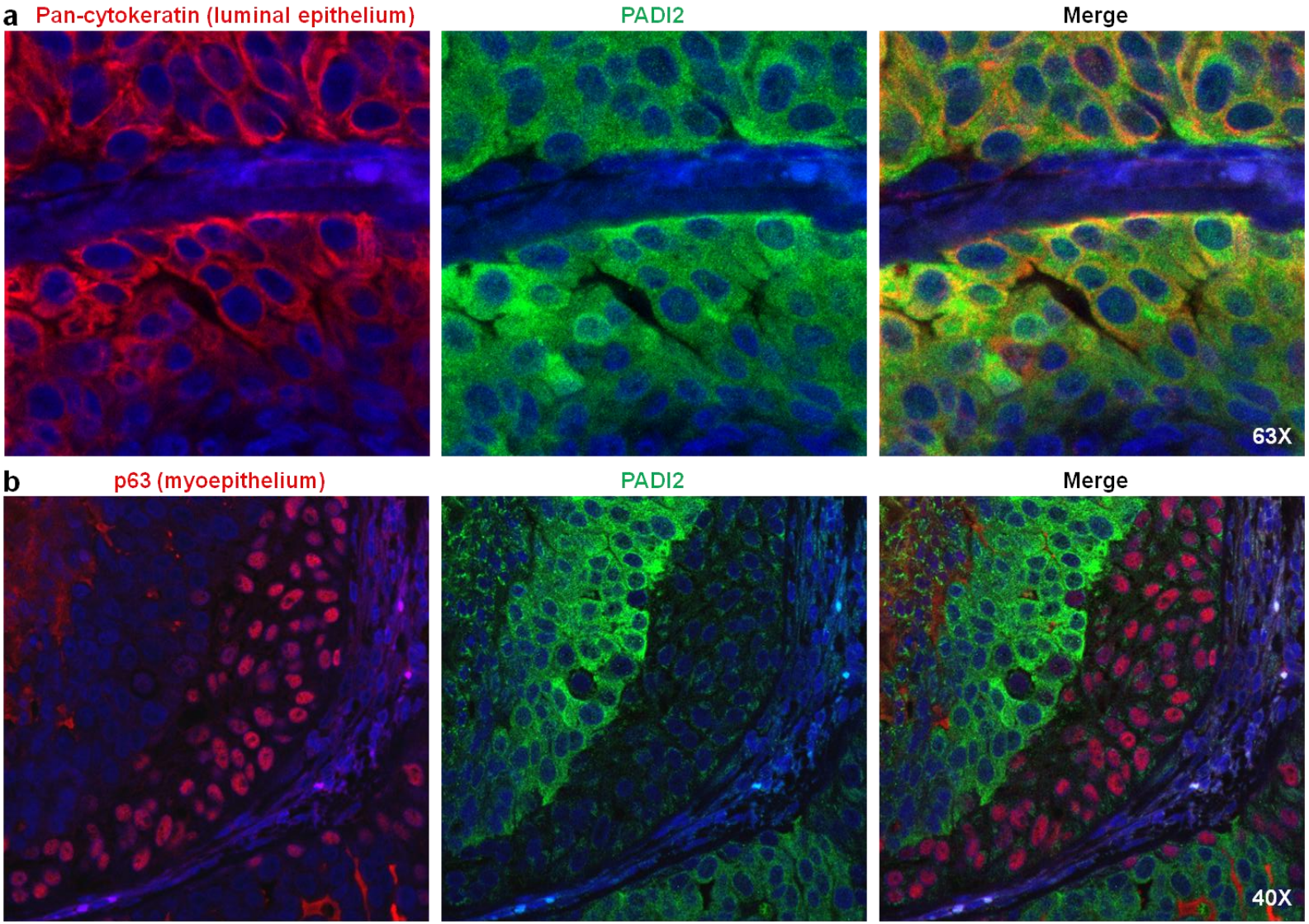
a
Pan-cytokeratin (luminal epithelium)
PADI2
Merge
63X
b
p63 (myoepithelium)
PADI2
Merge
40X

and Figure 2.10), while no detectable PADI2 signal was observed in the p63 positive myoepithelial cells (**Figure 2.9c, panel IV and VI, and Figure 2.10**).

Treatment of MCF10DCIS xenografts with Cl-amidine suppresses tumor growth

Given the inhibitory effects of Cl-amidine on MCF10DCIS monolayer and spheroid growth, we next tested whether the treatment of mice with this inhibitor would suppress the growth of MCF10DCIS-derived tumors. For this study, mouse fat-pads were injected with MCF10DCIS cells (1×10^6) and the tumors were allowed to establish and grow for ~2 weeks as described previously [18-20, 47]. Mice were randomly assigned into treatment or control groups and administered daily intra-peritoneal (IP) injections of either Cl-amidine (50 mg/kg/day) or vehicle (PBS). Note, that the choice of dose and route of administration were based on the previous demonstration that Cl-amidine reduces disease severity in the murine collagen induced arthritis model of rheumatoid arthritis [5]. Treatment continued for 14 days, at which point the tumors were harvested. Results from our xenograft study show that Cl-amidine treatment (n = 7/group) caused a significant reduction in the size of the tumors (**Figure 2.11a**). Moreover, the analysis of tumor morphology by H&E and PAS staining showed that, while tumors from the sham-injected group displayed an advanced, potentially invasive, tumor phenotype (**Figure 2.11b, panel II**), tumors from the Cl-amidine treated group (**Figure 2.11b, panel I**) were much more benign in appearance. For example, the basement membrane of Cl-amidine treated tumors remained largely intact (**Figure 2.11c**) and had considerably less membrane breaching and leukocyte infiltration compared to the control group. These findings suggest that PADI2 plays an important role in comedo-DCIS progression and that the inhibition of PADI activity can suppress tumor progression *in vivo*.

Figure 2.11: Cl-amidine decreases the growth of MCF10DCIS tumors in a xenograft model of comedo-DCIS. (a) Average tumor volumes after 1, 7, and 14 days of daily IP injections of Cl-amidine (50mg/kg/day) or PBS as vehicle control. MCF10DCIS cells (1×10^6) were injected subcutaneously into female nude (nu/nu) mice (Charles River). After 2 weeks of tumor growth (tumor volumes ~100-200 mm^3), mice were randomly treated with intraperitoneal injections of Cl-amidine at 50 mg/kg/day (n = 7) or PBS as a vehicle control (n = 7). Tumor volume was measured weekly by digital caliper, and the differences between tumor volumes were evaluated by the non-parametric Mann–Whitney–Wilcoxon test (MWW). Results are reported as mean ± SD (Day 14, $p = 0.002$). (b) PAS stained sections (10X, scale bar = 200 μm) from representative treated (I) and control tumors (II), arrows in (I) show an intact basement membrane (BM), while the arrow in (II) shows breaching of the BM with infiltrating leukocytes. (c) BM integrity was scored on a scale from 1-3 by S.M., with values being expressed as the mean ± SD. The treated tumors have a lower score, indicating a higher level of BM integrity (* $p < 0.05$ MWW).

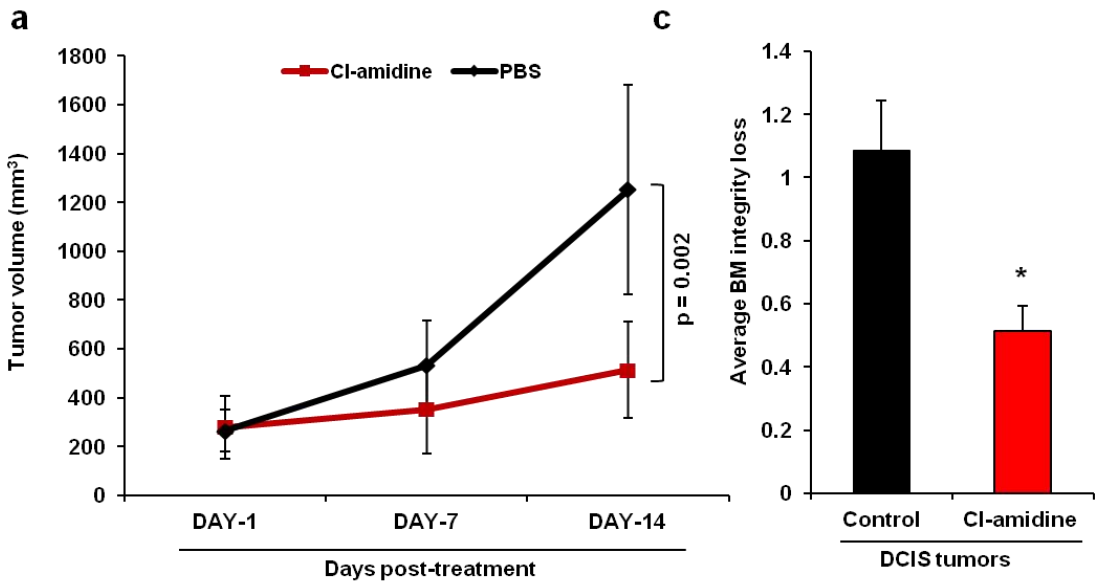
a
c
Cl-amidine
PBS
Tumor volume (mm³)
1800
1600
1400
1200
1000
800
600
400
200
0
p = 0.002
DAY-1
DAY-7
DAY-14
Days post-treatment
Average BM integrity loss
1.4
1.2
1
0.8
0.6
0.4
0.2
0
*
Control
Cl-amidine
DCIS tumors

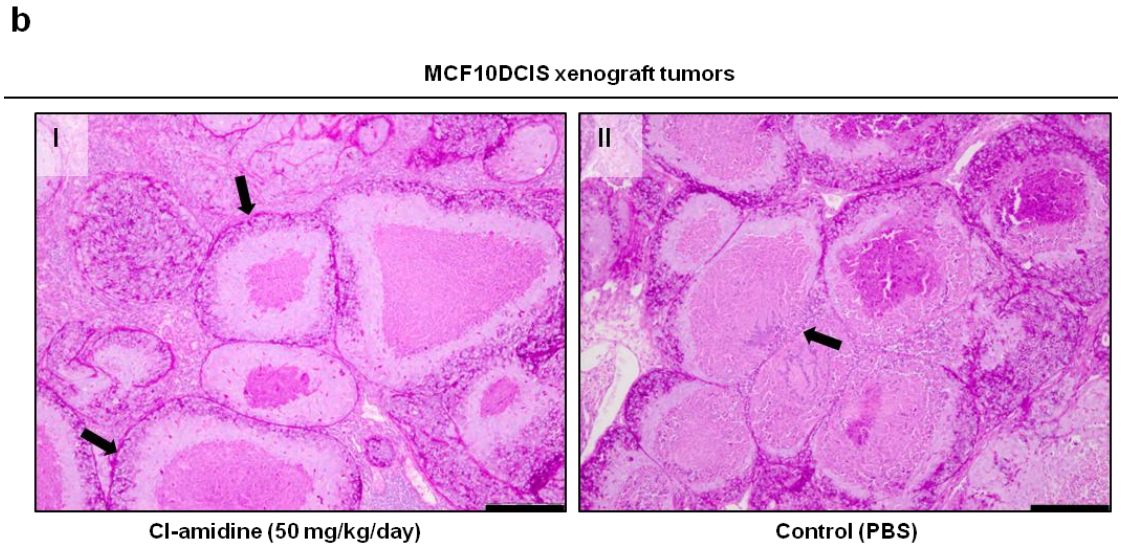
b
MCF10DCIS xenograft tumors
I
II
Cl-amidine (50 mg/kg/day)
Control (PBS)

2.5 Discussion

In this study, we show that PADI2 is specifically upregulated during mammary tumor progression and that the PADI inhibitor, Cl-amidine, is effective in inhibiting the growth of PADI2 overexpressing cell lines in both 2D and 3D cultures. In addition, we demonstrate here for the first time that Cl-amidine is successful in suppressing tumor growth in a xenograft mouse model of comedo-DCIS. Lastly, we document that PADI2 expression is highly correlated with HER2/ERBB2 overexpressing and luminal subtype breast cancers.

Given the previous correlations between PADI2 and the HER2/ERBB2 oncogene, the goal of this study was to carry out an initial test of the hypothesis that PADI2 plays a role in breast cancer progression. To accomplish this, we utilized the well-established MCF10AT model [16, 17] and found that PADI2 expression was highly upregulated in MCF10DCIS cells, a cell line that forms comedo-DCIS lesions that spontaneously progress to invasive tumors [30, 47]. Our finding that PADI2 expression is highest in comedo-DCIS lesions (defined by their necrotic centers) was perhaps not too surprising, given the close association of PADIs with inflammatory events. We are currently investigating the potential links between inflammatory signaling in these MCF10DCIS lesions and PADI2 activity.

Interestingly, PADI2 expression in the MCF10AT series coincided with HER2/ERBB2 upregulation, which, again, was not entirely unexpected given previous reports correlating *PADI2* expression with *HER2/ERBB2* [15]. While we did find that HER2/ERBB2 and PADI2 protein expression correlated well across the MCF10AT cell lines, PADI2 protein levels are particularly high in the MCF10DCIS line, relative to HER2/ERBB2. We cannot currently explain this finding; however, it is possible that cell-line-specific factors are stabilizing the PADI2 transcript, thus allowing for increased protein expression [52, 53].

While our data show a potential relationship between PADI2 and HER2/ERBB2 in the MCF10AT model, we wanted to examine this correlation at higher resolution. To accomplish this we queried our RNA-seq dataset of 57 breast cancer cell lines with known subtype and HER2/ERBB2 status and found that: (a) *PADI2* expression is highest in luminal cell lines and that (b) *PADI2* expression is highly correlated with HER2/ERBB2+ across the basal-NM, claudin-low, and luminal lines. The observation that *PADI2* is upregulated in the luminal subtype confirms previous gene expression data where *PADI2* was identified as one of the top upregulated genes in luminal breast cancer lines compared to basal lines [13, 14]. In order to test whether the observed correlation between *PADI2* and *HER2/ERBB2* would be retained at the protein level, we also tested a small sample of cell lines representing the four common breast cancer subtypes and found that PADI2 expression was only observed in the HER2/ERBB2+ BT-474 and SK-BR-3 lines. However, we did observe some discordance seen between *PADI2* transcript and protein levels, but we predict this difference may be due to post-transcriptional regulatory mechanisms. This prediction is based, in part, upon the observation that PADI2 possesses a long 3'UTR [54] that contains several AU-rich elements [55, 56] that have been shown to bind the stabilizing regulatory factor HuR [57]. HuR binding has been shown to enhance the stability of mRNAs involved in proliferation [58-60], while also playing a role in breast cancer, as cytoplasmic accumulation of HuR promotes tamoxifen resistance in BT-474 cells [61] and the stability of *HER2/ERBB2* transcripts in SK-BR-3 cells [53]. Interestingly, from these studies, the level of HuR was reported to be high in both BT-474 and SK-BR-3 cells, while it was relatively low in MCF7 cells. It is important to note that that while we observed low levels of PADI2 protein expression in MCF7 (Additional file, Figure S1a), recent work from our lab has confirmed the expression of PADI2 in MCF7 cells [50, 51].

We also examined two mouse models of mammary tumorigenesis, the luminal MMTV-neu and the basal MMTV-*Wnt-1* and found that, as predicted, PADI2 levels are highest in the HER2/ERBB2 overexpressing MMTV-neu mice compared to normal mammary tissue and to hyperplastic and primary MMTV-*Wnt-1* tumors. Taken together, these findings indicate that PADI2 is predominantly expressed in luminal epithelial cells, and that there appears to be a strong relationship between PADI2 and HER2/ERBB2 expression in breast cancer. Subsequent studies are now underway to test whether PADI2 plays a functional role in HER2/ERBB2 driven breast cancers, potentially by functioning as an inflammatory mediator.

Previous studies have shown that the inhibition of PADI enzymatic activity by Cl-amidine is effective in decreasing the growth of several cancer cell lines (i.e. HL-60, HT-29, U2OS, and MCF7 cells), and that administering the drug in combination with doxorubicin or the HDAC inhibitor SAHA can have synergistic cytotoxic effects on cells [8, 9, 11, 46]. Cl-amidine is highly specific for all PADI enzymes, with dose-dependent cytotoxicity and little to no effect in non-cancerous cell lines (i.e. HL-60 granulocytes and NIH3T3 cells) [11]. Our studies expand on these previous results by showing that Cl-amidine suppresses the growth of the transformed lines of the MCF10AT model, especially the MCF10DCIS cell line, in both 2D and 3D cultures. In addition, we show for the first time that Cl-amidine is successful in treating tumors *in vivo* using a mouse model of comedo-DCIS from xenografted MCF10DCIS cells. Given that, the loss of basement membrane integrity is an important event during the progression of DCIS to invasive disease, it is significant that Cl-amidine treated xenografts maintain their basement membrane integrity and show reduced leukocytic infiltration across the basement membrane compared to the control group. These observations suggest that Cl-amidine treatment might enhance the ability of tumor

ductular myoepithelial cells to deposit continuous and organized basement membranes.

While we chose the subcutaneous model of MCF10DCIS tumorigenesis, future studies on the effect of Cl-amidine could examine alternate methods of transplantation, such as the previously described intraductal method [49]. In addition, different models of DCIS could be examined, such as xenografted SUM-225 cells, which show high *HER2/ERBB2* and *PADI2* levels (see Figure 3 for relative levels). Of note, we found that while Cl-amidine suppressed tumor growth, the drug was well tolerated by mice in this study. Similarly, our previous work found that doses of Cl-amidine up to 75 mg/kg/day in a mouse model of Colitis [3], and up to100 mg/kg/day in a mouse model of RA [5], were well tolerated without side effects. Further work into studying the pharmacokinetics and biodistribution of Cl-amidine, or perhaps the development of an isozyme specific inhibitor of PADI2, will be an important step in helping to find a potent drug for the treatment of DCIS patients.

The actual mechanisms by which Cl-amidine reduces cellular proliferation have yet to be fully elucidated, though evidence here suggests that PADI2 may play a role (direct or indirect) in regulating the expression of both cell cycle and tumor promoting genes. Previous reports have shown that Cl-amidine effectively upregulates a number of p53-regulated genes, including *p21*, *PUMA*, and *GADD45* [8, 46]. Our qRT-PCR cell cycle array results confirm that two of these genes, *p21* and *GADD45α*, are upregulated after treatment of MCF10DCIS cells with Cl-amidine by 17.68- and 13.53-fold, respectively. Furthermore, we have identified additional genes downregulated by Cl-amidine, including *MKI67*, *MCM5*, and *MCM2*, each with known functions in cancer progression**.** We have also quantitatively analyzed for apoptosis levels (Caspase-3) after Cl-amidine treatment via flow-cytometry, and see a dose-dependent decrease in proliferation and increase in apoptosis. Moreover, we also

show that the cells arrest in S-phase after Cl-amidine treatment, thus leading to S-phase coupled apoptosis, which is a known response to DNA damage [45]. Taken together, the observed inhibitory effects of Cl-amidine on tumor growth may be due to the suppression of genes involved in oncogenesis and the activation of genes involved in apoptosis, though additional work is needed to define the mechanisms behind these potential relationships.

Conclusions

In summary, we provide here an important new line of evidence demonstrating that PADI2 may play a role in the oncogenic progression of cancer and, in particular, breast cancer. Using the MCF10AT model, we show that PADI2 is highly upregulated following transformation at both the mRNA and protein level, with highest levels in the cell line that recapitulates human comedo-DCIS. Furthermore, we show that, across a wide array of breast cancer cell lines, *PADI2* is specifically overexpressed in the luminal subtype, while also being highly correlated with HER2/ERBB2 overexpression. This observation suggests that PADI2 may function as a biomarker for HER2/ERBB2+ lesions. Lastly, our preclinical mouse xenograft study suggests that the PADI inhibitor, Cl-amidine, could potentially be utilized as a therapeutic agent for the treatment of comedo-DCIS tumors.

Acknowledgements/Contributions

Thanks to: Dr. Sunish Mohanan for help with the IHC and 3D-spheroid experiments and pathological analysis (Figs. 2.6c-d, 2.11c); Dr. Obi Griffith for help with RNA-seq and ALEXA-seq analysis (Figs. 2.2d, 2.4, 2.4, Table 2.1); Lynne Anguish for help with the flow-cytometry experiments (Figs. 2.6e-f, 2.11c); and Dr. Paul Thomson for generating the Cl-amidine used in the experiments.

2.6 References

1. Vossenaar, E.R., Zendman, A.J., van Venrooij, W.J. & Pruijn, G.J. PAD, a growing family of citrullinating enzymes: genes, features and involvement in disease. *Bioessays* **25**, 1106-18 (2003).

2. Balandraud, N. et al. A rigorous method for multigenic families' functional annotation: the peptidyl arginine deiminase (PADs) proteins family example. *BMC genomics* **6**, 153 (2005).

3. Chumanevich, A.A. et al. Suppression of colitis in mice by Cl-amidine: a novel peptidylarginine deiminase inhibitor. *American journal of physiology. Gastrointestinal and liver physiology* **300**, G929-38 (2011).

4. Lange, S. et al. Protein deiminases: New players in the developmentally regulated loss of neural regenerative ability. *Developmental biology* (2011).

5. Willis, V.C. et al. N-alpha-benzoyl-N5-(2-chloro-1-iminoethyl)-L-ornithine amide, a protein arginine deiminase inhibitor, reduces the severity of murine collagen-induced arthritis. *J Immunol* **186**, 4396-404 (2011).

6. Wang, Y. et al. Human PAD4 regulates histone arginine methylation levels via demethylimination. *Science (New York, N.Y.)* **306**, 279-83 (2004).

7. Zhang, X. et al. Genome-Wide Analysis Reveals PADI4 Cooperates with Elk-1 to Activate c-Fos Expression in Breast Cancer Cells. *PLoS genetics* **7**, e1002112 (2011).

8. Yao, H. et al. Histone Arg modifications and p53 regulate the expression of OKL38, a mediator of apoptosis. *J Biol Chem* **283**, 20060-8 (2008).

9. Li, P. et al. Coordination of PAD4 and HDAC2 in the regulation of p53-target gene expression. *Oncogene* **29**, 3153-62 (2010).

10. Tanikawa, C. et al. Regulation of protein Citrullination through p53/PADI4 network in DNA damage response. *Cancer Res* **69**, 8761-9 (2009).

11. Slack, J.L., Causey, C.P. & Thompson, P.R. Protein arginine deiminase 4: a target for an epigenetic cancer therapy. *Cell Mol Life Sci* **68**, 709-20 (2011).

12. Montañez-Wiscovich, M.E. et al. LMO4 is an essential mediator of ErbB2/HER2/Neu-induced breast cancer cell cycle progression. *Oncogene* **28**, 3608-18 (2009).

13. Mackay, A. et al. A high-resolution integrated analysis of genetic and expression profiles of breast cancer cell lines. *Breast cancer research and treatment* **118**, 481-98 (2009).

14. Blick, T. et al. Epithelial mesenchymal transition traits in human breast cancer cell lines parallel the CD44(hi/)CD24 (lo/-) stem cell phenotype in human breast cancer. *Journal of mammary gland biology and neoplasia* **15**, 235-52 (2010).

15. Bertucci, F. et al. Identification and validation of an ERBB2 gene expression signature in breast cancers. *Oncogene* **23**, 2564-2575 (2004).

16. Heppner, G.H. & Wolman, S.R. MCF-10AT: A Model for Human Breast Cancer Development. *The Breast Journal* **5**, 122-129 (1999).

17. Dawson, P.J., Wolman, S.R., Tait, L., Heppner, G.H. & Miller, F.R. MCF10AT: a model for the evolution of cancer from proliferative breast disease. *The American journal of pathology* **148**, 313-9 (1996).

18. Hu, M. et al. Role of COX-2 in epithelial-stromal cell interactions and progression of ductal carcinoma in situ of the breast. *Proceedings of the National Academy of Sciences of the United States of America* **106**, 3372-7 (2009).

19. Hu, M. et al. Regulation of In Situ to Invasive Breast Carcinoma Transition. *Cancer Cell* **13**, 394-406 (2008).

20. Shekhar, M.P. et al. Comedo-ductal carcinoma in situ: A paradoxical role for programmed cell death. *Cancer Biol Ther* **7** (2008).

21. Causey, C.P. & Thompson, P.R. An improved synthesis of haloaceteamidine-based inactivators of protein arginine deiminase 4 (PAD4). *Tetrahedron Lett* **49**, 4383-4385 (2008).

22. Santini, M.T. & Rainaldi, G. Three-dimensional spheroid model in tumor biology. *Pathobiology* **67**, 148-57 (1999).

23. Carlsson, J. & Yuhas, J.M. Liquid-overlay culture of cellular spheroids. *Recent Results Cancer Res* **95**, 1-23 (1984).

24. Kelm, J.M., Timmins, N.E., Brown, C.J., Fussenegger, M. & Nielsen, L.K. Method for generation of homogeneous multicellular tumor spheroids applicable to a wide variety of cell types. *Biotechnology and bioengineering* **83**, 173-80 (2003).

25. Nakashima, K. et al. Molecular characterization of peptidylarginine deiminase in HL-60 cells induced by retinoic acid and 1alpha,25-dihydroxyvitamin D(3). *J Biol Chem* **274**, 27786-92 (1999).

26. Lamensa, J.W. & Moscarello, M.A. Deimination of human myelin basic protein by a peptidylarginine deiminase from bovine brain. *J Neurochem* **61**, 987-96 (1993).

27. Cherrington, B.D., Morency, E., Struble, A.M., Coonrod, S.a. & Wakshlag, J.J. Potential role for peptidylarginine deiminase 2 (PAD2) in citrullination of canine mammary epithelial cell histones. *PloS one* **5**, e11768 (2010).

28. Livak, K.J. & Schmittgen, T.D. Analysis of relative gene expression data using real-time quantitative PCR and the 2(-Delta Delta C(T)) Method. *Methods* **25**, 402-8 (2001).

29. Griffith, M. et al. Alternative expression analysis by RNA sequencing. *Nat Methods* **7**, 843-7.

30. Miller, F.R., Santner, S.J., Tait, L. & Dawson, P.J. MCF10DCIS.com xenograft model of human comedo ductal carcinoma in situ. *J Natl Cancer Inst* **92**, 1185-6 (2000).

31. Kadota, M. et al. Delineating genetic alterations for tumor progression in the MCF10A series of breast cancer cell lines. *PloS one* **5**, e9201 (2010).

32. Neve, R.M. et al. A collection of breast cancer cell lines for the study of functionally distinct cancer subtypes. *Cancer cell* **10**, 515-27 (2006).

33. Santner, S.J. et al. Malignant MCF10CA1 cell lines derived from premalignant human breast epithelial MCF10AT cells. *Breast Cancer Res Treat* **65**, 101-10 (2001).

34. Tait, L., Dawson, P., Wolman, S., Galea, K. & Miller, F. Multipotent human breast stem cell line MCF1OAT. *International journal of oncology* **9**, 263-7 (1996).

35. So, J., Lee, H., Kramata, P., Minden, A. & Suh, N. Differential Expression of Key Signaling Proteins in MCF10 Cell Lines, a Human Breast Cancer Progression Model. *Mammalian genome : official journal of the International Mammalian Genome Society* **4**, 31-40 (2012).

36. Tsukamoto, A.S., Grosschedl, R., Guzman, R.C., Parslow, T. & Varmus, H.E. Expression of the int-1 gene in transgenic mice is associated with mammary gland hyperplasia and adenocarcinomas in male and female mice. *Cell* **55**, 619-25 (1988).

37. Li, Y., Hively, W.P. & Varmus, H.E. Use of MMTV-Wnt-1 transgenic mice for studying the genetic basis of breast cancer. *Oncogene* **19**, 1002-9 (2000).

38. Baker, R. et al. Pea3 transcription factors and wnt1-induced mouse mammary neoplasia. *PLoS One* **5**, e8854.

39. Huang, S. et al. Changes in gene expression during the development of mammary tumors in MMTV-Wnt-1 transgenic mice. *Genome Biol* **6**, R84 (2005).

40. Luo, Y. et al. Inhibitors and inactivators of protein arginine deiminase 4: functional and structural characterization. *Biochemistry* **45**, 11727-36 (2006).

41. Jones, J.E. et al. Synthesis and screening of a haloacetamidine containing library to identify PAD4 selective inhibitors. *ACS Chem Biol* **7**, 160-5 (2011).

42. Shevde, L.A. et al. Spheroid-forming subpopulation of breast cancer cells demonstrates vasculogenic mimicry via hsa-miR-299-5p regulated de novo expression of osteopontin. *J Cell Mol Med* **14**, 1693-706.

43. McElwee, J.L. et al. Identification of PADI2 as a potential breast cancer biomarker and therapeutic target. *BMC Cancer* **12**, 500 (2012).

44. Harkin, D.P. et al. Induction of GADD45 and JNK/SAPK-dependent apoptosis following inducible expression of BRCA1. *Cell* **97**, 575-86 (1999).

45. Cho, Y.J. & Liang, P. S-phase-coupled apoptosis in tumor suppression. *Cell Mol Life Sci* **68**, 1883-96 (2011).

46. Li, P. et al. Regulation of p53 target gene expression by peptidylarginine deiminase 4. *Mol Cell Biol* **28**, 4745-58 (2008).

47. Tait, L.R. et al. Dynamic stromal-epithelial interactions during progression of MCF10DCIS.com xenografts. *Int J Cancer* **120**, 2127-34 (2007).

48. Miller, F.R. Xenograft models of premalignant breast disease. *Journal of mammary gland biology and neoplasia* **5**, 379-91 (2000).

49. Behbod, F. et al. An intraductal human-in-mouse transplantation model mimics the subtypes of ductal carcinoma in situ. *Breast Cancer Res* **11**, R66 (2009).

50. Cherrington, B.D. et al. Potential Role for PAD2 in Gene Regulation in Breast Cancer Cells. *PLoS One* **7**, e41242 (2012).

51. Zhang, X. et al. Peptidylarginine deiminase 2-catalyzed histone H3 arginine 26 citrullination facilitates estrogen receptor α target gene activation. *Proceedings of the National Academy of Sciences of the United States of America* (In press).

52. Delacroix, L., Begon, D., Chatel, G., Jackers, P. & Winkler, R. Distal ERBB2 promoter fragment displays specific transcriptional and nuclear binding activities in ERBB2 overexpressing breast cancer cells. *DNA Cell Biol* **24**, 582-94 (2005).

53. Scott, G.K. et al. Destabilization of ERBB2 transcripts by targeting 3' untranslated region messenger RNA associated HuR and histone deacetylase-6. *Mol Cancer Res* **6**, 1250-8 (2008).

54. Vossenaar, E.R. et al. Expression and activity of citrullinating peptidylarginine deiminase enzymes in monocytes and macrophages. *Ann Rheum Dis* **63**, 373-81 (2004).

55. Barreau, C., Paillard, L. & Osborne, H.B. AU-rich elements and associated factors: are there unifying principles? *Nucleic Acids Res* **33**, 7138-50 (2005).

56. Gruber, A.R., Fallmann, J., Kratochvill, F., Kovarik, P. & Hofacker, I.L. AREsite: a database for the comprehensive investigation of AU-rich elements. *Nucleic Acids Res* **39**, D66-9.

57. Lopez de Silanes, I. et al. Global analysis of HuR-regulated gene expression in colon cancer systems of reducing complexity. *Gene Expr* **12**, 49-59 (2004).

58. Wang, W., Caldwell, M.C., Lin, S., Furneaux, H. & Gorospe, M. HuR regulates cyclin A and cyclin B1 mRNA stability during cell proliferation. *EMBO J* **19**, 2340-50 (2000).

59. Wang, W. et al. HuR regulates p21 mRNA stabilization by UV light. *Mol Cell Biol* **20**, 760-9 (2000).

60. Wang, W., Yang, X., Cristofalo, V.J., Holbrook, N.J. & Gorospe, M. Loss of HuR is linked to reduced expression of proliferative genes during replicative senescence. *Mol Cell Biol* **21**, 5889-98 (2001).

61. Hostetter, C. et al. Cytoplasmic accumulation of the RNA binding protein HuR is central to tamoxifen resistance in estrogen receptor positive breast cancer cells. *Cancer Biol Ther* **7**, 1496-506 (2008).

CHAPTER THREE

PADI2 AS A POTENTIAL THERAPEUTIC TARGET IN HER2/ERBB2-POSITIVE BREAST CANCER

* Manuscript from: John L. McElwee; Sachi Horibata; Xuesen Zhang; Sunish Mohanan; Josephine I. Chen; Dalton McLean; Lynne J. Anguish; Paul R. Thompson; and Scott A. Coonrod. PADI2 as a potential therapeutic target in HER2/ERBB2-positive breast cancer. *In preparation*.

3.1 Summary

Introduction:

We have recently reported that the expression of peptidylarginine deiminase 2 (PADI2) is correlated with HER2 expression in breast cancer cell lines and appears to play a role in the proliferation of mammary tumors *in vitro* and *in vivo*; however, the functional relationship between these two genes has yet to be investigated. Thus, the goals of this study were to examine the role of PADI2 in HER2-positive breast cancer, and to validate our next generation PADI inhibitor in the treatment of these tumors.

Methods:

Using molecular genetics approaches, we looked to identify whether PADI2 expression was upstream or downstream of HER2. Lentiviral transduction of MCF10DCIS and BT474 cells was used to examine the role of PADI2 knockdown on HER2 signaling and cellular malignancy. Chromatin-immunoprecipitation (ChIP) was performed to identify whether PADI2 binds the HER2 promoter and/or upstream intronic ERE. Lastly, we used our next-generation PADI inhibitor, BB-Cl-amidine, to examine the role of PADI2 signaling on HER2-positive breast cancers.

Results:

We have previously shown a role for PADI2 in ER-target gene signaling via the citrullination of histone H3 arginine 26 (H3R26). This study shows that PADI2 appears to play a role in HER2-signaling as part of an oncogenic positive-feedback loop. First, we show using MCF10DCIS and BT474 cells stably knocked-downed for PADI2, that HER2 expression levels are decreased. Next, we show that PADI2 binds the HER2 promoter and downstream ERE, and that reduced levels of PADI2 are concomitant with reduced levels of citrullinated H3R26 (H3Cit26). The reduction in

PADI2 signaling has a negative effect on the expression of genes downstream of HER2 signaling, and these results can be replicated with our next-generation PADI inhibitor, BB-Cl-amidine. Interestingly, we also report that increased HER2 signaling can upregulate PADI2 expression. Lastly, we established that the next-generation PADI inhibitor, BB-Cl-amidine, is nearly 100X more potent than first-generation Cl-amidine in reducing the growth of cancer cells.

Conclusion:

Taken together, these results suggest an enhanced role for PADI2 in HER2 expressing breast cancers, and that the PADI inhibitor, BB-Cl-amidine, represents a potential novel therapy for the treatment of patients with HER2-positive mammary tumors.

Key words: Peptidylarginine deiminase, PAD2/PADI2, HER2/ERBB2, Breast Cancer, BB-Cl-amidine, Citrullination, Histone H3 Arginine 26

3.2 Introduction

Breast cancer is the most frequently diagnosed cancer in women, with over 1 million new cases in the world each year [1]. Approximately 75% of breast cancers are ER-positive, with anywhere between 15-20% of breast cancers positive for HER2 amplification or overexpression [2]. Between ER and HER2, the majority of breast cancers express at least one or both of these markers. While there are drugs targeting both of these hormone receptors, about ~30% of patients with ER-positive breast cancers fail to respond to treatments such as tamoxifen; in addition, the majority of those patients that do initially respond develop resistance over time [3]. Interestingly, the most commonly documented mechanism of resistance to tamoxifen occurs via EGFR and HER2 overexpression [4-6]. The same problem exists for patients with HER2-positive tumors, as greater than 60% of patients fail to respond to trastuzumab monotherapy, with initial responders developing resistance within 1 year [7, 8]. In addition, a significant portion of those patients treated with trastuzumab must discontinue treatment because of cardiotoxic side effects, owing to the role of HER2 receptor signaling in the heart [9]. This has highlighted the critical need to discover and validate novel targets for both ER- and HER2-positive tumors, so that additional treatments may be used in combination with, or in the place of, current therapies to overcome issues with *de novo* and acquired resistance.

Recently, in addition to genetic mutations, numerous studies have found that epigenetics plays a direct role in the etiology of breast cancer [10-12]. The PADIs are a family of posttranslational modification enzymes that convert positively charged arginine residues on substrate proteins to neutrally charged citrulline, and this activity is alternatively called citrullination or deimination. Protein citrullination has recently been implicated in many diseases, including cancer [13-19]. PADI2 has historically been defined as a cytoplasmic protein; however, recent evidence from our lab shows that

PADI2 can localize to the nucleus and directly bind chromatin to influence target gene expression [13, 14, 16]. In the canine mammary gland, estrous cycle regulated PADI2 expression in epithelial tissue correlates with citrulline levels, potentially indicating a role in gene expression. Recent evidence from our lab supports this prediction, as Zhang et al. have shown that PADI2 catalyzed citrullination of histone H3 arginine 26 (H3R26) facilitates ER target gene activation [16]. PADI2-mediated citrullination of H3R26 likely facilitates transcriptional activation by creating an open, permissive, chromatin architecture around the EREs of E2-induced genes. Following this, we established a new line of evidence demonstrating that PADI2 plays a role in the oncogenic progression of breast cancer using the basal-like MCF10AT model. Furthermore, we showed using RNA-seq, that *PADI2* is highly correlated with *HER2/ERBB2* overexpression across 57 breast cancer cell lines. We concluded this study with the first preclinical evidence showing that the PADI inhibitor, Cl-amidine, could be utilized as a therapeutic agent for the treatment of tumors *in vivo*.

These findings led to additional questions, mainly, what was the functional relationship between PADI2 and HER2 in breast cancer. In this study, we present an additional role for PADI2 in the expression of the HER2 oncogene. Interestingly, PADI2 appears to function both upstream and downstream of HER2, potentially indicating a role in an oncogenic positive-feedback loop with HER2. Since our previous evidence suggested that PADI2 could act as an ER co-activator via the citrullination of H3R26, we were curious whether PADI2 regulates *HER2* expression using the same mechanism. Using both *PADI2* shRNA and our next-generation PADI inhibitor BB-Cl-amidine, we show that the reduction of PADI2, as well as the inhibition of PADI2-mediated citrullination of H3R26 (BB-Cl-amidine), leads to decreased expression of HER2. Conversely, HER2 regulation of *PADI2* gene

expression is most likely downstream of PI3K signaling. Lastly, we validate our next-generation PADI inhibitor, BB-Cl-amidine, in the treatment of breast cancer cells.

Taken together, these results suggest an enhanced role for PADI2 in HER2 expressing breast cancers. Given the role of PADI2 in ER- and HER2-positive tumors, PADI2 inhibitors may have therapeutic value for over 85% of all breast cancers, thus potentially benefiting a large majority of patients.

3.3 Materials and Methods

The Cancer Genome Atlas (TCGA) data analysis

Data are from the sequencing of mammary tumors as part of the TCGA project [20]. User generated gene-based heat map was performed using the UCSC browser via the TCGA portal (https://genome-cancer.ucsc.edu/proj/site/hgHeatmap/) [21]. Survivability data was generated using the cBio Cancer Genomics Portal (http://cbioportal.org), which is an open-access resource for exploration of the TCGA data sets [22].

Cell culture and treatment with BB-Cl-amidine and small-molecule inhibitors

Cell lines from the MCF10AT breast cancer progression model used were the non-tumorigenic MCF10A, MCF10AT1kC1.2 (MCF10AT), and MCF10DCIS.com (MCF10DCIS) cells, and were obtained from Dr. Fred Miller (Barbara Ann Karmanos Cancer Institute, Detroit, MI, USA). This biological system has been extensively reviewed [23, 24] and culture conditions described [25-27]. The BT474, SKBR3, CHO-K1, and NIH-3T3 cell lines were obtained from ATCC and cultured according to manufacturer's directions. MCF10A cells overexpressing GFP or HER2 were a generous gift of Dr. Zachary Hartman, MD Anderson Cancer Center, and have been previously described elsewhere [28, 29]. All cells were maintained in a humidified atmosphere of 5% CO_2 at 37^o C. For the experimental treatment of cell lines with

inhibitors, cells were seeded in 6-well plates (2×10^4) and treated with select inhibitors: LY294002 (#9901, Cell Signaling), PD98059 (#9900, Cell Signaling), AG1478 (#658548, Calbiochem), Triciribine (#124012, Calbiochem), Rapamycin (R0395, Sigma), Lapatinib (SC-202205, Santa Cruz), and BB-Cl-amidine, which was a generous gift of Dr. Paul Thompson (The Scripps Research Institute, Florida).

Generation of stable cell lines

The MCF10DCIS and BT474 cell lines where stably transduced with lentivirus expressing shRNA for PADI2 or non-targeting shRNA control. Mission shRNA lentivirus plasmids for PADI2 (TRCN0000051447 – NM_007365.1-995s1c1) and non-targeting control (SHC002) were purchased from Sigma. Lentivirus was prepared and transduced according to manufacturer's instructions. Stable clones were generated after selection with 2 µg/ml of puromycin for 2-3-weeks. The MCF10AT cell line was previously generated from MCF10A cells that were stably transfected with T24 H-Ras under G418 selection [30]. Because of this, we generated a pcDNA3.1-hyg (+) vector expressing FLAG-PADI2 by subcloning FLAG-PADI2 from the previously validated pcDNA3.1-neo (+) overexpression vector (pcDNA3.1-FLAG-PADI2 [16]) using NheI and XhoI restriction sites. MCF10AT cells were transfected with the pcDNA3.1-hyg-FLAG-PADI2 plasmid using X-tremeGene 9 (Roche), and stable clones selected in 100 µg/ml hygromycin.

Transient siRNA

Pooled small interfering RNA (siRNA) oligonucleotides (ON-TARGET plus human SMARTpool) against *PADI2* and *ERBB2* were purchased from Dharmacon RNA Technologies (Thermo Scientific). For siRNA transfection of MCF10DCIS and BT474 cell lines, cells were seeded at 100,000/well in 6-well plates, and transfected

with 50–100 nM of the pooled oligonucleotide mixture by using X-tremeGENE siRNA transfection reagent (Roche) following manufacturer's protocols. Cells were grown for 72h before subsequent analysis by western blot or qPCR.

Chromatin-immunoprecipitation (ChIP)

Chromatin immunoprecipitation (ChIP) experiments were performed as previously described[16, 31]. Briefly, MCF10DCIS and BT474 cells were grown to ~80 to 90% confluence, cross-linked with 1% PFA for 10 min at 37^{o}C, and quenched with glycine (125 mM) for 5 min at 4^{o}C. The cells were lysed (1% SDS, 10 mM EDTA, 50 mM Tris·HCl, pH 7.9, 1x protease inhibitor cocktail) and sonicated under conditions yielding fragments ranging from 300bp to 700bp. The material was clarified by centrifugation, diluted 10-fold in dilution buffer (0.5% Triton X-100, 2 mM EDTA, 150 mM NaCl, 20 mM Tris·HCl, pH 7.9, 1x protease inhibitor cocktail), and pre-cleared with protein A-agarose beads. The pre-cleared, chromatin-containing supernatant was used in immunoprecipitation reactions with antibodies against PADI2 (12110-1-AP, ProteinTech) and H3Cit26 (ab19847, Abcam). Ten percent of the supernatant was saved as reference control. The immunoprecipitated genomic DNA was cleared of protein and residual RNA by digestion with proteinase K and RNase (Roche), respectively. The DNA was then extracted with phenol:chloroform:isoamyl alcohol and precipitated with ethanol. ChIP analysis of the *HER2/ERBB2* promoter and downstream ERE (intron 4) was performed using quantitative real-time PCR (qPCR) to determine the enrichment of immunoprecipitated DNA relative to the input DNA, using primers as previously described [32]. Each ChIP experiment was conducted a minimum of three times with independent chromatin isolates to ensure reproducibility.

Immunofluorescence (IF)

Immunofluorescence experiments were performed using a standard protocol as previously described [13]. Briefly, BT474 cells treated with BB-Cl-amidine were probed with primary antibody for anti-ERBB2 (A0485, Dako). The IF slides were incubated in streptavidin conjugated-488 (Invitrogen), washed, and then mounted using Vectashield containing DAPI (Vector Laboratories). Negative control for IF was rabbit IgG antibody at the appropriate concentration.

Western blotting

Western blotting was carried out as previously described [13]. Primary antibodies against the following proteins were incubated overnight at 4^{o}C: PADI2 (12110-1-AP, ProteinTech), ERBB2 (A0485, Dako), pERBB2-Y1248 (2247S, Cell Signaling), EGFR (ab2430, Abcam), pEGFR-Y1173 (4407, Cell Signaling), AKT (4691P, Cell Signaling), pAKT-S473 (4060P, Cell Signaling), MAPK (4695, Cell Signaling), pMAPK-T202/Y204 (4370P, Cell Signaling), AIB1 (2126S, Cell Signaling), ER-alpha (SC-542, Santa Cruz), FLAG-M2 (F1804, Sigma), and Ki67 (ab15580-100, Abcam). To confirm equal protein loading, membranes were stripped and re-probed with anti-β-actin (ab8227, Abcam).

Quantitative real-time PCR (qPCR)

RNA was purified using the Qiagen RNAeasy kit, including on-column DNase treatment to remove genomic DNA. The resulting RNA was reverse transcribed using the ABI High Capacity RNA-to-cDNA kit according to the manufacturer's protocol (Applied Biosystems). TaqMan Gene Expression Assays (ABI) for human *PADI2* (Hs00247108_m1), *ERBB2* (Hs01001580_m1), *EGFR* (Hs01076078_m1), *AIB1* (Hs00180722_m1), *ESR1* (Hs00174860_m1), and *GAPDH* (4352934E), were used for

qPCR. In addition, primer sequences for gene expression analysis via SYBR-qPCR can be found in **Table 3.1**. Expression levels were analyzed using the $2^{-\Delta\Delta C(t)}$ method [33]. Data are shown as means ± SD from three independent experiments, and were separated using Student's t-test.

Flow-cytometry

Monolayers of MCF10DCIS, BT474, CHO-K1, and NIH3T3 cells were seeded into 25 cm^2 flasks (2 x 10^6 cells) and treated with increasing concentrations of BB-Cl-amidine or vehicle (DMSO, 0.6125µM, 1.25 µM, 2.5 µM, and 5.0 µM). Cells were harvested after 48h using Accutase (Innovative Cell Technologies), fixed, permeabilized, and blocked in FACS Buffer (0.1M Dulbecco's phosphate buffered saline, 0.02% sodium azide, 1.0% bovine serum albumin, and 0.1% Triton X-100) containing 10% normal goat serum and stained (except the isotype controls) with rabbit anti-cleaved Caspase-3 antibody (Cell Signaling). Isotype controls were treated with normal rabbit IgG (Vector Laboratories). All samples were stained with secondary goat anti-rabbit IgG conjugated to Alexa-488 (Invitrogen) and DAPI (Invitrogen) according to the manufacturer's instructions. Cells were analyzed on a FACS-Calibur (BD Biosciences) or a Gallios (Beckman Coulter) flow-cytometer and data analyzed for percent apoptotic cells (cleaved caspase-3-positive) and cell cycle analysis with FlowJo software (TreeStar Inc.). Data are shown as means ± SD from three independent experiments, and were separated using Student's t-test.

Assays for cellular malignancy

Anchorage-independent growth assays were performed on MCF10DCIS-P2KD and MCF10AT-PADI2 cells, along with their respective control cell lines (MCF10DCIS-SC and MCF10AT-emtpy). Briefly, the cells were plated at a density of 5,000 cells/ml

in medium containing 0.3% agarose onto media containing 0.6% agarose in 6-well dishes. Cultures were fed once a week and colonies counted after 3-weeks of growth. Each assay was repeated and means represent ± SD from three independent experiments (* $p < 0.05$). Focus formation assays were carried out on cells grown in 6-well plates. Cells were fixed with 4% PFA and stained with crystal violet for subsequent analysis of focus formation.

Statistical analysis

All experiments were independently repeated at least three times unless otherwise indicated. Values were expressed as the mean ± the SD. Means were separated using Student's t-test

3.4 Results

PADI2 is overexpressed in HER2-positive and basal-like tumors and is correlated with poor prognosis

While we have previously shown that *PADI2* is highly correlated with *HER2* expression levels across 57 breast cancer cell lines, we wanted to see whether this relationship holds up in primary mammary tumors. Recently, data from The Cancer Genome Atlas (TCGA) was published [20], with various sources currently available to access this data. The UCSC cancer browser offers the opportunity to view data in user generated gene-based heat maps [21]. We examined a small group of genes known to be involved in PADI2 signaling in breast cancer. Consistent with our previous findings, we see the same relationship between *PADI2* and *HER2*, as *PADI2* expression clusters with HER2-positive tumors (**Figure 3.1**). Interestingly, we also see that *PADI2* is upregulated in basal-like breast cancers, along with EGFR, which is known to be a marker for basal tumors; however, our previous data potentially supports this

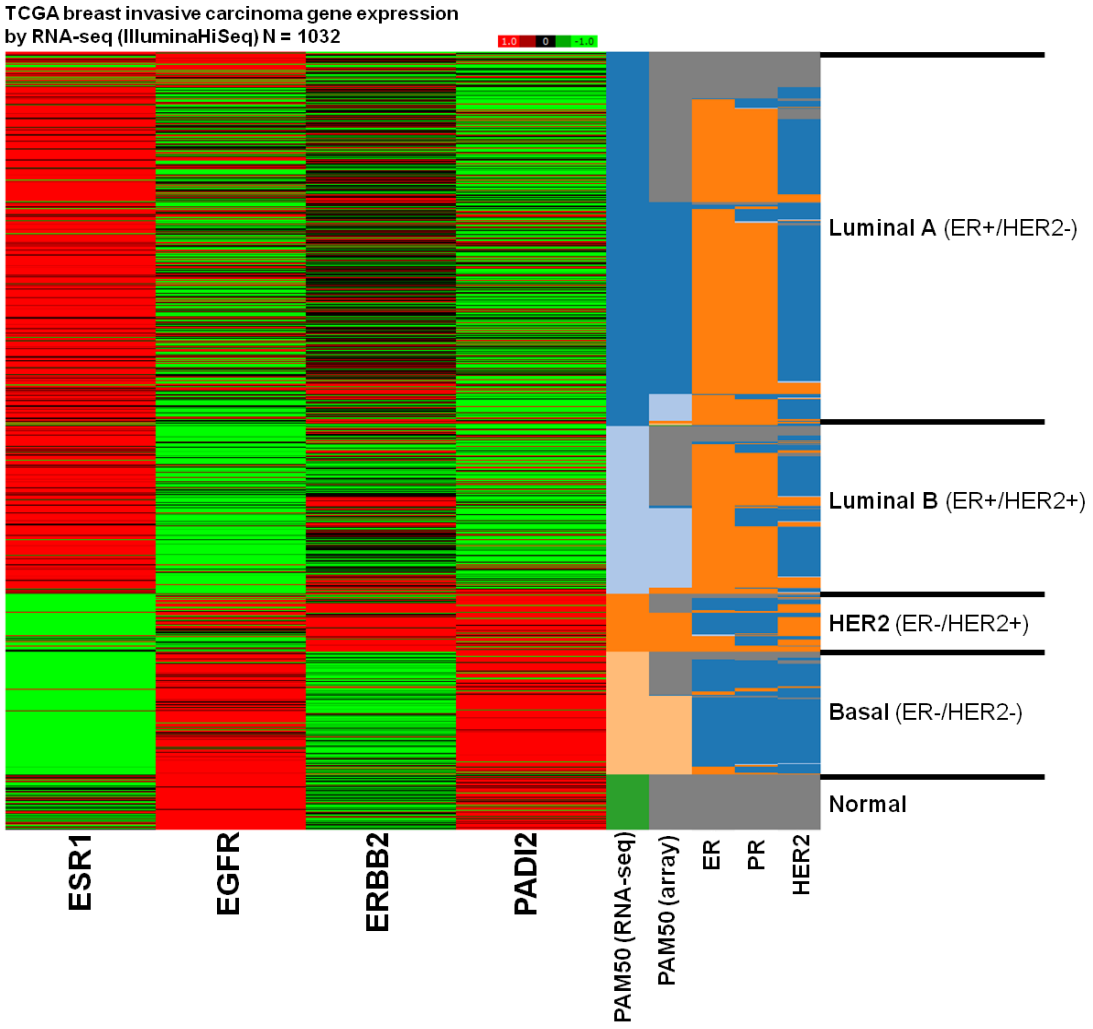

Figure 3.1: PADI2 expression clusters with HER2-positive and basal-like tumors. TCGA heat map displaying gene expression for genes known to play a role in PADI2 signaling: estrogen receptor-alpha (*ESR1*), epidermal growth factor receptor (*EGFR*), erythroblastic leukemia viral oncogene homolog-2 (*ERBB2*), and peptidylarginine deiminase-2 (*PADI2*). Gene mRNA levels were determined by Illumina HiSeq 2000 RNA Sequencing platform by the University of North Carolina TCGA genome characterization center. Breast cancer subtypes are based on RNA-seq and array data. Mammary tumors (N = 1032) are from the TCGA breast cancer panel (as presented in TCGA, N*ature*, 2012 [20]). Data were collected from UCSC browser (TCGA portal), and heat map generated as detailed in Goldman et al., *Nuc. Acids Res.*, 2013 [21].

relationship, as we have shown *PADI2* is upregulated in the transformed cell lines of the basal MCF10AT model of breast cancer progression [15]. Surprisingly, we do not see any correlation between *PADI2* and *ESR1* (ER) expression levels, though our previous data suggest that *PADI2* expression is upregulated upon estrogen stimulation in ER-positive breast cancer [16]. However, more work is needed to investigate this disparity. The TCGA data are also associated with clinical progression and outcome for each of the patients and associated primary tumors. We queried the cBio Cancer Genomics Portal, which is offered through Memorial Sloan Kettering Cancer Center (MSKCC) [22], and show that PADI2 upregulation in mammary tumors leads to decreased survivability and worse prognosis (p-value = 0.0435) (**Figure 3.2**). Interestingly, we see these data hold up for basal-like tumors, with elevated PADI2 significantly decreasing survivability in these patients (p-value = 0.0036).

Knockdown of PADI2 reduces HER2/ERBB2 expression levels

The coordinated increase in *PADI2* and *HER2* expression levels suggested a direct relationship, and given our previously established role for PADI2 as an ER co-activator, we wanted to assess the potential effect of PADI2 on HER2 signaling. Using lentiviral delivery of shRNA targeting PADI2 (or scrambled control), we generated two different breast cancer cell lines that stably knocked-downed *PADI2* expression. We first targeted the MCF10DCIS cell line, which we previously described as having high PADI2 expression levels *in vitro* and *in vivo*. This cell line is part of the MCF10AT model of breast cancer progression, and faithfully recapitulates highly invasive human comedo-like ductal carcinoma *in situ* tumors [34]. We found that when we knocked-down *PADI2* in MCF10DCIS cells, HER2 expression levels were reduced at both the protein and mRNA levels (**Figure 3.3a and b**). Interestingly, we also saw a slight reduction in the activated form of HER2/ERBB2, indicated by

Figure 3.2: PADI2 upregulation in mammary tumors leads to decreased survivability and worse prognosis. TCGA data showing that PADI2 upregulation significantly decreases survivability across all mammary tumors (a) and the basal subtype (b). Kaplan-Meier estimates of disease specific survival (event of death from breast cancer) across 447 samples for all mammary tumors (16/447, p-value 0.0435) and 81 cases for basal-like tumors (10/81, p-value 0.0036).

a

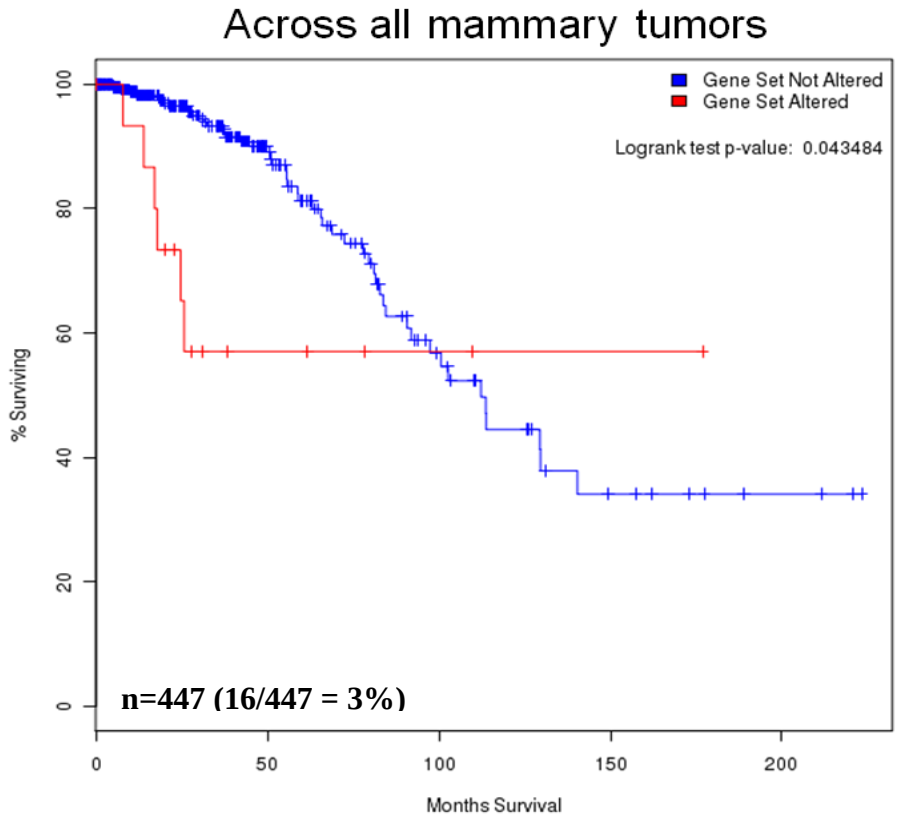
Across all mammary tumors
Gene Set Not Altered
Gene Set Altered
Logrank test p-value: 0.043484
% Surviving
0
20
40
60
80
100
0
50
100
150
200
Months Survival
n=447 (16/447 = 3%)

b

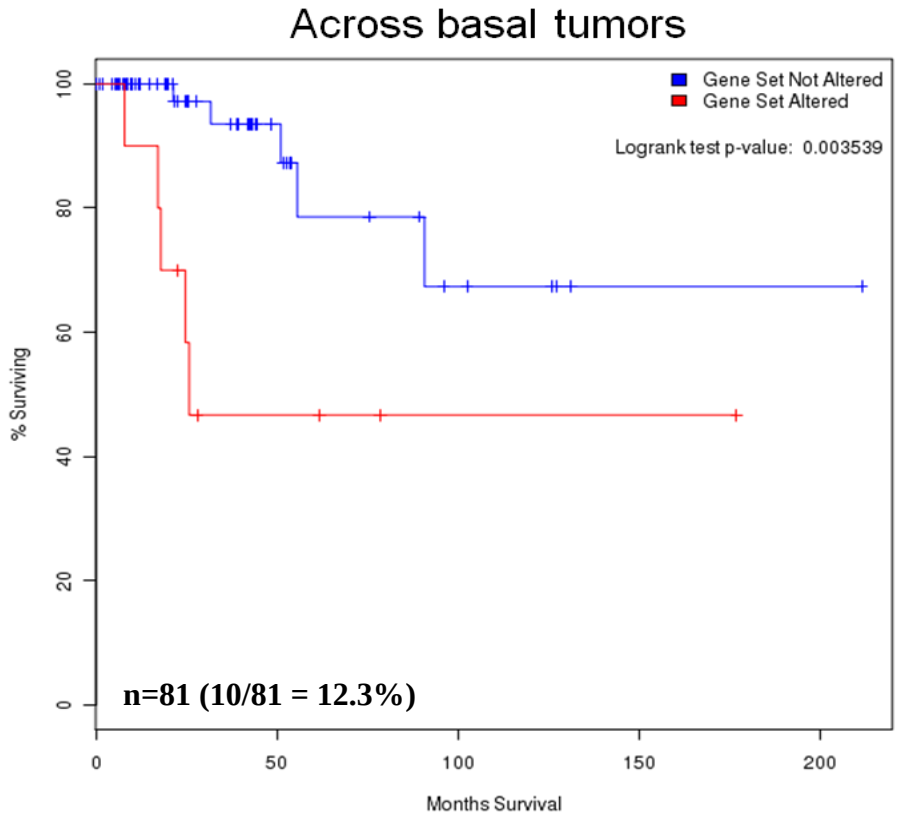
Across basal tumors
Gene Set Not Altered
Gene Set Altered
Logrank test p-value: 0.003539
% Surviving
0
20
40
60
80
100
0
50
100
150
200
Months Survival
n=81 (10/81 = 12.3%)

phosphorylation at tyrosine-1248 (pERBB2). We have previously shown, along with others, that MCF10DCIS cells have upregulated HER2/ERBB2 expression levels (when compared to their isogenic parental cell line, MCF10A) [15, 35, 36], but we wanted to compare whether we see this same effect in the HER2-amplified BT474 cell line. This cell line was chosen due to its high levels of HER2/ERBB2 and PADI2 expression. Again, we see the same effect on HER2 /ERBB2 expression when we knockdown PADI2, with the effect on pERBB2 levels more pronounced in BT474 than MCF10DCIS (**Figure 3.3a and b**). The reduction in activated HER2/ERBB2 in both cell lines could potentially be a byproduct of the decreased HER2/ERBB2 protein levels; however, we cannot rule out additional mechanisms. To validate these findings, we examined whether ER or the ER co-activator AIB1 had any changes in expression levels upon PADI2 knockdown (**Figure 3.4a and b**). As expected, we see that ER levels are reduced, which we have previously described in MCF7 cells [16]. However, the reduction of AIB1 protein, a known ER cofactor that has been implicated in tamoxifen resistance, was surprising [5, 32]. While we have previously established a role for PADI2 in ER-target gene signaling, these data suggest that PADI2 might also play a role in the development of tamoxifen resistance through ER/HER2 cross talk.

PADI2 binds the HER2/ERBB2 promoter and downstream ERE and potentially acts as a co-activator of HER2 signaling

Given our previously findings linking PADI2 and histone H3 arginine (H3R26) citrullination (H3Cit26) with ER-target gene expression, and our results here showing PADI2 knockdown leads to decreased HER2 expression levels, we predicted that PADI2 might directly regulate HER2 via the same mechanism. To test this hypothesis, we used chromatin immunoprecipitation (ChIP) to assay PADI2 binding to the *HER2/ERBB2* promoter and downstream estrogen response element (ERE) in both

Figure 3.3: Stable knockdown of *PADI2* leads to decreased HER2/ERBB2 expression at both protein and mRNA levels. (a) Western blot analyses of PADI2, ERBB2, and phosphorylated ERBB2 protein levels (pERBB2-Y1248) in MCF10DCIS (DCIS) or BT474 cells stably expressing a scrambled control shRNA (SC) or shRNA directed against *PADI2* (P2KD). Equal loading was determined by probing the membrane with β-actin antibody. (b) Relative *PADI2* and *ERBB2* mRNA levels in MCF10DCIS and BT474 P2KD cell lines compared to scrambled control. *PADI2* and *ERBB2* mRNA levels were determined by qPCR (TaqMan) using scrambled control (SC) cells as the reference and with *GAPDH* normalization. Expression levels were analyzed using the $2^{-\Delta\Delta C(t)}$ method, and data are expressed as the mean ± SD from three independent experiments (* $p < 0.05$).

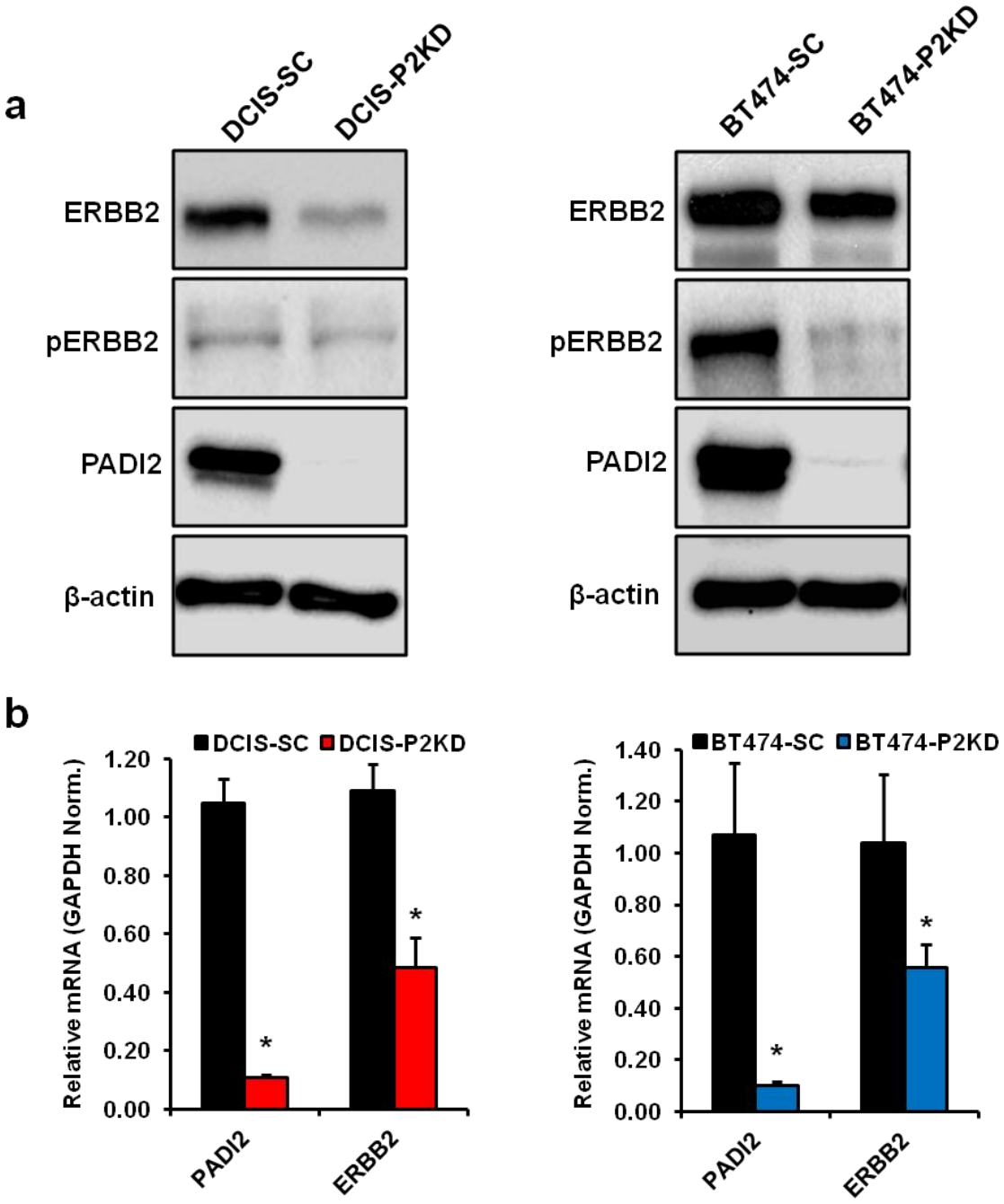
a
DCIS-SC
DCIS-P2KD
BT474-SC
BT474-P2KD
ERBB2
pERBB2
PADI2
β-actin
b
DCIS-SC
DCIS-P2KD
BT474-SC
BT474-P2KD
Relative mRNA (GAPDH Norm.)
1.20
1.00
0.80
0.60
0.40
0.20
0.00
1.40
*
PADI2
ERBB2

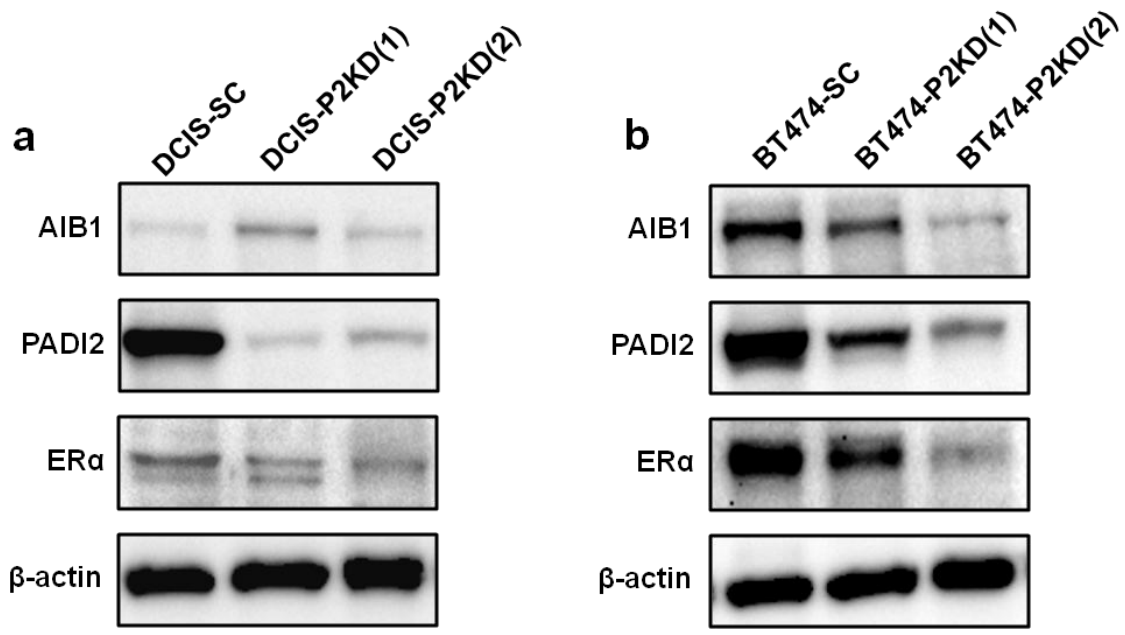

Figure 3.4: ***PADI2*** **stable knockdown leads to a decrease in the expression of estrogen receptor-alpha and ER-cofactor AIB1**. (a) Western blot analyses of PADI2, ER-alpha (ERα), and the ERα co-activator AIB1 protein levels in MCF10DCIS (DCIS) or BT474 cells stably expressing a scrambled control shRNA (SC) or shRNA directed against *PADI2* (P2KD). Two different stable clones were tested, (1) and (2), with (2) being the clone selected for further analysis in both MCF10DCIS and BT474 cell lines. Equal loading was determined by probing the membrane with β-actin antibody.

MCF10DCIS and BT474 cells. Results show that the strong association of PADI2 with ETS elements at the *HER2/ERBB2* promoter, in addition to the recently identified downstream intronic ERE, is lost upon PADI2 knockdown in both the MCF10DCIS (**Figure 3.5a**) and BT474 (**Figure 3.5b**) cell lines. Furthermore, we also found a sharp reduction in the H3Cit26 modification at both of these sites in PADI2-depleted (PADI2-KD) cell lines (**Figure 3.5a and b**), suggesting that PADI2-catalyzed H3Cit26 modification may regulate *HER2/ERBB2* expression. To examine whether PADI2-KD has any effects on genes known to be downstream of HER2 signaling, we analyzed the expression of a subset of genes using qPCR. We first looked at the MCF10DCIS cell line, and as expected, we see a reduction of *HER2/ERBB2* gene levels, along with genes known to be downstream of HER2, including *JAB1* [37, 38], *PEA3* [39, 40], *FOXAI* [41], *FOXMI* [42, 43], and *GRB7* [44] (**Figure 3.6**). The same group of genes is also reduced in the BT474 cell line (**Figure 3.7**), indicating similar results in both cell lines upon PADI2-KD. HER2/ERBB2 signaling is known to drive the proliferation of breast cancer cells, leading to the upregulation of genes known to be involved with cell cycle progression, such as the cyclins and cyclin dependent kinases (CDKs). Interestingly, we show that PADI2-KD in both MCF10DCIS and BT474 cells leads to a reduction across these genes, as well as in the proliferation markers, *Ki67* and *PCNA* (**Figures 3.6 and 3.7**). Surprisingly, we also see an increase in markers of inflammation, *IL6* and *IL8*, upon PADI2-KD in both cell lines. While PADI2 has been implicated in multiple inflammatory diseases, these results are surprising given the role of both of these genes in tumor progression. However, recent evidence suggests that both IL6 and IL8 are involved in inflammatory positive-feedback loops during the progression of HER2-positive breast cancer [29, 45, 46]. Not surprisingly, we also see a reduction in ER (*ESR1*), as well as the nuclear receptor co-activators *SRC1* and *AIB1*. The expression of co-activator proteins, such as SRC1,

<u>Figure 3.5:</u> PADI2 and H3Cit26 bind the *HER2/ERBB2* promoter and intronic ERE in MCF10DCIS and BT474 cells. Chromatin-immunoprecipitation (ChIP) qPCR was used to analyze the binding of PADI2 and citrullinated H3R26 (H3Cit26) to the *HER2/ERBB2* promoter and/or downstream ERE in MCF10DCIS (a) and BT474 (b) cells. ChIP-qPCR data are presented as % input for MCF10DCIS and signal/background for BT474. Error bars indicate ± SEM of three independent experiments.

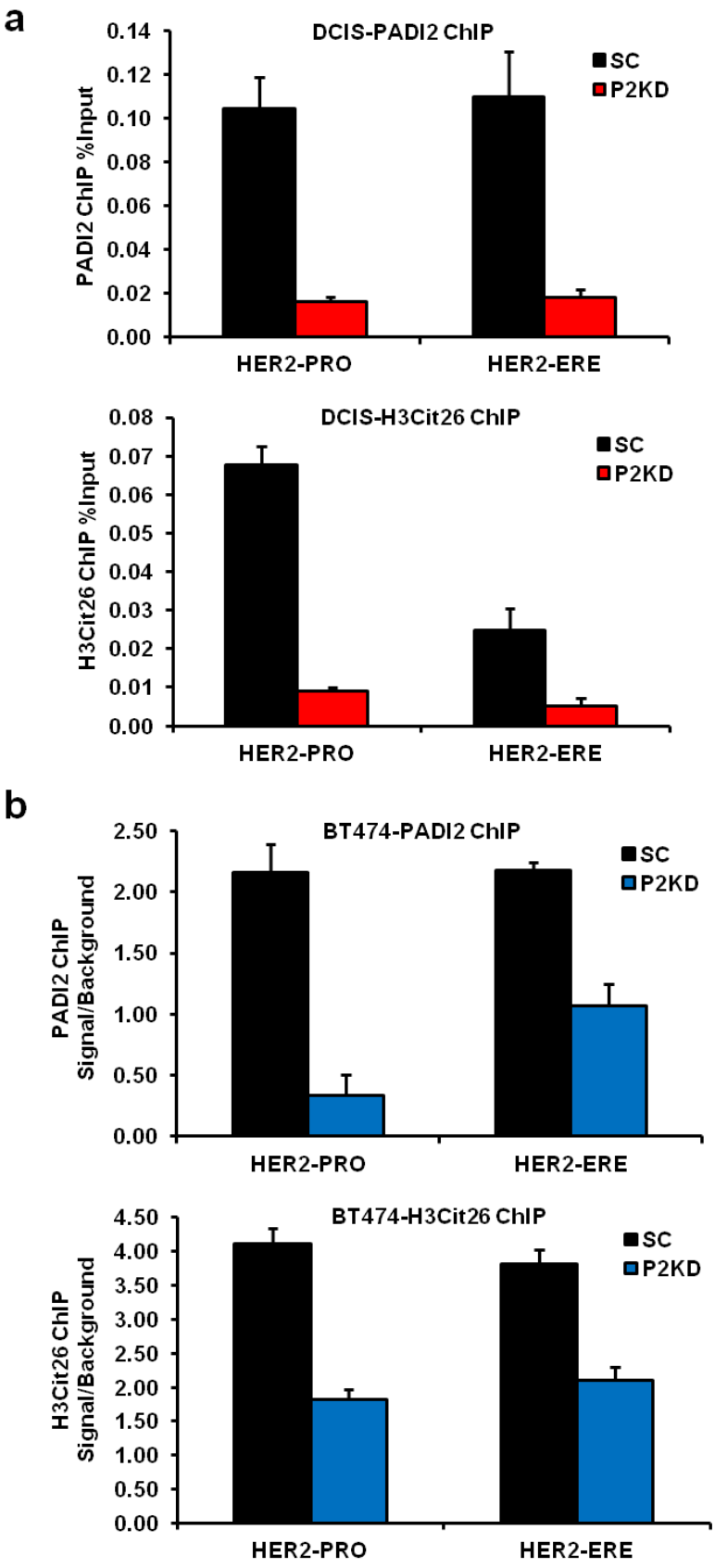
a
DCIS-PADI2 ChIP
PADI2 ChIP %Input
0.14
0.12
0.10
0.08
0.06
0.04
0.02
0.00
SC
P2KD
HER2-PRO
HER2-ERE
DCIS-H3Cit26 ChIP
H3Cit26 ChIP %Input
0.08
0.07
0.06
0.05
0.04
0.03
0.02
0.01
0.00
SC
P2KD
HER2-PRO
HER2-ERE
b
BT474-PADI2 ChIP
PADI2 ChIP Signal/Background
2.50
2.00
1.50
1.00
0.50
0.00
SC
P2KD
HER2-PRO
HER2-ERE
BT474-H3Cit26 ChIP
H3Cit26 ChIP Signal/Background
4.50
4.00
3.50
3.00
2.50
2.00
1.50
1.00
0.50
0.00
SC
P2KD
HER2-PRO
HER2-ERE

Figure 3.6: Stable knockdown of *PADI2* reduces expression of genes downstream of HER2/ERBB2 and ER signaling in MCF10DCIS cells. Genes known to be expressed downstream of HER2 and ER (full gene list and primers can be found in **Table 3.1**) were tested by SYBR qPCR on MCF10DCIS (DCIS) cells stably expressing a scrambled control shRNA or shRNA directed against *PADI2* (P2KD). Relative mRNA levels in MCF10DCIS P2KD cell lines compared to scrambled control. Total RNA was isolated from cells and respective mRNA levels were determined by SYBR qPCR using scrambled control cells as the reference (represented by dashed line = ~1) and with *GAPDH* normalization. Expression levels were analyzed using the $2^{-\Delta\Delta C(t)}$ method, and data are expressed as the mean ± SD from three independent experiments.

DCIS-PADI2-KD
Relative mRNA (GAPDH Norm.)
0.00
0.50
1.00
1.50
2.00
2.50
3.00
3.50
4.00
4.50
PADI2
NRG1
EGFR
HER2
HER3
VEGFA
IGFR1
FOXA1
FOXM1
PEA3
GRB7
JAB1
ESR1
SRC1
AIB1
PI3K
AKT1
AKT2
AKT3
mTOR
MEK1
ERK1
ERK2
p53
PUMA
PARP1
BCL2
BAX
BIRC5
GADD45α
p21
p27
CDK1
CDK2
CDK4
CDK6
CCNB1
CCND1
CCND2
CCNE1
RB1
MYC
HRAS
KRAS
NRAS
KI67
PCNA
ECAD
NCAD
VIM
FN1
SNAIL
SLUG
TWIST
IL6
IL8
GSK3β
COX2
MMP2
NFKB1
RELA
TGFβ
BCAT
SMAD2
SMAD3
SMAD4
26.16
5.17

<u>Figure 3.7:</u> Stable knockdown of *PADI2* reduces expression of genes downstream of HER2/ERBB2 and ER signaling in BT474 cells. Genes known to be expressed downstream of HER2 and ER (full gene list and primers can be found in **Table 3.1**) were tested by SYBR qPCR on BT474 cells stably expressing a control scrambled shRNA or shRNA directed against *PADI2* (P2KD). Relative mRNA levels in BT474-P2KD cell lines compared to scrambled control. Total RNA was isolated from cells and respective mRNA levels were determined by SYBR qPCR using scrambled control cells as the reference (represented by dashed line = ~1) and with *GAPDH* normalization. Expression levels were analyzed using the $2^{-\Delta\Delta C(t)}$ method, and data are expressed as the mean ± SD from three independent experiments.

BT474-PADI2-KD
Relative mRNA (GAPDH Norm.)
0.00
0.50
1.00
1.50
2.00
2.50
3.00
3.50
4.00
4.50
PADI2
NRG1
EGFR
HER2
HER3
VEGFA
IGFR1
FOXA1
FOXM1
PEA3
GRB7
JAB1
ESR1
SRC1
AIB1
PI3K
AKT1
AKT2
AKT3
mTOR
MEK1
ERK1
ERK2
p53
PUMA
PARP1
BCL2
BAX
BIRC5
GADD45a
p21
p27
CDK1
CDK2
CDK4
CDK6
CCNB1
CCND1
CCND2
CCNE1
RB1
MYC
HRAS
KRAS
NRAS
KI67
PCNA
ECAD
NCAD
VIM
FN1
SNAIL
SLUG
TWIST
IL6
IL8
GSK3β
COX2
MMP2
NFKB1
RELA
TGFβ
BCAT
SMAD2
SMAD3
SMAD4
8.03
11.28
5.07

AIB1, and Polyomavirus Enhancer Activator-3 (PEA3), has been shown to correlate with endocrine resistance in breast cancer [47].

PADI2 expression levels correlate with cellular malignancy

Given the reduction in expression of genes downstream of HER2 signaling, including those involved in proliferation and ER/HER2 cross talk in breast cancer, we wanted to see what effects the knockdown of PADI2 has on cellular malignancy. We tested the ability of our PADI2 knocked-down MCF10DCIS cells to form colonies in soft-agar. The ability of cells to grow under anchorage-independent conditions is a hallmark of malignant transformation. We show that both the size (**Figure 3.8a**) and number (**Figure 3.8b**) of colonies are severely reduced in the PADI2-KD (DCIS-P2KD) cells, when compared to scrambled control shRNA cells (DCIS-SC). However, we did not see any effect on anchorage-independent growth of BT474-P2KD cells (data not shown). In addition, we assayed the focus-forming activity for both MCF10DCIS (**Figure 3.8c**) and BT474 (**Figure 3.8d**) cells, with both showing a marked reduction in PADI2-KD cell lines compared to the scrambled control. Conversely, we tested the ability of PADI2 overexpression to enhance malignancy in MCF10AT cells lines. While we do not see any significant difference in the number of colonies grown on soft-agar, the MCF10AT-PADI2 cells have larger colonies (**Figure 3.9a and b**). We also found a slight increase in HER2/ERBB2 expression in the stably overexpressing MCF10AT-PADI2 cells, when compared to the control empty vector cells (MCF10AT-empty) (**Figure 3.9c**).

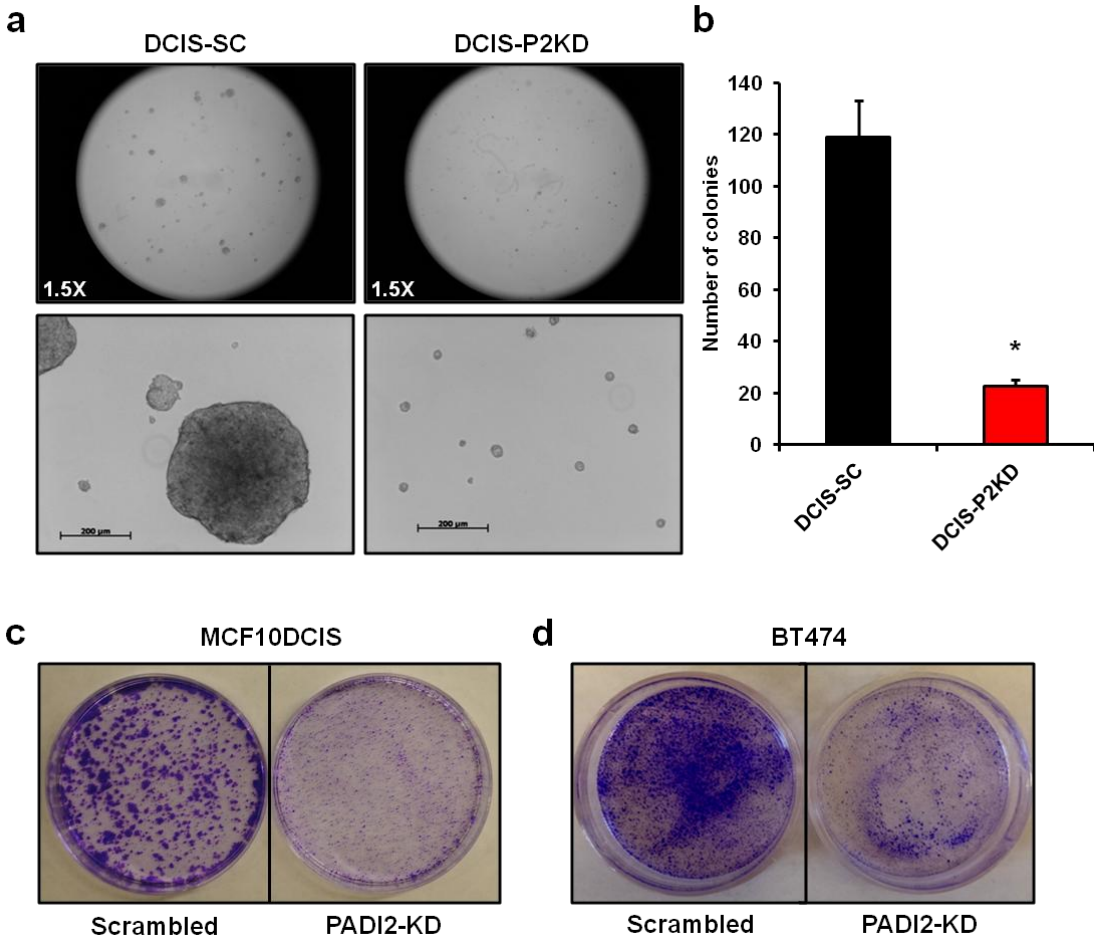

<u>Figure 3.8:</u> ***PADI2*** **knockdown (KD) decreases cellular malignancy in breast cancer cells.** (a) MCF10DCIS cells stably overexpressing shRNA for *PADI2* or scrambled control were plated at a density of 5,000 cells/ml in medium containing 0.3% agarose onto media containing 0.6% agarose in 6-well dishes. Cultures were fed once a week and colonies counted (b) after 3-weeks of growth. The data shown in (b) are expressed as the mean ± SD from three independent experiments (* $p < 0.05$). MCF10DCIS (c) and BT474 (d) cells stably expressing scrambled or *PADI2* shRNA were grown for 1-week, fixed with 4% PFA, and stained with crystal violet for subsequent analysis of focus formation.

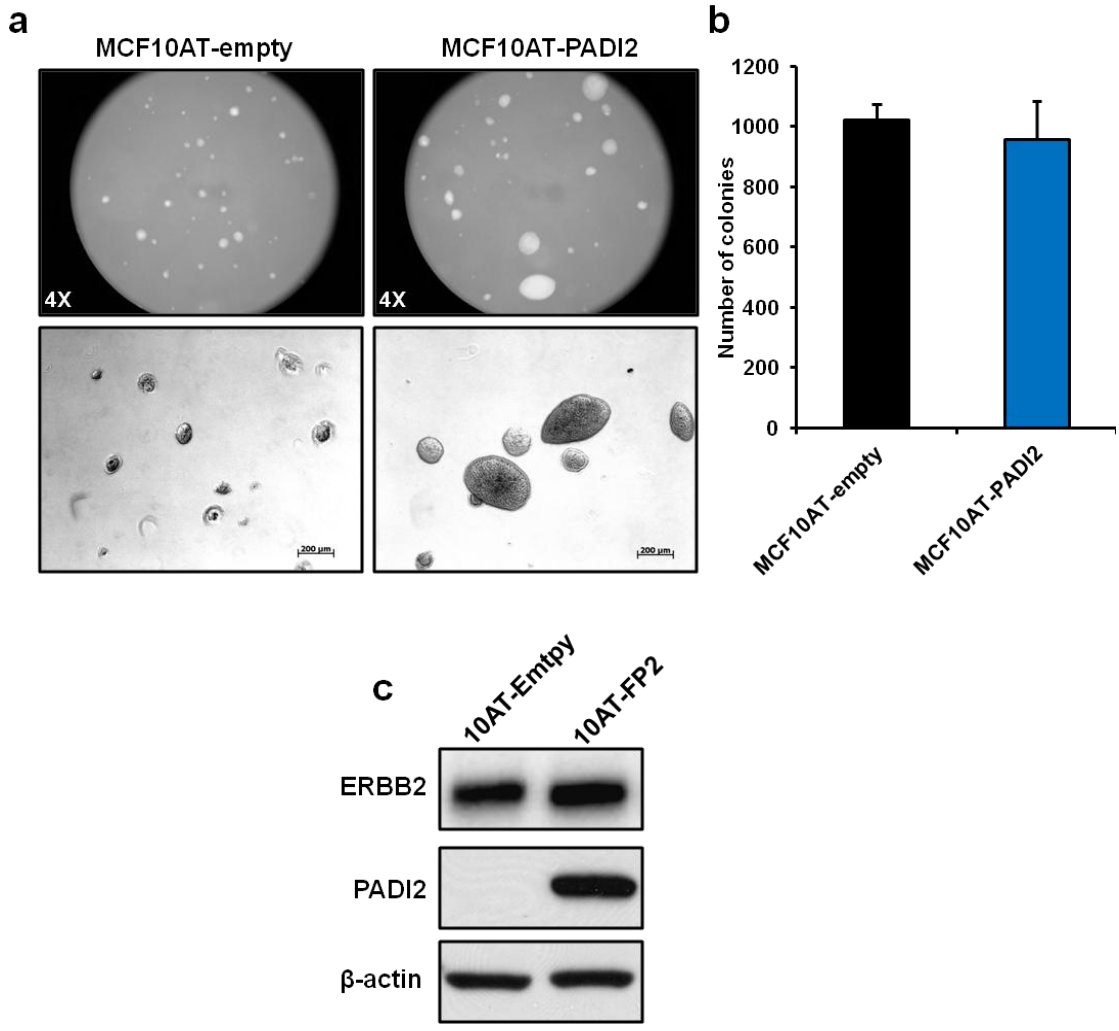

<u>Figure 3.9:</u> Stable overexpression of PADI2 in premalignant MCF10AT cells leads to increased colony size in anchorage-independent growth. (a) MCF10AT cells stably overexpressing FLAG-tagged PADI2 (pcDNA3.1-FLAG-PADI2) or an empty vector control were plated at a density of 5,000 cells/ml in medium containing 0.3% agarose onto media containing 0.6% agarose in 6-well dishes. Cultures were fed once a week and colonies counted (b) after 3-weeks of growth. The data shown in (b) are expressed as the mean ± SD from three independent experiments (* $p < 0.05$). (c) Western blot of PADI2 and ERBB2 protein levels in MCF10AT cells overexpressing PADI2 or empty vector. (β-actin = loading control)

Inhibition of PADI2 activity reduces HER2/ERBB2 associated oncogenic signaling and cellular malignancy

To investigate whether PADI2 expression is important for HER2 gene expression and downstream signaling, we next tested the pharmacological inhibition of PADI2 on breast cancer cells *in vitro.* We have recently developed a next-generation PADI inhibitor, biphenyl-benzimidazole-Cl-amidine (BB-Cl-amidine), which has increased cellular permeability, stability, and potency compared to first-generation Cl-amidine. BB-Cl-amidine is a derivative of Cl-amidine (**Figure 3.10a**), and has much of the same properties, including the ability to bind irreversibly to the active site of PADIs, thereby blocking activity *in vitro* and *in vivo* [48]. BB-Cl-amidine functions as a "pan-PADI" inhibitor as it blocks the activity of all PADIs, though PADI2 has been shown to be the predominant isozyme expressed in both MCF10DCIS and BT474 cells (McElwee et al.[15] and data not shown). We found that BB-Cl-amidine leads to a dose-dependent reduction in HER2/ERBB2 protein expression in MCF10DCIS cells and the HER2-positive SKBR3 cell line (**Figure 3.10b**). Furthermore, we see the same dose-dependent reduction at the mRNA level in both cell lines (**Figure 3.10c**), indicating that PADI2 activity has a potential effect on *HER2/ERBB2* gene transcription. When we knocked-down PADI2 in BT474 cells, we noticed that there was a reduction in both ER and AIB1 [47] (**Figure 3.4**), both of which are involved, along with HER2/ERBB2 and EGFR [4-6], in the development of acquired resistance to hormone-therapy. Similarly, we found that BB-Cl-amidine reduces HER2/ERBB2 and EGFR, along with both of their tyrosine phosphorylated activated forms (pERBB2-Y1248 and pEGFR-Y1173) (**Figure3.11a**). As expected, we also see a dose-dependent reduction in both ER and AIB1 levels (**Figure 3.11a**). This reduction in protein expression is concomitant with a reduction in gene expression (**Figure 3.11b**). Furthermore, this reduced growth-factor/ER cross talk leads to a reduction in cellular

<u>Figure 3.10:</u> The PADI inhibitor, BB-Cl-amidine, leads to a dose-dependent reduction of HER2/ERBB2 protein and mRNA. (a) The chemical structure of next-generation PADI inhibitor, biphenyl-benzimidazole-Cl-amidine (BB-CLA); BB-CLA has increased cellular permeability, stability, and potency compared to first-generation Cl-amidine. (b) MCF10DCIS and BT474 cells were treated for 24h with increasing concentrations of BB-Cl-amidine or vehicle (DMSO, 500 nM, 1.25 µM, 2.5 µM, and 5.0 µM). Whole-cell lysates were analyzed by western blot for PADI2 and ERBB2 proteins, with β-actin serving as a loading control. (c) Relative *PADI2* and *ERBB2* mRNA levels in MCF10DCIS and BT474 cells treated with BB-Cl-amidine compared to vehicle control (DMSO). *PADI2* and *ERBB2* mRNA levels were determined by qPCR (TaqMan) using DMSO treated cells as the reference and with *GAPDH* normalization. Expression levels were analyzed using the $2^{-\Delta\Delta C(t)}$ method, and data are expressed as the mean ± SD from three independent experiments (* $p < 0.05$).

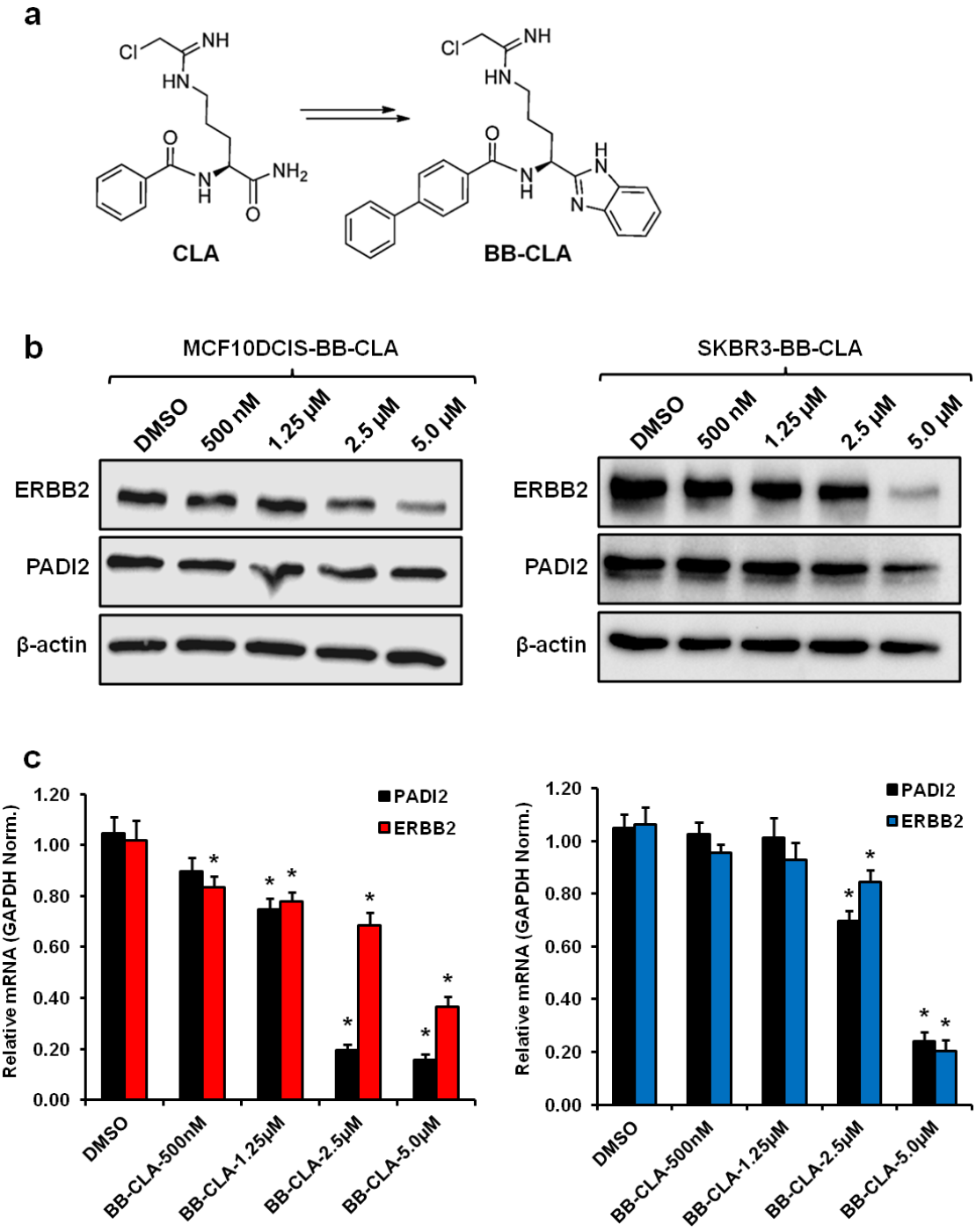
a
CLA
BB-CLA
b
MCF10DCIS-BB-CLA
SKBR3-BB-CLA
DMSO
500 nM
1.25 μM
2.5 μM
5.0 μM
ERBB2
PADI2
β-actin
c
Relative mRNA (GAPDH Norm.)
PADI2
ERBB2
DMSO
BB-CLA-500nM
BB-CLA-1.25μM
BB-CLA-2.5μM
BB-CLA-5.0μM

<u>Figure 3.11:</u> BB-Cl-amidine leads to decreased malignancy of breast cancer cells and dose-dependent reduction in the expression of genes involved in ER-signaling and tamoxifen resistance pathways. (a) Western blot analysis of proteins involved in ER-signaling and tamoxifen resistance in BT474 cells after treatment of cells for 24h with vehicle (DMSO) or increasing doses of BB-Cl-amidine (500 nM, 1.25 μM, 2.5 μM, and 5.0 μM). Whole-cell lysates were analyzed by western blot for the indicated proteins, including active forms of ERBB2 (phosphorylated -ERBB2, Y1248) and EGFR (phosphorylated-EGFR, Y1173), with β-actin serving as a loading control. Total RNA was isolated after 24h of treatment and analyzed for *ERBB2*, *EGFR*, *AIB1*, *PADI2*, and *ESR1* mRNA expression using qPCR (TaqMan). Values represent the averages of three independent experiments (* $p < 0.05$) using DMSO treated cells as the reference and with *GAPDH* normalization. (c) MCF10DCIS and BT474 cells were treated with increasing doses of BB-Cl-amidine over the course of 1-week, with replacement of media and drug every 3 days. Cells were fixed with 4% PFA and stained with crystal violet for subsequent analysis.

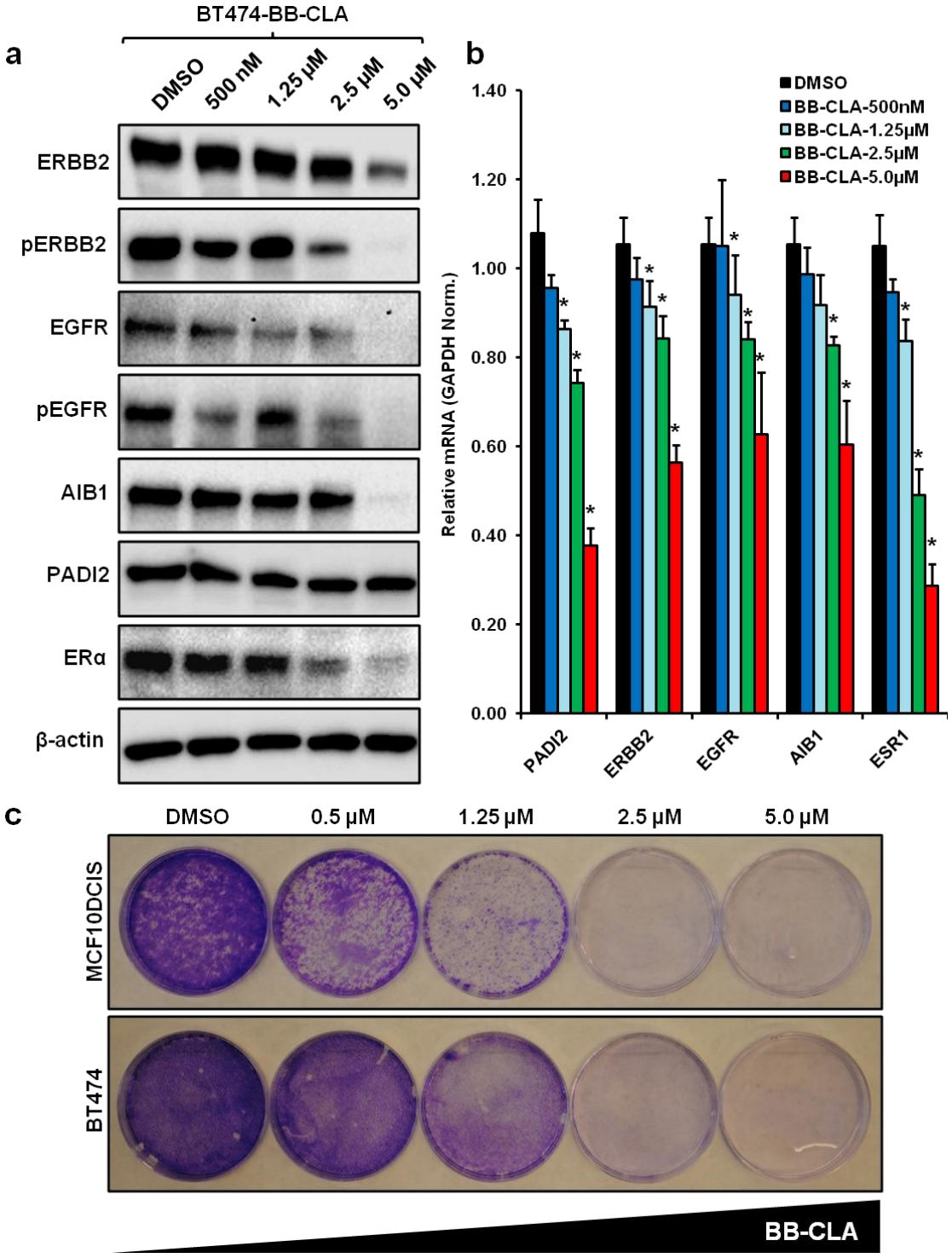
a
BT474-BB-CLA
DMSO
500 nM
1.25 μM
2.5 μM
5.0 μM
ERBB2
pERBB2
EGFR
pEGFR
AIB1
PADI2
ERα
β-actin
b
DMSO
BB-CLA-500nM
BB-CLA-1.25μM
BB-CLA-2.5μM
BB-CLA-5.0μM
Relative mRNA (GAPDH Norm.)
1.40
1.20
1.00
0.80
0.60
0.40
0.20
0.00
PADI2
ERBB2
EGFR
AIB1
ESR1
c
DMSO
0.5 μM
1.25 μM
2.5 μM
5.0 μM
MCF10DCIS
BT474
BB-CLA

growth and malignancy in treated breast cancer cells. Both MCF10DCIS and BT474 cells show a dose-dependent decrease in focus formation when treated with BB-Cl-amidine (**Figure 3.11c**). Since we observed a reduction in expression of genes known to be downstream of HER2 signaling upon PADI2 knockdown, we wanted to see whether the inhibition of PADI2 activity has the same effect. As predicted, we show the same reduction in the genes downstream of HER2 signaling (**Figures 3.12 and 3.13**); however, the decrease is not as pronounced as that seen in the PADI2-KD cells. Interestingly, we saw an increased reduction in expression of those genes involved in cellular proliferation (cyclins and CDKs) when compared to the PADI2-KD. This might indicate additional targeting of BB-Cl-amidine beyond PADI2. Surprisingly, we do not see increased *IL6* and *IL8* gene expression as we did with PADI2-KD, again suggesting that some of the effects of BB-Cl-amidine differ from the genetic knockdown of PADI2. As previously shown with our first-generation PADI inhibitor, we see increased expression of genes involved with DNA-damage and apoptosis, including *p21*, *PUMA*, and *GADD45α*, potentially indicating that BB-Cl-amidine leads to the same S-phase induced apoptosis seen with Cl-amidine [15]. To investigate whether there was an increase in apoptosis in the treated MCF10DCIS and BT474 cells, we examined the cells by flow-cytometry for activated caspase-3 levels. Results show a dose-dependent reduction in cellular proliferation (**Figure3.14a**), as well as the induction of activated caspase-3 (**Figure 3.14b**), upon treatment with BB-Cl-amidine in both breast cancer cell lines. Conversely, we do not see any adverse effects on growth or apoptosis in two normal cell lines, CHO-KI and NIH-3T3. Taken together, these results suggest that BB-Cl-amidine blocks the growth of MCF10DCIS and BT474 cells by inducing cell cycle arrest and apoptosis. This prediction is supported by our previous finding that Cl-amidine drives apoptosis in lymphocytic cell lines [17], and can reduce tumor growth *in vitro* and *in vivo*, ultimately leading to S-phase

<u>Figure 3.12:</u> BB-Cl-amidine treatment reduces the expression of genes downstream of HER2/ERBB2 and ER signaling in MCF10DCIS cells. Genes known to be expressed downstream of HER2 and ER (full gene list and primers can be found in **Table 3.1**) were tested by SYBR qPCR on MCF10DCIS (DCIS) cells treated with 2.5 µM of BB-Cl-amidine for 24h. Total RNA was isolated and respective mRNA levels were determined by SYBR qPCR using DMSO treated control cells as the reference (represented by dashed line = ~1) and with *GAPDH* normalization. Expression levels were analyzed using the $2^{-\Delta\Delta C(t)}$ method, and data are expressed as the mean ± SD from three independent experiments.

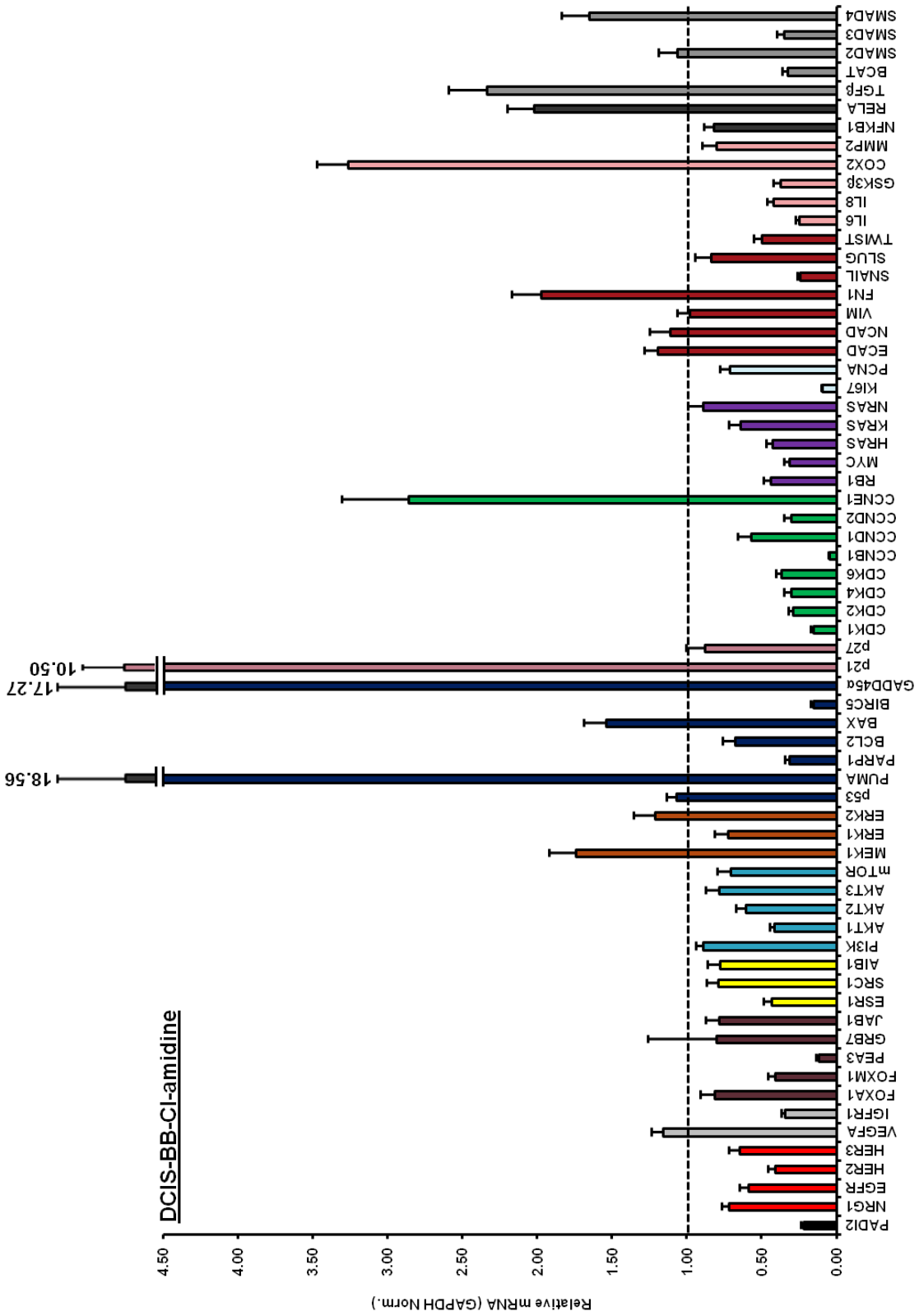
DCIS-BB-CI-amidine
Relative mRNA (GAPDH Norm.)
4.50
4.00
3.50
3.00
2.50
2.00
1.50
1.00
0.50
0.00
18.56
17.27
10.50
PADI2
NRG1
EGFR
HER2
HER3
VEGFA
IGFR1
FOXA1
FOXM1
PEA3
GRB7
JAB1
ESR1
SRC1
AIB1
PI3K
AKT1
AKT2
AKT3
mTOR
MEK1
ERK1
ERK2
p53
PUMA
PARP1
BCL2
BAX
BIRC5
GADD45a
p21
p27
CDK1
CDK2
CDK4
CDK6
CCNB1
CCND1
CCND2
CCNE1
RB1
MYC
HRAS
KRAS
NRAS
KI67
PCNA
ECAD
NCAD
VIM
FN1
SNAIL
SLUG
TWIST
IL6
IL8
GSK3β
COX2
MMP2
NFKB1
RELA
TGFβ
BCAT
SMAD2
SMAD3
SMAD4

Figure 3.13: BB-Cl-amidine treatment reduces the expression of genes downstream of HER2/ERBB2 and ER signaling in BT474 cells. Genes known to be expressed downstream of HER2 and ER (full gene list and primers can be found in **Table 3.1**) were tested by SYBR qPCR on BT474 cells treated with 2.5 µM of BB-Cl-amidine for 24h. Total RNA was isolated and respective mRNA levels were determined by SYBR qPCR using DMSO treated control cells as the reference (represented by dashed line = ~1) and with *GAPDH* normalization. Expression levels were analyzed using the $2^{-\Delta\Delta C(t)}$ method, and data are expressed as the mean ± SD from three independent experiments.

BT474-BB-Cl-amidine
Relative mRNA (GAPDH Norm.)
0.00
0.50
1.00
1.50
2.00
2.50
3.00
3.50
4.00
4.50
9.97
11.23
8.43
PADI2
NRG1
EGFR
HER2
HER3
VEGFA
IGFR1
FOXA1
FOXM1
PEA3
GRB7
JAB1
ESR1
SRC1
AIB1
PI3K
AKT1
AKT2
AKT3
mTOR
MEK1
ERK1
ERK2
p53
PUMA
PARP1
BCL2
BAX
BIRC5
GADD45a
p21
p27
CDK1
CDK2
CDK4
CDK6
CCNB1
CCND1
CCND2
CCNE1
RB1
MYC
HRAS
KRAS
NRAS
KI67
PCNA
ECAD
NCAD
VIM
FN1
SNAIL
SLUG
TWIST
IL6
IL8
GSK3β
COX2
MMP2
NFKB1
RELA
TGFβ
BCAT
SMAD2
SMAD3
SMAD4

Figure 3.14: BB-Cl-amidine treatment leads to a decrease in cellular proliferation and increased apoptosis in BT474 and MCF10DCIS breast cancer cell lines, with no significant negative effects on growth seen in normal CHO-K1 or NIH-3T3 cells. (a) BT474 and MCF10DCIS cells were treated with increasing concentrations of BB-Cl-amidine or vehicle (DMSO, 0.6125μM, 1.25 μM, 2.5 μM, and 5.0 μM) and analyzed by flow-cytometry for proliferation (a) and apoptosis (b). (a) Cell counts (DAPI) show a dose-dependent decrease in growth of BT474 and MCF10DCIS cells after 48h of BB-Cl-amidine compared to DMSO treatment. Normal cell lines, CHO-KI and NIH-3T3, were largely unaffected by treatment. (b) BT474 and MCF10DCIS cells show increased apoptosis upon treatment with BB-Cl-amidine, compared to normal cells (CHO-KI and NIH-3T3). Data represent cell number and percent apoptotic cells (cleaved Caspase-3 positive) after 48h of treatment and are expressed as the mean ± SD from three independent experiments (* $p < 0.05$).

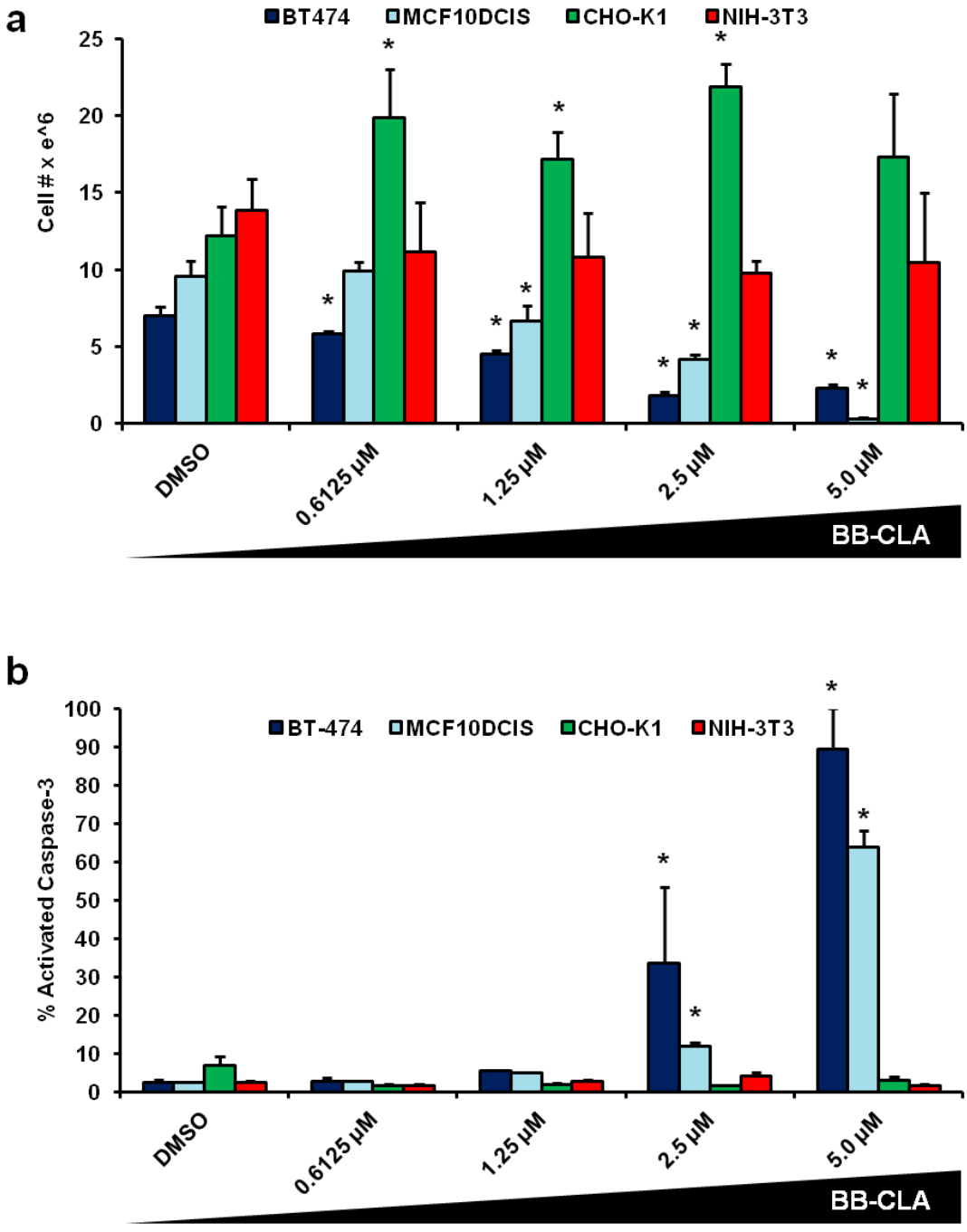
a
BT474
MCF10DCIS
CHO-K1
NIH-3T3
Cell # x e^6
25
20
15
10
5
0
DMSO
0.6125 µM
1.25 µM
2.5 µM
5.0 µM
BB-CLA
b
BT-474
MCF10DCIS
CHO-K1
NIH-3T3
% Activated Caspase-3
100
90
80
70
60
50
40
30
20
10
0
DMSO
0.6125 µM
1.25 µM
2.5 µM
5.0 µM
BB-CLA

induced apoptosis [15]. Importantly, the lack of an apoptotic effect on CHO-K1 and NIH-3T3 cells suggests that BB-Cl-amidine may primarily target tumor cells for killing. Consistent with this possibility is the fact that our first-generation PADI inhibitor, Cl-amidine, did not affect the growth of "normal" MCF10A cells [15], in addition to non-tumorigenic NIH3T3 cells and HL60 granulocytes [49]. We also found that BB-Cl-amidine slightly decreased the cell surface expression of HER2/ERBB2 and potentially facilitated the internalization of the receptor in BT474 cells (**Figure 3.15**). This has been previously noted to occur with the PI3K inhibitor, LY294002, but the mechanism behind this phenomenon is still under investigation [50].

HER2/ERBB2 upregulates PADI2 expression through PI3K pathway signaling

HER2/ERBB2 signaling often occurs within positive feedback loops, including genes such as *ADAM12* [51], *ERα36* [52], *BEX2* [53], *MED1* [54], and the inflammatory gene, *IL6* [29]. These signaling loops enhance the oncogenic signaling of HER2 and drive tumorigenesis, and in the case of MED1, tamoxifen resistance. Interestingly, we find that PADI2 appears to be both upstream and downstream of HER2/ERBB2 signaling. When we treat BT474 cells with the dual-tyrosine kinase inhibitor (EGFR/HER2), lapatinib, we see reduced protein levels of PADI2 (**Figure 3.16b**). Based on this, we wanted to test whether the overexpression of HER2/ERBB2 in MCF10A cells, which have very low basal levels of PADI2, can upregulate the expression of PADI2. Surprisingly, MCF10A-HER2 cells show an increase in both PADI2 protein and mRNA (**Figure 3.16b**). Using siRNA to transiently knockdown *HER2/ERBB2*, we show that in BT474 cells, reduced *HER2/ERBB2* leads to a decrease in *PADI2* expression (**Figure 3.17a**). We see the same effect in MCF10DCIS cells, albeit to a lesser extent (**Figure 3.17b**). Signaling downstream of HER2/ERBB2 is known to occur through either the MAPK or PI3K pathway. To determine which signaling

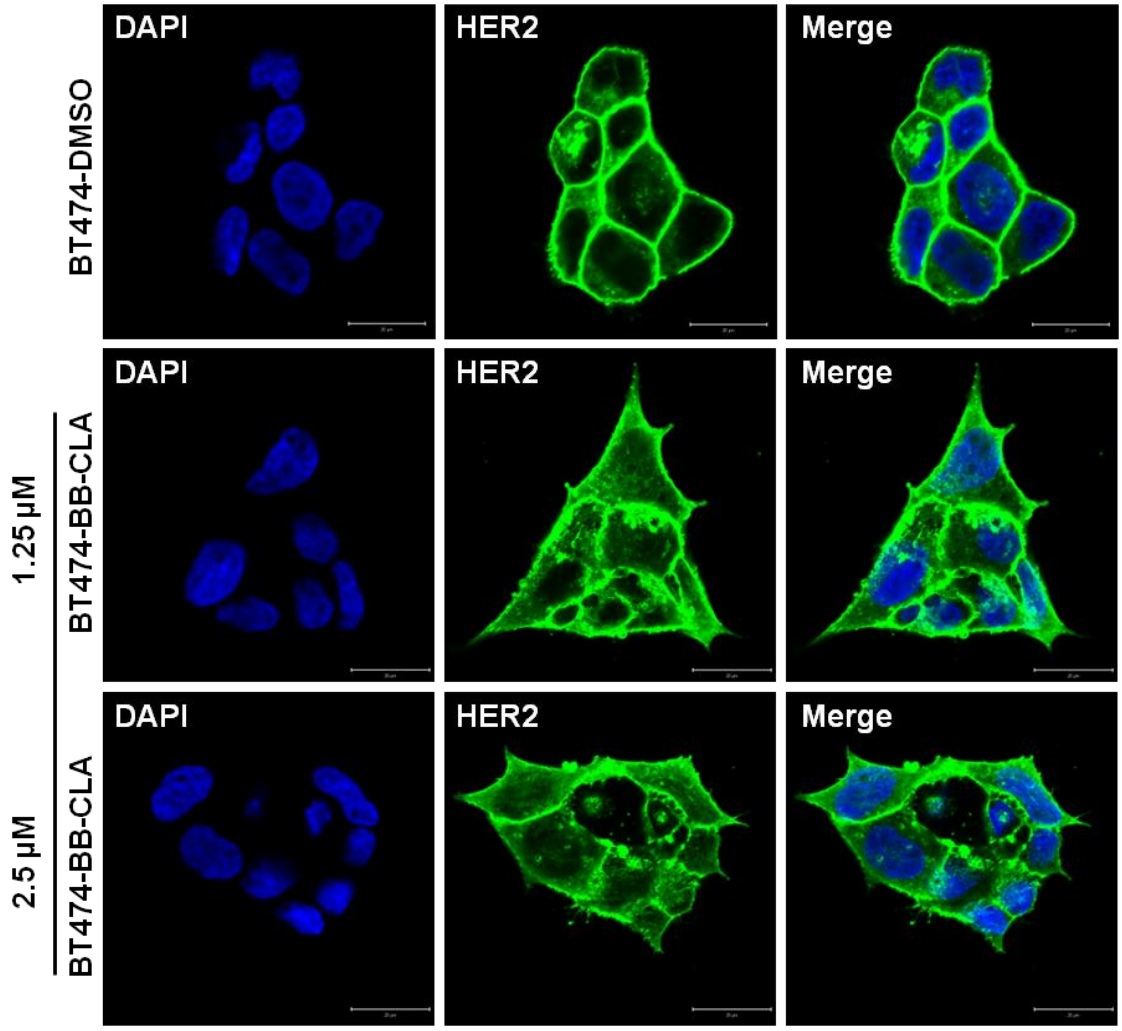

Figure 3.15: Immunofluorescence examination of HER2/ERBB2 localization in BT474 cells after treatment with BB-Cl-amidine shows increased internalization of the receptor. BT474 cells were treated with either 1.25 µM or 2.5 µM of BB-Cl-amidine for 48h. Cells were probed with anti-HER2/ERBB2 (green) and nuclei were stained with DAPI (blue).

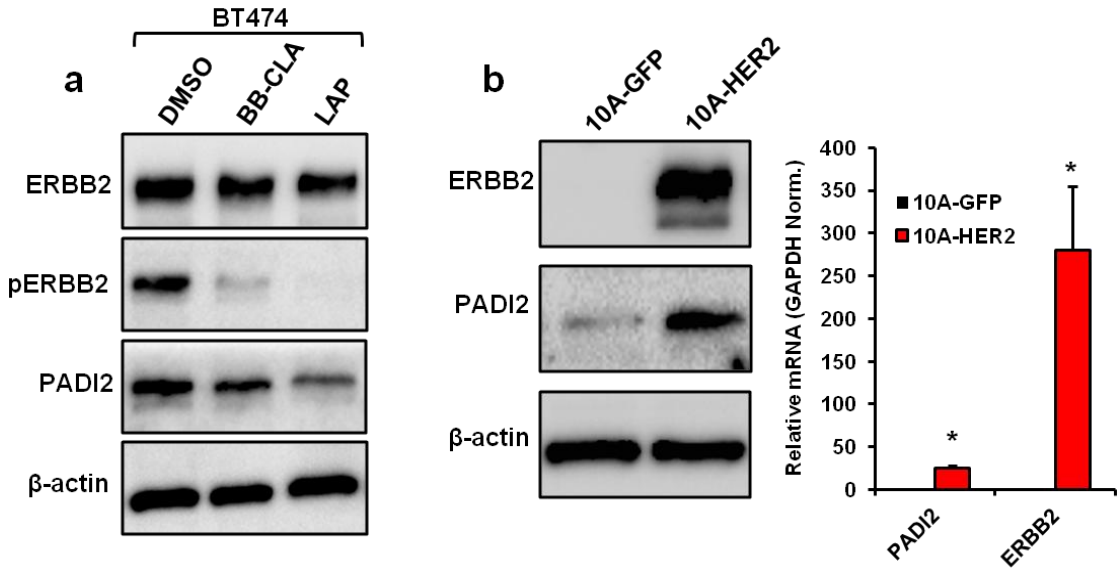

<u>Figure 3.16:</u> PADI2 expression is downstream of HER2/ERBB2 signaling. (a) Western blot analysis of ERBB2/pERBB2 (Y1248) and PADI2 protein expression in BT474 cells treated with BB-Cl-amidine (BB-CLA, 2.5 μM) and lapatinib (LAP, 1 μM) for 24h. (b) MCF10A cells stably overexpressing HER2 (10A-HER2) or GFP (10A-GFP) were analyzed by western blot for ERBB2 and PADI2 expression. β-actin was used as a loading control for both blots. Total RNA from GFP or HER2 expressing MCF10A cells was isolated and *PADI2* and *ERBB2* mRNA levels were determined by qPCR (TaqMan) using MCF10A-GFP control cells as the reference with *GAPDH* normalization. Expression levels were analyzed using the $2^{-\Delta\Delta C(t)}$ method, and data are expressed as the mean ± SD from three independent experiments.

Figure 3.17: Transient siRNA knockdown of *ERBB2/HER2* in BT474 and MCF10DCIS cells reduces *PADI2* expression. BT474 (a) and MCF10DCIS (b) cells were transfected with siRNA targeting *PADI2* and *ERBB2*, or control non-targeting siRNA, for 72h. Western blot analyses of siRNA treated BT474 (a) and MCF10DCIS (b) cells for ERBB2 and PADI2 protein expression with β-actin serving as a loading control. Total RNA from *PADI2* and *ERBB2* siRNA transfected BT474 (a) and MCF10DCIS (b) cells was isolated and *PADI2* and *ERBB2* mRNA levels were determined by qPCR (TaqMan) using control siRNA as the reference with *GAPDH* normalization. Expression levels were analyzed using the $2^{-\Delta\Delta C(t)}$ method, and data are expressed as the mean ± SD from three independent experiments.

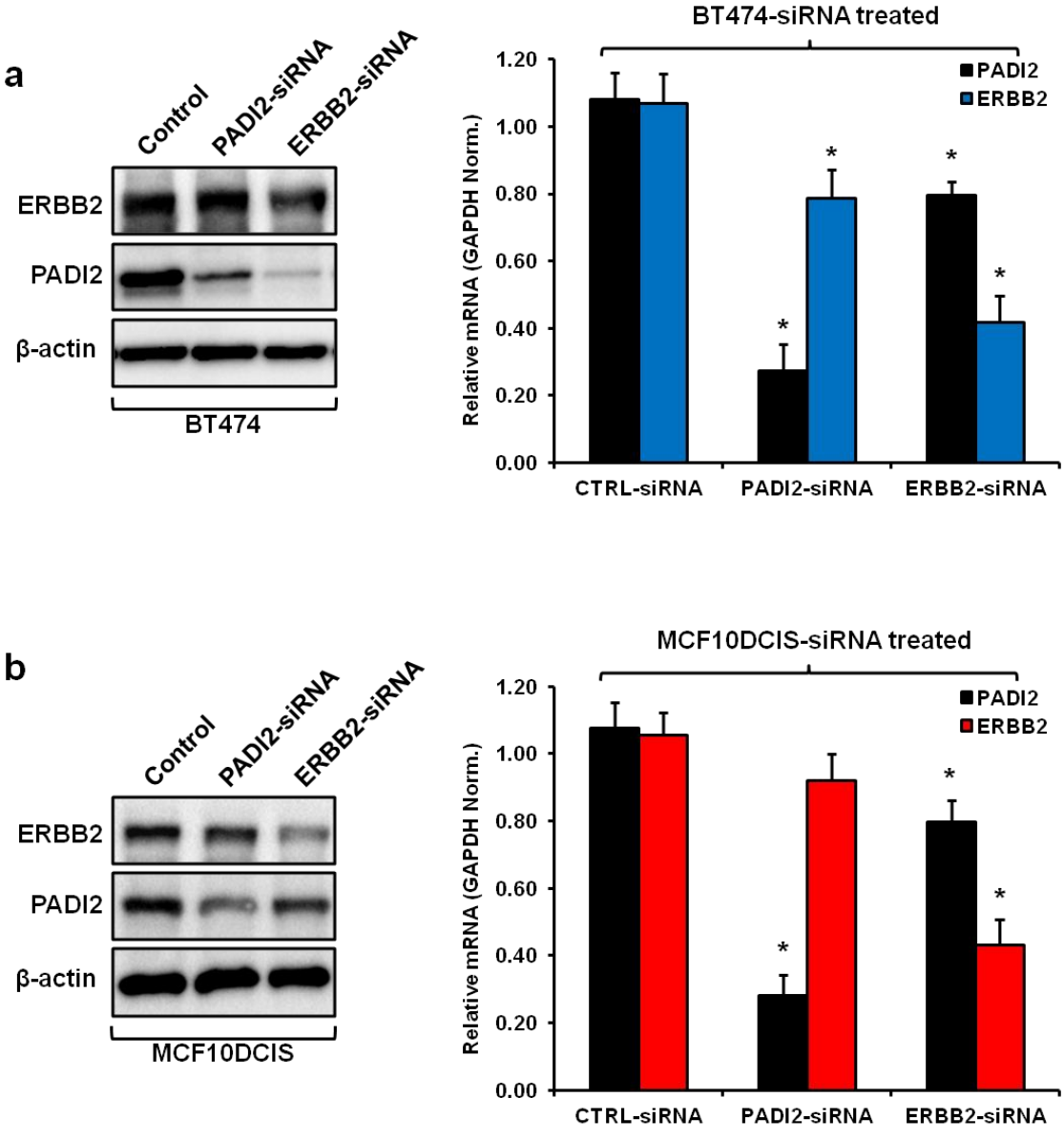
a
Control
PADI2-siRNA
ERBB2-siRNA
ERBB2
PADI2
β-actin
BT474
BT474-siRNA treated
PADI2
ERBB2
Relative mRNA (GAPDH Norm.)
1.20
1.00
0.80
0.60
0.40
0.20
0.00
CTRL-siRNA
PADI2-siRNA
ERBB2-siRNA
b
Control
PADI2-siRNA
ERBB2-siRNA
ERBB2
PADI2
β-actin
MCF10DCIS
MCF10DCIS-siRNA treated
PADI2
ERBB2
Relative mRNA (GAPDH Norm.)
1.20
1.00
0.80
0.60
0.40
0.20
0.00
CTRL-siRNA
PADI2-siRNA
ERBB2-siRNA

pathway may affect PADI2 expression, we treated BT474 cells with inhibitors for both the PI3K and MAPK pathways. We found that PADI2 signaling is reduced when PI3K pathway inhibitors (LY294002-PI3K, triciribine-Akt, and rapamycin-mTOR) were used (**Figure 3.18a**), while the MAPK pathway inhibitor (PD98059-MEK1) had no effect, indicating that PADI2 expression is downstream of the PI3K-AKT-mTOR axis.

PADI inhibitor BB-Cl-amidine enhances HER2/ERBB2 and PI3K pathway inhibitors

As we previously noted here, BB-Cl-amidine treatment leads to a marked reduction in activated HER2/ERBB2 and EGFR. This potentially suggests that PADI2 may act directly on proteins, and that reducing PADI2-mediated citrullination might have an effect on these proteins phosphorylation levels. To test this, we treated BT474 cells with BB-Cl-amidine and the same PI3K pathway inhibitors, along with lapatinib, as well as combinations of the two. Interestingly, we found that BB-Cl-amidine reduces both phospho-AKT (serine-473) and phospho-MAPK (threonine-202/ tyrosine-204) levels (**Figure 3.18b**). Furthermore, the combination of BB-Cl-amidine with the PI3K inhibitors, and lapatinib, had synergistic effects and greatly reduced cellular proliferation in BT474 cells (**Figure 3.19**). We confirmed these results by testing decreasing levels of lapatinib along with a low-dose of BB-Cl-amidine (500 nM), and confirmed that the combination of the two had a much greater effect on the growth of BT474 cells (**Figure 3.20a**). However, we did not see the same effect on the MCF10DCIS cells (**Figure 3.20b**). This was not surprising, as MCF10DCIS cells have been reported to be resistant to lapatinib treatment due to an activating mutation in the PIK3CA gene (H1047R) [55, 56]. The following results establish a novel role for any PADI inhibitor, and potentially indicate an enhanced role for this small molecule in the treatment of breast cancers. Future studies might examine whether PADI2 knockdown might have any effect on the lapatinib resistance of MCF10DCIS cells.

Figure 3.18: PADI2 expression is downstream of HER2/ERBB2 signaling via the PI3K-ATK-mTOR pathway, and BB-Cl-amidine can reduce activation of both PI3K and MAPK signaling. (a) Western blot analysis of protein expression in BT474 cells treated with the following small molecule inhibitors: AG1478 (EGFR, 10 μM), lapatinib ([LAP] EGFR/HER2, 1 μM), LY294002 (PI3K, 20 μM), triciribine (Akt, 1 μM), rapamycin (mTOR, 100 nM), and PD98059 (MAPK/MEK, 20 μM). Antibodies against ERBB2/pERBB2 (Y1248), PADI2, phospho-AKT (S473), and phospho-MAPK (T202/Y204) were used, with β-actin serving as a loading control. (b) BT474 cells were treated for 48h with BB-Cl-amidine, BB-Cl-amidine and lapatinib together, or with a combination of BB-Cl-amidine plus PI3K pathway inhibitors (LY294002, triciribine, and rapamycin). Whole-cell lysates were probed for ERBB2/pERBB2 (Y1248), AKT/pAKT (S473), and MAPK/pMAPK (T202/Y204), with β-actin serving as a loading control.

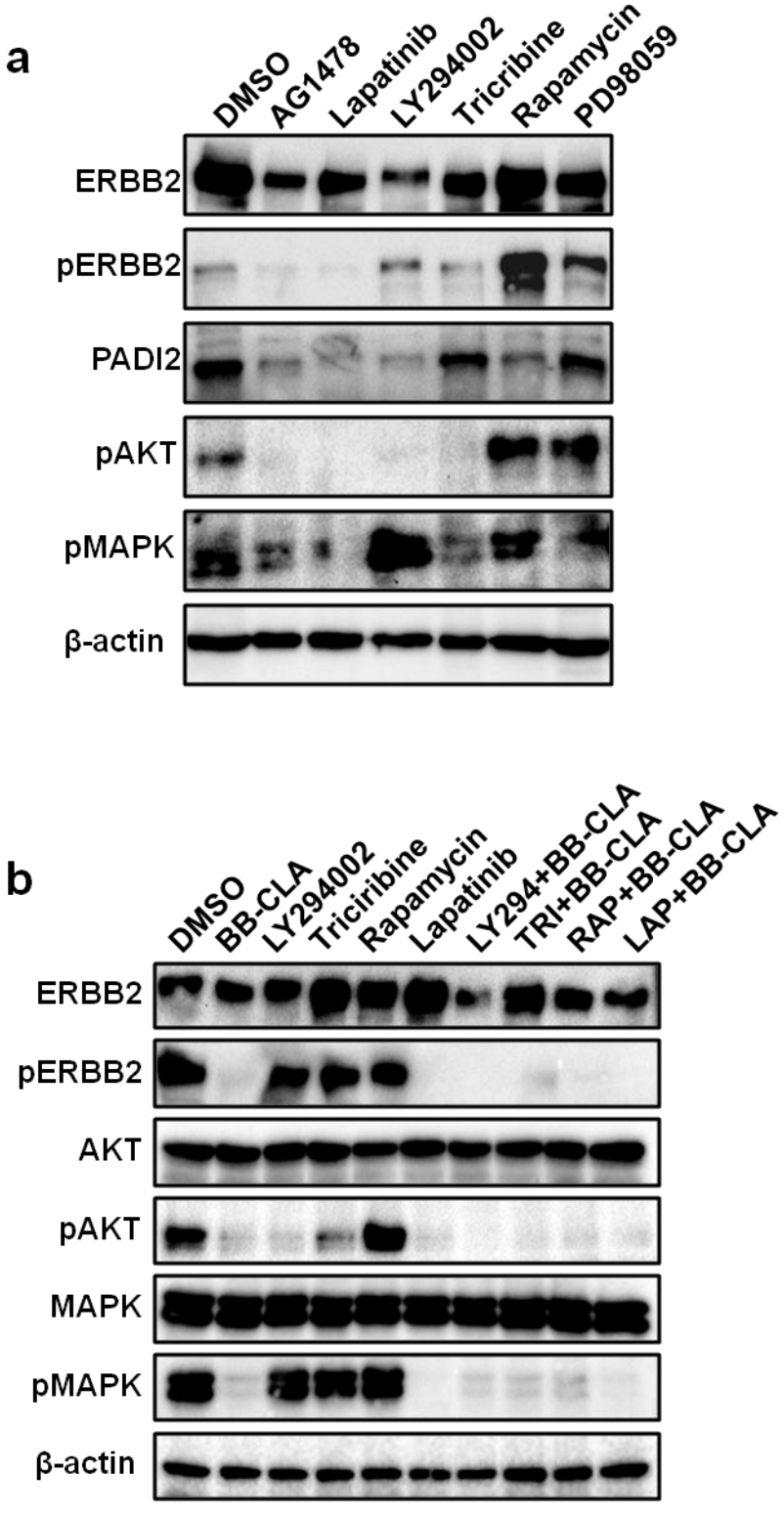
a
DMSO
AG1478
Lapatinib
LY294002
Tricribine
Rapamycin
PD98059
ERBB2
pERBB2
PADI2
pAKT
pMAPK
β-actin
b
DMSO
BB-CLA
LY294002
Triciribine
Rapamycin
Lapatinib
LY294+BB-CLA
TRI+BB-CLA
RAP+BB-CLA
LAP+BB-CLA
ERBB2
pERBB2
AKT
pAKT
MAPK
pMAPK
β-actin

Figure 3.19: BB-Cl-amidine enhances the effect of small molecular inhibitors that target the HER2/ERBB2 and the PI3K pathways. Epithelial morphology of BT474 cells treated with BB-Cl-amidine alone, or in combination with LY294002 (PI3K, 20 μM), triciribine (Akt, 1 μM), rapamycin (mTOR, 100 nM), and lapatinib ([LAP] EGFR/HER2, 1 μM).

DMSO
LY294002-PI3Ki (20μM)
Triciribine-AKTi (1μM)
Rapamycin-RAP (100nM)
Lapatinib-LAP (1μM)
BB-CLA (2.5μM)
BB-CLA (2.5μM) + PI3Ki (20μM)
BB-CLA (2.5μM) + AKTi (1μM)
BB-CLA (2.5μM) + RAP (100nM)
BB-CLA (2.5μM) + LAP (1μM)

<u>Figure 3.20:</u> BB-Cl-amidine has a synergistic effect with lapatinib in the treatment of BT474, but not MCF10DCIS breast cancer cells. BT474 (a) or MCF10DCIS (b) cells were treated with increasing concentrations of BB-Cl-amidine or lapatinib alone, or with a combination of BB-Cl-amidine (0.5 μM) and increasing concentrations of lapatinib. BT474 cells were treated over the course of 3-weeks, and MCF10DCIS cells 1-week, with new media and drug added every 3d. Cells were fixed with 4% PFA and stained with crystal violet for subsequent analysis of focus formation.

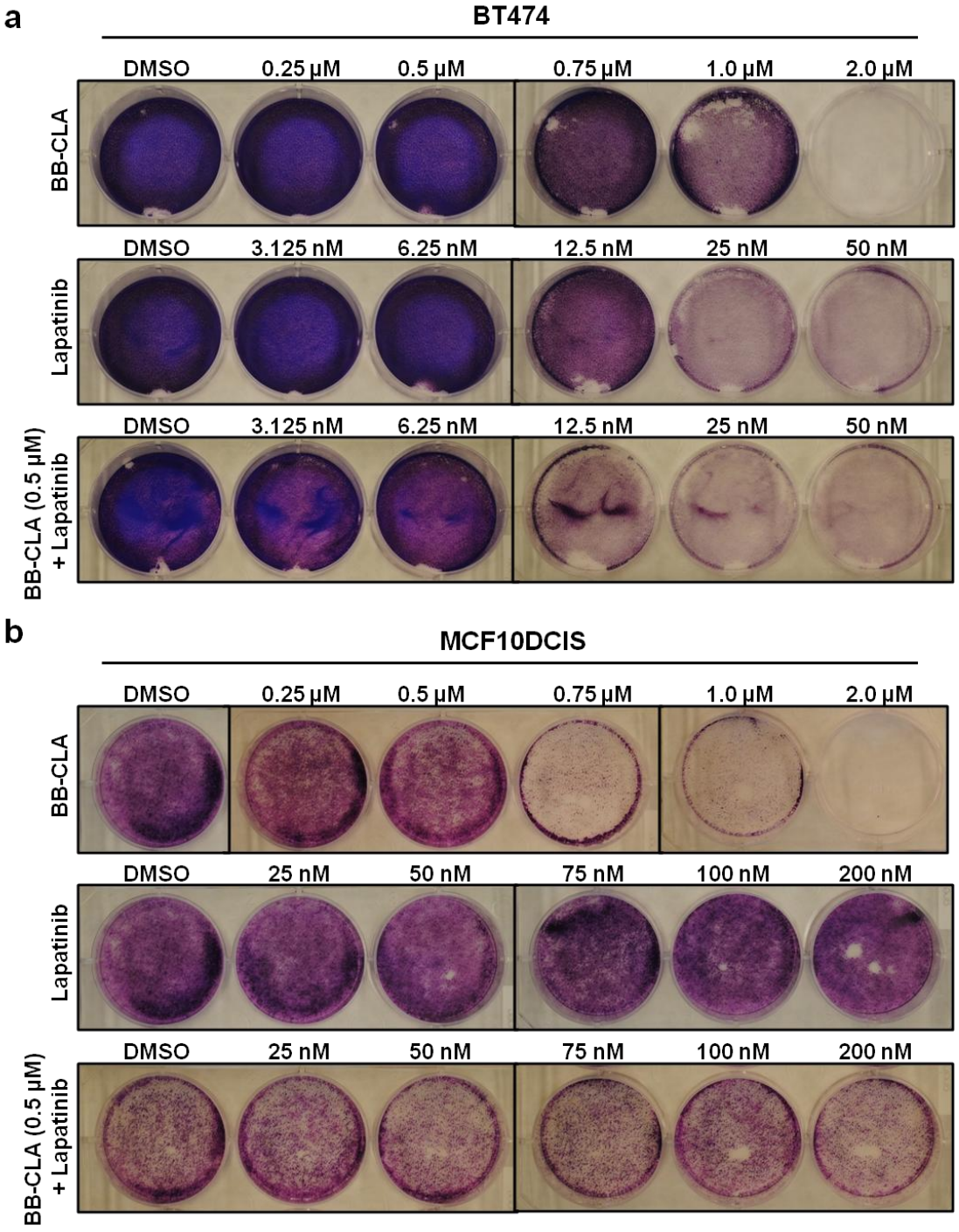
a
BT474
DMSO
0.25 µM
0.5 µM
0.75 µM
1.0 µM
2.0 µM
BB-CLA
DMSO
3.125 nM
6.25 nM
12.5 nM
25 nM
50 nM
Lapatinib
DMSO
3.125 nM
6.25 nM
12.5 nM
25 nM
50 nM
BB-CLA (0.5 µM) + Lapatinib
b
MCF10DCIS
DMSO
0.25 µM
0.5 µM
0.75 µM
1.0 µM
2.0 µM
BB-CLA
DMSO
25 nM
50 nM
75 nM
100 nM
200 nM
Lapatinib
DMSO
25 nM
50 nM
75 nM
100 nM
200 nM
BB-CLA (0.5 µM) + Lapatinib

3.5 Discussion

Our previous work has established a role for PADI2 as an epigenetic regulator of ER-target gene expression in mammary tumorigenesis [16], in addition to establishing a correlation between PADI2 and HER2/ERBB2 expression across 57 breast cancer cell lines [15]. The work presented here looks to expand on both of these studies, and to establish a role for PADI2 in the expression of the HER2 oncogene. We set out to explore the functional relationship between PADI2 and HER2, i.e. whether PADI2 enhances HER2 expression or vice-versa. Interestingly, PADI2 appears to function both upstream and downstream of HER2, potentially indicating a role in an oncogenic positive-feedback loop with HER2. Previous evidence from our lab has shown that PADI2 can act as an ER co-activator via the citrullination of H3R26 [16] , so we were curious to see if PADI2 regulates *HER2* expression using the same mechanism. Interestingly, a recent report by Hurtado et al. has found that ER can regulate HER2/ERBB2 expression by binding to an estrogen response element (ERE) within intron 4 of the HER2/ERBB2 gene [32]. Therefore, it is possible that, similar to other ER target genes, PADI2 regulates HER2/ERBB2 expression by functioning as an ER co-factor. We show here that PADI2 strongly binds the *HER2* proximal promoter (ETS region), in addition to the recently characterized ERE. In the presence of the PADI inhibitor, BB-Cl-amidine, we see a dose-dependent reduction in HER2 protein and mRNA. We also see the reduction of HER2 protein and mRNA in cells that were stably transfected with shRNA for *PADI2*. Furthermore, there was also a concomitant reduction in the growth and malignant progression of these cells upon inhibition or shRNA knockdown of PADI2. It is interesting to speculate how PADI2 can function both as an ER and HER2 cofactor, especially with regard to mammary tumorigenesis. Previous evidence suggests that histone acetylation and phosphorylation play key roles in inducing HER2 expression [57], and we have previously shown that histone

citrullination enhances histone acetylation and vice-versa [58]. Therefore, provided with what we know about PADI2 as a co-activator of ER target genes, we can hypothesize that HER2 gene expression might work in the same fashion. Recent evidence from our lab using *in vitro* biochemical assays with bulk histones revealed that the H3Cit26 modification was found only on peptides that contained acetylated H3K27 (H3K27ac); thus, suggesting that H3K237ac enhances PADI2-mediated H3R26 citrullination [16]. ER is known to associate with a number of multi-protein complexes, including heat shock proteins (HSPs) [59], steroid receptor co-activators (SRCs) [60], p300-containing co-activator complexes [61], and HDAC containing co-repressor complexes [62]. The p300 co-activator is known to have intrinsic histone acetyltransferase (HAT) activity, which helps to relax the chromatin structure at gene promoters, leading to gene activation. Studies have shown that p300 can function as an ER co-activator, and is required for acetylation at H3K27 [61]. This supports our hypothesis that ER uses p300-mediated H3K27 acetylation and PADI2-mediated H3R26 citrullination to promote chromatin decondensation, allowing for the binding of ER and associated co-factors (i.e. SRC1 or AIB1) to EREs and enhancing ER-target and potentially HER2 gene transcription.

Alternatively, PADI2 may activate HER2 expression by functioning as an ETS co-factor (e.g. PEA3), thereby enhancing HER2 transcription. PEA3 is a well-known ETS co-factor and transcriptional activator of HER2 [63, 64], and the primers used for detecting PADI2 at the *HER2* promoter are within the known PEA3 binding site [32]. Interestingly, one of the most commonly documented mechanisms of tamoxifen resistance is the overexpression of growth factor receptors, particularly EGFR and HER2 [4-6]. In addition, the expression of previously mentioned co-activator proteins, SRC1, AIB1, and Polyomavirus Enhancer Activator-3 (PEA3), have been shown to correlate with endocrine resistance in breast cancer [47]. Particularly, the AIB1 gene has been shown to be critical in the development of tamoxifen resistance via ER/HER2

cross-talk [5, 32], as MCF7 breast cancer cells overexpressing HER2 (MCF-7/HER2-18) showed cross-phosphorylation and activation of ER and EGFR/HER2 receptors when treated with tamoxifen [65]. This was coincident with the phosphorylation and activation of the signaling molecules AKT and MAPK, as well as AIB1. We show here that the targeting of PADI2 by both shRNA and BB-Cl-amidine leads to a reduction in both SRC and AIB1 at the mRNA levels, and ER and AIB1 at the protein levels, as well as both activated EGFR and HER2/ERBB2. This has potential implications for the treatment of patients with acquired resistance to endocrine therapies.

Finally, we also provide evidence that PADI2 functions in a positive-feedback loop with HER2/ERBB2. We found using inhibitors for MAPK and PI3K pathways, that HER2/ERBB2 induces PADI2 expression downstream of PI3K-AKT-mTOR signaling. Interestingly, we also note that using the PADI2 inhibitor BB-Cl-amidine, along with lapatinib, had synergistic inhibitory effects on the growth and malignant nature of tumor cells *in vitro*. Currently, PI3K-AKT and mTOR inhibitors are effective therapies for the treatment of breast cancer, but they are often plagued by acquired resistance through the upregulation of receptor tyrosine kinase (RTK) activation via MAPK-ERK signaling [66]. Surprisingly, we showed that BB-Cl-amidine treatment can reduce both pMAPK and pAKT, in addition to pERBB2; thus, relieving the RTK-activation seen when cells are treated with the mTOR inhibitor rapamycin.

Conclusions

Taken together, these results suggest an enhanced role for PADI2 in HER2 expressing breast cancers, and that the PADI inhibitor, BB-Cl-amidine, represents a potential novel therapy for the treatment of patients with HER2-positive mammary tumors, and potentially for those with acquired resistance to endocrine therapies

Acknowledgements/Contributions

Thanks to: Dr. Xuesen Zhang for help with ChIP experiment replicates (Fig. 3.5); Sachi Horibata for help with the anchorage-independent growth and focus formation assays (Figs. 3.8, 3.9a-b, 3.11c, 3.20); Lynne Anguish for help with the flow-cytometry experiments (Fig. 3.14); and Dr. Paul Thomson for generating the BB-Cl-amidine used in the experiments.

Table 3.1: Primer sequences for genes tested by SYBR-qPCR

Gene Name	Primer Name	Sequence
AIB1 (*SRC3*, *NCOA3*)	AIB1-F	AGCTGAGCTGCGAGGAAA
	AIB1-R	GAGTCCACCATCCAGCAAGT
AKT1	AKT1-F	GGCTATTGTGAAGGAGGGTTG
	AKT1-R	TCCTTGTAGCCAATGAAGGTG
AKT2	AKT2-F	CTCACACAGTCACCGAGAGC
	AKT2-R	TGGGTCTGGAAGGCATACTT
AKT3	AKT3-F	TTGCTTTCAGGGCTCTTGAT
	AKT3-R	CATAATTTCTTTTGCATCATCTGG
β-actin (*ACTB*)	B-ACTIN-F	CCAACCGCGAGAAGATGA
	B-ACTIN-R	CCAGAGGCGTACAGGGATAG
BAX	BAX-F	AGCAAACTGGTGCTCAAGG
	BAX-R	TCTTGGATCCAGCCCAAC
β-Catenin (*CTNNB1*)	BCAT-F	GCTTTCAGTTGAGCTGACCA
	BCAT-R	CAAGTCCAAGATCAGCAGTCTC
BCL2	BCL2-F	AGTACCTGAACCGGCACCT
	BCL2-R	GCCGTACAGTTCCACAAAGG
BIRC5 (Survivin)	BIRC5-F	AGAACTGGCCCTTCTTGGA
	BIRC5-R	CAAGTCTGGCTCGTTCTCAGT
Cyclin B1 (*CCNB1*)	CCNB1-F	CATGGTGCACTTTCCTCCTT
	CCNB1-R	AGGTAATGTTGTAGAGTTGGTGTCC
Cyclin D1 (*CCND1*)	CCND1-F	GAAGATCGTCGCCACCTG
	CCND1-R	GACCTCCTCCTCGCACTTCT
Cyclin D2 (*CCND2*)	CCND2-F	GGACATCCAACCCTACATGC
	CCND2-R	CGCACTTCTGTTCCTCACAG

Cyclin E1 (*CCNE1*)	CCNE1-F	GGCCAAAATCGACAGGAC
	CCNE1-R	GGGTCTGCACAGACTGCAT
CDK1 (CDC2)	CDK1-F	AACTGGCTGATTTTGGCCTTG
	CDK1-R	TGAGTAACGAGCTGACCCCA
CDK2	CDK2-F	AAAGCCAGAAACAAGTTGACG
	CDK2-R	GTACTGGGCACACCCTCAGT
CDK4	CDK4-F	GTGCAGTCGGTGGTACCTG
	CDK4-R	TTCGCTTGTGTGGGTTAAAA
CDK6	CDK6-F	TGATCAACTAGGAAAAATCTTGGA
	CDK6-R	GGCAACATCTCTAGGCCAGT
COX-2 (*PTGS2*)	COX2-F	GCTTTATGCTGAAGCCCTATGA
	COX2-R	TCCAACTCTGCAGACATTTCC
E-cadherin (*CDH1*)	ECAD-F	TGGAGGAATTCTTGCTTTGC
	ECAD-R	CGCTCTCCTCCGAAGAAAC
EGFR (*HER1*, *ERBB1*)	EGFR-F	GATCCAAGCTGTCCCAATG
	EGFR-R	GGCACAGATGATTTTGGTCAG
ERK1 (*MAPK3*-p44)	ERK1-F	CCCTAGCCCAGACAGACATC
	ERK1-R	GCACAGTGTCCATTTTCTAACAGT
ERK2 (*MAPK1*-p42)	ERK2-F	TCTGCACCGTGACCTCAA
	ERK2-R	GCCAGGCCAAAGTCACAG
ESR1	ESR1-F	TTACTGACCAACCTGGCAGA
	ESR1-R	ATCATGGAGGGTCAAATCCA
FN1	FN1-F	CTGGCCGAAAATACATTGTAAA
	FN1-R	CCACAGTCGGGTCAGGAG
FOXA1	FOXA1-F	AGGGCTGGATGGTTGTATTG
	FOXA1-R	ACCGGGACGGAGGAGTAG

FOXM1	FOXMI-F	ACTTTAAGCACATTGCCAAGC
	FOXMI-R	CGTGCAGGGAAAGGTTGT
GADD45α (*GADD45A*)	GADD45a-F	TTTGCAATATGACTTTGGAGGA
	GADD45a-R	CATCCCCCACCTTATCCAT
GRB7	GRB7-F	GGAACGGGTGTCCTGCTAC
	GRB7-R	AACCAGTTGTGTGCCCTTGT
GSK3β (*GSK3B*)	GSK3β-F	GACATTTCACCTCAGGAGTGC
	GSK3β-R	GTTAGTCGGGCAGTTGGTGT
HER2 (*ERBB2*)	HER2-F	TGCTGTCCTGTTCACCACTC
	HER2-R	TCATCCTCATCATCTTCACATTG
HER3 (*ERBB3*)	HER3-F	CTGATCACCGGCCTCAAT
	HER3-R	GGAAGACATTGAGCTTCTCTGG
HRAS	HRAS-F	GGACGAATACGACCCCACTAT
	HRAS-R	TGTCCAACAGGCACGTCTC
IGFR1	IGFR1-F	TCAGCGCTGCTGATGTGTA
	IGFR1-R	GGCTCATGGTGATCTTCTCC
IL6	IL6-F	GCCCTGAGAAAGGAGACATGTAA
	IL6-R	TTGTTTTCTGCCAGTGCCTC
IL8	IL8-F	ACTGAGAGTGATTGAGAGTGGAC
	IL8-R	AACCCTCTGCACCCAGTTTTC
JAB1 (*COPS5*)	JAB1-F	CGAAGCCCTGGACTAAGGAT
	JAB1-R	CTGGCATGCATCACCATCT
KI67 (*MKI67*)	KI67-F	TTACAAGACTCGGTCCCTGAA
	KI67-R	TTGCTGTTCTGCCTCAGTCTT
KRAS	KRAS-F	TGGACGAATATGATCCAACAAT
	KRAS-R	TCCCTCATTGCACTGTACTCC

MEK1 (*MAP2K1*)	MEK1-F	TCTGCAGTTAACGGGACCA
	MEK1-R	GCTGCTGCTCATCAAGCTC
MMP2	MMP2-F	CCCCAAAACGGACAAAGAG
	MMP2-R	CTTCAGCACAAACAGGTTGC
MTOR (*FRAP1*)	mTOR-F	AGCTGCATGGGGTTTAGGT
	mTOR-R	CCCGAGGGATCATACAGGT
MYC	MYC-F	CACCAGCAGCGACTCTGA
	MYC-R	GATCCAGACTCTGACCTTTTGC
N-cadherin (*CDH2*)	NCAD-F	CTCCATGTGCCGGATAGC
	NCAD-R	CGATTTCACCAGAAGCCTCTAC
NFKB1(p105/p50)	NFKB1-F	CTGGCAGCTCTTCTCAAAGC
	NFKB1-R	TCCAGGTCATAGAGAGGCTCA
NRAS	NRAS-F	GCAAGTCATTTGCGGATATTAAC
	NRAS-R	CATCCGAGTCTTTTACTCGCTTA
NRG1	NRG1-F	GATCAGCAAATTAGGAAATGACAG
	NRG1-R	GGCATACCAGTGATGATCTCG
p21 (*CDKN1A*)	p21-F	CCTGTCACTGTCTTGTACCCT
	p21-F	GCGTTTGGAGTGGTAGAAATCT
p27 (*CDKN1B*)	p27-F	TTTGACTTGCATGAAGAGAAGC
	p27-R	AGCTGTCTCTGAAAGGGACATT
p53 (*TP53*)	p53-F	CCCCAGCCAAAGAAGAAAC
	p53-R	AACATCTCGAAGCGCTCAC
PADI2	PADI2-F	TCTCAGGCCTGGTCTCCAT
	PADI2-R	AAGATGGGAGTCAGGGGAAT
PARP1	PARP1-F	TGGAGGACGACAAGGAAAAC
	PARP1-R	TGTTGCTACCGATCACCGTA

PCNA	PCNA-F	TGGAGAACTTGGAAATGGAAA
	PCNA-R	GAACTGGTTCATTCATCTCTATGG
PEA3 (*ETV4*)	PEA3-F	ACTTCGCCTACGACTCAGATG
	PEA3-R	GAGGTTTCTCATAGCCATAGCC
PI3K (*PIK3CA*-p110α)	PI3K-F	CACGAGATCCTCTCTCTGAAATC
	PI3K-R	GGTAGAATTTCGGGGATAGTTACA
PUMA (*BBC3*)	PUMA-F	GACCTCAACGCACAGTACGA
	PUMA-R	GAGATTGTACAGGACCCTCCA
RB1	RB1-F	TCCTGAGGAGGACCCAGAG
	RB1-R	AGGTTCTTCTGTTTCTTCAAACTCA
RELA (p65)	RELA-F	ACCGCTGCATCCACAGTT
	RELA-R	GATGCGCTGACTGATAGCC
SMAD2	SMAD2-F	CAGGACGATTAGATGAGCTTGA
	SMAD2-R	CCCCAAATTTCAGAGCAAGT
SMAD3	SMAD3-F	CCATCCCCGAAAACACTAAC
	SMAD3-R	TCCATCTTCACTCAGGTAGCC
SMAD4	SMAD4-F	CCTGTTCACAATGAGCTTGC
	SMAD4-R	GCAATGGAACACCAATACTCAG
SNAIL (*SNAI1*)	SNAIL-F	GCTGCAGGACTCTAATCCAGA
	SNAIL-R	ATCTCCGGAGGTGGGATG
SLUG (*SNAI2*)	SLUG-F	TGGTTGCTTCAAGGACACAT
	SLUG-R	GCAAATGCTCTGTTGCAGTG
SRC1 (*NCOA1*)	SRC1-F	ATGAGATCAGGCATGCAACA
	SRC1-R	TGTGCCAACATTTGAGCATT
TGFβ (*TGFB1*)	TGFB-F	ACTACTACGCCAAGGAGGTCAC
	TGFB-R	TGCTTGAACTTGTCATAGATTTCG

TWIST1	TWIST1-F	AGCTACGCCTTCTCGGTCT
	TWIST1-R	CCTTCTCTGGAAACAATGACATC
VEGFA	VEGFA-F	GCAGCTTGAGTTAAACGAACG
	VEGFA-R	GGTTCCCGAAACCCTGAG
VIM	VIM-F	GGCTCGTCACCTTCGTGAAT
	VIM-R	GAGAAATCCTGCTCTCCTCGC

3.6 References

1. Coughlin, S.S. & Ekwueme, D.U. Breast cancer as a global health concern. *Cancer Epidemiol* **33**, 315-8 (2009).

2. Jemal, A., Siegel, R., Xu, J. & Ward, E. Cancer statistics, 2010. *CA Cancer J Clin* **60**, 277-300 (2010).

3. Osborne, C.K. & Schiff, R. Mechanisms of endocrine resistance in breast cancer. *Annu Rev Med* **62**, 233-47 (2010).

4. Knowlden, J.M. et al. Elevated levels of epidermal growth factor receptor/c-erbB2 heterodimers mediate an autocrine growth regulatory pathway in tamoxifen-resistant MCF-7 cells. *Endocrinology* **144**, 1032-44 (2003).

5. Shou, J. et al. Mechanisms of tamoxifen resistance: increased estrogen receptor-HER2/neu cross-talk in ER/HER2-positive breast cancer. *J Natl Cancer Inst* **96**, 926-35 (2004).

6. Arpino, G., Wiechmann, L., Osborne, C.K. & Schiff, R. Crosstalk between the estrogen receptor and the HER tyrosine kinase receptor family: molecular mechanism and clinical implications for endocrine therapy resistance. *Endocr Rev* **29**, 217-33 (2008).

7. Slamon, D.J. et al. Studies of the HER-2/neu proto-oncogene in human breast and ovarian cancer. *Science* **244**, 707-12 (1989).

8. Esteva, F.J. et al. Phase II study of weekly docetaxel and trastuzumab for patients with HER-2-overexpressing metastatic breast cancer. *J Clin Oncol* **20**, 1800-8 (2002).

9. Seidman, A. et al. Cardiac dysfunction in the trastuzumab clinical trials experience. *J Clin Oncol* **20**, 1215-21 (2002).

10. Huang, Y., Nayak, S., Jankowitz, R., Davidson, N.E. & Oesterreich, S. Epigenetics in breast cancer: what's new? *Breast Cancer Res* **13**, 225 (2011).

11. Jovanovic, J., Ronneberg, J.A., Tost, J. & Kristensen, V. The epigenetics of breast cancer. *Mol Oncol* **4**, 242-54 (2010).

12. Vo, A.T. & Millis, R.M. Epigenetics and breast cancers. *Obstet Gynecol Int* **2012**, 602720 (2012).

13. Cherrington, B.D., Morency, E., Struble, A.M., Coonrod, S.a. & Wakshlag, J.J. Potential role for peptidylarginine deiminase 2 (PAD2) in citrullination of canine mammary epithelial cell histones. *PloS one* **5**, e11768 (2010).

14. Cherrington, B.D. et al. Potential role for PAD2 in gene regulation in breast cancer cells. *PLoS One* **7**, e41242 (2012).

15. McElwee, J.L. et al. Identification of PADI2 as a potential breast cancer biomarker and therapeutic target. *BMC Cancer* **12**, 500 (2012).

16. Zhang, X. et al. Peptidylarginine deiminase 2-catalyzed histone H3 arginine 26 citrullination facilitates estrogen receptor alpha target gene activation. *Proc Natl Acad Sci U S A* **109**, 13331-6 (2012).

17. Chumanevich, A.A. et al. Suppression of colitis in mice by Cl-amidine: a novel peptidylarginine deiminase inhibitor. *American journal of physiology. Gastrointestinal and liver physiology* **300**, G929-38 (2011).

18. Lange, S. et al. Protein deiminases: New players in the developmentally regulated loss of neural regenerative ability. *Developmental biology* (2011).

19. Willis, V.C. et al. N-alpha-benzoyl-N5-(2-chloro-1-iminoethyl)-L-ornithine amide, a protein arginine deiminase inhibitor, reduces the severity of murine collagen-induced arthritis. *J Immunol* **186**, 4396-404 (2011).

20. TCGA. Comprehensive molecular portraits of human breast tumours. *Nature* **490**, 61-70 (2012).

21. Goldman, M. et al. The UCSC Cancer Genomics Browser: update 2013. *Nucleic Acids Res* **41**, D949-54 (2013).

22. Cerami, E. et al. The cBio cancer genomics portal: an open platform for exploring multidimensional cancer genomics data. *Cancer Discov* **2**, 401-4 (2012).

23. Heppner, G.H. & Wolman, S.R. MCF-10AT: A Model for Human Breast Cancer Development. *The Breast Journal* **5**, 122-129 (1999).

24. Dawson, P.J., Wolman, S.R., Tait, L., Heppner, G.H. & Miller, F.R. MCF10AT: a model for the evolution of cancer from proliferative breast disease. *The American journal of pathology* **148**, 313-9 (1996).

25. Hu, M. et al. Role of COX-2 in epithelial-stromal cell interactions and progression of ductal carcinoma *in situ* of the breast. *Proceedings of the National Academy of Sciences of the United States of America* **106**, 3372-7 (2009).

26. Hu, M. et al. Regulation of *In situ* to Invasive Breast Carcinoma Transition. *Cancer Cell* **13**, 394-406 (2008).

27. Shekhar, M.P. et al. Comedo-ductal carcinoma *in situ*: A paradoxical role for programmed cell death. *Cancer Biol Ther* **7** (2008).

28. Hartman, Z.C. et al. An adenoviral vaccine encoding full-length inactivated human Her2 exhibits potent immunogenicty and enhanced therapeutic efficacy without oncogenicity. *Clin Cancer Res* **16**, 1466-77 (2010).

29. Hartman, Z.C. et al. HER2 overexpression elicits a proinflammatory IL-6 autocrine signaling loop that is critical for tumorigenesis. *Cancer Res* **71**, 4380-91 (2011).

30. Miller, F.R. et al. Xenograft model of progressive human proliferative breast disease. *J Natl Cancer Inst* **85**, 1725-32 (1993).

31. Zhang, X. et al. Genome-wide analysis reveals PADI4 cooperates with Elk-1 to activate c-Fos expression in breast cancer cells. *PLoS Genet* **7**, e1002112 (2011).

32. Hurtado, A. et al. Regulation of ERBB2 by oestrogen receptor-PAX2 determines response to tamoxifen. *Nature* **456**, 663-6 (2008).

33. Livak, K.J. & Schmittgen, T.D. Analysis of relative gene expression data using real-time quantitative PCR and the 2(-Delta Delta C(T)) Method. *Methods* **25**, 402-8 (2001).

34. Miller, F.R., Santner, S.J., Tait, L. & Dawson, P.J. MCF10DCIS.com xenograft model of human comedo ductal carcinoma *in situ*. *J Natl Cancer Inst* **92**, 1185-6 (2000).

35. Shekhar, M.P., Kato, I., Nangia-Makker, P. & Tait, L. Comedo-DCIS is a precursor lesion for basal-like breast carcinoma: identification of a novel p63/Her2/neu expressing subgroup. *Oncotarget* **4**, 231-41 (2013).

36. So, J., Lee, H., Kramata, P., Minden, A. & Suh, N. Differential Expression of Key Signaling Proteins in MCF10 Cell Lines, a Human Breast Cancer Progression Model. *Mammalian genome : official journal of the International Mammalian Genome Society* **4**, 31-40 (2012).

37. Hsu, M.C. et al. Jab1 is overexpressed in human breast cancer and is a downstream target for HER-2/neu. *Mod Pathol* **21**, 609-16 (2008).

38. Hsu, M.C., Chang, H.C. & Hung, W.C. HER-2/neu transcriptionally activates Jab1 expression via the AKT/beta-catenin pathway in breast cancer cells. *Endocr Relat Cancer* **14**, 655-67 (2007).

39. O'Hagan, R.C. & Hassell, J.A. The PEA3 Ets transcription factor is a downstream target of the HER2/Neu receptor tyrosine kinase. *Oncogene* **16**, 301-10 (1998).

40. Benz, C.C. et al. HER2/Neu and the Ets transcription activator PEA3 are coordinately upregulated in human breast cancer. *Oncogene* **15**, 1513-25 (1997).

41. Naderi, A., Meyer, M. & Dowhan, D.H. Cross-regulation between FOXA1 and ErbB2 signaling in estrogen receptor-negative breast cancer. *Neoplasia* **14**, 283-96 (2012).

42. Francis, R.E. et al. FoxM1 is a downstream target and marker of HER2 overexpression in breast cancer. *Int J Oncol* **35**, 57-68 (2009).

43. Koo, C.Y., Muir, K.W. & Lam, E.W. FOXM1: From cancer initiation to progression and treatment. *Biochim Biophys Acta* **1819**, 28-37 (2011).

44. Nencioni, A. et al. Grb7 upregulation is a molecular adaptation to HER2 signaling inhibition due to removal of Akt-mediated gene repression. *PLoS One* **5**, e9024 (2010).

45. Aceto, N. et al. Co-expression of HER2 and HER3 receptor tyrosine kinases enhances invasion of breast cells via stimulation of interleukin-8 autocrine secretion. *Breast Cancer Res* **14**, R131 (2012).

46. Korkaya, H. et al. Activation of an IL6 inflammatory loop mediates trastuzumab resistance in HER2+ breast cancer by expanding the cancer stem cell population. *Mol Cell* **47**, 570-84 (2012).

47. Fleming, F.J. et al. Expression of SRC-1, AIB1, and PEA3 in HER2 mediated endocrine resistant breast cancer; a predictive role for SRC-1. *J Clin Pathol* **57**, 1069-74 (2004).

48. Luo, Y. et al. Inhibitors and inactivators of protein arginine deiminase 4: functional and structural characterization. *Biochemistry* **45**, 11727-36 (2006).

49. Slack, J.L., Causey, C.P. & Thompson, P.R. Protein arginine deiminase 4: a target for an epigenetic cancer therapy. *Cell Mol Life Sci* **68**, 709-20 (2011).

50. Tseng, P.H. et al. Overcoming trastuzumab resistance in HER2-overexpressing breast cancer cells by using a novel celecoxib-derived phosphoinositide-dependent kinase-1 inhibitor. *Mol Pharmacol* **70**, 1534-41 (2006).

51. Rao, V.H. et al. A positive feedback loop between HER2 and ADAM12 in human head and neck cancer cells increases migration and invasion. *Oncogene* **31**, 2888-98 (2011).

52. Kang, L., Guo, Y., Zhang, X., Meng, J. & Wang, Z.Y. A positive cross-regulation of HER2 and ER-alpha36 controls ALDH1 positive breast cancer cells. *J Steroid Biochem Mol Biol* **127**, 262-8 (2011).

53. Naderi, A., Liu, J. & Francis, G.D. A feedback loop between BEX2 and ErbB2 mediated by c-Jun signaling in breast cancer. *Int J Cancer* **130**, 71-82 (2011).

54. Cui, J. et al. Cross-talk between HER2 and MED1 regulates tamoxifen resistance of human breast cancer cells. *Cancer Res* **72**, 5625-34 (2012).

55. Kalaany, N.Y. & Sabatini, D.M. Tumours with PI3K activation are resistant to dietary restriction. *Nature* **458**, 725-31 (2009).

56. Farnie, G., Willan, P.M., Clarke, R.B. & Bundred, N.J. Combined inhibition of ErbB1/2 and Notch receptors effectively targets breast ductal carcinoma *in situ* (DCIS) stem/progenitor cell activity regardless of ErbB2 status. *PLoS One* **8**, e56840.

57. Mishra, S.K., Mandal, M., Mazumdar, A. & Kumar, R. Dynamic chromatin remodeling on the HER2 promoter in human breast cancer cells. *FEBS Lett* **507**, 88-94 (2001).

58. Kan, R. et al. Potential role for PADI-mediated histone citrullination in preimplantation development. *BMC Dev Biol* **12**, 19 (2012).

59. Chambraud, B., Berry, M., Redeuilh, G., Chambon, P. & Baulieu, E.E. Several regions of human estrogen receptor are involved in the formation of receptor-heat shock protein 90 complexes. *J Biol Chem* **265**, 20686-91 (1990).

60. Margeat, E. et al. The human estrogen receptor alpha dimer binds a single SRC-1 coactivator molecule with an affinity dictated by agonist structure. *J Mol Biol* **306**, 433-42 (2001).

61. Hanstein, B. et al. p300 is a component of an estrogen receptor coactivator complex. *Proc Natl Acad Sci U S A* **93**, 11540-5 (1996).

62. Kawai, H., Li, H., Avraham, S., Jiang, S. & Avraham, H.K. Overexpression of histone deacetylase HDAC1 modulates breast cancer progression by negative regulation of estrogen receptor alpha. *Int J Cancer* **107**, 353-8 (2003).

63. Kurpios, N.A., Sabolic, N.A., Shepherd, T.G., Fidalgo, G.M. & Hassell, J.A. Function of PEA3 Ets transcription factors in mammary gland development and oncogenesis. *J Mammary Gland Biol Neoplasia* **8**, 177-90 (2003).

64. Shepherd, T.G., Kockeritz, L., Szrajber, M.R., Muller, W.J. & Hassell, J.A. The pea3 subfamily ets genes are required for HER2/Neu-mediated mammary oncogenesis. *Curr Biol* **11**, 1739-48 (2001).

65. Benz, C.C. et al. Estrogen-dependent, tamoxifen-resistant tumorigenic growth of MCF-7 cells transfected with HER2/neu. *Breast Cancer Res Treat* **24**, 85-95 (1992).

66. Serra, V. et al. PI3K inhibition results in enhanced HER signaling and acquired ERK dependency in HER2-overexpressing breast cancer. *Oncogene* **30**, 2547-57 (2011).

CHAPTER FOUR

PADI2 OVEREXPRESSION IN TRANSGENIC MICE LEADS TO PREMALIGNANT SKIN LESIONS AND PROGRESSION TO SQUAMOUS CELL CARCINOMA

* Manuscript from: John L. McElwee[†]; Sunish Mohanan[†]; Sachi Horibata; Kelly Sams; Dalton McLean; Iva Cvitaš; and Scott A. Coonrod. PADI2 overexpression in transgenic mice leads to premalignant skin lesions and progression to squamous cell carcinoma. *In preparation.*

4.1 Summary

Introduction:

Peptidylarginine deiminases (PADIs) are a family of posttranslational modification enzymes that convert positively charged arginine residues on substrate proteins to neutrally charged citrulline. This activity, called citrullination or deimination, has been shown to have wide-ranging effects on target protein structure, function, and protein-protein interactions. PADI2 has been implicated in various diseases, including multiple sclerosis, inflammatory diseases such as RA and COPD, and more recently, cancer. We have recently reported that PADI2 and HER2 expression is correlated in breast cancer cell lines, and that PADI2 plays a role in the proliferation of mammary tumors *in vitro* and *in vivo*. The goal of this study was to analyze whether the transgenic expression of PADI2 driven by the MMTV-LTR promoter can induce oncogenesis in hormone-responsive epithelium.

Methods:

To examine whether the overexpression of PADI2 is sufficient to drive tumorigenesis in epithelial tissue, we cloned human FLAG-tagged PADI2 cDNA downstream of the hormone-responsive MMTV-LTR promoter. We generated four founder lines in FVB mice expressing the MMTV-FLAG-PADI2 transgene, and performed phenotypic and genetic analysis of these mice. Lastly, we have created stable cell lines overexpressing FLAG-PADI2 in the human skin cancer cell line A431 to validate our findings in the transgenic mice.

Results:

The ectopic expression of human PADI2 in mouse epithelium is sufficient to promote neoplasia, as we report that ~20% of transgenic mice develop skin lesions.

Interestingly we found that in a subset of these mice, these lesions further progress to more invasive squamous cell carcinomas, as noted by histopathological features. In addition, we note that these skin lesions express high levels of transgene, as well as display markers of invasion/EMT (decreased E-cadherin) and inflammation (Il6/Il8). We confirmed these results in the human squamous cell carcinoma cell line A431, where we report that stable expression of FLAG-PADI2 increases markers of inflammation (IL6/IL8) and EMT, ultimately increasing the cellular malignancy and invasiveness of these cells.

Conclusion:

Collectively, these studies provide functional and mechanistic evidence establishing PADI2 as a potential novel oncogene in the development of skin neoplasia, and might offer a new target for cancer therapy.

Key words: Peptidylarginine deiminase, PAD2/PADI2, MMTV-LTR, MMTV-FLAG-PADI2, Skin Neoplasia/Lesions, Squamous Cell Carcinoma, A431

4.2 Introduction

The peptidylarginine deiminase family of posttranslational modification enzymes converts positively charged arginine residues on substrate proteins to neutrally charged citrulline. This activity, alternatively called citrullination or deimination, has been shown to have wide-ranging effects on target protein structure, function, and protein-protein interactions. The PADI enzyme family is thought to have arisen by gene duplication and localizes within the genome to a highly organized cluster at 1p36.13 in humans. At the protein level, each of the five well-conserved PADI members shows a relatively distinct pattern of substrate specificity and tissue distribution [1, 2]. Increasingly, the dysregulation of PADI activity is associated with a range of diseases, including rheumatoid arthritis (RA), multiple sclerosis, ulcerative colitis, neural degeneration, COPD, and cancer [3-5]. While the presumptive function of PADI activity in most diseases is linked to inflammation, the role that PADIs play in cancer progression is still under investigation. Others have shown that citrullination of the p53 tumor suppressor protein by PADI4 affects the expression of p53-target genes *p21*, *OKL38*, *CIP1* and *WAF1* [6-8]. While PADI2 has historically been defined as a cytoplasmic protein, recent evidence from our lab shows that PADI2 can localize to the nucleus and directly bind chromatin to influence target gene expression [9-12].

Our recent studies suggest a role for PADI2 in the oncogenic progression of breast cancer, more specifically, HER2-positive tumors, as RNA-seq data reveal that *PADI2* is highly correlated with *HER2/ERBB2* overexpression across 57 breast cancer cell lines. We concluded this study with the first preclinical evidence showing that the PADI inhibitor, Cl-amidine, could be utilized as a therapeutic agent for the treatment of tumors *in vivo*.

To further investigate the involvement of PADI2 in the oncogenesis of epithelial tumors, we generated FVB mice expressing FLAG-PADI2 under the control

of the hormone-responsive mammary tumor virus (MMTV) promoter. However, while transgenic expression of human *PADI2* in mammary glands was detected, the MMTV-FLAG-PADI2 mice failed to develop any mammary tumors. While expression from the MMTV-LTR promoter is normally found to be localized to the mammary and salivary gland, other tissues have been implicated, including the skin and ovaries [13, 14]. Our results confirm this, as we see increased transgenic human *PADI2* transcript levels in the all four of those tissues. Surprisingly, we discovered that 20% of the mice developed skin lesions after five months. These tumors expressed high levels of transgenic human *PADI2* and display markers of increased invasiveness and epithelial to mesenchymal transition (EMT). Furthermore, some of these tumors display the hallmarks of malignant progression to highly invasive squamous cell carcinomas.

Previous studies have reported that three PADI isozymes, PADI1, PADI2, and PADI3, show expression in the epidermis, with all three displaying the ability to target filaggrin for citrullination, a key protein involved in tissue hydration and barrier functions [15]. PADI1 and PADI3 have been the primary isozymes characterized in the epidermis to date; with PADI3 being found to deiminate trichohyalin in hair follicles [16, 17] and PADI1 deiminating keratin (K1 and K10) and filaggrin during epidermal differentiation [18, 19]. Moreover, the overexpression of PADI1 (along with PADI2 and PADI3), has been shown to generate abnormal levels of citrullinated keratin K1 in the epidermis of psoriatic patients [20]. This suggests that aberrant expression of PADIs, including PADI2, might play a role in diseases of the skin, including cancer.

Interestingly, the original cloning of human *PADI2* cDNA was from the human skin cancer cell line, HSC-1, which is derived from a cutaneous squamous carcinoma [21]. We report here a novel model of skin neoplasia in FVB transgenic mice, driven by human PADI2 under the MMTV-LTR promoter; thus, establishing a novel role for PADI2 in the progression of cancer.

4.3 Materials and Methods

Generation of MMTV-FLAG-PADI2 mice

To generate the MMTV-FLAG-PADI2 construct, a human PADI2 cDNA fragment was removed from pcDNA3.1-FLAG-PADI2 [11], and cloned into the EcoRI sites of the MMTV-SV40-Bssk plasmid (Addgene plasmid #1824) that was originally generated in the laboratory of Dr. Philip Leder at Harvard Medical School [22]. The linear MMTV-FLAG-PADI2 construct was purified and microinjected into the pronuclei of fertilized embryos from super-ovulated FVB mice, and 2-cell stage embryos were transferred to pseudopregnant mothers. The microinjection and embryo transfer was performed by the Stem Cell and Transgenics Core at the Cornell University College of Veterinary Medicine. Mice were genotyped for the presence of human PADI2 transgene by PCR with the primers hPADI2-cds-F/R (**see Table 4.1**).

Lentivirus and plasmids for stable FLAG-PADI2 expression in A431 cells

The human squamous cell carcinoma A431 cell line was obtained from ATCC and cultured according to manufacturer's directions. To generate A431 cells overexpressing FLAG-tagged PADI2, two separate plasmids were generated. First, for stably and transiently transfected A431, FLAG-PADI2 was subcloned (NheI/XhoI) from pcDNA3.1-FLAG-PADI2 [11] into the pIRES2-EGFP vector (Clontech). This vector has bicistronic expression of both FLAG-PADI2 and EGFP by means of an internal ribosome entry site (IRES). A431 cells were transfected with pIRES2-FLAG-PADI2 using X-tremeGENE 9 (Roche) and stable cells were selected in 800 µg/ml G418 for 2-weeks. To generate lentiviral-transduced cells, the FLAG-PADI2-IRES-EGFP fragment was excised from the pIRES2-FLAG-PADI2 plasmid by digestion with MluI and SspI. The linearized fragment was blunted with T4 DNA polymerase (NEB), and subcloned into the BamHI-SalI digested/T4 blunted pLenti-PGK-GFP-

Puro plasmid (Addgene #19070) that was originally generated by Campeau et al. at the University of Massachusetts Medical School [23]. This plasmid was verified by restriction digest and sequencing, and transduction of A431 cells was performed as previously described in Campeau et al. using 3rd generation lentiviral packaging/envelope vectors (pLP1-pMDLg/pRRE, Addgene #12251; pLP2-pRSV-Rev, Addgene #12253; and pVSV-G-pMD2.G, Addgene #12259). Stably transduced cells were selected in 1 μg/ml puromycin for 2-weeks.

Immunohistochemistry (IHC) and immunofluorescence (IF)

IHC and IF experiments were carried out using a standard protocol as previously described [9]. Primary antibodies are as follows: anti-PADI2 (12110-1-AP, ProteinTech), anti-FLAG-M2 (F1804, Sigma), anti-Ki67 (ab15580, Abcam), and anti-GFP (ab290, Abcam). Sections prepared for IHC were incubated in DAB chromagen solution (Vector Laboratories) according to the manufacturer's protocol, washed, and then counterstained with hematoxylin. The IF slides were incubated in streptavidin conjugated-488 (Invitrogen), washed, and then mounted using Vectashield containing DAPI (Vector Laboratories). Negative controls for both IHC and IF experiments were either rabbit or mouse IgG antibody at the appropriate concentrations. Tumor sections were examined for general morphological differences after hematoxylin and eosin (H&E) staining.

Western blotting

Western blotting was carried out as previously described [9]. Primary antibodies against PADI2 (12110-1-AP, ProteinTech) and FLAG-M2 (F1804, Sigma) were incubated overnight at 4°C. To confirm equal protein loading, membranes were stripped and re-probed with anti-β-actin (ab8227, Abcam).

RNA isolation, semi-quantitative, and quantitative Real-Time PCR (qRT-PCR)

RNA was purified using the Qiagen RNAeasy kit, including on-column DNase treatment to remove genomic DNA. The resulting RNA was reverse transcribed using the ABI High Capacity RNA-to-cDNA kit according to the manufacturer's protocol (Applied Biosystems). Semi-quantitative PCR was performed using primers (see **Table 4.2**) for human *PADI2* and mouse *Padi1*, *Padi2*, *Padi3*, and *Padi4*, using mouse *Gapdh* as the loading control. TaqMan Gene Expression Assays (ABI) were used to measure relative mRNA levels for the transgenic human *PADI2* (Hs00247108_m1), along with endogenous mouse *Padi1* (Mm00478062_m1), *Padi2* (Mm00447020_m1), *Padi3* (Mm00478075_m1), and *Padi4* (Mm01341658_m1). Mouse *Gapdh* (4352932E) was used as the loading control. In addition, primer sequences for gene expression analysis via SYBR-qPCR can be found in **Table 4.3** for mouse genes, and **Table 4.4** for human genes. Expression levels were analyzed using the $2^{-\Delta\Delta C(t)}$ method [24]. Data are shown as means ± SD from three independent experiments, and were separated using Student's t-test.

Assays for cellular malignancy and invasion

Collagen coated inserts for 24-well plate wells (Falcon BD Fluoroblok; Catalog number: 351152, 8 µm pore size) were used to conduct transwell migration assays. Briefly, cells were trypsinized into an individual cell suspension, washed with DPBS, and added on the coated filters in serum-free DMEM (10,000 cells per filter). The lower chamber of the companion plate (Falcon BD Labware) was filled with DMEM supplemented with 10% FBS. At different time points (4 and 24 hours) of incubation, the filters were removed for evaluation. Cells that had migrated to the other side of the membrane were fixed in 4% paraformaldehyde (PFA), and stained with DAPI for visualization of the nuclei. The nuclei were counted under fluorescent

wide-field microscope. Values for cell invasion are expressed as the mean number of cells/20X microscopic field over five fields per filter for triplicate experiments. Focus formation assays were carried out using stable A431 cells (pIRES2-EGFP-FLAG-PADI2 or empty vector control) that were grown in 6-well plates. After 4d, cells were fixed with 4% PFA, and stained with crystal violet for subsequent analysis of focus formation. After imaging, the crystal violet was removed from the cells with 10% acetic acid and absorbance levels were measured (600 nM).

Statistical analysis

All experiments were independently repeated at least three times unless otherwise indicated. Values were expressed as the mean $\pm$ the SD. Means were separated using Student's t-test.

4.4 Results

Generation of MMTV-FLAG-PADI2 transgenic mice

To assess the potential role of PADI2 in the oncogenesis of epithelial tissue, we generated a mouse model in which the human *PADI2* gene is overexpressed under control of the hormone-responsive MMTV-LTR promoter. The transgenic construct consists of a MMTV-LTR promoter placed upstream of the human FLAG-tagged PADI2 cDNA, followed by an SV40 splice/polyadenylation site (**Figure 4.1**). MMTV-FLAG-PADI2 mice were generated, and seven potential founders were tested for the presence of transgene by PCR. We identified 4 founders (indicated in red, **Figure 4.2a**), 4807, 4853, 4680, and 4863, that carried germline transmission of the FLAG-PADI2 transgene. While founder 4854 initially appeared to be a low-copy founder line, we failed to see transmission of the transgene to subsequent generations at Mendelian ratios, perhaps indicating mosaicism. Using semi-quantitative RT-PCR,

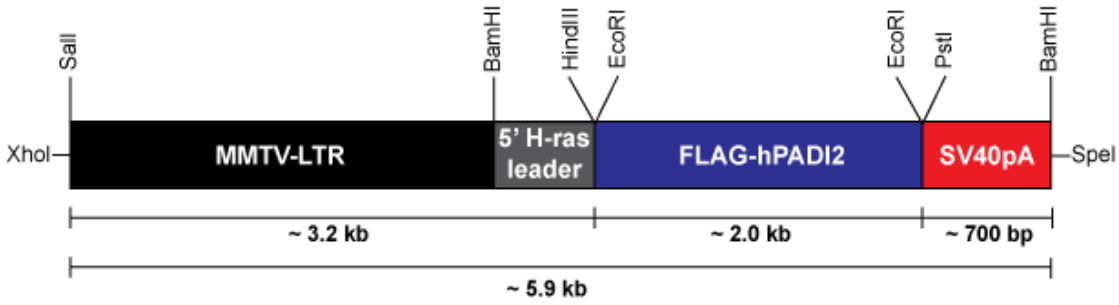

<u>Figure 4.1:</u> MMTV-FLAG-PADI2 transgenic construct. Schematic of the linearized MMTV-FLAG-hPADI2 transgene, containing a FLAG-tagged human *PADI2* cDNA fragment that was cloned between the EcoRI sites of the MMTV-SV40-Bssk plasmid [22]. The construct used for generation of FLAG-hPADI2-transgenic mice (also referred to as FLAG-PADI2) consists of FLAG-PADI2 under the control of the hormone-responsive MMTV-LTR promoter-enhancer with an SV40 splice-polyadenylation signal (SV40pA).

Figure 4.2: Generation of MMTV-FLAG-PADI2 transgenic mice. (a) PCR screening of DNA extracted from mouse tails for the presence of integrated human *PADI2* transgene (TG – hPADI2). Four founders were identified (red); primers for mouse *Padi4* were used as a wild-type (WT – mPADI4) control for amplification. Primer sequences can be found in **Table 4.1**. (b) Semi-quantitative RT-PCR was performed on tissues known to have high expression in MMTV-LTR transgenic mice: skin, salivary gland (SG), mammary gland (MG), and ovary (note: 4807 founder line was not used due to breeding issues and this line was subsequently terminated). Total RNA was isolated from tissues and relative mRNA levels for the transgenic human *PADI2*, along with endogenous mouse *Padi1*, *Padi2*, *Padi3*, and *Padi4* are shown. Mouse *Gapdh* was used as the loading control. (c) Quantitative RT-PCR (qPCR) for the human *PADI2* transgene was performed across the same tissues, using WT skin as the reference, with mouse *Gapdh* normalization. Expression levels were analyzed using the $2^{-\Delta\Delta C(t)}$ method, and data are expressed as the mean ± SD from three independent experiments (* $p < 0.05$).

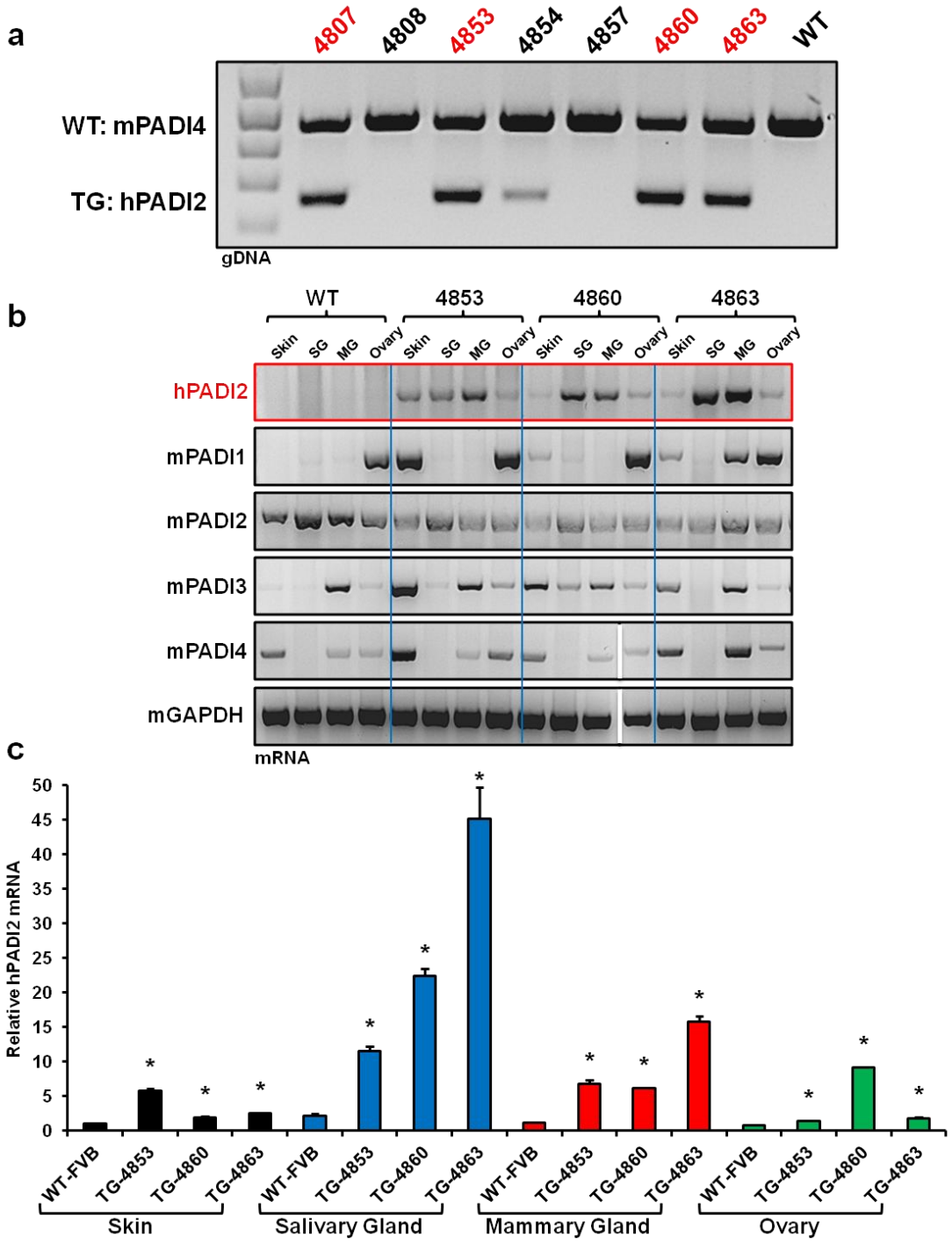
a
4807
4808
4853
4854
4857
4860
4863
WT
WT: mPADI4
TG: hPADI2
gDNA
b
WT
4853
4860
4863
Skin
SG
MG
Ovary
hPADI2
mPADI1
mPADI2
mPADI3
mPADI4
mGAPDH
mRNA
c
Relative hPADI2 mRNA
50
45
40
35
30
25
20
15
10
5
0
WT-FVB
TG-4853
TG-4860
TG-4863
Skin
Salivary Gland
Mammary Gland
Ovary

we confirmed the presence of FLAG-PADI2 transcript in the skin, salivary gland, mammary gland, and ovary of the transgenic mice (**Figure 4.2b**). These four tissues were chosen for analysis as they have previously been shown to have high expression of MMTV-LTR driven transgenes [14]. We note that the subsequent analysis is for only three founders (4853, 4860, 4863), as founder line 4807 had breeding issues and was subsequently terminated. Quantitative real-time PCR analysis (qPCR) of these founders for the four same tissues was performed; in comparison to other founders, founder 4853 showed the highest expression in skin, while founder 4863 had the highest expression in salivary and mammary glands (**Figure 4.2c**).

We first analyzed the mammary glands of the transgenic mice, as we have previously established a link between PADI2 and breast cancer. Our initial goal was to generate MMTV-driven transgenic mice to investigate the effects of ectopic PADI2 overexpression in mammary epithelium *in vivo*. However, while PADI2 transgenic expression in the mammary glands was detected at high levels in both virgin (**Figure 4.3a**) and multiparous mice (**Figure 4.3b**), we failed to detect any gross abnormalities or any observable phenotype in the mammary gland of these mice.

PADI2 transgenic mice develop skin lesions with the potential to advance to invasive squamous cell carcinomas

While expression from the MMTV-LTR promoter is predominantly localized to the mammary and salivary gland, other tissues have been implicated, including the skin and ovaries [13, 14]. Surprisingly, we discovered that 20% of the mice developed skin lesions after five months (**Table 4.2**). These lesions are characterized by gross abnormalities, such as alopecia, multifocal epidermal ulceration often covered in sero-cellular crust, dysplasia, and thickening of the adjacent epidermis (**Figure 4.4a**). These lesions occur on both the dorsum and ventrum of transgenic mice. We note that we

Figure 4.3: MMTV-FLAG-PADI2 expression in the mammary gland.

(a) Confocal immunofluorescence analysis of FLAG (red) expression in virgin mouse mammary gland of a transgenic mouse. The luminal epithelial cells of mammary acini strongly express FLAG-PADI2 protein. (b) Immunohistochemical staining for PADI2 and FLAG in a multiparous mammary gland. The representative image shows a hyperplastic mammary gland with acinar epithelial cells strongly expressing both PADI2 and FLAG, confirming proper expression of the tagged transgene.

a

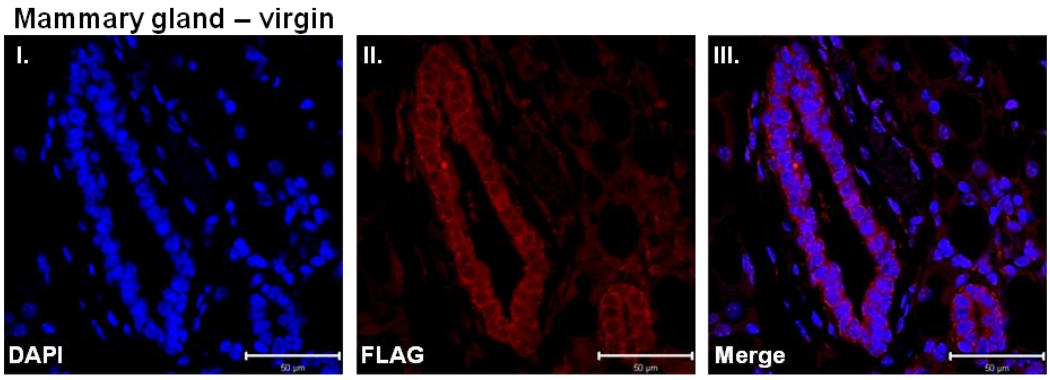
Mammary gland – virgin
I.
II.
III.
DAPI
FLAG
Merge

b

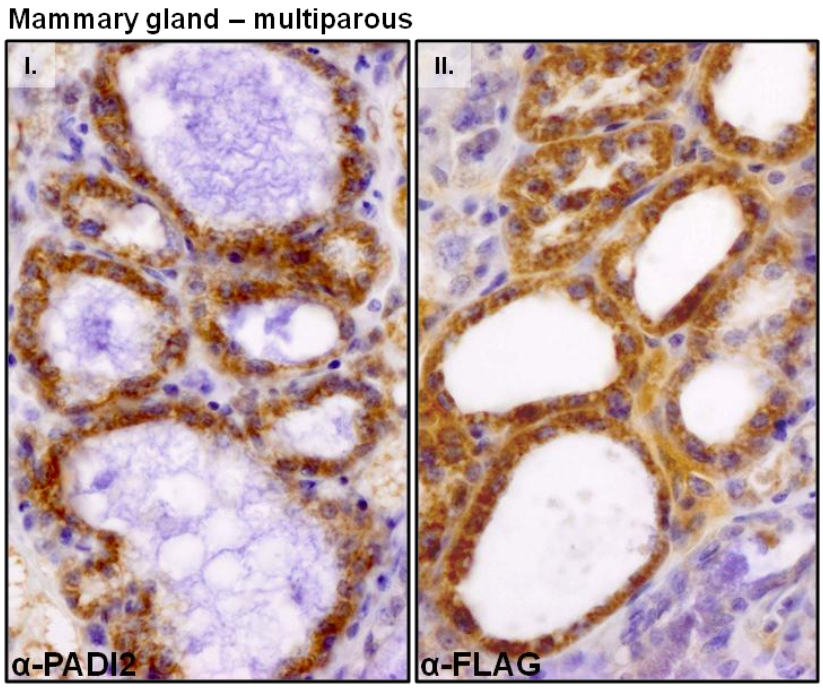
Mammary gland – multiparous
I.
II.
α-PADI2
α-FLAG

Table 4.2: Occurrence of skin lesions in MMTV-FLAG-PADI2 mice

	Total mice	WT mice	Tg mice
Mice > 5 months old (#)	86	31	55
Mice with lesions (#)	11	0	11
% of mice with lesions	13	0	20

have yet to see any of these lesions in the wild-type FVB mice, indicating that the phenotype is most likely a result of the FLAG-PADI2 transgene. Histological evaluation of skin lesions by H&E reveals highly neoplastic tissue, with features consistent with invasive squamous cell carcinoma (SCC). There are nests of neoplastic cells arising from the epidermis invading the dermis and subcutis (**Figure 4.4b, i**). Epidermis overlying the neoplasm is extensively ulcerated and the adjacent epidermal layers are hyperplastic (**Figure 4.4b, i**). Concentric layers of keratin surrounding tumor cells form keratin pearls, which are a characteristic of SCC (**Figure 4.4b, ii and iii**). The nests and islands of neoplastic cells within the subcutis show high degree of anisokaryosis and anisocytosis, with the nuclei often containing one to two prominent nucleoli (**Figure 4.4b, iv**). Clusters of neoplastic cells are surrounded by loose collagenous stroma with a marked loss of adnexal structures, consistent with a desmoplastic response (**Figure 4.4b, iii and iv**). Moreover, these skin lesions often contain carcinoma cells that are found budding off from the primary neoplasm (**Figure 4.4b, iv**), again indicating an invasive component to these tumors.

These skin lesions express high levels of transgenic PADI2, as immunohistochemical analysis shows PADI2 protein expression in the hyperplastic epidermis, neoplastic islands, and in hair follicular epithelium (**Figure 4.5a, i**). In addition, we see high expression of PADI2 protein in the neoplastic epithelium surrounding the keratin pearl (**Figure 4.5a, ii and iii**). Furthermore, these tumors are characterized by budding nests of carcinoma cells, which invade the adjacent stroma from the primary neoplasm. We note that PADI2 protein expression is high in these invasive cells (**Figure 4.5a, iv**). Because the PADI2 antibody can also detect endogenous mouse Padi2, we also stained for FLAG, and found that we see identical expression within the proliferating basal layers of hyperplastic/neoplastic epidermis; thus, suggesting that the increased PADI2 expression is a result of the transgene. We

<u>Figure 4.4:</u> Transgenic FLAG-PADI2 expression in the epidermis of mice leads to the development of skin lesions. (a) Representative gross lesion showing the skin phenotype, which includes alopecia, multifocal epidermal ulceration often covered in a sero-cellular crust, and thickening of the adjacent epidermis. (b) Histological evaluation of the skin sections by H&E reveals features consistent with invasive squamous cell carcinoma. (i) Nests of neoplastic cells arising from the epidermis are shown invading the deep dermis and subcutis, with the epidermis overlying the neoplasm extensively ulcerated. (i) and (ii) Adjacent epidermal layers are hyperplastic with the loss of adnexal structures and increase in desmoplastic response (iii). Carcinoma cells are often found budding off from the primary neoplasm (iv).

a Representative MMTV-FP2+ lesion

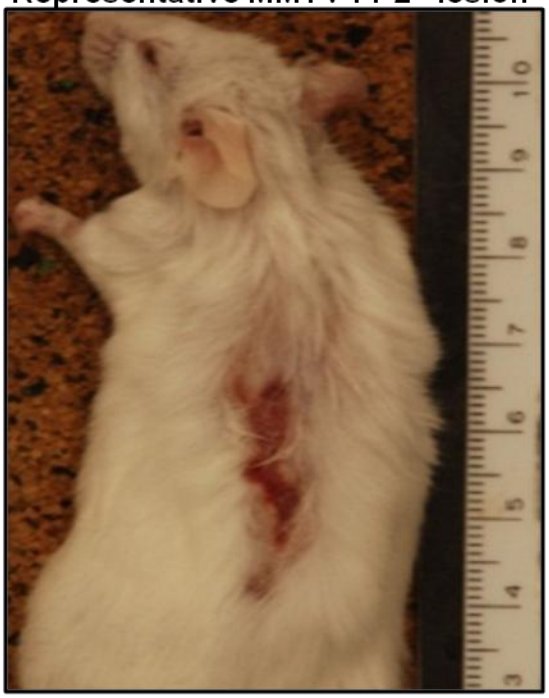

b H&E – MMTV-FP2+ skin lesion

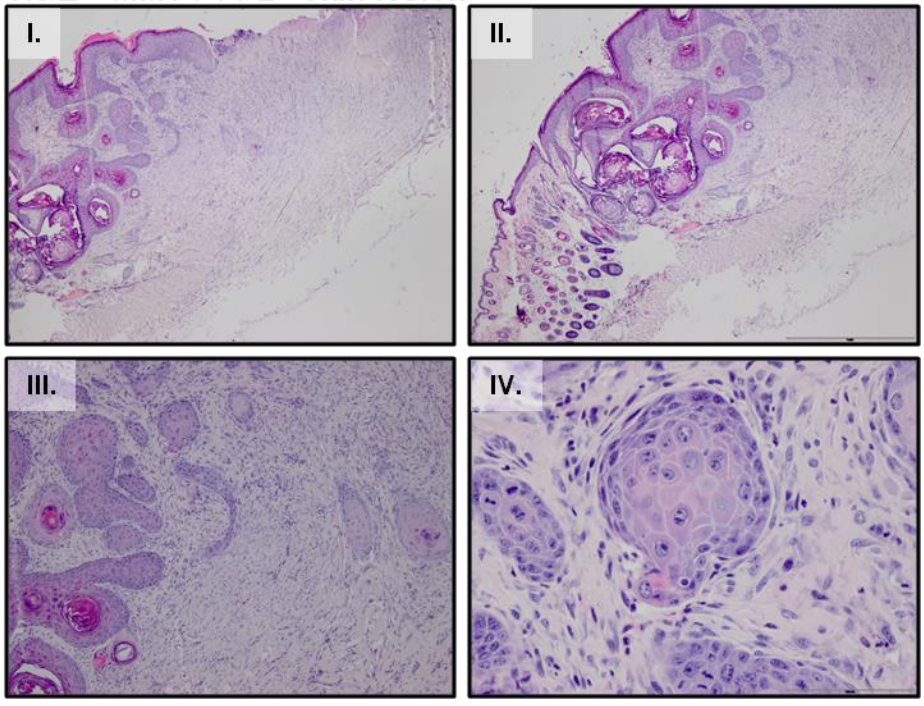

Figure 4.5: FLAG-PADI2 expression is high in the skin lesions of transgenic mice. (a) Immunohistochemical analysis of FLAG-PADI2 protein expression in skin neoplasms from transgenic mice. (i) Lower magnification image showing PADI2 protein expression in the hyperplastic epidermis, neoplastic islands, and in the hair follicular epithelium. (ii) – (iii) PADI2 protein expression in neoplastic cells surrounding concentric layers of keratin (arrow = keratin pearl). (iv) Representative image showing high levels of PADI2 protein expression in budding nest of carcinoma cells (broken arrow). (b) FLAG expression in skin neoplasms from transgenic mice. Scattered clusters of neoplastic cells show strong FLAG-tag expression. This staining is especially evident in the proliferating basal layers of hyperplastic or neoplastic epidermis.

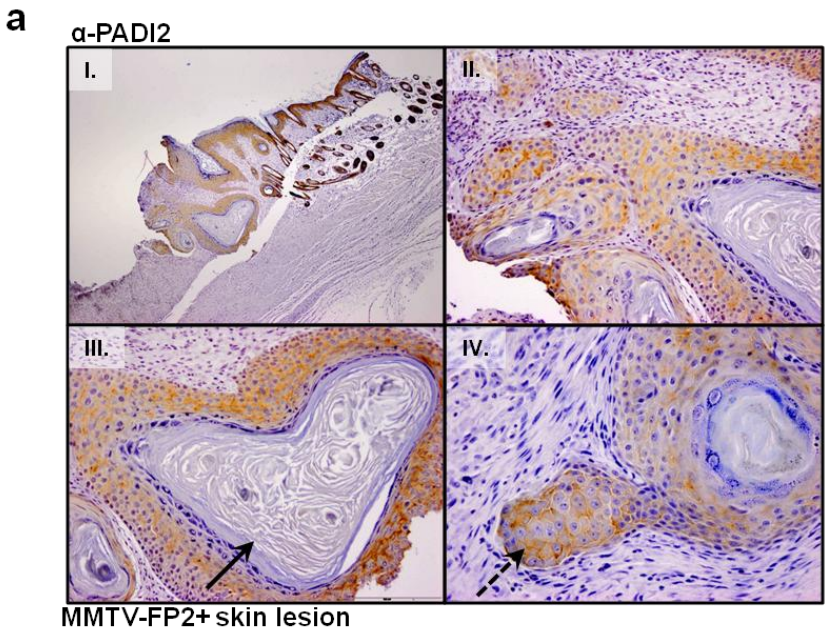
a
α-PADI2
I.
II.
III.
IV.
MMTV-FP2+ skin lesion

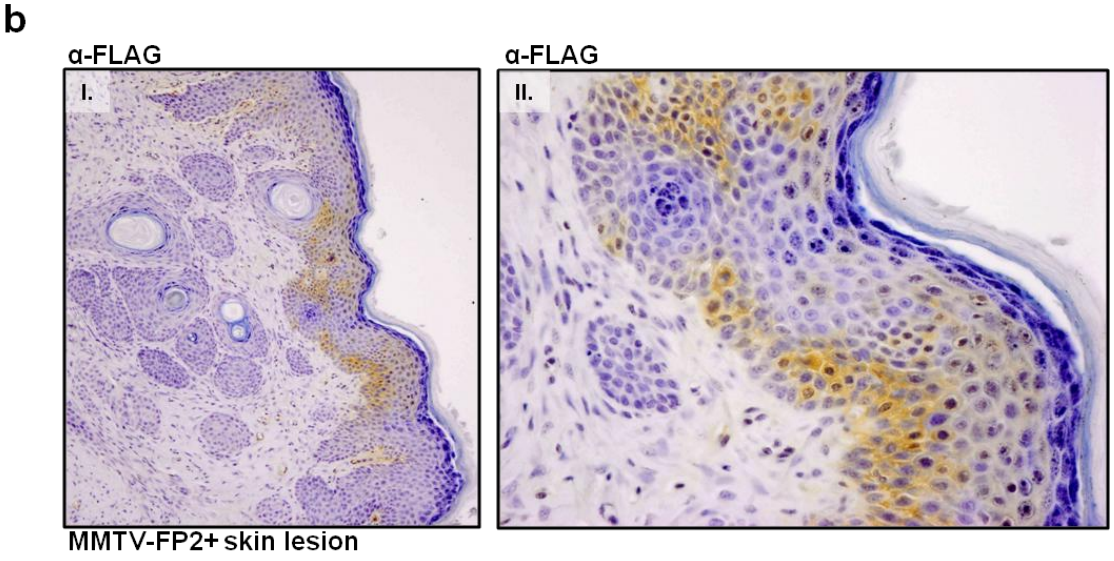
b
α-FLAG
I.
α-FLAG
II.
MMTV-FP2+ skin lesion

confirmed this using indirect-immunofluorescence to co-stain for FLAG and PADI2 expression in the skin lesions of transgenic mice. PADI2 and FLAG both co-localize to the neoplastic epithelial cells of a squamous cell carcinoma (**Figure 4.6, i-iv**). While PADI2 shows strong staining in multiple layers of the epidermis, we find that FLAG (i.e. transgene) is slightly more restricted to the basal layer, which is known to be more stem-cell like and highly proliferative [25]. Interestingly, we also see a slight increase in the proliferative marker, Ki67, within the FLAG staining section of the SCC lesion (**Figure 4.6b, ii-iv**). Therefore, this indicates that transgene expression in the skin might lead to an increase in proliferation, which is also supported by the identification of a subset of these lesions as highly proliferative and invasive SCC. We also note that we do not see any expression of the FLAG transgene in normal skin from wild-type mice (**Figure 4.7, i-vi**), as well as very little to any in adjacent normal skin from transgenic mice (data not shown).

Transgenic skin lesions have decreased levels of endogenous mouse Padis and increased markers of inflammation and EMT

Since we know that other PADIs can play a role in diseases of the skin, we were curious to see what the levels of other PADIs might be in the lesions from transgenic mice. Using semi-quantitative RT-PCR, we show human PADI2 transgene levels are present as expected in the lesions, as well as varying degrees of endogenous mouse Padis (**Figure 4.8a**). We show by qPCR that representative lesions (2) and (4) have the highest transgene expression (**Figure 4.8b**), and that these two lesions have the highest levels of protein expression (lesion 2 = SCC, **Figure 4.8c**). Surprisingly, we noticed what appeared to be a protein-dimer in the western blot that was probed with anti-FLAG. Previous evidence has indicated that PADI4 can associate as a dimer, and that PADI-activity (i.e. citrullination) is highest in dimerized PADI4 [26]. Interestingly,

Figure 4.6: Confocal immunofluorescence analysis of PADI2, FLAG, and Ki67 expression in neoplastic skin lesions of the FLAG-PADI2 transgenic mouse. (a) Representative image showing co-staining (iv) of FLAG (red, ii) and PADI2 (green, iii) in the neoplastic epithelial cells of a squamous cell carcinoma from a transgenic mouse. Nuclei are stained with DAPI (blue, i). Endogenous Padi2 shows strong positive staining in 2-3 layers of epidermal cells, while FLAG-PADI2 is predominantly localized to the basal cell layer. Scattered tumor cell islands underlying the epidermis show high levels of PADI2 expression. (b) Representative image showing co-staining (iv) of the proliferative marker, FLAG (red, ii), and Ki67 (green, iii) in neoplastic epithelial cells of squamous cell carcinoma. Tumor islands that are strongly positive for FLAG-PADI2 expression levels contain an increased number of Ki67 positive cells (iv). Nuclei are stained with DAPI (blue, i)

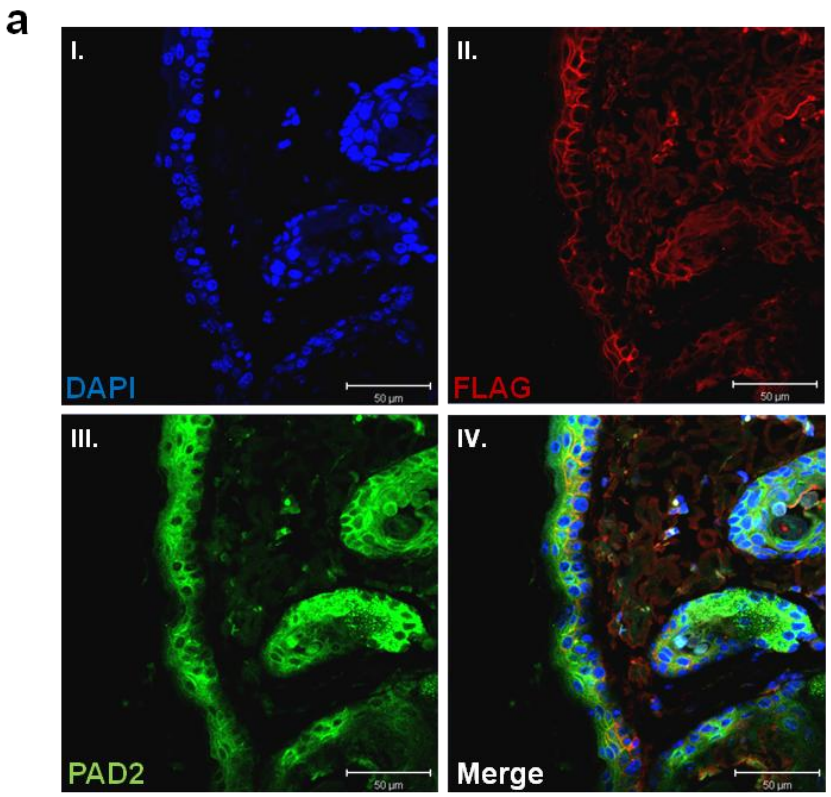
a
I.
II.
DAPI
FLAG
III.
IV.
PAD2
Merge
MMTV-FP2+ skin lesion
b
I.
II.
DAPI
FLAG
III.
IV.
KI67
Merge
MMTV-FP2+ skin lesion

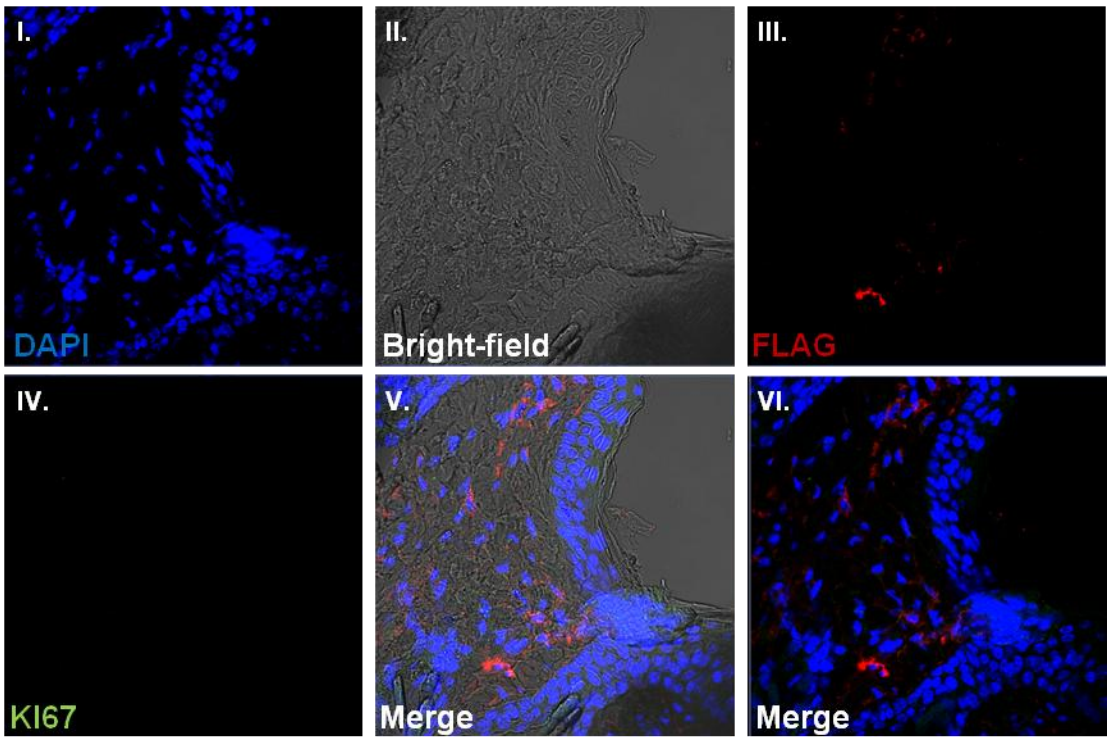

<u>Figure 4.7:</u> Normal skin from wild-type mice is absent for transgene expression, and has low levels of the proliferation marker, Ki67. (a) Representative image showing co-staining (vi) of FLAG (red, iii) and Ki67 (green, iv) in normal skin sections from a wild-type (WT) mouse. Bright-field image (ii and v). Both FLAG-tag and PADI2 protein expression are absent, concomitant with reduced Ki67 levels. Nuclei are stained with DAPI (blue, i)

Figure 4.8: Transgene expression in the skin lesions of MMTV-FLAG-PADI2 mice. (a) Semi-quantitative RT-PCR on four representative skin lesions from transgenic mice (Lesions 1-4). Total RNA was isolated from lesions and normal wild-type skin, and relative mRNA levels for the transgenic human *PADI2*, along with endogenous mouse *Padi1*, *Padi2*, *Padi3*, and *Padi4* are shown. Mouse *Gapdh* was used as the loading control. (b) Quantitative RT-PCR (TaqMan) for the human *PADI2* transgene was performed across the same lesions, using normal WT skin as the reference, along with mouse *Gapdh* normalization. Expression levels were analyzed using the $2^{-\Delta\Delta C(t)}$ method, and data are expressed as the mean ± SD from three independent experiments (* $p < 0.05$). (c) Representative western blot for skin from WT and transgenic (TG) mice, along with lesions (3) and (4), as well as (2), which is noted as a SCC skin tumor. Whole-cell lysates were probed for FLAG expression, with a predicted protein size of ~75 kDa (note the presence of a suspected homodimer at 150 kDa). β-actin was used as a loading control.

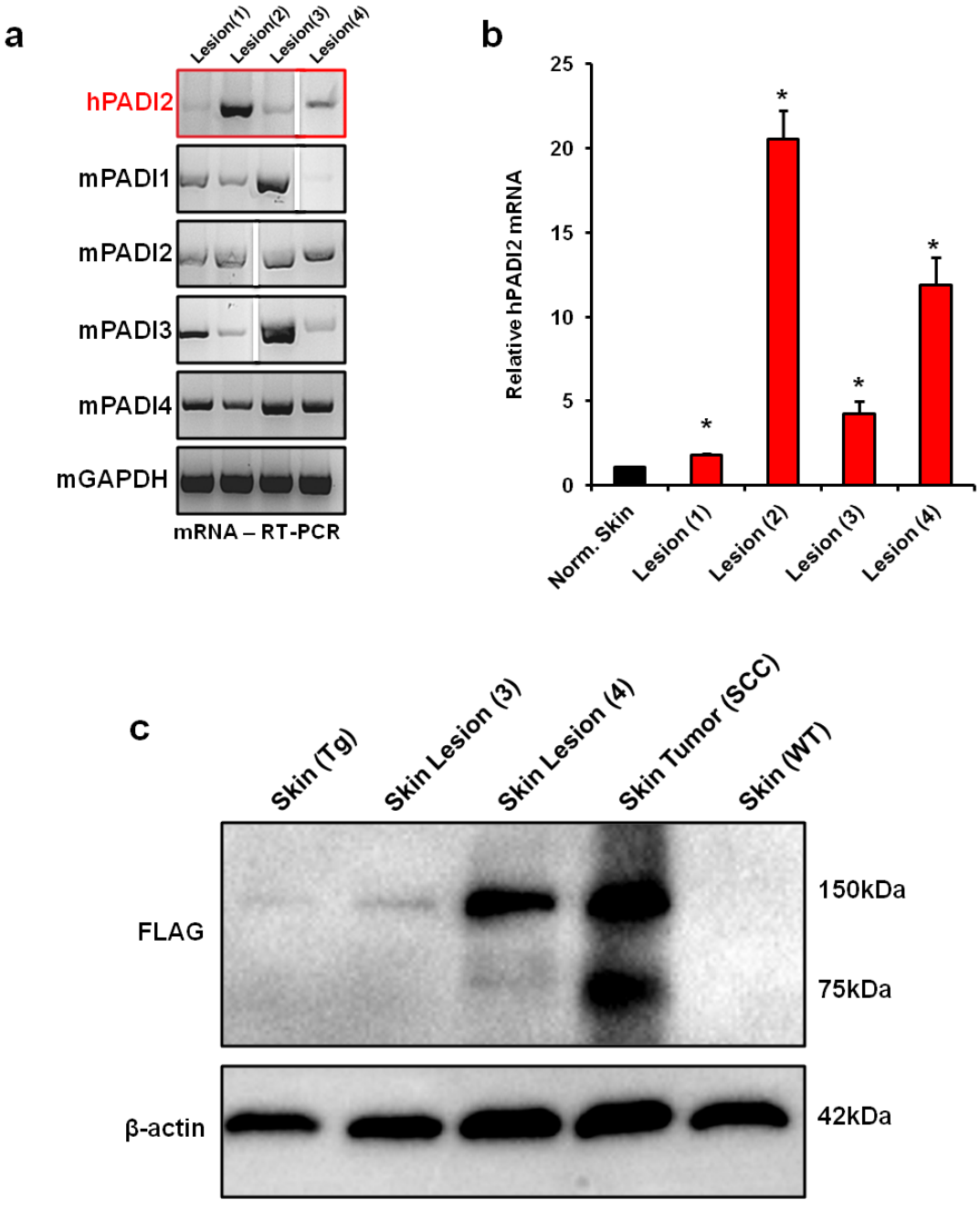
a
Lesion(1)
Lesion(2)
Lesion(3)
Lesion(4)
hPADI2
mPADI1
mPADI2
mPADI3
mPADI4
mGAPDH
mRNA – RT-PCR
b
Relative hPADI2 mRNA
25
20
15
10
5
0
*
Norm. Skin
Lesion (1)
Lesion (2)
Lesion (3)
Lesion (4)
c
Skin (Tg)
Skin Lesion (3)
Skin Lesion (4)
Skin Tumor (SCC)
Skin (WT)
FLAG
150kDa
75kDa
β-actin
42kDa

Liu et al. predict that PADI2 also functions as a dimer, as they report a high degree of conservation between the two family members, especially at the residues important for dimerization [26]. We wanted to quantify the levels of endogenous mouse Padis by qPCR, and show that in lesions (2) and (4), which have the highest levels of human *PADI2,* also have the lowest levels of mouse *Padi1*, *Padi3,* and *Padi4* (**Figure 4.9**). There is no observable difference reported for endogenous mouse *Padi2* levels. To gain better perspective as to the potential pathways involved in the progression of MMTV-FLAG-PADI2 skin lesions, we examined genes known to be involved in inflammation and invasion in cancer. We chose these genes based on previous reports indicating a role for PADI2 in inflammatory diseases, coupled with our report here of the invasive nature of these carcinomas. Interestingly, when we examined the two representative lesions with the highest levels of transgenic *PADI2* (lesions 2 and 4), we found that they have sharply elevated levels of *Il6* and *Il8* (*Cxcl15*) gene expression (**Figure 4.10**). Furthermore, these two lesions also display markers of EMT, as E-cadherin is decreased, along with a concomitant increase in vimentin (*Vim*) and the E-cadherin repressor, *Snai1* (**Figure 4.10**).

Overexpression of PADI2 in human squamous cell carcinoma A431 cells increases invasiveness and malignancy

Transgenic MMTV-FLAG-PADI2 mice show that ectopic expression of PADI2 is sufficient to drive tumorigenesis in epithelial cells and that this expression correlates with an increase in markers of invasion and EMT. We wanted to see if could replicate these results in a human skin cancer cell line, A431. The A431 cell line is a human squamous carcinoma cell line that was isolated from a vulva epidermoid carcinoma. To test the oncogenic potential of PADI2 in this cell line, we first transiently expressed FLAG-PADI2 using standard plasmids for mammalian protein expression

Figure 4.9: Lesions from MMTV-FLAG-PADI2 transgenic mice that express the highest levels of human *PADI2*, have decreased mouse *Padi1*, *Padi3*, and *Padi4*. Total RNA from transgenic skin lesions (1-4) and normal wild-type skin was isolated and reverse transcribed to cDNA. The relative mRNA levels for human transgenic *PADI2*, along with mouse *Padi1*, *Padi2*, *Padi3*, and *Padi4*, were determined by qPCR (TaqMan) using normal WT skin as the reference, along with *Gapdh* normalization. Expression levels were analyzed using the $2^{-\Delta\Delta C(t)}$ method, and data are expressed as the mean ± SD from three independent experiments (* $p < 0.05$).

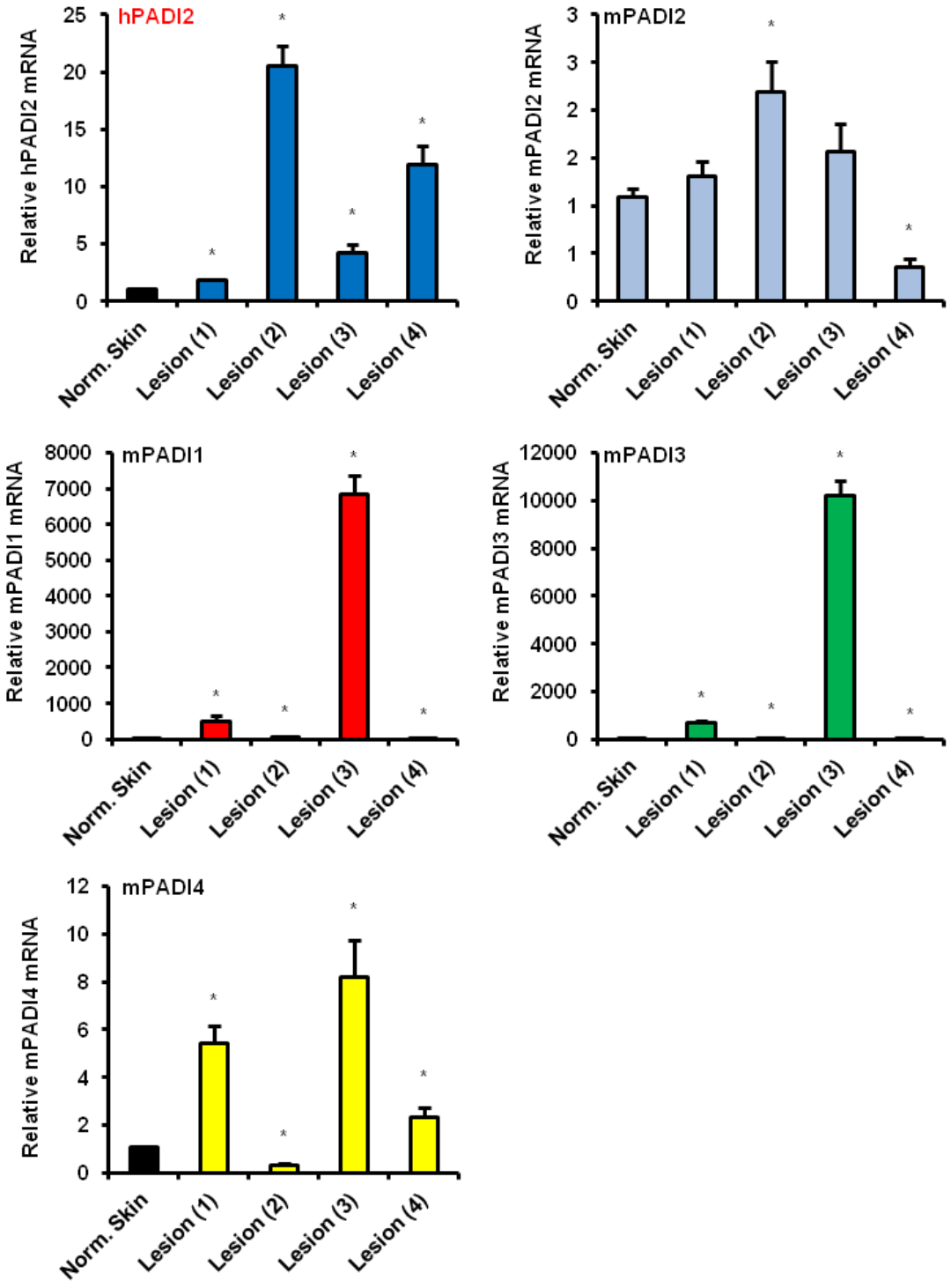
hPADI2
Relative hPADI2 mRNA
25
20
15
10
5
0
mPADI2
Relative mPADI2 mRNA
3
3
2
2
1
1
0
mPADI1
Relative mPADI1 mRNA
8000
7000
6000
5000
4000
3000
2000
1000
0
mPADI3
Relative mPADI3 mRNA
12000
10000
8000
6000
4000
2000
0
mPADI4
Relative mPADI4 mRNA
12
10
8
6
4
2
0
Norm. Skin
Lesion (1)
Lesion (2)
Lesion (3)
Lesion (4)

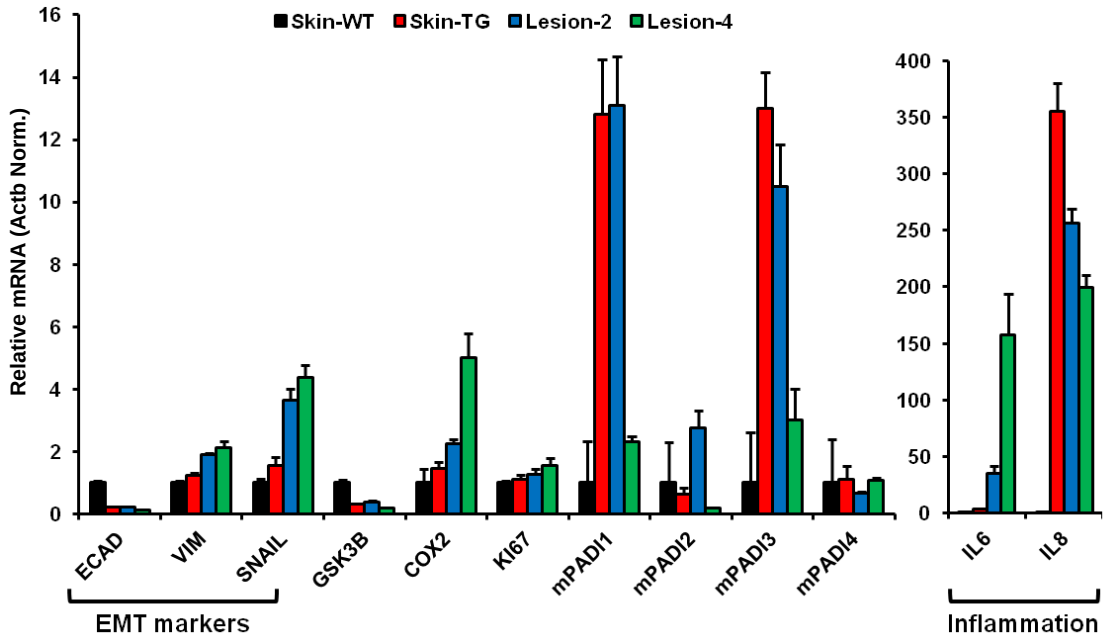

Figure 4.10: Skin lesions from MMTV-FLAG-PADI2 transgenic mice express markers of inflammation and EMT. Total RNA from transgenic skin lesions (1-4), along with transgenic and wild-type (WT) skin, was isolated and reverse transcribed to cDNA. Relative mRNA levels for the representative genes (see **Table 4.3** for gene list and primer sequences) were determined by qPCR (SYBR) using normal WT skin as the reference, along with β-actin (*Actb*) normalization. Expression levels were analyzed using the $2^{-\Delta\Delta C(t)}$ method, and data are expressed as the mean ± SD from three independent experiments (* $p < 0.05$).

(pcDNA3.1-FLAG-PADI2) and (pIRES2-FLAG-PADI2) and associated empty vectors. We found that in both of the cell lines expressing high levels of FLAG-PADI2 (**Figure 4.11a and b**), E-cadherin protein levels were reduced when compared to the empty vector control cells (**Figure 4.11a**). In addition, we see a concomitant increase in vimentin in these two cell lines. We examined the FLAG-PADI2 overexpressing A431 cells for expression of genes involved in inflammation and EMT, and found the results were similar to those seen in the transgenic mice. Both *IL6* and *IL8* gene levels are increased, while we see a reduction in E-cadherin, along with concomitant increases in *SNAIL* and *SLUG* (**Figure 4.11b**).

Given the data from our transiently transfected A431 cells, along with our data from the transgenic mice, we decided to test whether stable overexpression of FLAG-PADI2 might have an effect on the cellular malignancy and/or invasiveness of A431 cells. Using both lentiviral transduction of FLAG-PADI2, and traditional transfection, we created two stable cell lines overexpressing various levels of PADI2. The lentiviral generated stable cell line (pLenti-FLAG-PADI2) is under the control of the phosphoglycerate kinase (PGK) promoter, which is weaker than the cytomegalovirus promoter used in the pIRES2-FLAG-PADI2 stably transfected cells. After selecting for 2-3 weeks, we assayed for PADI2 levels, showing, as expected, that pLenti-FLAG-PADI2 (pLenti-FP2) had slightly less expression of PADI2 than pIRES2-FLAG-PADI2 (pIRES-FP2) (**Figure 4.12a**). Next, we tested the invasive properties of these cell lines by measuring their ability to migrate through a collagen matrix. For both cell lines, we see a significant increase in cellular migration after 24h, while the pIRES2-FP2 cell line also has a significant increase after 4h (**Figure 4.12b**). These results suggest that PADI2 dosage might correlate with invasion. Recent evidence from our lab suggests that PADI2 can be expressed in the nucleus, as well as the cytoplasm [10]; therefore, we decided to analyze the localization of PADI2 *in vitro* using indirect-

<u>Figure 4.11:</u> Transient overexpression of FLAG-PADI2 increases markers of inflammation and EMT in the human squamous cell carcinoma A431 cell line. (a) Human squamous cell carcinoma cells, A431, were transiently transfected with FLAG-PADI2 (pcDNA3.1-FP2 or pIRES2-FP2) or empty vector (pcDNA3.1-emtpy). Western blot analysis of protein expression for EMT markers, E-cadherin and vimentin, along with PADI2, was performed on transfected A431 cells. β-actin was used as a loading control. Total RNA was isolated and relative *PADI2* levels for the FLAG-PADI2 transfected A431 cells, relative to empty vector control (*ACTB* normalized), were analyzed by qPCR (SYBR). Additional genes were also analyzed, see **Table 4.4** for full gene list and primer sequences. Expression levels were analyzed using the $2^{-\Delta\Delta C(t)}$ method, and data are expressed as the mean ± SD from three independent experiments (* $p < 0.05$).

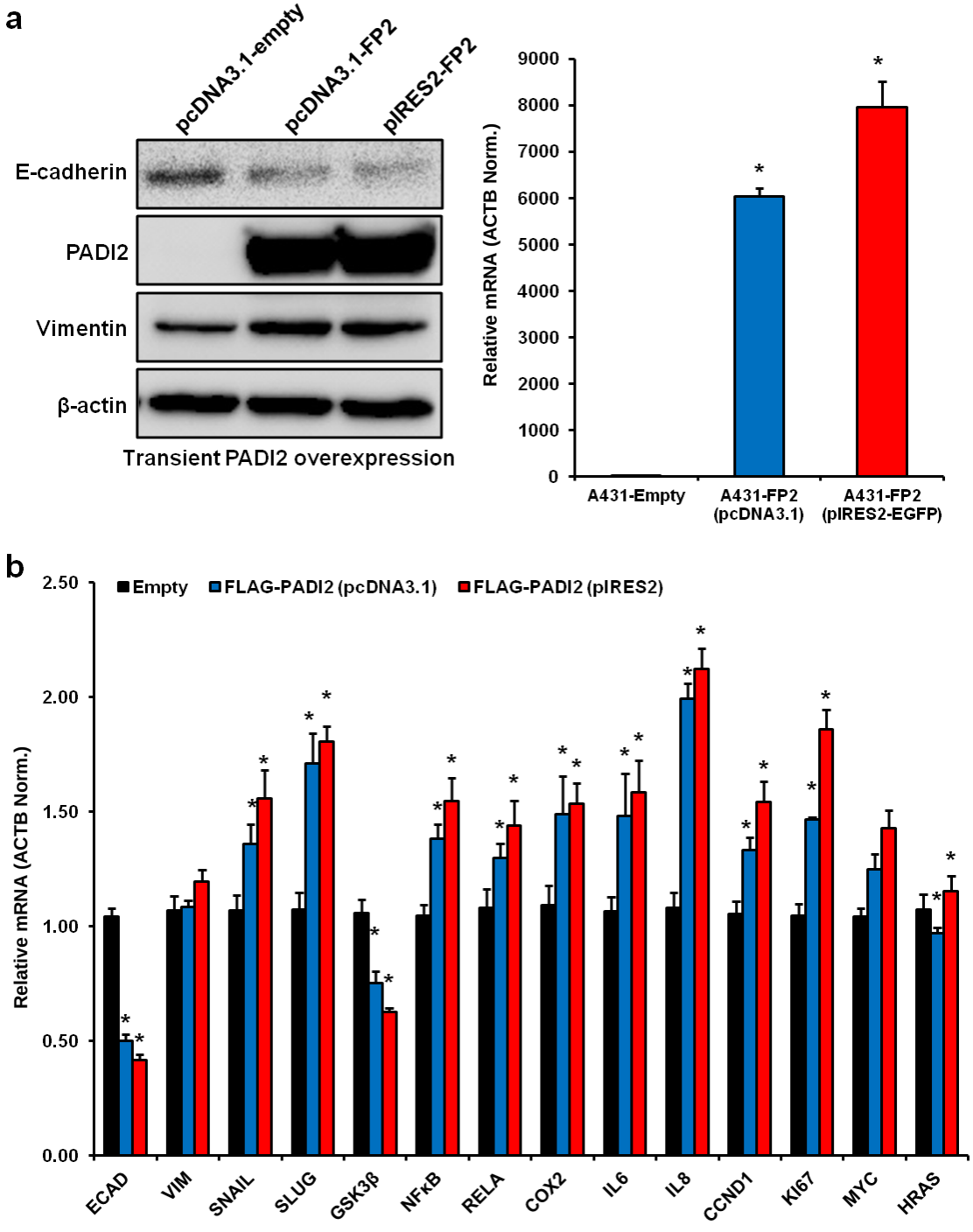
a
pcDNA3.1-empty
pcDNA3.1-FP2
pIRES2-FP2
E-cadherin
PADI2
Vimentin
β-actin
Transient PADI2 overexpression
Relative mRNA (ACTB Norm.)
9000
8000
7000
6000
5000
4000
3000
2000
1000
0
A431-Empty
A431-FP2 (pcDNA3.1)
A431-FP2 (pIRES2-EGFP)
b
Empty
FLAG-PADI2 (pcDNA3.1)
FLAG-PADI2 (pIRES2)
Relative mRNA (ACTB Norm.)
2.50
2.00
1.50
1.00
0.50
0.00
ECAD
VIM
SNAIL
SLUG
GSK3β
NFκB
RELA
COX2
IL6
IL8
CCND1
KI67
MYC
HRAS

Figure 4.12: A431 cells stably overexpressing PADI2 have increased invasion through a collagen matrix. (a) A431 cells were stably transfected with pIRES2-FLAG-PADI2 (pIRES2-FP2) or infected with lentivirus expressing FLAG-PADI2-EGFP (pLenti-FP2). Control vectors only express the *EGFP* gene (pIRES2-GFP and pLenti-GFP). Western blot analysis for PADI2 protein expression levels, β-actin was used as a loading control. Total RNA was isolated and relative *PADI2* levels for the FLAG-PADI2 transfected A431 cells, relative to GFP vector control (*ACTB* normalized), were analyzed by qPCR (SYBR). Expression levels were analyzed using the $2^{-\Delta\Delta C(t)}$ method, and data are expressed as the mean ± SD from three independent experiments (* $p < 0.05$). (b) Transwell migration assay through a collagen matrix – cells were seeded and allowed to migrate through a collagen matrix. After 4h or 24h, cells that migrated were counted under a microscope at 40X magnification. Data are expressed as the mean ± SD from three independent experiments (* $p < 0.05$).

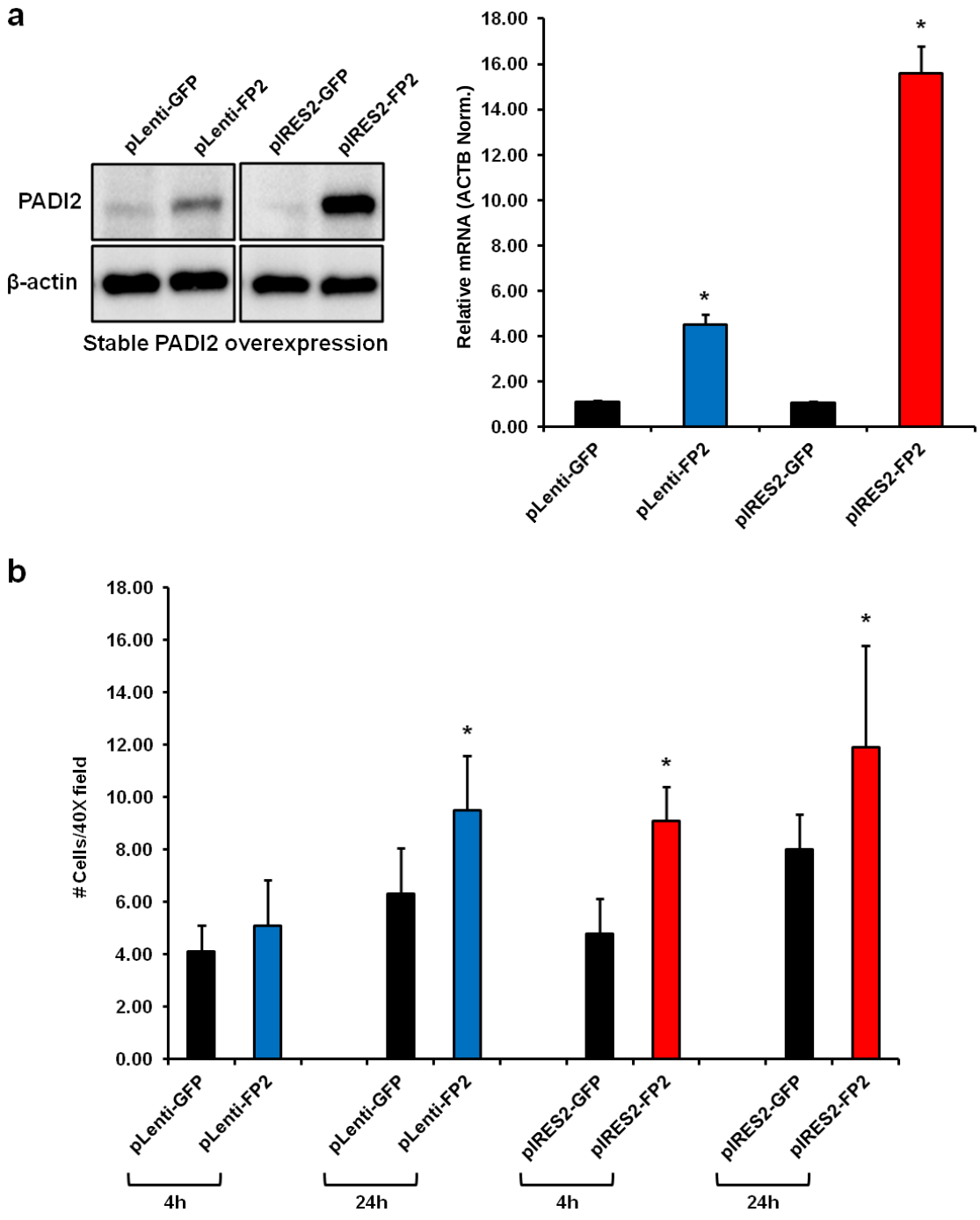
a
pLenti-GFP
pLenti-FP2
pIRES2-GFP
pIRES2-FP2
PADI2
β-actin
Stable PADI2 overexpression
Relative mRNA (ACTB Norm.)
18.00
16.00
14.00
12.00
10.00
8.00
6.00
4.00
2.00
0.00
*
*
pLenti-GFP
pLenti-FP2
pIRES2-GFP
pIRES2-FP2
b
Cells/40X field
18.00
16.00
14.00
12.00
10.00
8.00
6.00
4.00
2.00
0.00
*
*
*
pLenti-GFP
pLenti-FP2
pLenti-GFP
pLenti-FP2
pIRES2-GFP
pIRES2-FP2
pIRES2-GFP
pIRES2-FP2
4h
24h
4h
24h

immunofluorescence and confocal microscopy. Interestingly, we show that FLAG-PADI2 expression is predominantly nuclear in the stable A431-pIRES-FP2 cells (**Figure 4.13b**) compared to empty vector control cells (**Figure 4.13a**). Both the pLenti-FP2 and pIRES2-FP2 plasmids express GFP bicistronically via an internal ribosome entry site (IRES); therefore, we show that GFP in the pIRES2-FP2 stable cells is predominantly cytoplasmic (**Figure 4.13a, iii; and b, iii**), indicating different localization of the two overexpressed proteins (FLAG-PADI2 and GFP). Finally, we wanted to test the stable A431-pIRES2-FP2 cells for any increase in cellular malignancy. Assaying for focus formation, we show a significant increase in the FLAG-PADI2 overexpressing A431 cells compared to the empty vector control (**Figure 4.14a**). In addition, we show that the morphology of these cells also displays an elongated, fibroblast-like shape, indicative of cells that have undergone EMT (**Figure 4.14b**).

4.5 Discussion

In the present study, we have demonstrated that transgenic mice overexpressing PADI2 in the epidermis are sufficient to develop skin lesions that progress to invasive squamous cell carcinomas (SCC). Moreover, we have verified these results using the human squamous cell carcinoma cell line, A431, in which we stably overexpressed PADI2, resulting in the increased invasiveness and malignancy of these cells.

While *PADI2* transgenic expression in the mammary glands was detected, the MMTV-FLAG-PADI2 mice failed to develop any mammary tumors. Transgenic mice under control of the MMTV-LTR promoter can often have low expression in the mammary gland, or only noticeable expression in the mammary glands of lactating or multi-parous mice [27-29]. In addition, the MMTV promoter often becomes hypermethylated, and thus silenced [30]. While we have noted high expression in the

Figure 4.13: Co-localization of FLAG and GFP in A431 cells stably overexpressing FLAG-PADI2. (a) Confocal immunofluorescence analysis of the co-localization (iv) of FLAG (red, ii) and GFP (iii) in the nucleus and cytoplasm of A431 cells expressing the empty vector (pIRES2-GFP) or the FLAG-PADI2 expressing vector (b), which has bicistronic expression of both *PADI2* and *EGFP* (pIRES2-GFP-FLAG-PADI2). Note the nuclear expression of FLAG (*PADI2)*. Nuclei are stained with DAPI (blue, i).

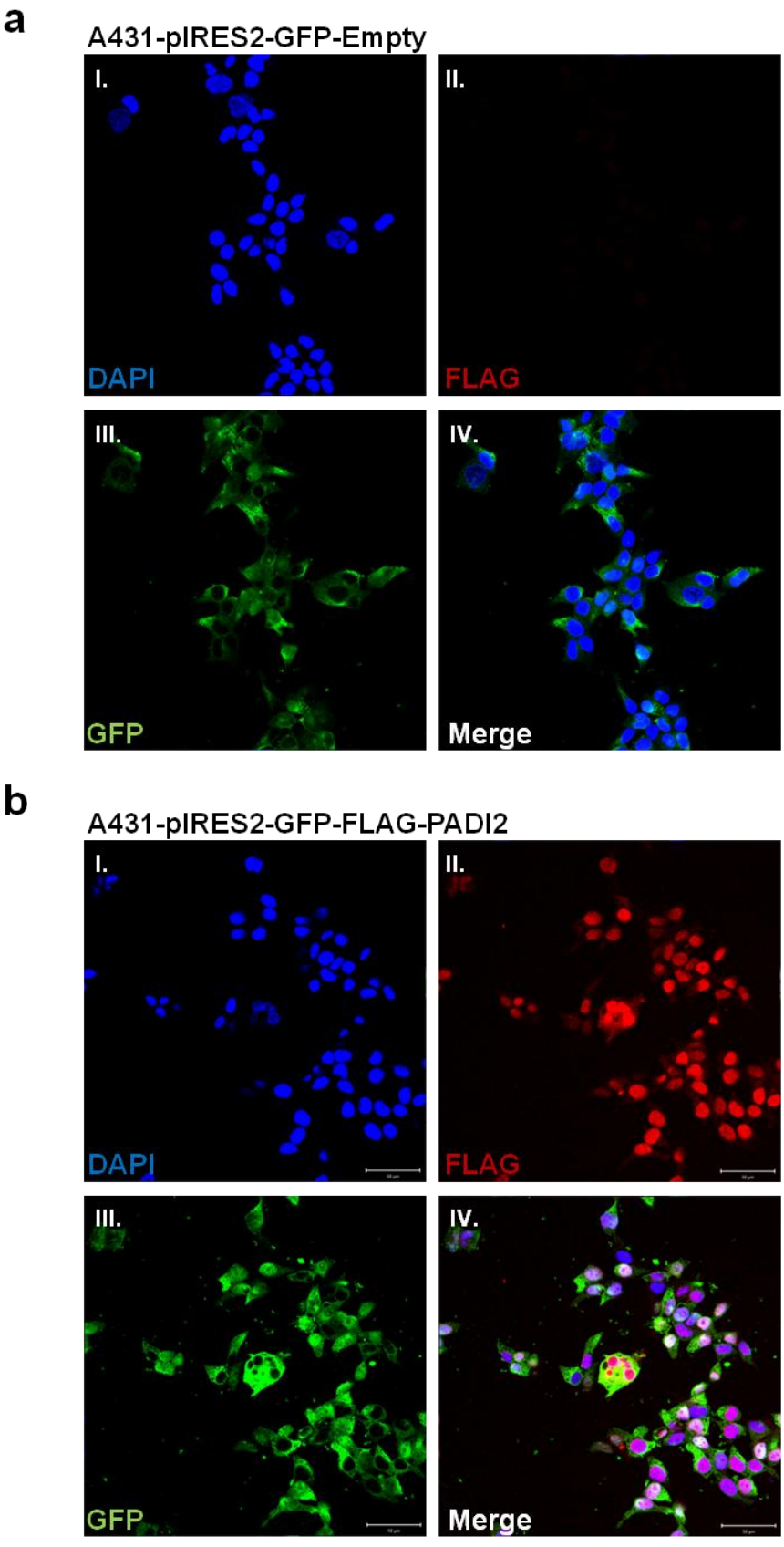
a
A431-pIRES2-GFP-Empty
I.
DAPI
II.
FLAG
III.
GFP
IV.
Merge
b
A431-pIRES2-GFP-FLAG-PADI2
I.
DAPI
II.
FLAG
III.
GFP
IV.
Merge

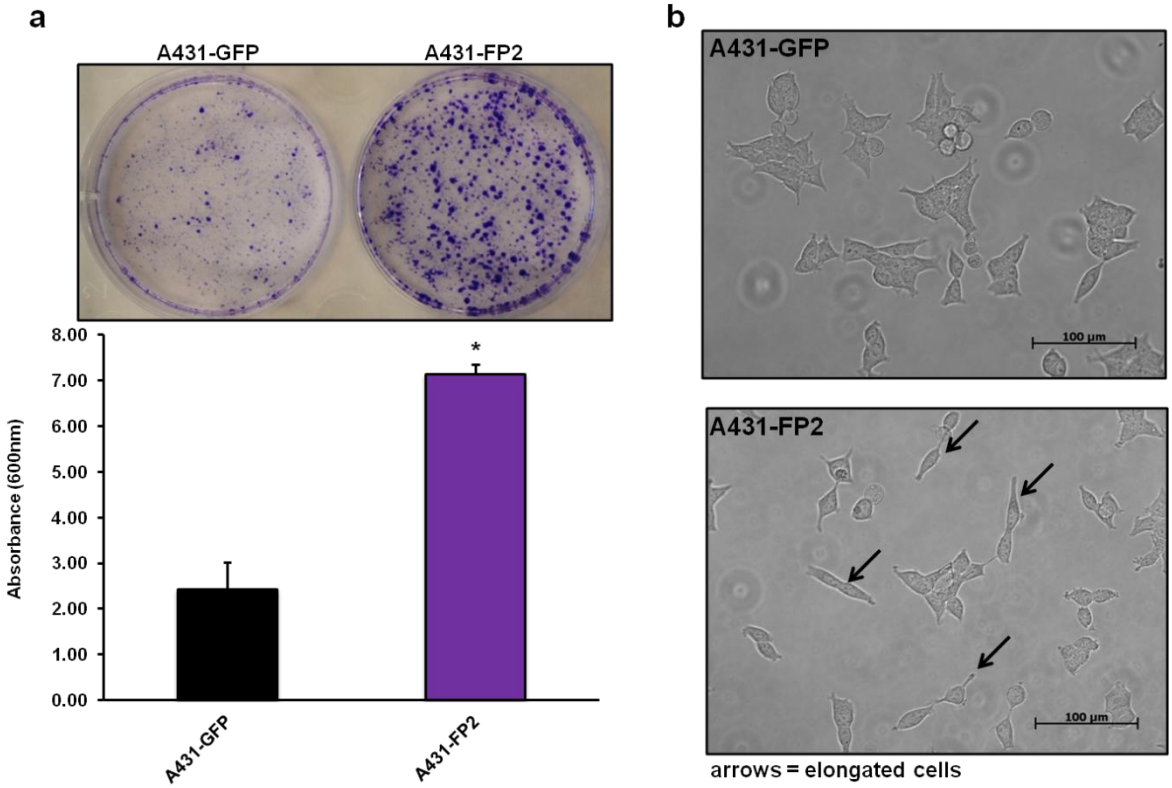

<u>Figure 4.14:</u> A431 skin cancer cells overexpressing FLAG-PADI2 show increased malignancy and EMT morphology. (a) Cells stably overexpressing FLAG-PADI2 (A431-FP2), or EGFP control (A431-GFP), were grown for 4d in a 6-well plate, fixed with 4% PFA, and stained with crystal violet for subsequent analysis of focus formation. After imaging, the crystal violet was removed from the cells with 10% acetic acid and absorbance levels were measured (600 nM). Data are expressed as the mean ± SD from three independent experiments (* $p < 0.05$). (b) Representative morphology of A431 cells overexpressing FLAG-PADI2, showing elongated cells with fibroblast-like shape, indicative of cells that have undergone EMT.

mammary glands of our transgenic mice, perhaps further analysis of transgenic *PADI2* expression over the life span of the mice might indicate age-related variation in expression. Future studies will examine the effectiveness of challenging our MMTV-FLAG-PADI2 mice, either genetically or chemically, to induce mammary carcinomas.

Recent research has shown that inflammation plays an important role in the development of advanced SCC tumors in mice [31]. As mentioned previously, numerous studies have documented a role for PADI-mediated citrullination in immune diseases characterized by inflammation. In addition, we recently identified a new role for PADI2 in inflammation, as we found that PADI2-mediated histone tail hypercitrullination is important during macrophage extracellular trap (MET) formation in inflamed tissues [32, 33]. Increasing evidence supports a pro-tumorigenic role for immune cells and inflammatory processes, with tumor-promoting inflammation recently defined as an emerging hallmark of cancer [34, 35]. Many inflammatory mediators, including cytokines and chemokines, are important for the growth and proliferation of pre-malignant cells [36]. These mediators often activate oncogenic transcription factors, such as NFκB and STAT3 [37-39]. PADI2 has been shown to regulate cytokine signaling in macrophages via citrullination of IKKγ, which controls NFκB expression activity [40]. Furthermore, PADI2 has also been shown to citrullinate CXCL8 (IL8) [41], again suggesting a role for regulating the inflammatory microenvironment of the cancer microenvironment.

We show here that *Il6* and *Il8* expression is increased in the skin lesions of MMTV-FLAG-PADI2 transgenic mice. These results were also confirmed using the A431 cell line overexpressing FLAG-PADI2. Both IL6 and IL8 have been shown to be important in the progression of cancer, having a critical role in tumor growth, angiogenesis, and EMT [42-51]. Further work is needed to identify exactly how PADI2 regulates the expression of these two inflammatory mediators.

Lastly, we show that, in addition to increased *Il6* and *Il8* expression, skin lesions in the MMTV-FLAG-PADI2 mice also display increased markers of invasiveness and EMT. Furthermore, the A431 cells overexpressing FLAG-PADI2 show increased invasion through a collagen matrix when compared to control transfected cells. Cells undergoing EMT are often at the leading edge of invasive tumors that are epithelial in origin. EMT is an important process during normal development by which epithelial cells acquire mesenchymal, fibroblast-like properties, and show reduced intercellular adhesion and increased motility. Several oncogenic pathways have been implicated in EMT, including Src, Ras, Ets, Wnt/β-catenin, as well as signaling downstream from the PI3K-AKT-axis resulting from IGF1, TGFβ, EGFR, and HER2 activation [52, 53]. Recently, studies have suggested a variety of epigenetic mechanisms may also play a role in EMT [54]. Interestingly, we have recently reported on a role for PADI4 in the progression of breast cancer and EMT, via the citrullination of GSK3β, which is known to regulate TGFβ [55]. Stadler et al. establish that PADI4 serves as a tumor suppressor, with dysregulation of PADI4-mediated citrullination of nuclear GSKβ activating TGFβ signaling, thereby inducing EMT in breast cancer cells and the production of more invasive tumors *in vivo*. Interestingly, the two representative skin lesions from MMTV-FLAG-PADI2 mice, which express the highest levels of transgenic *PADI2*, have markedly reduced levels of endogenous *Padi4*. Perhaps this indicates cross-talk between *PADI2* and *Padi4*, working in opposite fashion to promote tumorigenesis and invasiveness in tumors. Nevertheless, the critical molecular feature of EMT is the downregulation of E-cadherin, a cell adhesion molecule present in the plasma membrane of most normal epithelial cells. This is the earliest event in EMT; however, as the cell progresses from epithelial-like to mesenchymal-like cells, they are often accompanied by the increased expression of Snail1 (*Snai1*) and the intermediate filament vimentin. We show here that *Snail1* is

upregulated in the skin lesions of MMTV-FLAG-PADI2 mice, E-cadherin is reduced, and that vimentin levels increase, all indicative of EMT. This molecular evidence matches well with the invasive histology of the lesions, as we report that a subset of lesions advance to highly invasive squamous cell carcinomas. Snail expression is inversely correlated with E-cadherin expression, and has been shown to bind to E-boxes in the promoter of E-cadherin, directly repressing gene expression via various mechanisms [56, 57]. The most established method of repression is via the recruitment of HDAC containing complexes to the E-cadherin promoter, such as the Sin3A/HDAC1/HDAC2 complex [58]. We have already shown that PADI2 can function as an epigenetic regulator of genes in breast cancer cells [11]; however, further work is needed to characterize the mechanism behind PADI2 regulation of genes involved in both inflammation and EMT.

Conclusions

These tumors express high levels of transgenic human *PADI2* and display markers of increased invasiveness (i.e. EMT). Furthermore, a subset of these tumors shows the hallmarks of malignant progression from skin lesions to highly invasive squamous cell carcinomas. We have also replicated these results in the human squamous cell carcinoma cell line, A431. Collectively, these studies provide functional and mechanistic evidence establishing PADI2 as a potential novel oncogene in the progression of epidermal carcinomas.

Acknowledgements/Contributions

Thanks to: Dr. Sunish Mohanan for help with the IHC/IF experiments, invasion assay, and pathological analysis (Figs. 4.3, 4.4b, 4.5, 4.6, 4.7); and Sachi Horibata for help with the anchorage-independent growth and focus formation assays (Fig 4.14).

Table 4.1: Primers for Semi-quantitative RT-PCR

Primer Name	Sequence	Amplicon
mPADI4-gDNA-F	CCCACCCTGTGTGAGTTCTT	395bp
mPADI4-gDNA-R	GCCCAGAGCTTCATGTCTTC	
hPADI2-cds-F	ATTGAGATCTCCCTGGATGTG	194bp
hPADI2-cds-R	TCCTTGAGATCTTCCTTGCTG	
mPADI1-cds-F	CGTCTATAGTGATGTGCCCA	219bp
mPADI1-cds-R	CTCCTGTGACTCAAAGTATGAC	
mPADI2-cds-F	CAAGATCCTGTCCAATGAGAG	189bp
mPADI2-cds-R	ATCATGTTCACCATGTTAGGGA	
mPADI3-cds-F	GATTCTTAACAACCAGAGCCT	183bp
mPADI3-cds-R	CAGCATATTCACCAAGTCGG	
mPADI4-cds-F	CTACTCTGACCAAGAAAGCC	193bp
mPADI4-cds-R	ATTTGGACCCATAACTCGCT	
mGAPDH-cds-F	GGGCATCTTGGGCTACAC	209bp
mGAPDH-cds-R	GGTCCAGGGTTTCTTACTCC	

Table 4.3: Primers for mouse quantitative RT-PCR (SYBR)

Primer Name	Sequence
mECAD-F	ATCCTCGCCCTGCTGATT
mECAD-R	ACCACCGTTCTCCTCCGTA
mVIM-F	TGCGCCAGCAGTATGAAA
mVIM-R	GCCTCAGAGAGGTCAGCAAA
mSNAIL-F	CTTGTGTCTGCACGACCTGT
mSNAIL-R	CAGGAGAATGGCTTCTCACC
mCOX2-F	GATGCTCTTCCGAGCTGTG
mCOX2-R	GGATTGGAACAGCAAGGATTT
mGSK3B-F	TCCTTATCCCTCCACATGCT
mGSK3B-R	CCACGGTCTCCAGCATTAGT
mIL6-F	GCTACCAAACTGGATATAATCAGGA
mIL6-R	CCAGGTAGCTATGGTACTCCAGAA
mIL8-F	TGCTCAAGGCTGGTCCAT
mIL8-R	GACATCGTAGCTCTTGAGTGTCA
mKI67-F	CAAGAGGAAGTCTCTTGGCACT
mKI67-R	ACTCTTGTTTCCCTGGAGACTG
mPADI1-F	ATGACCCCCAACACTCAGC
mPADI1-R	CGGCCGTGGATATCTGTC
mPADI2-F	GATCCTCATCGGAAGCAGTT
mPADI2-R	AGTCGCGTACCACCTTGG
mPADI3-F	CCCCTAGCAATGACCTCAAC
mPADI3-R	ATAGGCCAGGGGCAAATG
mPADI4-F	TGACCCTACAGGTGAAAGCA
mPADI4-R	GGGTCCATAGTATGAAACTCGAA
mACTB-F	CTAAGGCCAACCGTGAAAAG
mACTB-R	ACCAGAGGCATACAGGGACA

Table 4.4: Primers for human quantitative RT-PCR (SYBR)

Primer Name	Sequence
hPADI2-F	TCTCAGGCCTGGTCTCCAT
hPADI2-R	AAGATGGGAGTCAGGGGAAT
hECAD-F	TGGAGGAATTCTTGCTTTGC
hECAD-R	CGCTCTCCTCCGAAGAAAC
hVIM-F	GGCTCGTCACCTTCGTGAAT
hVIM-R	GAGAAATCCTGCTCTCCTCGC
hGSK3β-F	GACATTTCACCTCAGGAGTGC
hGSK3β-R	GTTAGTCGGGCAGTTGGTGT
hSNAIL-F	GCTGCAGGACTCTAATCCAGA
hSNAIL-R	ATCTCCGGAGGTGGGATG
hSLUG-F	TGGTTGCTTCAAGGACACAT
hSLUG-R	GCAAATGCTCTGTTGCAGTG
hNFκB-F	CTGGCAGCTCTTCTCAAAGC
hNFκB-R	TCCAGGTCATAGAGAGGCTCA
hRELA-F	ACCGCTGCATCCACAGTT
hRELA-R	GATGCGCTGACTGATAGCC
hCOX2-F	GCTTTATGCTGAAGCCCTATGA
hCOX2-R	TCCAACTCTGCAGACATTTCC
hIL6-F	GCCCTGAGAAAGGAGACATGTAA
hIL6-R	TTGTTTTCTGCCAGTGCCTC
hIL8-F	ACTGAGAGTGATTGAGAGTGGAC
hIL8-R	AACCCTCTGCACCCAGTTTTC
hCCND1-F	GAAGATCGTCGCCACCTG
hCCND1-R	GACCTCCTCCTCGCACTTCT
hKI67-F	TTACAAGACTCGGTCCCTGAA
hKI67-R	TTGCTGTTCTGCCTCAGTCTT
hMYC-F	CACCAGCAGCGACTCTGA
hMYC-R	GATCCAGACTCTGACCTTTTGC
hHRAS-F	GGACGAATACGACCCCACTAT
hHRAS-R	TGTCCAACAGGCACGTCTC
hACTB-F	CCAACCGCGAGAAGATGA
hACTB-R	CCAGAGGCGTACAGGGATAG

4.6 References

1. Vossenaar, E.R., Zendman, A.J., van Venrooij, W.J. & Pruijn, G.J. PAD, a growing family of citrullinating enzymes: genes, features and involvement in disease. *Bioessays* **25**, 1106-18 (2003).

2. Balandraud, N. et al. A rigorous method for multigenic families' functional annotation: the peptidyl arginine deiminase (PADs) proteins family example. *BMC genomics* **6**, 153 (2005).

3. Chumanevich, A.A. et al. Suppression of colitis in mice by Cl-amidine: a novel peptidylarginine deiminase inhibitor. *American journal of physiology. Gastrointestinal and liver physiology* **300**, G929-38 (2011).

4. Lange, S. et al. Protein deiminases: New players in the developmentally regulated loss of neural regenerative ability. *Developmental biology* (2011).

5. Willis, V.C. et al. N-alpha-benzoyl-N5-(2-chloro-1-iminoethyl)-L-ornithine amide, a protein arginine deiminase inhibitor, reduces the severity of murine collagen-induced arthritis. *J Immunol* **186**, 4396-404 (2011).

6. Yao, H. et al. Histone Arg modifications and p53 regulate the expression of OKL38, a mediator of apoptosis. *J Biol Chem* **283**, 20060-8 (2008).

7. Li, P. et al. Coordination of PAD4 and HDAC2 in the regulation of p53-target gene expression. *Oncogene* **29**, 3153-62 (2010).

8. Tanikawa, C. et al. Regulation of protein Citrullination through p53/PADI4 network in DNA damage response. *Cancer Res* **69**, 8761-9 (2009).

9. Cherrington, B.D., Morency, E., Struble, A.M., Coonrod, S.a. & Wakshlag, J.J. Potential role for peptidylarginine deiminase 2 (PAD2) in citrullination of canine mammary epithelial cell histones. *PloS one* **5**, e11768 (2010).

10. Cherrington, B.D. et al. Potential Role for PAD2 in Gene Regulation in Breast Cancer Cells. *PLoS One* **7**, e41242 (2012).

11. Zhang, X. et al. Peptidylarginine deiminase 2-catalyzed histone H3 arginine 26 citrullination facilitates estrogen receptor alpha target gene activation. *Proc Natl Acad Sci U S A* **109**, 13331-6 (2012).

12. Zhang, X. et al. Genome-Wide Analysis Reveals PADI4 Cooperates with Elk-1 to Activate c-Fos Expression in Breast Cancer Cells. *PLoS genetics* **7**, e1002112 (2011).

13. Hennighausen, L., Wall, R.J., Tillmann, U., Li, M. & Furth, P.A. Conditional gene expression in secretory tissues and skin of transgenic mice using the MMTV-LTR and the tetracycline responsive system. *J Cell Biochem* **59**, 463-72 (1995).

14. Wagner, K.U. et al. Spatial and temporal expression of the Cre gene under the control of the MMTV-LTR in different lines of transgenic mice. *Transgenic research* **10**, 545-53 (2001).

15. Méchin, M.-C. et al. Deimination is regulated at multiple levels including auto-deimination of peptidylarginine deiminases. *Cellular and molecular life sciences : CMLS* **67**, 1491-503 (2010).

16. Kanno, T. et al. Human peptidylarginine deiminase type III: molecular cloning and nucleotide sequence of the cDNA, properties of the recombinant enzyme, and immunohistochemical localization in human skin. *J Invest Dermatol* **115**, 813-23 (2000).

17. Nishijyo, T., Kawada, A., Kanno, T., Shiraiwa, M. & Takahara, H. Isolation and molecular cloning of epidermal- and hair follicle-specific peptidylarginine deiminase (type III) from rat. *J Biochem* **121**, 868-75 (1997).

18. Akiyama, K. & Senshu, T. Dynamic aspects of protein deimination in developing mouse epidermis. *Exp Dermatol* **8**, 177-86 (1999).

19. Nakashima, K. et al. Molecular characterization of peptidylarginine deiminase in HL-60 cells induced by retinoic acid and 1alpha,25-dihydroxyvitamin D(3). *J Biol Chem* **274**, 27786-92 (1999).

20. Chavanas, S. et al. Peptidylarginine deiminases and deimination in biology and pathology: relevance to skin homeostasis. *J Dermatol Sci* **44**, 63-72 (2006).

21. Ishigami, A. et al. Human peptidylarginine deiminase type II: molecular cloning, gene organization, and expression in human skin. *Arch Biochem Biophys* **407**, 25-31 (2002).

22. Ornitz, D.M., Moreadith, R.W. & Leder, P. Binary system for regulating transgene expression in mice: targeting int-2 gene expression with yeast GAL4/UAS control elements. *Proceedings of the National Academy of Sciences of the United States of America* **88**, 698-702 (1991).

23. Campeau, E. et al. A versatile viral system for expression and depletion of proteins in mammalian cells. *PLoS One* **4**, e6529 (2009).

24. Livak, K.J. & Schmittgen, T.D. Analysis of relative gene expression data using real-time quantitative PCR and the 2(-Delta Delta C(T)) Method. *Methods* **25**, 402-8 (2001).

25. Boehnke, K., Falkowska-Hansen, B., Stark, H.J. & Boukamp, P. Stem cells of the human epidermis and their niche: composition and function in epidermal regeneration and carcinogenesis. *Carcinogenesis* **33**, 1247-58.

26. Liu, Y.L., Chiang, Y.H., Liu, G.Y. & Hung, H.C. Functional role of dimerization of human peptidylarginine deiminase 4 (PAD4). *PLoS One* **6**, e21314 (2011).

27. Vargo-Gogola, T. & Rosen, J.M. Modelling breast cancer: one size does not fit all. *Nat Rev Cancer* **7**, 659-72 (2007).

28. Blanco-Aparicio, C. et al. Mice expressing myrAKT1 in the mammary gland develop carcinogen-induced ER-positive mammary tumors that mimic human breast cancer. *Carcinogenesis* **28**, 584-94 (2007).

29. Yao, Y. et al. Increased susceptibility to carcinogen-induced mammary tumors in MMTV-Cdc25B transgenic mice. *Oncogene* **18**, 5159-66 (1999).

30. Zhou, H. et al. MMTV promoter hypomethylation is linked to spontaneous and MNU associated c-neu expression and mammary carcinogenesis in MMTV c-neu transgenic mice. *Oncogene* **20**, 6009-17 (2001).

31. Gasparoto, T.H. et al. Inflammatory events during murine squamous cell carcinoma development. *J Inflamm (Lond)* **9**, 46.

32. Mohanan, S., Horibata, S., McElwee, J.L., Dannenberg, A.J. & Coonrod, S.A. Identification of macrophage extracellular trap-like structures in mammary gland adipose tissue: a preliminary study. *Front Immunol* **4**, 67 (2013).

33. Wang, Y. et al. Histone hypercitrullination mediates chromatin decondensation and neutrophil extracellular trap formation. *J Cell Biol* **184**, 205-13 (2009).

34. Hanahan, D. & Weinberg, Robert A. Hallmarks of Cancer: The Next Generation. *Cell* **144**, 646-674 (2011).

35. Mantovani, A., Allavena, P., Sica, A. & Balkwill, F. Cancer-related inflammation. *Nature* **454**, 436-44 (2008).

36. Karin, M. & Greten, F.R. NF-kappaB: linking inflammation and immunity to cancer development and progression. *Nat Rev Immunol* **5**, 749-59 (2005).

37. Grivennikov, S.I. & Karin, M. Dangerous liaisons: STAT3 and NF-kappaB collaboration and crosstalk in cancer. *Cytokine Growth Factor Rev* **21**, 11-9 (2009).

38. Yu, H., Kortylewski, M. & Pardoll, D. Crosstalk between cancer and immune cells: role of STAT3 in the tumour microenvironment. *Nat Rev Immunol* **7**, 41-51 (2007).

39. Karin, M. Nuclear factor-kappaB in cancer development and progression. *Nature* **441**, 431-6 (2006).

40. Lee, H.J. et al. Peptidylarginine deiminase 2 suppresses inhibitory {kappa}B kinase activity in lipopolysaccharide-stimulated RAW 264.7 macrophages. *J Biol Chem* **285**, 39655-62 (2010).

41. Proost, P. et al. Citrullination of CXCL8 by peptidylarginine deiminase alters receptor usage, prevents proteolysis, and dampens tissue inflammation. *J Exp Med* **205**, 2085-97 (2008).

42. Ancrile, B., Lim, K.H. & Counter, C.M. Oncogenic Ras-induced secretion of IL6 is required for tumorigenesis. *Genes Dev* **21**, 1714-9 (2007).

43. Sparmann, A. & Bar-Sagi, D. Ras-induced interleukin-8 expression plays a critical role in tumor growth and angiogenesis. *Cancer Cell* **6**, 447-58 (2004).

44. Aceto, N. et al. Co-expression of HER2 and HER3 receptor tyrosine kinases enhances invasion of breast cells via stimulation of interleukin-8 autocrine secretion. *Breast Cancer Res* **14**, R131 (2012).

45. Fernando, R.I., Castillo, M.D., Litzinger, M., Hamilton, D.H. & Palena, C. IL-8 signaling plays a critical role in the epithelial-mesenchymal transition of human carcinoma cells. *Cancer Res* **71**, 5296-306 (2011).

46. Freund, A. et al. IL-8 expression and its possible relationship with estrogen-receptor-negative status of breast cancer cells. *Oncogene* **22**, 256-65 (2003).

47. Freund, A. et al. Mechanisms underlying differential expression of interleukin-8 in breast cancer cells. *Oncogene* **23**, 6105-14 (2004).

48. Hartman, Z.C. et al. Growth of triple-negative breast cancer cells relies upon coordinate autocrine expression of the proinflammatory cytokines IL-6 and IL-8. *Cancer Res* **73**, 3470-80 (2013).

49. Hartman, Z.C. et al. HER2 overexpression elicits a proinflammatory IL-6 autocrine signaling loop that is critical for tumorigenesis. *Cancer Res* **71**, 4380-91 (2011).

50. Korkaya, H. et al. Activation of an IL6 inflammatory loop mediates trastuzumab resistance in HER2+ breast cancer by expanding the cancer stem cell population. *Mol Cell* **47**, 570-84 (2012).

51. Iliopoulos, D., Hirsch, H.A. & Struhl, K. An epigenetic switch involving NF-kappaB, Lin28, Let-7 MicroRNA, and IL6 links inflammation to cell transformation. *Cell* **139**, 693-706 (2009).

52. Larue, L. & Bellacosa, A. Epithelial-mesenchymal transition in development and cancer: role of phosphatidylinositol 3' kinase/AKT pathways. *Oncogene* **24**, 7443-54 (2005).

53. Tse, J.C. & Kalluri, R. Mechanisms of metastasis: epithelial-to-mesenchymal transition and contribution of tumor microenvironment. *J Cell Biochem* **101**, 816-29 (2007).

54. Stadler, S.C. & Allis, C.D. Linking epithelial-to-mesenchymal-transition and epigenetic modifications. *Semin Cancer Biol* **22**, 404-10 (2012).

55. Stadler, S.C. et al. Dysregulation of PAD4-mediated citrullination of nuclear GSK3beta activates TGF-beta signaling and induces epithelial-to-mesenchymal transition in breast cancer cells. *Proc Natl Acad Sci U S A* **110**, 11851-6 (2013).

56. Hajra, K.M., Chen, D.Y. & Fearon, E.R. The SLUG zinc-finger protein represses E-cadherin in breast cancer. *Cancer Res* **62**, 1613-8 (2002).

57. Bolos, V. et al. The transcription factor Slug represses E-cadherin expression and induces epithelial to mesenchymal transitions: a comparison with Snail and E47 repressors. *J Cell Sci* **116**, 499-511 (2003).

58. Peinado, H., Olmeda, D. & Cano, A. Snail, Zeb and bHLH factors in tumour progression: an alliance against the epithelial phenotype? *Nat Rev Cancer* **7**, 415-28 (2007).

CHAPTER FIVE

DISCUSSION – SUMMARY AND FUTURE ROLE FOR PADI2 IN ONCOGENESIS

5.1 Summary of findings

At the onset of this project, little was known about the function of PADI2 during breast cancer progression and metastasis. While PADI2-mediated citrullination has been associated with various other diseases (**Chapter 1**), PADI4 was previously the only PADI family member with an established role in the development of cancer. The goal of this thesis research was to gain better insight into the potential role for PADI2 in the progression of breast cancer, elucidate the PADI2-mediated mechanisms during tumorigenesis, and validate PADI2 as a novel therapeutic target *in vitro* and *in vivo* using inhibitors of PADI-mediated activity (citrullination).

To meet the first goal, we used an *in vitro* model of breast cancer progression (MCF10AT) to provide us with evidence that PADI2 might be upregulated upon the malignant transformation of cells (**Chapter 2**). Following this, we turned to genomics based tools (RNA-seq) to allow us to gain a better perspective of PADI2 expression across a large set of breast cancer cells. The value of using global gene expression profiling to drive scientific hypotheses cannot be understated. Armed with subtype and full transcriptome data for all 57 breast cancer cell lines, we were able to identify that PADI2 is highly correlated with luminal (ER-positive) and HER2-positive breast cancers. Furthermore, we showed for the first time that PADI2 is potentially a novel target for cancer therapy using the PADI-inhibitor Cl-amidine both *in vitro* and *in vivo*.

These findings led to additional questions, mainly, what was the functional relationship between PADI2 and HER2 in breast cancer. Thus, in **Chapter 3**, we set out to explore whether PADI2 enhances HER2 expression or vice-versa. Interestingly, PADI2 appears to function both upstream and downstream of HER2, potentially indicating a role in an oncogenic positive-feedback loop with HER2. Previous evidence from our lab has shown that PADI2 can act as an ER co-activator via the

citrullination of H3R26, so we were curious to see if PADI2 regulates *HER2* expression using the same mechanism. Using both *PADI2* shRNA and PADI inhibitors, we showed that the reduction of PADI2, as well as the inhibition of PADI2-mediated citrullination of H3R26 (BB-Cl-amidine), leads to decreased expression of HER2. Conversely, HER2 regulation of *PADI2* gene expression is most likely downstream of PI3K signaling. Using inhibitors for both the MAPK or PI3K pathways, which are both downstream of HER2, we showed that PADI2 expression is reduced downstream of PI3K-AKT-mTOR signaling. Interestingly, we also noticed that using the PADI2 inhibitor BB-Cl-amidine, along with lapatinib, had synergistic inhibitory effects on the growth and malignant nature of tumor cells *in vitro*. Currently, PI3K-AKT and mTOR inhibitors are effective therapies for the treatment of breast cancer, but they are often plagued by acquired resistance through the upregulation of RTK activation (e.g. phosphorylation of HER2) via MAPK-ERK signaling [1]. Surprisingly, we showed that BB-Cl-amidine treatment can also lead to a reduction in phosphorylated MAPK (pMAPK), as well as pHER2; thus, relieving the RTK-activation seen when cells are treated with the mTOR inhibitor rapamycin. Taken together, these results suggest an enhanced role for PADI2 in HER2 expressing breast cancers, and that the PADI inhibitor, BB-Cl-amidine, represents a potential novel therapy for the treatment of patients with HER2-positive mammary tumors.

Lastly, we wanted to examine whether PADI2 was sufficient for tumorigenesis *in vivo*, so we decided to generate a transgenic model of human *PADI2* overexpression under control of the hormone-responsive MMTV-LTR promoter in FVB mice (**Chapter 4**). However, while *PADI2* transgenic expression in the mammary glands was detected, the MMTV-FLAG-PADI2 mice failed to develop any mammary tumors. While expression from the MMTV-LTR promoter is found predominantly in the mammary and salivary gland, other tissues have been implicated, including the skin

and ovaries [2, 3]. Surprisingly, we discovered that 20% of the mice developed skin lesions after five months. These tumors expressed high levels of transgenic human PADI2 and displayed markers of increased invasiveness (i.e. EMT). Furthermore, a subset of these tumors showed the hallmarks of malignant progression to highly invasive squamous cell carcinomas.

Collectively, these studies provide functional and mechanistic evidence establishing PADI2 as a potential novel oncogene and target for cancer therapy. However, there are still some unanswered questions regarding the molecular mechanisms behind this role. Specifically, how does PADI2-mediated citrullination of H3R26 lead to the increase of HER2 gene expression? Secondly, is there a role for PADI2 at the tumor-stroma interface, perhaps through the enhanced expression of markers of inflammation and invasion? Lastly, more work is needed to fully understand the role of PADI2 in tumorigenesis *in vivo*. While the MMTV-FLAG-PADI2 mouse model is promising, due to the spontaneous development of skin lesions in transgenic mice, we would like to investigate whether PADI2 enhances the development of tumors in oncogenically challenged mice. The following sections will outline several hypotheses and approaches to further explore these questions, beginning with our current working model of how PADI2 regulates HER2 expression.

5.2 Model for PADI2-mediated citrullination and regulation of HER2

Breast cancer is the second most common cancer in women in the US, with ~40,000 women dying from the disease each year. As covered in **chapter 1**, approximately 75% of breast cancers are ER-positive, with anywhere between 15-20% of breast cancers positive for HER2 amplification or overexpression [4]. Between ER and HER2, the majority of breast cancers express at least one or both of these markers. While there are drugs targeting both of these hormone receptors, about ~30% of patients with

ER-positive breast cancers fail to respond to treatments such as tamoxifen; in addition, the majority of those patients that do initially respond develop resistance over time [5]. Interestingly, the most commonly documented mechanism of resistance to tamoxifen occurs via EGFR and HER2 overexpression [6-8]. The same problem exists for patients with HER2-positive tumors, as greater than 60% of patients fail to respond to trastuzumab monotherapy, with initial responders developing resistance within 1 year [9, 10]. In addition, a significant portion of those patients treated with trastuzumab must discontinue treatment because of cardiotoxic side effects, owing to the role of HER2 receptor signaling in the heart [11]. This has highlighted the critical need to discover and validate novel targets for both ER- and HER2-positive tumors, so that additional treatments may be used in combination with, or in the place of, current therapies to overcome issues with *de novo* and acquired resistance.

Our previous work has established a role for PADI2 as an epigenetic regulator of ER-target gene expression in breast cancer cells, but our recent evidence, presented here, establishes a role for PADI2 in the expression of the HER2 oncogene. We show that PADI2 strongly binds the *HER2* proximal promoter (ETS region), in addition to the recently characterized ERE located downstream in intron 4 [12]. In the presence of the PADI inhibitor, BB-Cl-amidine, we see a dose-dependent reduction in HER2 protein and mRNA. We also see the reduction of HER2 protein and mRNA in cells that were stably transfected with shRNA for *PADI2*. Furthermore, there was also a concomitant reduction in the growth and malignant progression of these cells upon inhibition/knockdown of PADI2. It is interesting to speculate how PADI2 can function both as an ER and HER2 cofactor, especially with regard to mammary tumorigenesis. Previous evidence suggests that histone acetylation and phosphorylation play key roles in inducing HER2 expression [13], and we have previously shown that histone citrullination enhances histone acetylation and vice-versa [14]. Therefore, using what we

know about PADI2 as a co-activator of ER target genes, we can hypothesize that HER2 gene expression might work in the same fashion. Recent evidence from our lab using *in vitro* biochemical assays with bulk histones revealed that the H3Cit26 modification was found only on peptides that contained acetylated H3K27 (H3K27ac); thus, suggesting that H3K237ac enhances PADI2-mediated H3R26 citrullination [15]. ER is known to associate with a number of multi-protein complexes (see **Chapter 1**), including: heat shock proteins (HSPs) [16], steroid receptor co-activators (SRCs) [17], p300-containing co-activator complexes [18], and HDAC containing co-repressor complexes [19]. The p300 co-activator is known to have intrinsic histone acetyltransferase (HAT) activity, which helps to relax the chromatin structure at gene promoters, leading to gene activation. Studies have shown that p300 can function as an ER co-activator, and is required for acetylation at H3K27 [18]. This supports our hypothesis that ER uses p300-mediated H3K27 acetylation and PADI2-mediated H3R26 citrullination to promote chromatin decondensation, allowing for the binding of ER and associated co-factors (i.e. SRC or AIB1) to EREs and enhancing gene transcription (**Figure 5.1a**). Previous studies have shown that ER binds poorly to nucleosomal DNA *in vitro* [20]; based on this and additional studies [21, 22], we predict that this is due to H3 tail occluding ER binding to the ERE, due to electrostatic interactions with DNA (**Figure 5.1b**). Recent work has shown that p300 and H3K27ac are enriched at active enhancers and ER binding sites [23]. We predict that ER recruits p300 (HAT) to acetylate H3K27, which weakens the H3 tail-DNA binding, allowing for weak binding of ER to the ERE (**Figure 5.1c**). Based on our previous findings by Zhang et al., we suggest that ER then recruits PADI2 (**Figure 5.1d**), which subsequently citrullinates H3R26, further weakening the interaction and allowing for stable ER binding to nucleosomal ERE (**Figure 5.1e**). Future experiments in our lab

<u>Figure 5.1:</u> PADI2-mediated citrullination of histone H3 arginine 26 (H3R26) yields the citrulline modification (H3Cit26), which can have an effect on ER nucleosomal ERE binding. (a) Our working model predicts that acetylation of H3 lysine 27 (H3K27) by p300 promotes PADI2-mediated citrullination of H3R26; thus, weakening H3 tail-DNA interaction and allowing for binding of ER to nucleosomal EREs. (b) H3 tail (red) blocks the ER binding to ERE. (c) ER recruits HAT to acetylate (Ac) H3K27, partially weakening H3 tail-DNA binding. (d) ER then recruits PADI2 to citrullinate H3R26 (Cit), further weakening interaction and allowing for stable ER binding to nucleosomal ERE (e).

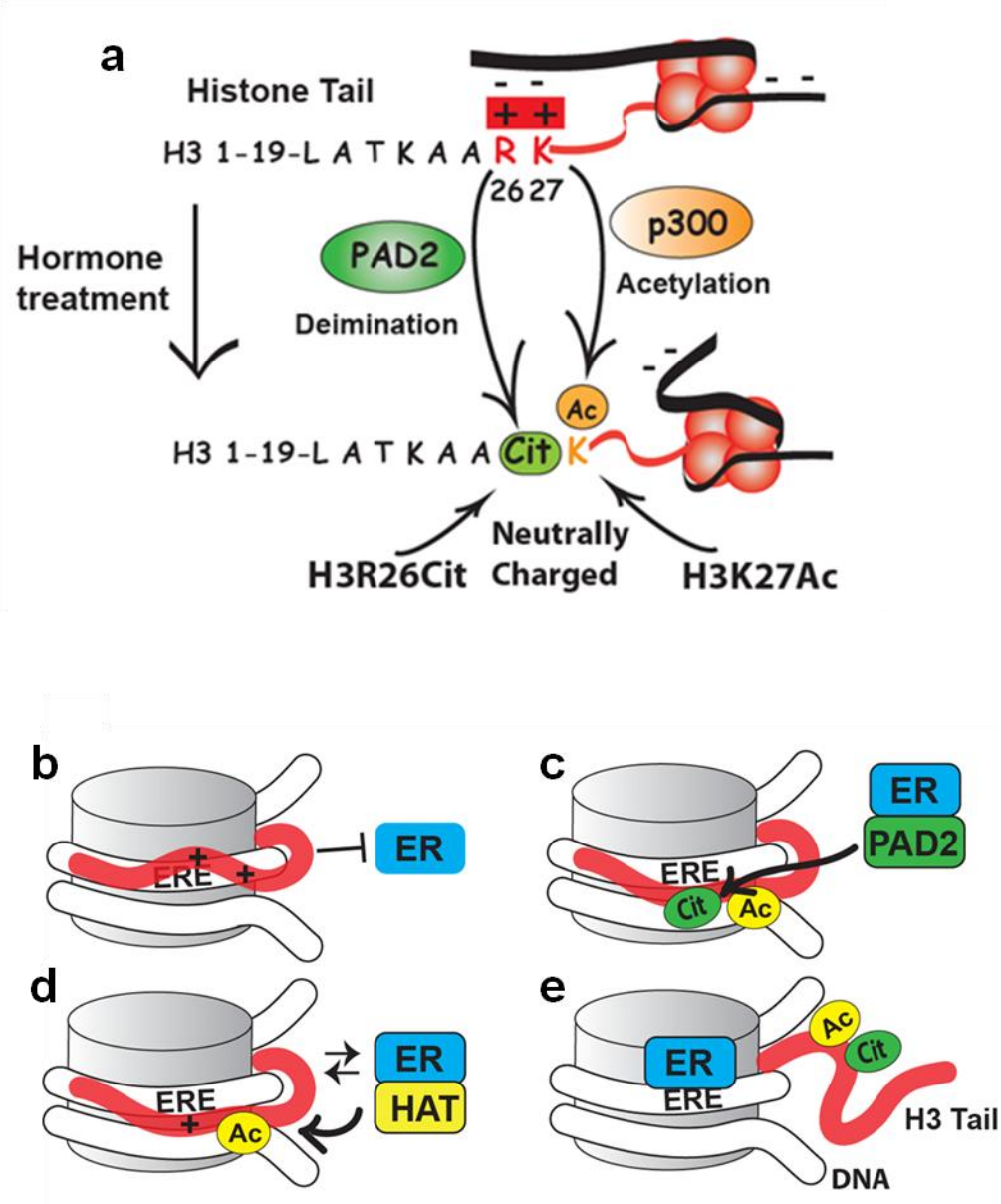
a
Histone Tail
H3 1-19-L A T K A A R K
26 27
Hormone treatment
PAD2
Deimination
p300
Acetylation
Ac
H3 1-19-L A T K A A Cit K
H3R26Cit
Neutrally Charged
H3K27Ac
b
ERE
ER
c
ER
PAD2
ERE
Cit
Ac
d
ERE
Ac
ER
HAT
e
ER
ERE
Ac
Cit
H3 Tail
DNA

will help to elucidate whether HER2 expression may be regulated by "cross-talk" between PADI2-catalyzed histone citrullination and histone acetylation and/or phosphorylation via similar mechanisms. To examine whether p300-mediated H3K27 acetylation is necessary for the H3Cit26 modification, we can perform estrogen (E2) stimulation experiments on MCF7 cells (and/or BT474 for HER2 studies) that have been stably transfected with shRNA targeting p300. Conversely, we can test whether we see an increase in H3Cit26 levels with H3R27ac by treating MCF7 cells with the HDAC inhibitor TSA, then measuring H3Cit26 levels in E2 stimulated cells versus control. As previously outlined, PADI2 can act as an ER co-activator via PADI-mediated citrullination of H3R26, leading to the upregulation of ER-target genes (**Figure 5.2a**). Similarly, we predict that either ER, or potentially other ER co-factors such as AIB1 or SRC1, will recruit PADI2 to the downstream ERE, thus promoting activation of HER2 via the citrullination of H3R26 (**Figure 5.2b**). We can assess the relative importance of these genes by first performing standard siRNA experiments, or potentially shRNA for stable cell lines. Preliminary evidence suggests that siRNA of ER reduces PADI2 expression, but whether this has any effect on HER2 expression or H3Cit26 levels remains to be investigated. Alternatively, PADI2 may activate HER2 expression by functioning as an ETS co-factor (e.g. PEA3), thereby enhancing HER2 transcription. PEA3 is a well-known ETS co-factor and transcriptional activator of HER2 [24, 25], and the primers used for detecting PADI2 at the *HER2* promoter are within the known PEA3 binding site.

We have shown conclusively using both molecular genetics (PADI2-KD) and pharmacological inhibition (BB-Cl-amidine), that the absence of PADI2 leads to decreased transcription of *HER2*, as well as downstream genes (**Figure 5.2c**). More work is needed to elucidate these mechanisms, including testing whether PADI2 overexpression can drive *HER2* expression using the *HER2* promoter luciferase-

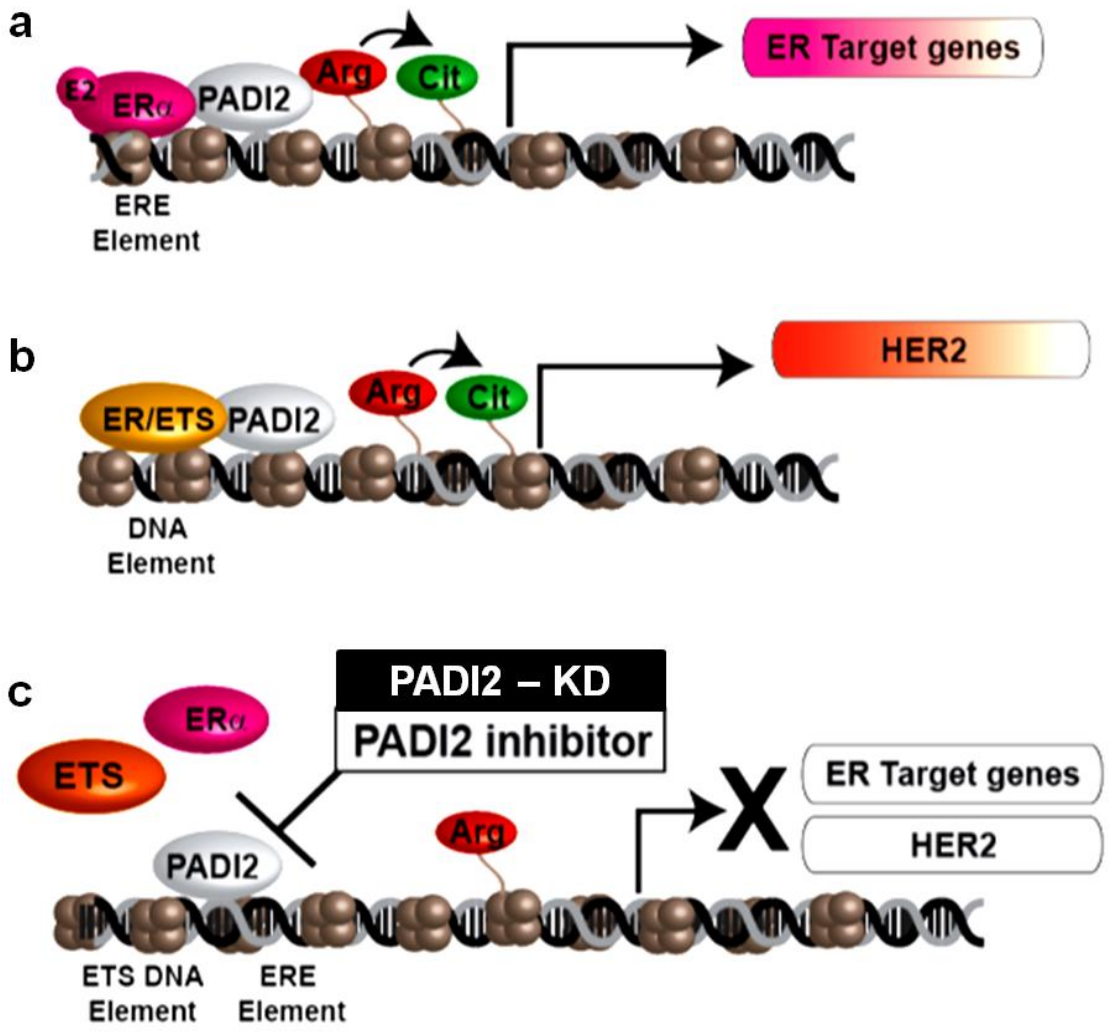

<u>Figure 5.2:</u> PADI2 appears to be a transcriptional co-activator of both ER target gene and *HER2* expression using the same mechanism. (a) PADI2-mediated citrullination of H3R26 leads to the upregulation of ER-target genes. (b) It is predicted that either ER or additional ETS factors (e.g. PEA3) will recruit PADI2 to known ETS binding elements on the *HER2* promoter, leading to H3Cit26 promoted acetylation and subsequent activation of *HER2* transcription. (c) Using both the genetic knockdown and pharmacological inhibition of PADI2, we have shown that the absence of PADI2 leads to decreased transcription of *HER2*, as well as downstream genes.

reporter plasmid (pNeuLite) [26]. This should help clarify whether PADI2 binding to the promoter is sufficient to drive *HER2* expression; however, previous evidence from studies of PEA3 indicates that these results might be contradictory [26]. In addition, it would be interesting to identify additional genes that might serve as co-regulators of the PADI2-HER2 oncogenic loop using genomics based approaches. Based on our results presented here, and previous links between PADI2 and inflammation, cytokines IL6 and IL8 are great candidates.

5.3 PADI2 involvement in inflammation and EMT

As mentioned previously, numerous studies have documented the role of PADIs and increased citrullination in immune diseases characterized by inflammation (**Chapter 1**). In addition, the PADI inhibitor Cl-amidine has also been shown to reduce the inflammatory symptoms in mouse models of colitis and RA [27]. Recently, a new link between PADIs and inflammation has been established, implicating a role for PADI4 and PADI2 in catalyzing histone tail hypercitrullination during NET formation and MET formation, respectively, in inflamed tissues [28, 29]. PADIs also play a role in the citrullination of various genes involved in inflammatory diseases; for example, the citrullination of vimentin has been shown to correlate with the proliferation of fibroblast-like synoviocytes (from patients with RA), thereby stimulating TNFα and IL1 production in these cells [30]. Interestingly, the citrullination of vimentin, in addition to promoting an inflammatory microenvironment, might also have implications in tumor cell migration. Increasing evidence supports a pro-tumorigenic role for immune cells and inflammatory processes, with tumor-promoting inflammation being defined as an emerging hallmark of cancer [31, 32]. Many inflammatory mediators (e.g. cytokines/chemokines) are important for the growth and proliferation of pre-malignant cells [33]. These mediators often activate oncogenic transcription factors, such as NFκB

and STAT3 [34-36]. Conversely, HER family signaling, and oncogenes such as Ras and Myc, can initiate an inflammatory response [32, 37-39]. Downstream signaling from these various pathways leads to the induction of an inflammatory loop; thus, setting the stage for further recruitment of factors involved in cancer cell survival, proliferation, invasiveness (EMT), and eventual metastasis (**Figure 5.3**). PADI family members have previously been shown to promote the inflammatory microenvironment, as PADI2 can regulate cytokine signaling in macrophages via citrullination of IKKγ, which controls NFκB expression activity [40]. Furthermore, PADI2 has also been shown to citrullinate CXCL8 (IL8) [41], again suggesting a role for regulating the inflammatory milieu of the cancer microenvironment.

We have shown using MMTV-FLAG-PADI2 mice that *Il6* and *Il8* expression are both increased in the skin lesions of mice. This relationship between PADI2-driven tumors and IL6-IL8 upregulation was confirmed in the squamous cell carcinoma cell line, A431, that was stably transfected with FLAG-tagged PADI2 (A431-FP2). Both IL6 and IL8 have been shown to be important in the progression of cancer, having a critical role in tumor growth, angiogenesis, and EMT [37-39, 42-48]. Further work is needed to identify exactly how PADI2 regulates the expression of these two inflammatory mediators. Future experiments will use ChIP to examine whether PADI2 binds to either gene's promoter; in addition, co-immunoprecipitation (Co-IP) will help examine whether there are any protein-protein interactions. Interestingly, while we see PADI2 upregulation increases *IL6* and *IL8* transcription in skin cancer, we see the opposite effect in breast cancer cells. The highly invasive MCF10DCIS cell line and the luminal B BT474 cell line show the upregulation of both *IL6* and *IL8* transcription when PADI2 is stably knocked-downed via shRNA. However, this effect is less pronounced (or lost) when cell lines were treated with BB-Cl-amidine. Since BB-Cl-amidine is a pan-PADI inhibitor, the targeting of additional PADIs might explain this

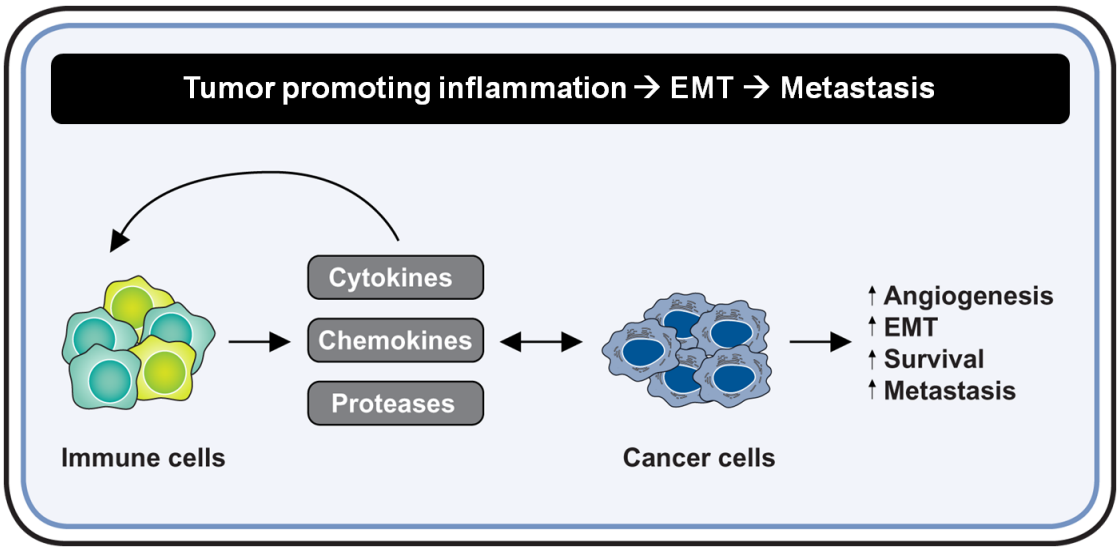

<u>Figure 5.3:</u> Tumor-promoting inflammation is an emerging hallmark of cancer. Inflammation may contribute to tumor initiation via the release of signaling molecules such as EGF, VEGF, and other proangiogenic factors. In addition, the production of cytokines and chemokines enhance the inflammatory state, which helps to facilitate cancer cell survival, proliferation, and invasiveness (via EMT). (Figure adapted from Genentech, via Grivennikov and Karin, *Current. Opinion. in Gen. & Dev*., 2010 [49])

discrepancy. Supporting this hypothesis, we see a 2-fold induction of *IL6* and *IL8* in BT474 cells upon BB-Cl-amidine treatment, which might be explained by the fact that this cell line predominantly expresses the PADI2 isozyme (data not shown). In contrast, MCF10DCIS cells, which also express *PADI1* and *PADI3* (data not shown), show a reduction in *IL6* and *IL8* when we treat with BB-Cl-amidine. Previous studies have shown that activation of inflammatory loops can occur upon treatment with drugs, as the development of trastuzumab resistance often occurs as a result of the concomitant upregulation of IL6. In addition, the tumor drug taxol (paclitaxel), which has also been shown to be a moderate PADI inhibitor [50], leads to the transcriptional activation of *IL8* in both human ovarian and lung carcinoma cell lines [51-53]. Interestingly, Lee et al. show that this increase in IL8 actually plays a role in reducing the rate of tumor growth *in vivo*, most likely mediated by increased neutrophil infiltration [54]. Further work is needed to elucidate the pathways involved in PADI2 regulation of *IL6* and *IL8* expression.

In the PADI2 overexpressing mice, we show that, in addition to increased *Il6* and *Il8* expression, transgenic skin lesions also display markers of invasiveness and EMT. Furthermore, A431-FP2 cells show increased invasion through a collagen matrix when compared to control transfected cells. Cells undergoing EMT are often at the leading edge of invasive tumors that are epithelial in origin. EMT is an important process during normal development by which epithelial cells acquire mesenchymal, fibroblast-like properties, and show reduced intercellular adhesion and increased motility (**Figure 5.4**). Several oncogenic pathways have been implicated in EMT, including Src, Ras, Ets, Wnt/β-catenin, as well as signaling downstream from the PI3K-AKT-axis resulting from IGF1, as well as TGFβ, EGFR, and HER2 activation [55, 56]. Recently, studies have suggested a variety of epigenetic mechanisms may also play a role in EMT [57]. Nevertheless, the critical molecular feature of EMT is the

Figure 5.4: Overview of epithelial to mesenchymal transition (EMT). Epithelial-to-mesenchymal transition (EMT) describes a series of molecular and morphologic changes that occur in epithelial cells. During EMT, normal polarized epithelial cells undergo a functional transition into more fibroblastic-like mobile/invasive mesenchymal cells. The common markers for each stage are listed. E-cadherin expression is usually the first to be downregulated during this transition, while Vimentin expression is upregulated. Snail and Slug, which bind to E-boxes in the promoter of E-cadherin leading to direct repression, are also upregulated. This process is usually accompanied by the loss/degradation of the basement membrane, allowing for distant site metastasis of tumor cells.

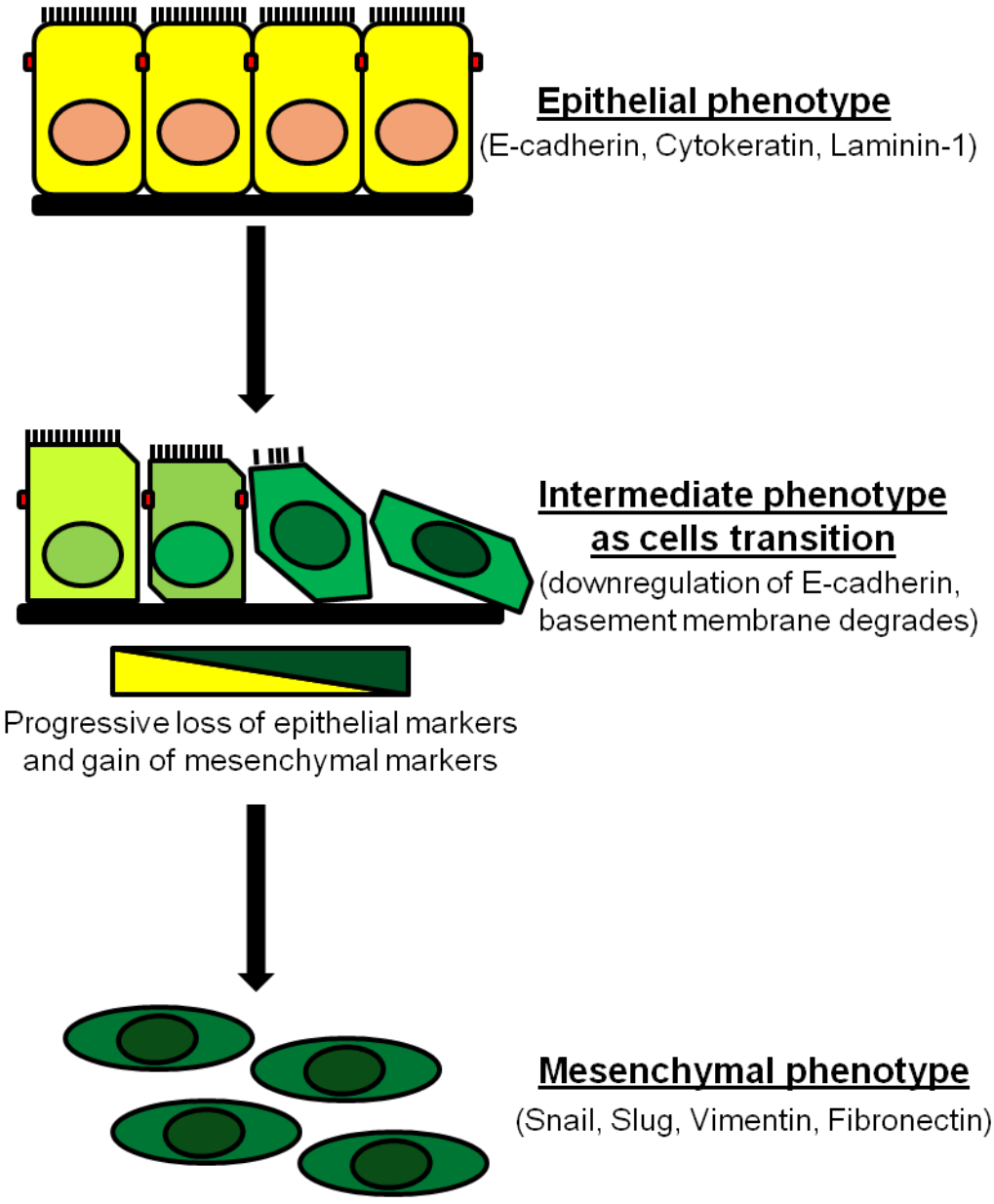
Epithelial phenotype
(E-cadherin, Cytokeratin, Laminin-1)
Intermediate phenotype
as cells transition
(downregulation of E-cadherin,
basement membrane degrades)
Progressive loss of epithelial markers
and gain of mesenchymal markers
Mesenchymal phenotype
(Snail, Slug, Vimentin, Fibronectin)

downregulation of E-cadherin, a cell adhesion molecular present in the plasma membrane of most normal epithelial cells. Reduced E-cadherin expression in breast cancer often correlates with poor differentiation, increased invasiveness, aggressive metastatic behavior, and an unfavorable prognosis [58-60]. This is the earliest event in EMT, though as the cell progresses from epithelial-like to mesenchymal-like cells, they are often accompanied by the increased expression of Snail1 (*Snai1*) and Snail2/Slug (*Slug*), the intermediate filament vimentin, and the eventual degradation of the basement membrane by proteases (MMPs) [61]. We show that *Snail1* is upregulated in the skin lesions of MMTV-FLAG-PADI2 mice, E-cadherin is reduced, and that vimentin levels increase, all indicative of EMT. This molecular evidence matches well with the invasive histology of the lesions, as some lesions advance to highly invasive squamous cell carcinomas. Snail and Slug are inversely correlated with E-cadherin expression, as both have been shown to bind to E-boxes in the promoter of E-cadherin, directly repressing gene expression via various mechanisms [62, 63]. The most established method of repression is via the recruitment of HDAC containing complexes to the E-cadherin promoter, such as the Sin3A/HDAC1/HDAC2 complex [64]. Further work will be needed to characterize the mechanism that PADI2 regulates EMT. The first experiment should look at whether PADI2 directly binds the E-cadherin promoter to regulate transcription, in addition to looking at both Snail and Slug. The stable A431-FLAG-PADI2 (A431-FP2) cell line could be effectively used to analyze chromatin binding of PADI2, as well as H3Cit26, to see whether potential gene regulation occurs via the same mechanism as *HER2* and ER-target genes. In addition, it would be interesting to evaluate the transcriptomic differences between these two cell lines, to gain a better idea of what genes are involved in PADI2-mediated oncogenesis. With regard to PADI2 overexpression in breast cancer, various animal models could be used to analyze what effect PADI2 has on the invasiveness of

tumors *in vivo*. Stadler et al. have shown that *PADI4* knockdown in xenografted MCF7 breast cancer cells leads to an increase in tumor invasiveness and associated EMT markers via the citrullination of GSK3β, which subsequently activates TGFβ signaling. Alternatively, we could use the MCF10DCIS cells, which are known to recapitulate invasive comedo-DCIS cancers when xenografted into nude mice. Preliminary evidence shows that when we knockdown *PADI2*, E-cadherin is upregulated and cellular migration is decreased in MCF10DCIS cells. Again, this suggests a direct relationship between PADI2 and E-cadherin expression. The xenografted MCF10DCIS tumors would provide a valuable model to further investigate this relationship. It would also be of interest to cross our MMTV-FLAG-PADI2 mice, in addition to our recently acquired PADI2$^{-/-}$ mice, to known mouse models of breast cancer (e.g. MMTV-neu) to see whether these tumors show increased/decreased invasiveness based on PADI2 gene dosage. While the MMTV-FLAG-PADI2 mouse model is imperfect, genetic crosses might prove valuable in delineating a role for PADI2 in the progression of cancer.

5.4 Reflections on PADI2 transgenic mouse – can it be improved?

Genetic crosses can help to bring out phenotypes in transgenic mice that might not have been evident during the initial evaluation. However, generating double transgenic mice is both time consuming and expensive. The simplest method of evaluating modifying factors (i.e. your transgene of interest) in the study of molecular carcinogenesis is via chemical carcinogenesis. Mammary tumors in rodents can be produced following the administration of DMBA (7,12-dimethylbenz[a]anthracene) by oral gavage, which usually results in the activation of oncogenes, most frequently hRas [65, 66]. Other genes have been shown to be upregulated upon treatment with DMBA, including the aryl hydrocarbon receptor (AhR), as well as cyclin D1 and c-

Myc, and hyperphosphorylated pRb [67]. Transgenic mice under control of the MMTV-LTR promoter can often have low expression in the mammary gland, or only noticeable expression in the mammary glands of lactating or multi-parous mice [68-70]. Another study has suggested that this is due to the MMTV promoter often becoming hypermethylated, and thus silenced [71]. Interestingly, this study employed the chemical carcinogen normally used for generating mammary carcinomas in rats, NMU (N-methyl-N-nitrosourea), to generate tumors in the MMTV-neu (unactivated) mouse. Since global hypomethylation is a normal event found in the early stage of breast cancer development [72], it is possible this result was a "side-effect" of using the chemical carcinogen. However, this reinforces the value of chemical carcinogens in the promotion of tumors in genetically modified mouse models lacking an observable phenotype. We have currently started the DMBA treatment of MMTV-FLAG-PADI2 mice via oral gavage using the experimental design detailed in **Table 5.1**. Preliminary results look promising; however, more time is needed to determine whether the transgenic mice have any increase in tumor burden or latency, or any change in morphology (e.g. increased clinically invasive features).

Research has shown that squamous cell carcinomas (SCCs), which are responsible for the majority of non-melanoma skin cancer related deaths, are the result of accumulating genetic alterations [73]. Understanding the role these genetic lesions play in the etiology of skin cancer is essential for designing improved therapies for cancer treatment and prevention. This is where the full potential of our MMTV-FLAG-PADI2 mice, within which a subset of skin lesions develops to SCC, can be realized. However, the current problem is that only 20% of our mice show the phenotype of skin lesions, and only a proportion of those develop to fully invasive SCCs. The need to examine these tumors on an alternative background, whether genetic or chemically manipulated, cannot be understated. More than 50% of human

cutaneous SCCs carry mutations in the p53 gene, most of which are missense mutations resulting in the change of a single amino acid and expression of altered forms of p53 [74]. Transgenic mice with this mutant p53 allele have been shown to develop normally, without any obvious epidermal phenotype or development of spontaneous tumors. However, these mice demonstrate an increased susceptibility to the two-stage chemical carcinogenesis protocol, with both an increase in the rate and number of papillomas compared to wild-type controls [75]. Since it is likely that the MMTV-FLAG-PADI2 mice need additional mutations to promote oncogenesis, crossbreeding experiments with mice such as the p53 mutant, or potentially mutant hRas and/or kRas mice, would offer a unique opportunity to test this hypothesis. Several mouse models have previously documented that overexpression of oncogenic hRas or kRas in the skin can induce tumor formation [76-80]. The Ras oncogene is also often mutated in SCCs (10%–30% of human skin SCCs) [80, 81], and as previously mentioned, activating Ras mutations can be induced by DMBA, which is the initiating event of the two-step chemical carcinogenesis protocol. Mice subjected to chemical carcinogenesis protocols by initiation with DMBA and tumor promotion with 12-*O*-tetradecanoylphorbol-13-acetate (TPA) develop skin tumors that exhibit hRas mutations in more than 90% of the cases [82, 83]. Our MMTV-FLAG-PADI2 mice are on the FVB background, which is known to be highly sensitive to chemical induction with DMBA [84]. A description of the general protocol can be found in **Table 5.1**, while an overview of the procedure and expected results is detailed in **Figure 5.5**. Briefly, the initiation stage occurs with the chemical carcinogen DMBA, which is applied topically to the mice. The hRas gene is the primary target of DMBA, with activating mutations (A182T transversion in codon 61 of the *HRAS1* gene), detectable in mice as early as 3-4 weeks [85, 86]. About 1-2 weeks after the initiation stage, the mutated cells are promoted with TPA to clonally expand the mutated cells. The topical application

Table 5.1: Challenge of MMTV-FLAG-PADI2 mice with DMBA or DMBA/TPA

Experimental Groups	Wild type and PADI2-Tg mice (n=20); Wild type and PADI2-KO mice (n=20); Vehicle control (n=10).
Method	Mammary tumorigenesis – DMBA Oral gavage (1 mg/wk. for 6 weeks), Tumors arise in 15-18 wks. after first treatment. (DMBA = 7,12-dimethylbenz[a]anthracene) Cutaneous tumorigenesis – DMBA/TPA treatment (DMBA - 200 nmol over 3X3 mm shaved area; TPA – 7 days post DMBA, 17 nmol, 3 times a week for 20 weeks).
Evaluation	Number of tumors developed (e.g. # papillomas from DMBA/TPA), size, histopathology features.
Expected Results	PADI2 transgenic mice will develop a higher tumor load with more invasive clinical features.

Figure 5.5: Two-stage model of skin carcinogenesis in mice. Initiation occurs with the topical application of a sub-carcinogenic dose of a mutagenic agent, in this case DMBA (7,12-dimethylbenz[a]anthracene). DMBA has been shown to induce mutations in target genes in keratinocyte stem cells (e.g. hRas and kRas). Following initiation (generally 1-2 weeks after), repeated topical application of a tumor promoting agent, such as the phorbol ester, 12-*O*-tetradecanoylphorbol-13-acetate (TPA) continue weekly (2-3X) until the end of the study, which is usually anywhere between 20-50 weeks after initiation. Papillomas begin to arise ~6-12 weeks of promotion with TPA, with a subset advancing to squamous cell carcinomas (SCC) after ~20 weeks. Representative H&E stained sections of normal and hyperplastic skin, a papilloma, and SCC. The two-stage skin carcinogenesis protocol allows for the evaluation of genes (e.g. PADI2) and cell-signaling pathways involved in the progression of tumors. (Figure obtained from Abel et al., *Nat. Protocols*, 2009 [87])

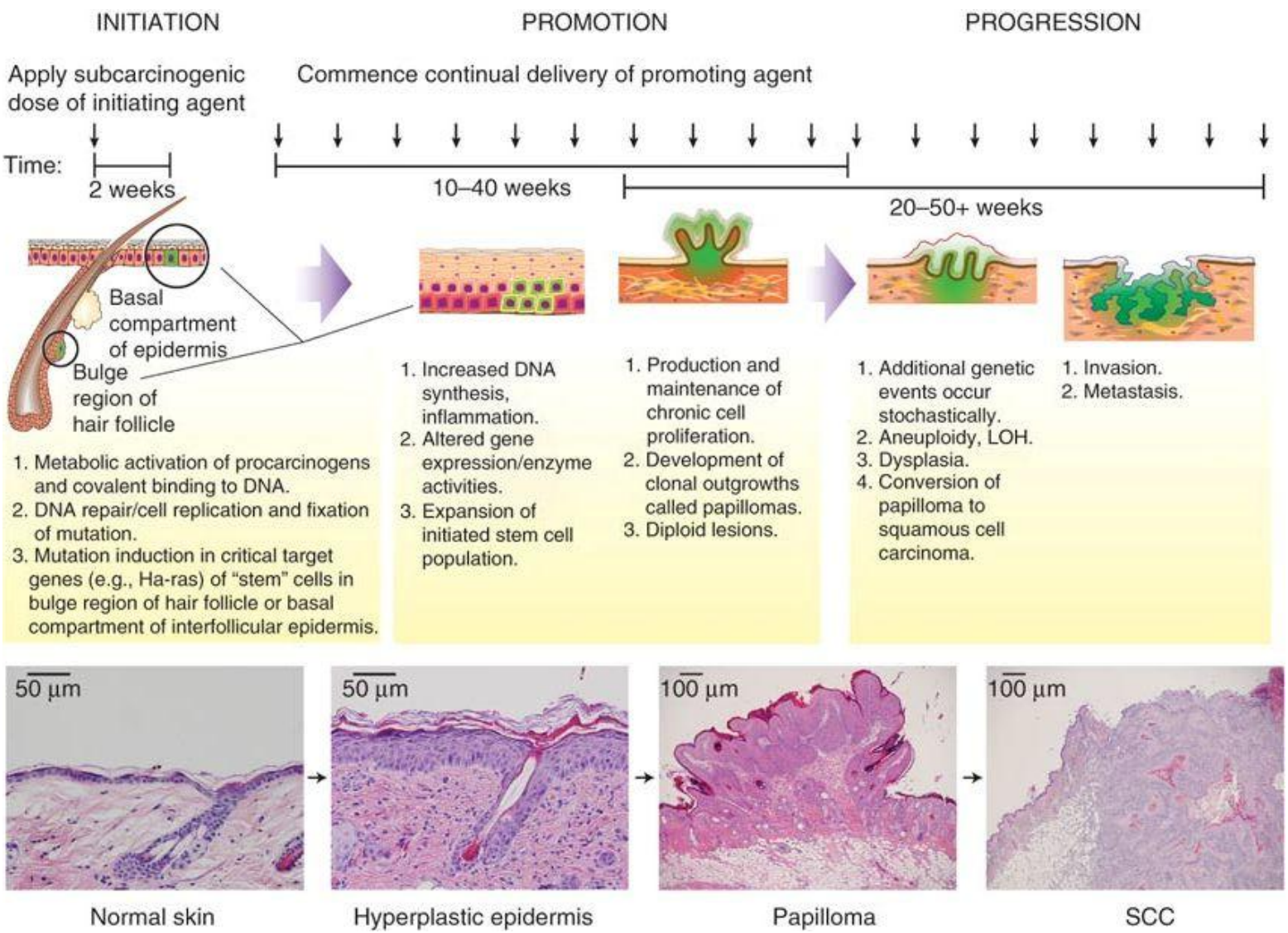
INITIATION
PROMOTION
PROGRESSION
Apply subcarcinogenic dose of initiating agent
Commence continual delivery of promoting agent
Time:
2 weeks
10–40 weeks
20–50+ weeks
Basal compartment of epidermis
Bulge region of hair follicle
1. Metabolic activation of procarcinogens and covalent binding to DNA.
2. DNA repair/cell replication and fixation of mutation.
3. Mutation induction in critical target genes (e.g., Ha-ras) of "stem" cells in bulge region of hair follicle or basal compartment of interfollicular epidermis.
1. Increased DNA synthesis, inflammation.
2. Altered gene expression/enzyme activities.
3. Expansion of initiated stem cell population.
1. Production and maintenance of chronic cell proliferation.
2. Development of clonal outgrowths called papillomas.
3. Diploid lesions.
1. Additional genetic events occur stochastically.
2. Aneuploidy, LOH.
3. Dysplasia.
4. Conversion of papilloma to squamous cell carcinoma.
1. Invasion.
2. Metastasis.
50 µm
50 µm
100 µm
100 µm
Normal skin
Hyperplastic epidermis
Papilloma
SCC

of TPA leads to sustained epidermal hyperplasia, stimulating an increase in cellular signaling, production of growth factors, oxidative stress, and tissue inflammation [88]. Papillomas generally appear in all of the mice within ~6-12 weeks following initiation, with a subset progressing to invasive SCCs in as early as 20 weeks. The percentage of mice that progress to SCC depends on a number of factors, including DMBA and TPA dosage, as well as genetic background [84, 89]. Up to 50% of papillomas in mice on the FVB background may progress to SCC [84]. This is especially important to our research, as we are interested in the role of PADI2 signaling in the progression of lesions to SCC, so the prediction is that we see an increase in the number of SCCs in the treated transgenic mice versus wild-type control. Preliminary results look promising, as we currently see a statistically significant increase in the number of papillomas in the treated transgenic mice compared to wild-type controls. However, more time will need to elapse before a full analysis of the data can confirm these initial results. The two-stage skin carcinogenesis model is often cited as recapitulating the natural progression of cancer, where the slow accumulation of mutations occurs before tumor formation. While we are currently using this model to test whether PADI2 acts as a genetic modifier or proto-oncogene in tumor progression, it could potentially be used to evaluate the effectiveness of therapeutic agents, such as our PADI inhibitors. For example, previous research has shown that the mTOR inhibitor, rapamycin, was successful in causing the regression of carcinogen-induced skin tumor lesions [90].

Taken together, there are many available options, both genetically and experimentally, to improve upon our MMTV-FLAG-PADI2 transgenic mouse. We have postulated placing the FLAG-PADI2 gene under the control of different promoters, including the ubiquitous CAG (CMV early enhancer/chicken β-actin) promoter, to fully evaluate the potential role for PADI2 as an oncogene in all tissues. The current working plan was to clone FLAG-PADI2 into a two different bicistronic

vectors, both expressing a reporter construct containing the coding sequence for a either a membrane localized red fluorescent protein (Myr-TdTomato), or a nuclear localized green fluorescent protein (H2B-GFP), separated by a 2A sequence [91]. The use of 2A peptides has emerged as an attractive alternative to the internal ribosomal entry site (IRES), resulting in the cotranslational 'cleavage' of the two proteins in a transgene, and leading to bicistronic expression of both proteins at equimolar levels. To gain a better view at tissue-specific expression of *PADI2*, and to further evaluate the role of PADI-driven carcinogenesis in the skin, we have planned to express *PADI2* under the control of promoters specific to the basal layer of epidermis in mice. The mammalian keratin-14 (K14) and keratin-4 (K5) promoters have been extensively used to drive expression of transgenes in the epidermis of mice [92, 93], and are both potential options. However, much more work on the DMBA treated mice is needed before we move onto this next stage. Regardless, we currently have an abundance of evidence linking PADI2 to the oncogenesis of mouse epidermis.

5.5 Linking it all together – summary of PADI2 involvement in cancer

The objective of these studies was to gain insight into the potential function of PADI2 in the progression of breast cancer. This thesis has advanced our understanding of PADI2 biology, while establishing a role for PADI2 as a novel oncogene and therapeutic target of cancer therapy (an overview of the potential functions of PADI2 in cancer, as described from experimental evidence offered in this thesis, is reviewed in **Figure 5.6**). We show here, for the first time, that PADI2 is capable of transforming epithelial cells both *in vitro* and *in vivo*. In addition, we have the ability to specifically block the growth of these transformed cells, in addition to other carcinomas, with PADI inhibitors. While previous work has shown that PADI2-mediated citrullination of H3R26 plays a pivotal role in ER-target gene activation, we show here that this co-

<u>Figure 5.6:</u> Overview of the potential role of PADI2 in cancer pathogenesis. This body of work has shown that PADI2 can play a role in the progression of breast cancer through regulation at gene promoters via the citrullination of H3 arginine 26 (H3R26). This leads to chromatin decondensation, and ultimately the upregulation of both ER-target genes and *HER2*. These two pathways are known to be important in the neoplastic transformation of mammary epithelial tissue. Using the MMTV-FLAG-PADI2 mouse, we have also shown PADI2 expression to have an effect on the tumor microenvironment, either through the upregulation of pro-inflammatory genes (e.g. IL6/IL8) or increased invasiveness due to the alteration of known EMT markers (e.g. E-cadherin). (Adapted from Qiagen)

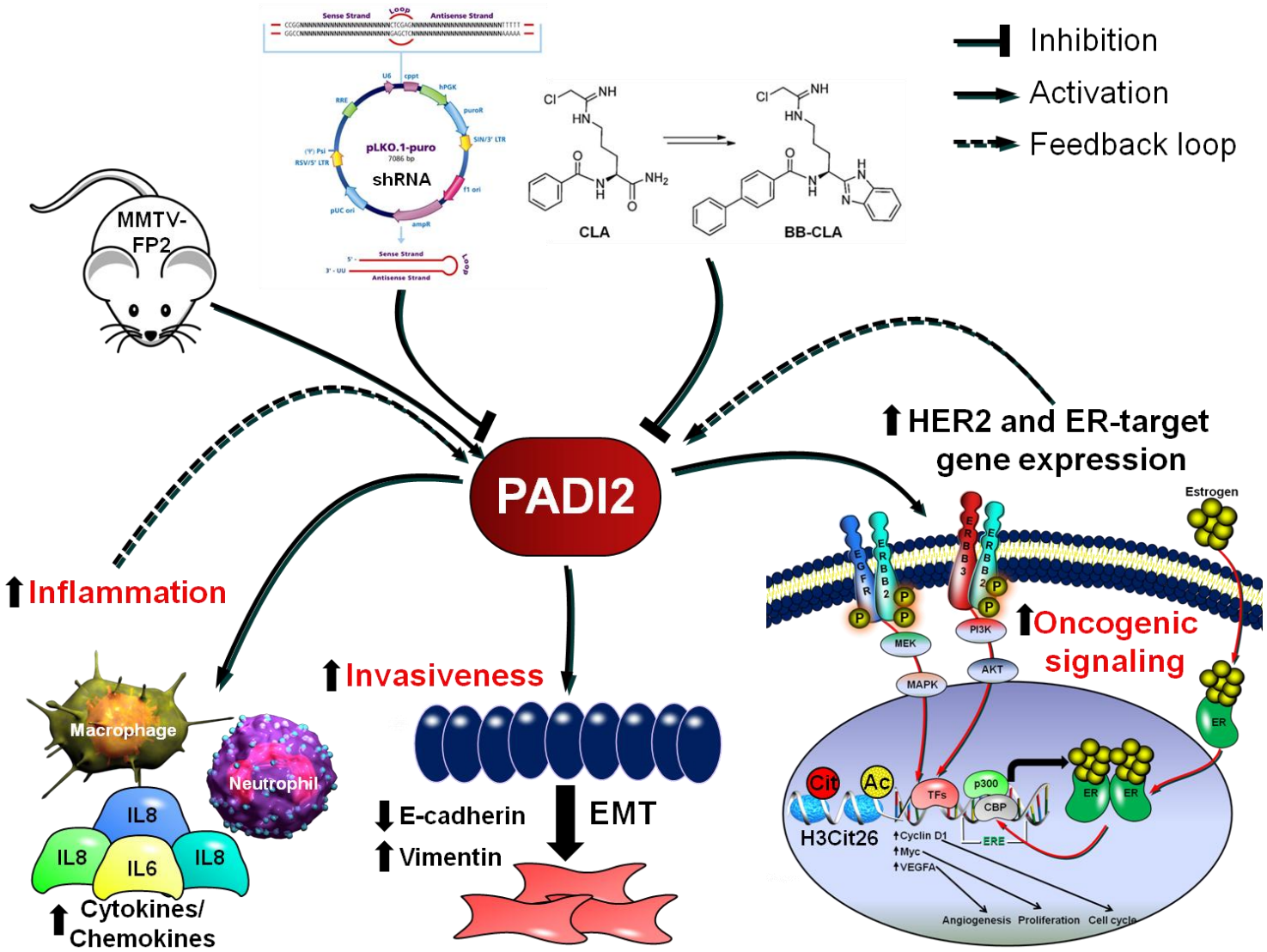
Inhibition
Activation
Feedback loop
MMTV-FP2
pLKO.1-puro
7086 bp
shRNA
CLA
BB-CLA
PADI2
Inflammation
Macrophage
Neutrophil
IL8
IL8
IL6
IL8
Cytokines/ Chemokines
Invasiveness
E-cadherin
Vimentin
EMT
HER2 and ER-target gene expression
Estrogen
EGFR
ERBB2
ERBB3
ERBB2
P
PI3K
MEK
AKT
MAPK
Oncogenic signaling
ER
Cit
Ac
TFs
p300
CBP
ER
ER
H3Cit26
Cyclin D1
Myc
VEGFA
ERE
Angiogenesis
Proliferation
Cell cycle

activator function extends to the *HER2* oncogene via the same mechanism. Using molecular genetics, we have discovered that PADI2 operates both upstream and downstream of HER2 signaling, potentially functioning as part of an oncogenic positive-feedback loop. In addition, we show that the PADI inhibitor, BB-Cl-amidine, is a powerful next-generation small molecule drug that blocks tumor growth at near-nanomolar levels. Furthermore, we show a synergistic effect for BB-Cl-amidine in the treatment of HER2-positive breast cancers when used in conjunction with the dual EGFR/HER2 inhibitor, lapatinib. Given the role of PADI2 in ER- and HER2-positive tumors, PADI2 inhibitors may have therapeutic value for over 85% of all breast cancers, thus potentially benefiting a large majority of patients. Lastly, we show evidence that *PADI2* expression is sufficient to drive oncogenic transformation in the murine epidermis, as ~20% of MMTV-FLAG-PADI2 transgenic mice develop skin lesions. Moreover, a subset of these lesions expresses markers of inflammation and EMT, having progressed to highly invasive squamous cell carcinomas. The knowledge gained from MMTV-FLAG-PADI2 mice further extends the reach of PADI2 as an oncogene to additional organ systems, and paves the way for future studies.

5.6 References:

1. Serra, V. et al. PI3K inhibition results in enhanced HER signaling and acquired ERK dependency in HER2-overexpressing breast cancer. *Oncogene* **30**, 2547-57 (2011).

2. Hennighausen, L., Wall, R.J., Tillmann, U., Li, M. & Furth, P.A. Conditional gene expression in secretory tissues and skin of transgenic mice using the MMTV-LTR and the tetracycline responsive system. *J Cell Biochem* **59**, 463-72 (1995).

3. Wagner, K.U. et al. Spatial and temporal expression of the Cre gene under the control of the MMTV-LTR in different lines of transgenic mice. *Transgenic research* **10**, 545-53 (2001).

4. Jemal, A., Siegel, R., Xu, J. & Ward, E. Cancer statistics, 2010. *CA Cancer J Clin* **60**, 277-300 (2010).

5. Osborne, C.K. & Schiff, R. Mechanisms of endocrine resistance in breast cancer. *Annu Rev Med* **62**, 233-47 (2010).

6. Knowlden, J.M. et al. Elevated levels of epidermal growth factor receptor/c-erbB2 heterodimers mediate an autocrine growth regulatory pathway in tamoxifen-resistant MCF-7 cells. *Endocrinology* **144**, 1032-44 (2003).

7. Shou, J. et al. Mechanisms of tamoxifen resistance: increased estrogen receptor-HER2/neu cross-talk in ER/HER2-positive breast cancer. *J Natl Cancer Inst* **96**, 926-35 (2004).

8. Arpino, G., Wiechmann, L., Osborne, C.K. & Schiff, R. Crosstalk between the estrogen receptor and the HER tyrosine kinase receptor family: molecular mechanism and clinical implications for endocrine therapy resistance. *Endocr Rev* **29**, 217-33 (2008).

9. Slamon, D.J. et al. Studies of the HER-2/neu proto-oncogene in human breast and ovarian cancer. *Science* **244**, 707-12 (1989).

10. Esteva, F.J. et al. Phase II study of weekly docetaxel and trastuzumab for patients with HER-2-overexpressing metastatic breast cancer. *J Clin Oncol* **20**, 1800-8 (2002).

11. Seidman, A. et al. Cardiac dysfunction in the trastuzumab clinical trials experience. *J Clin Oncol* **20**, 1215-21 (2002).

12. Hurtado, A. et al. Regulation of ERBB2 by oestrogen receptor-PAX2 determines response to tamoxifen. *Nature* **456**, 663-6 (2008).

13. Mishra, S.K., Mandal, M., Mazumdar, A. & Kumar, R. Dynamic chromatin remodeling on the HER2 promoter in human breast cancer cells. *FEBS Lett* **507**, 88-94 (2001).

14. Kan, R. et al. Potential role for PADI-mediated histone citrullination in preimplantation development. *BMC Dev Biol* **12**, 19 (2012).

15. Zhang, X. et al. Peptidylarginine deiminase 2-catalyzed histone H3 arginine 26 citrullination facilitates estrogen receptor alpha target gene activation. *Proc Natl Acad Sci U S A* **109**, 13331-6 (2012).

16. Chambraud, B., Berry, M., Redeuilh, G., Chambon, P. & Baulieu, E.E. Several regions of human estrogen receptor are involved in the formation of receptor-heat shock protein 90 complexes. *J Biol Chem* **265**, 20686-91 (1990).

17. Margeat, E. et al. The human estrogen receptor alpha dimer binds a single SRC-1 coactivator molecule with an affinity dictated by agonist structure. *J Mol Biol* **306**, 433-42 (2001).

18. Hanstein, B. et al. p300 is a component of an estrogen receptor coactivator complex. *Proc Natl Acad Sci U S A* **93**, 11540-5 (1996).

19. Kawai, H., Li, H., Avraham, S., Jiang, S. & Avraham, H.K. Overexpression of histone deacetylase HDAC1 modulates breast cancer progression by negative regulation of estrogen receptor alpha. *Int J Cancer* **107**, 353-8 (2003).

20. He, H.H. et al. Nucleosome dynamics define transcriptional enhancers. *Nat Genet* **42**, 343-7 (2010).

21. Lee, D.Y., Hayes, J.J., Pruss, D. & Wolffe, A.P. A positive role for histone acetylation in transcription factor access to nucleosomal DNA. *Cell* **72**, 73-84 (1993).

22. Luger, K., Mader, A.W., Richmond, R.K., Sargent, D.F. & Richmond, T.J. Crystal structure of the nucleosome core particle at 2.8 A resolution. *Nature* **389**, 251-60 (1997).

23. Hah, N., Murakami, S., Nagari, A., Danko, C.G. & Kraus, W.L. Enhancer transcripts mark active estrogen receptor binding sites. *Genome Res* **23**, 1210-23.

24. Kurpios, N.A., Sabolic, N.A., Shepherd, T.G., Fidalgo, G.M. & Hassell, J.A. Function of PEA3 Ets transcription factors in mammary gland development and oncogenesis. *J Mammary Gland Biol Neoplasia* **8**, 177-90 (2003).

25. Shepherd, T.G., Kockeritz, L., Szrajber, M.R., Muller, W.J. & Hassell, J.A. The pea3 subfamily ets genes are required for HER2/Neu-mediated mammary oncogenesis. *Curr Biol* **11**, 1739-48 (2001).

26. Xing, X. et al. The ets protein PEA3 suppresses HER-2/neu overexpression and inhibits tumorigenesis. *Nat Med* **6**, 189-95 (2000).

27. Chumanevich, A.A. et al. Suppression of colitis in mice by Cl-amidine: a novel peptidylarginine deiminase inhibitor. *American journal of physiology. Gastrointestinal and liver physiology* **300**, G929-38 (2011).

28. Mohanan, S., Horibata, S., McElwee, J.L., Dannenberg, A.J. & Coonrod, S.A. Identification of macrophage extracellular trap-like structures in mammary gland adipose tissue: a preliminary study. *Front Immunol* **4**, 67 (2013).

29. Wang, Y. et al. Histone hypercitrullination mediates chromatin decondensation and neutrophil extracellular trap formation. *J Cell Biol* **184**, 205-13 (2009).

30. Fan, L.Y. et al. Citrullinated vimentin stimulates proliferation, pro-inflammatory cytokine secretion, and PADI4 and RANKL expression of fibroblast-like synoviocytes in rheumatoid arthritis. *Scand J Rheumatol* **41**, 354-8 (2012).

31. Hanahan, D. & Weinberg, Robert A. Hallmarks of Cancer: The Next Generation. *Cell* **144**, 646-674 (2011).

32. Mantovani, A., Allavena, P., Sica, A. & Balkwill, F. Cancer-related inflammation. *Nature* **454**, 436-44 (2008).

33. Karin, M. & Greten, F.R. NF-kappaB: linking inflammation and immunity to cancer development and progression. *Nat Rev Immunol* **5**, 749-59 (2005).

34. Grivennikov, S.I. & Karin, M. Dangerous liaisons: STAT3 and NF-kappaB collaboration and crosstalk in cancer. *Cytokine Growth Factor Rev* **21**, 11-9 (2009).

35. Yu, H., Kortylewski, M. & Pardoll, D. Crosstalk between cancer and immune cells: role of STAT3 in the tumour microenvironment. *Nat Rev Immunol* **7**, 41-51 (2007).

36. Karin, M. Nuclear factor-kappaB in cancer development and progression. *Nature* **441**, 431-6 (2006).

37. Ancrile, B., Lim, K.H. & Counter, C.M. Oncogenic Ras-induced secretion of IL6 is required for tumorigenesis. *Genes Dev* **21**, 1714-9 (2007).

38. Aceto, N. et al. Co-expression of HER2 and HER3 receptor tyrosine kinases enhances invasion of breast cells via stimulation of interleukin-8 autocrine secretion. *Breast Cancer Res* **14**, R131 (2012).

39. Hartman, Z.C. et al. HER2 overexpression elicits a proinflammatory IL-6 autocrine signaling loop that is critical for tumorigenesis. *Cancer Res* **71**, 4380-91 (2011).

40. Lee, H.J. et al. Peptidylarginine deiminase 2 suppresses inhibitory {kappa}B kinase activity in lipopolysaccharide-stimulated RAW 264.7 macrophages. *J Biol Chem* **285**, 39655-62 (2010).

41. Proost, P. et al. Citrullination of CXCL8 by peptidylarginine deiminase alters receptor usage, prevents proteolysis, and dampens tissue inflammation. *J Exp Med* **205**, 2085-97 (2008).

42. Sparmann, A. & Bar-Sagi, D. Ras-induced interleukin-8 expression plays a critical role in tumor growth and angiogenesis. *Cancer Cell* **6**, 447-58 (2004).

43. Fernando, R.I., Castillo, M.D., Litzinger, M., Hamilton, D.H. & Palena, C. IL-8 signaling plays a critical role in the epithelial-mesenchymal transition of human carcinoma cells. *Cancer Res* **71**, 5296-306 (2011).

44. Freund, A. et al. IL-8 expression and its possible relationship with estrogen-receptor-negative status of breast cancer cells. *Oncogene* **22**, 256-65 (2003).

45. Freund, A. et al. Mechanisms underlying differential expression of interleukin-8 in breast cancer cells. *Oncogene* **23**, 6105-14 (2004).

46. Hartman, Z.C. et al. Growth of triple-negative breast cancer cells relies upon coordinate autocrine expression of the proinflammatory cytokines IL-6 and IL-8. *Cancer Res* **73**, 3470-80 (2013).

47. Korkaya, H. et al. Activation of an IL6 inflammatory loop mediates trastuzumab resistance in HER2+ breast cancer by expanding the cancer stem cell population. *Mol Cell* **47**, 570-84 (2012).

48. Iliopoulos, D., Hirsch, H.A. & Struhl, K. An epigenetic switch involving NF-kappaB, Lin28, Let-7 MicroRNA, and IL6 links inflammation to cell transformation. *Cell* **139**, 693-706 (2009).

49. Grivennikov, S.I. & Karin, M. Inflammation and oncogenesis: a vicious connection. *Curr Opin Genet Dev* **20**, 65-71 (2009).

50. Pritzker, L.B. & Moscarello, M.A. A novel microtubule independent effect of paclitaxel: the inhibition of peptidylarginine deiminase from bovine brain. *Biochim Biophys Acta* **1388**, 154-60 (1998).

51. Lee, L.F., Haskill, J.S., Mukaida, N., Matsushima, K. & Ting, J.P. Identification of tumor-specific paclitaxel (Taxol)-responsive regulatory elements in the interleukin-8 promoter. *Mol Cell Biol* **17**, 5097-105 (1997).

52. Lee, L.F. et al. Taxol-dependent transcriptional activation of IL-8 expression in a subset of human ovarian cancer. *Cancer Res* **56**, 1303-8 (1996).

53. Collins, T.S., Lee, L.F. & Ting, J.P. Paclitaxel up-regulates interleukin-8 synthesis in human lung carcinoma through an NF-kappaB- and AP-1-dependent mechanism. *Cancer Immunol Immunother* **49**, 78-84 (2000).

54. Lee, L.F. et al. IL-8 reduced tumorigenicity of human ovarian cancer *in vivo* due to neutrophil infiltration. *J Immunol* **164**, 2769-75 (2000).

55. Larue, L. & Bellacosa, A. Epithelial-mesenchymal transition in development and cancer: role of phosphatidylinositol 3' kinase/AKT pathways. *Oncogene* **24**, 7443-54 (2005).

56. Tse, J.C. & Kalluri, R. Mechanisms of metastasis: epithelial-to-mesenchymal transition and contribution of tumor microenvironment. *J Cell Biochem* **101**, 816-29 (2007).

57. Stadler, S.C. & Allis, C.D. Linking epithelial-to-mesenchymal-transition and epigenetic modifications. *Semin Cancer Biol* **22**, 404-10 (2012).

58. Wheelock, M.J. & Johnson, K.R. Cadherins as modulators of cellular phenotype. *Annu Rev Cell Dev Biol* **19**, 207-35 (2003).

59. Onder, T.T. et al. Loss of E-cadherin promotes metastasis via multiple downstream transcriptional pathways. *Cancer Res* **68**, 3645-54 (2008).

60. Berx, G. & Van Roy, F. The E-cadherin/catenin complex: an important gatekeeper in breast cancer tumorigenesis and malignant progression. *Breast Cancer Res* **3**, 289-93 (2001).

61. Rowe, R.G. & Weiss, S.J. Breaching the basement membrane: who, when and how? *Trends Cell Biol* **18**, 560-74 (2008).

62. Hajra, K.M., Chen, D.Y. & Fearon, E.R. The SLUG zinc-finger protein represses E-cadherin in breast cancer. *Cancer Res* **62**, 1613-8 (2002).

63. Bolos, V. et al. The transcription factor Slug represses E-cadherin expression and induces epithelial to mesenchymal transitions: a comparison with Snail and E47 repressors. *J Cell Sci* **116**, 499-511 (2003).

64. Peinado, H., Olmeda, D. & Cano, A. Snail, Zeb and bHLH factors in tumour progression: an alliance against the epithelial phenotype? *Nat Rev Cancer* **7**, 415-28 (2007).

65. Kumar, R., Medina, D. & Sukumar, S. Activation of H-ras oncogenes in preneoplastic mouse mammary tissues. *Oncogene* **5**, 1271-7 (1990).

66. Kumar, R., Sukumar, S. & Barbacid, M. Activation of ras oncogenes preceding the onset of neoplasia. *Science* **248**, 1101-4 (1990).

67. Currier, N. et al. Oncogenic signaling pathways activated in DMBA-induced mouse mammary tumors. *Toxicol Pathol* **33**, 726-37 (2005).

68. Vargo-Gogola, T. & Rosen, J.M. Modelling breast cancer: one size does not fit all. *Nat Rev Cancer* **7**, 659-72 (2007).

69. Blanco-Aparicio, C. et al. Mice expressing myrAKT1 in the mammary gland develop carcinogen-induced ER-positive mammary tumors that mimic human breast cancer. *Carcinogenesis* **28**, 584-94 (2007).

70. Yao, Y. et al. Increased susceptibility to carcinogen-induced mammary tumors in MMTV-Cdc25B transgenic mice. *Oncogene* **18**, 5159-66 (1999).

71. Zhou, H. et al. MMTV promoter hypomethylation is linked to spontaneous and MNU associated c-neu expression and mammary carcinogenesis in MMTV c-neu transgenic mice. *Oncogene* **20**, 6009-17 (2001).

72. Hon, G.C. et al. Global DNA hypomethylation coupled to repressive chromatin domain formation and gene silencing in breast cancer. *Genome Res* **22**, 246-58 (2012).

73. Boukamp, P. Non-melanoma skin cancer: what drives tumor development and progression? *Carcinogenesis* **26**, 1657-67 (2005).

74. Bolshakov, S. et al. p53 mutations in human aggressive and nonaggressive basal and squamous cell carcinomas. *Clin Cancer Res* **9**, 228-34 (2003).

75. Wang, X.J. et al. Expression of a p53 mutant in the epidermis of transgenic mice accelerates chemical carcinogenesis. *Oncogene* **17**, 35-45 (1998).

76. Brown, K., Strathdee, D., Bryson, S., Lambie, W. & Balmain, A. The malignant capacity of skin tumours induced by expression of a mutant H-ras transgene depends on the cell type targeted. *Curr Biol* **8**, 516-24 (1998).

77. Bailleul, B. et al. Skin hyperkeratosis and papilloma formation in transgenic mice expressing a ras oncogene from a suprabasal keratin promoter. *Cell* **62**, 697-708 (1990).

78. Greenhalgh, D.A. et al. Induction of epidermal hyperplasia, hyperkeratosis, and papillomas in transgenic mice by a targeted v-Ha-ras oncogene. *Mol Carcinog* **7**, 99-110 (1993).

79. Vitale-Cross, L., Amornphimoltham, P., Fisher, G., Molinolo, A.A. & Gutkind, J.S. Conditional expression of K-ras in an epithelial compartment that includes the stem cells is sufficient to promote squamous cell carcinogenesis. *Cancer Res* **64**, 8804-7 (2004).

80. Spencer, J.M., Kahn, S.M., Jiang, W., DeLeo, V.A. & Weinstein, I.B. Activated ras genes occur in human actinic keratoses, premalignant precursors to squamous cell carcinomas. *Arch Dermatol* **131**, 796-800 (1995).

81. Pierceall, W.E., Goldberg, L.H., Tainsky, M.A., Mukhopadhyay, T. & Ananthaswamy, H.N. Ras gene mutation and amplification in human nonmelanoma skin cancers. *Mol Carcinog* **4**, 196-202 (1991).

82. Balmain, A., Brown, K., Akhurst, R.J. & Fee, F.M. Molecular analysis of chemical carcinogenesis in the skin. *Br J Cancer Suppl* **9**, 72-5 (1988).

83. Balmain, A. & Brown, K. Oncogene activation in chemical carcinogenesis. *Adv Cancer Res* **51**, 147-82 (1988).

84. Hennings, H. et al. FVB/N mice: an inbred strain sensitive to the chemical induction of squamous cell carcinomas in the skin. *Carcinogenesis* **14**, 2353-8 (1993).

85. Nelson, M.A., Futscher, B.W., Kinsella, T., Wymer, J. & Bowden, G.T. Detection of mutant Ha-ras genes in chemically initiated mouse skin epidermis before the development of benign tumors. *Proc Natl Acad Sci U S A* **89**, 6398-402 (1992).

86. Brown, K., Buchmann, A. & Balmain, A. Carcinogen-induced mutations in the mouse c-Ha-ras gene provide evidence of multiple pathways for tumor progression. *Proc Natl Acad Sci U S A* **87**, 538-42 (1990).

87. Abel, E.L., Angel, J.M., Kiguchi, K. & DiGiovanni, J. Multi-stage chemical carcinogenesis in mouse skin: fundamentals and applications. *Nat Protoc* **4**, 1350-62 (2009).

88. DiGiovanni, J. Multistage carcinogenesis in mouse skin. *Pharmacol Ther* **54**, 63-128 (1992).

89. Ewing, M.W., Conti, C.J., Kruszewski, F.H., Slaga, T.J. & DiGiovanni, J. Tumor progression in Sencar mouse skin as a function of initiator dose and promoter dose, duration, and type. *Cancer Res* **48**, 7048-54 (1988).

90. Amornphimoltham, P., Leelahavanichkul, K., Molinolo, A., Patel, V. & Gutkind, J.S. Inhibition of Mammalian target of rapamycin by rapamycin causes the regression of carcinogen-induced skin tumor lesions. *Clin Cancer Res* **14**, 8094-101 (2008).

91. Trichas, G., Begbie, J. & Srinivas, S. Use of the viral 2A peptide for bicistronic expression in transgenic mice. *BMC Biol* **6**, 40 (2008).

92. Byrne, C., Tainsky, M. & Fuchs, E. Programming gene expression in developing epidermis. *Development* **120**, 2369-83 (1994).

93. Magin, T.M. Lessons from keratin transgenic and knockout mice. *Subcell Biochem* **31**, 141-72 (1998).